Dissertation

Effects of Lysophosphatidic Acid on Microglia Function

submitted by

Ioanna PLASTIRA

Pt. Metapt.

for the Academic Degree of

Doctor of Philosophy

(PhD)

at the

Medical University of Graz

Institute of Molecular Biology and Biochemistry

under the Supervision of

Prof. Dr. Wolfgang SATTLER

2017

“Declaration

I hereby declare that this thesis is my own original work and that I have fully acknowledged by name all of those individuals and organizations that have contributed to the research for this thesis. Due acknowledgement has been made in the text to all other material used. Throughout this thesis and in all related publications I followed the “Standards of Good Scientific Practice and Ombuds Committee at the Medical University of Graz“.

Date, April 2017

Ioanna Plastira

Parts of my dissertation have already been published in Journal of Neuroinflammation:

Plastira I, Bernhart E, Goeritzer M, Reicher H, Kumble VB, Kogelnik N, et al. 1-Oleyl-lysophosphatidic acid (LPA) promotes polarization of BV-2 and primary murine microglia towards an M1-like phenotype. Journal of neuroinflammation. 2016;13(1):205 (1)

Dedicated to my parents
and everyone who believed in me

Scientific research consists of seeing what everybody else has seen,
but thinking what nobody else has thought.
Albert Szent-Gyorgyi

Acknowledgements

Coming to the end of my PhD thesis I would like to thank the DK-MOLIN for giving me the opportunity to be part of a highly educational and well-organized program. Especially I would like to wholeheartedly thank my supervisor, Prof. Wolfgang Sattler, for welcoming me in his group and trusting me with such a beautiful and multidimensional project. For all his support and kindness the last 4.5 years, and for believing in me more than I believe in myself. He helped me to enhance my educational background, allowed me to take experimental risks, and was always there to ensure the successful progress of this project.

I would like to thank all the members of our group, my lab family, Eva, Madeleine, Nora, Vishwa, Jurgen, Helga, Anja and Andrea as well as Christoph, Andi, Sabine and Doris who are not part of it anymore. I am grateful for all their support, educational or not, and for creating an environment that makes you feel happy to work at every single day. A special thank you to Helga for her valuable help and for standing by my side when I needed it the most. For my lab trainer, Eva, a simple thank you may not be enough. She shared with me her valuable knowledge and experience and her efforts allowed me to grow as a scientist and mature as a person. I wouldn't and I couldn't ask for more.

Moreover I would like to thank Prof. Katerina Akassoglou and her research group at the Gladstone Institutes for Neurological Disease (UCSF) for accepting me at their lab for six months and providing me with an excellent working environment. It was an honor to work with such kind and highly educated people who made me feel comfortable and part of their group since the first day. I am also grateful for my mentor, Prof. Dagmar Kratky, for all her support and help through these 4.5 years.

I would like to express my gratitude for my friends and family who were always there during the good and the bad moments. For their constant support all these years and for making my life a bit brighter every single day. A big thank you to S.L., S.C., and the extraordinary J.K. for sharing with me the anxiety of the last months and giving me strength to successfully reach my goal.

Finally, I would like to thank my parents for standing by my side all these years, for their love and support and for sacrificing their convenience and welfare in order to make it possible for me to pursuit my dreams.

Abbreviations

Aβ	amyloid-β
AD	alzheimer's disease
Akt	protein kinase B
ALS	amylotrophic lateral sclerosis
AP-1	activator protein 1
APC	allophycocyanin
APP	amyloid precursor protein
Arg-1	Arginase 1
ATX	autotaxin
B2M	β2 microglobulin
BBB	blood brain barrier
BM	bone marrow
BrP-LPA	1-bromo-3(S)-hydroxy-4-(palmitoyloxy)butyl-phosphonate
BSA	bovine serum albumin
cAMP	cyclic adenosine monophosphate
CCL	C-C motif chemokine
CD	cluster of differentiation
CNS	central nervous system
COX-2	cyclooxygenase 2
CRT0066101	2-[4-[[(2R)-2-Aminobutyl]amino]-2-pyrimidinyl]-4-(1-methyl-1H-pyrazol-4-yl)-phenol hydrochloride
CSF	cerebrospinal fluid
CSF1R	colony stimulating factor 1 receptor
CXCL	C-X-C motif chemokine
CXCR	C-X-C motif chemokine receptors
DAG	diacylglycerol
DC	dendritic cells
DCFDA	2',7' –dichlorofluorescin diacetate
DLB	dementia with Lewy bodies
DMSO	dimethylsulfoxide
EAE	experimental autoimmune encephalomyelitis

ENPP2	ectonucleotide pyrophosphatase/ phosphodiesterase family member 2
ERK1/2	mitogen-activated protein kinase 1
FCS	fetal calf serum
FITC	fluorescein isothiocyanate
FTD	frontotemporal dementia
GBM	glioblastoma multiforme
DGK	diacylglycerol kinase
GM-CSF	granulocyte-macrophage colony-stimulating factor
GPCR	G protein-coupled receptors
GRN	granulin
GSK3	Glycogen synthase kinase 3
H_2O_2	hydrogen peroxide
HEPES	4-(2-hydroxyethyl)-1-piperazineethanesulfonic acid
HD	huntington's disease
HPRT	hypoxanthine-guanine phosphoribosyltransferase
HTT	huntingtin
IFN	interferon
IkBα	nuclear factor of kappa light polypeptide gene enhancer in B-cells inhibitor, alpha
IKKβ	inhibitor of nuclear factor kappa-B kinase subunit beta
IL	interleukin
iNOS	inducible nitric oxide synthase
IRF	interferon regulatory factor
ITGα	integrin alpha
ITGβ	integrin beta
JNK	c-Jun N-terminal kinases
LDH	lactate dehydrogenase
LPs	lysophospholipids
LPA	lysophosphatidic acid
LPAR	LPA receptors
LPPs	lipid phosphate phosphatases
LPS	lipopolysaccharide
MAPK	mitogen-activated protein kinase

miRNA	micro RNA
MMP	matrix metalloproteinase
mRNA	messenger RNA
MRC1	macrophage mannose receptor 1
MS	multiple sclerosis
MYC9	myosin, heavy chain 9, non-muscle
NF-kB	nuclear factor kappa-light-chain-enhancer of activated B cells
NFTs	neurofibrillary tangles
NO	nitric oxide
NOX2	phagocyte NADPH oxidase
NPC	neuroprogenitor cell
O_2• –	superoxide
o/n	over night
$ONOO^-$	peroxynitrite
P2RY	purinergic G protein-coupled receptors
PA	phosphatidic acid
PC	phosphatidylcholine
PD	parkinson's disease
PDL	poly-D-lysine
PE	phycoerythrin
PI3K	phsophoinositide 3-kinase
PKC	protein kinase C
PKD	protein kinase D
PLA	phospholipase A
PLC	phospholipase C
PLs	phospholipids
PMM	primary murine microglia
PPAR	peroxisome proliferator-activated receptor
PS	phosphatidylserine
qPCR	real-time PCR
Rac2	Ras-related C3 botulinum toxin substrate 2
RELMα	resistin-like alpha
Rho	Rho GTPase

RNS	reactive nitrogen species
ROCK	Rho-associated protein kinase
ROS	reactive oxygen species
Runx1	Runt-related transcription factor 1
SCs	Schwann cells
SOD1	superoxide dismutase 1
SP600125	1,9-Pyrazoloanthrone
STAT	signal transducer and activator of transcription
TBCB	tubulin-folding cofactor B
TBHP	tert-butylhydroperoxide
TCLPA5	5-(3-Chloro-4-cyclohexylphenyl)-1-(3-methoxyphenyl)-1H-pyrazole-3-carboxylic acid
TGF-β	transforming growth factor beta
TLR	toll-like receptors
TNFα	tumor necrosis factor alpha
TREM2	triggering receptor expressed on myeloid cells 2
TRP	transient receptor potential
VASP	vasodilator-stimulated phosphoprotein
VEGF	vascular endothelial growth factor
VIM	vimentin
VZ	ventricular zone
WASF2	Wiskott-Aldrich syndrome protein family member 2
YS	yolk sac

Zusammenfassung

Lysophosphatidsäure als Modulator der Mikroglia-Funktion

Microglia, die immunkompetenten Zellen des ZNS, reagieren unmittelbar auf Erkrankungen und Verletzungen des zentralen Nervensystems (ZNS), verändern ihre Morphologie, wandern in das geschädigte Gewebe ein und spielen eine wichtige Rolle bei der Regeneration des ZNS. Extrinsische Signale entscheiden letztendlich, ob Mikroglia einen neuroprotektiven oder neurodegenerativen Phänotyp entwickeln. Klassisch aktivierte (M1) Mikroglia synthetisieren proinflammatorische Faktoren, die zu neuronaler Schädigung führen können. Andererseits kann die Produktion von entzündungshemmenden Faktoren durch M2-polarisierte Mikroglia neuronales Überleben und Regeneration unterstützen. Bei chronisch entzündlichen Vörgängen, wie sie bei vielen neurodegenerativen Erkrankungen beobachtet werden, sind Mikroglia durch Überaktivierung, Dysfunktion, Sekretion von pro-inflammatorischen Faktoren und neuronaler Toxizität gekennzeichnet. Der entscheidende Beitrag von Mikroglia zur Homöostase im ZNS macht diese Klasse von immunkompetenten Zellen zu potentiellen therapeutischen Targets. Somit würde die Möglichkeit, den Polarisations-Phenotyp (M1 vs. M2) zu modulieren, einen neuen pharmakologischen Ansat bei der Behandlung von neurodegenerativen Erkrankungen, möglicherweise sogar bei Gehirntumoren ermöglichen.

Den bioaktiven Substanzen der Lysophosphatidsäure (LPA)-Familie wird zunehmend ein Einfluss auf unterschiedlichste Erkrankungen zugeschrieben. Die Spezies der LPA-Familie stellen ein Gemisch aus gesättigten oder ungesättigten Acyl-/Alkylresten, die an der sn-1 oder sn-2-Position eines Glycerophosphatmoleküls verestert sind, dar. Unterschiedliche LPA Spezies wurden in biologischen Flüssigkeiten, unter anderem auch in der Zerebrospinal-Flüssigkeit nachgewiesen. Der quantitativ grösste Teil von LPA wird durch Autotaxin (ATX)-katalysierte Hydrolyse von lyso-Phosphatidylcholin produziert. LPA-vermittelte Signale werden durch die Bindung an einen oder mehrere der sechs bis jetzt charakterisierten G-Protein gekoppelten LPA Rezeptoren (LPAR1-6) ausgelöst. Das Gehirn ist ein Organ in dem LPAR vorwiegend exprimiert werden. LPA löst unterschiedlichste biologische Reaktionen die durch LPAR-vermittelte Signaltransduktion, ausgelöst werden. Diese Rezeptoren spielen bei normaler Entwicklung aber auch bei Erkrankungen des ZNS eine entscheidende Rolle. Speziell bei neuroinflammatorischen

Erkrankungen wird die Expression von ATX auf Proteinebene induziert, was in weiterer Folge zu einem lokalen Anstieg der LPA Konzentrationen führt.

Die Ergebnisse der vorliegenden Studie belegen, dass LPA ein potenter Regulator der Mikrogliafunktion ist. Erhöhte LPA-Spiegel, wie sie unter entzündlichen Bedingungen beobachtet wurden, beeinflussten die Mikroglia-Morphologie und fördern die Motilität von Mikroglia. Die während der vorliegenden Dissertation gewonnenen Ergebnisse belegen, dass die LPA/LPAR5/ Proteinkinase D (PKD) - Achse die Chemokinese und Chemotaxis von Mikroglia reguliert. Darüber hinaus förderte LPA die Etablierung eines M1-ähnlichen Polarisationsphenotyp von Mikroglia. Dies wurde durch erhöhte Sekretion von pro-entzündlichen Mediatoren wie Cytokinen und Chemokinen, Stickstoffmonoxid und reaktiven Sauerstoffspezies, erhöhte Expression von M1-Markern und Mikroglia-vermittelter Neurotoxizität belegt. Die pharmakologische Hemmung der LPAR5/PKD/JNK-Achse führte zu signifikant verringerter Expression dieser entzündlichen Faktoren und unterdrückte die Expression von pro-inflammatorischen Transkriptionsfaktoren.

Die Ergebnisse der vorliegenden Dissertation stellen einen ersten Schritt zu einem tieferen Verständnis von LPA-vermittelten Wirkungen auf Mikroglia dar. Die Ergebnisse, die während meiner Doktorarbeit generiert wurden, sollten das Studium der LPA-vermittelten Signaltransduktion und ihren Auswirkungen auf die Mikroglia-Funktion bei neurodegenerativen Erkrankungen in ‚in vivo' Modellen weiterführen um mögliche neue pharmakologische und therapeutische Ansätze zu ermöglichen.

Abstract

Effects of Lysophosphatidic Acid on Microglia Function

Microglia, the immunocompetent cells of the CNS, rapidly respond to brain injury and disease, alter their morphology, migrate towards the damaged tissue and play an important role in CNS regeneration. Extrinsic signals determine whether microglia acquire - depending on disease context - a beneficial or detrimental phenotype. Classically activated (M1) microglia synthesize pro inflammatory factors that inflict neuronal damage, while the production of trophic and anti-inflammatory factors by M2 microglia can support neuronal survival and regeneration. Under chronic inflammation, as observed in many neurodegenerative diseases, microglia are characterized by overactivation, dysfunction, secretion of pro inflammatory factors and neuronal toxicity. Their crucial role in brain homeostasis makes these cells potential therapeutic targets, which necessitate a thorough understanding of polarization cascades, and pathways that modulate their function.

There is growing appreciation that the pathogenesis of many diseases is linked to dysregulated LPA signaling. LPA is a mixture of saturated or unsaturated acyl/alkyl residues esterified at the sn-1 or sn-2 position that are present in biological fluids including CSF. The majority of LPA is produced through autotaxin (ATX)-dependent cleavage of lysophosphatidylcholine and LPA signaling is mediated via six LPA receptors (LPAR1-6) that are all expressed in the brain. LPA has diverse biological functions mediated by downstream signaling through the different receptors. These receptors play prominent role in the central nervous system, and signaling is amplified at sites of inflammation where LPA concentrations are increased.

The results of the present study provide evidence that LPA is a potent regulator of microglia biology and function. Increased LPA levels, as observed under inflammatory conditions, affected microglial morphology and promoted the migrational response. The LPA/LPAR5/PKD axis regulated the expression of migratory genes indicating possible downstream targets via which LPA signaling controls microglia chemotaxis. In addition, LPA promoted am M1-like phenotype in microglia. I observed elevated secretion of pro inflammatory mediators such as cytokines, chemokines, NO, and ROS, increased expression of M1 markers and microglia-mediated neurotoxicity. Pharmacological inhibition of the LPAR5/PKD/JNK axis significantly decreased the expression of these pro-inflammatory factors and abolished the LPA-induced activation of pro-inflammatory

transcription factors, unraveling possible transcription programs that are involved in LPA-induced inflammatory response of microglia cells.

The outcome of this study comprises of an important step towards a better understanding of LPA-mediated effects on the immune cells of the CNS. The results obtained during my PhD thesis should foster the study of LPA signaling and its impact on microglia function in the diseased brain. Interference with different members of the LPA signaling pathway, depending on the context of disease, may unravel possible new targets for modulating neuroinflammation that, until now, were not considered.

1. Microglia

1.1 Origin and Development

The central nervous system (CNS) has been considered for a long time immune privileged due to its lack of lymphatic drainage and reduced capacity to present antigens (2). However, when necessary, it can mount immune reactions that depend upon specialized innate cells, including microglia, macrophages, and dendritic cells (DCs). Microglia are the resident macrophages of the CNS and uniformly distributed throughout the brain parenchyma and spinal cord (3). The density of resident microglia varies by brain regions. Increased densities are observed in in the gray matter, with the highest concentrations found in hippocampus, olfactory cortex, basal ganglia, and substantia nigra in the mid brain (4-6). Microglia comprise approximately 10-15% of glial cells and their function is crucial to maintenance of the CNS in both health and disease (7, 8).

Due to phenotypic similarities to peripheral monocytes/macrophages and DCs, microglia were proposed to be of hematopoietic origin and derive from circulating monocytes (3). Recent studies though confirmed that microglia are derived from primitive macrophages emanating during development from the yolk sack (YS) (9, 10). These primitive macrophages generated in the YS blood islands around E8.0 and spread into the embryos at the onset of blood circulation (around E8.5). Finally they colonize the neuroepithelium from E9.0/E9.5, giving rise to embryonic microglia (5) (**Figure 1**). In parallel, definitive hematopoiesis gives rise to progenitors that colonize the fetal liver (FL) from E10.5. Formation of the BBB from E13.5 isolates the developing brain from the contribution of FL and later of bone marrow (BM) hematopoiesis. Embryonic microglia expand, colonize the whole CNS, and maintain themselves until adulthood via proliferation during postnatal development as well in the injured adult brain. Under certain inflammatory conditions, the recruitment of BM derived progenitors can replenish to some extent the microglial population.

Transcriptome analysis has revealed that microglia have a very distinct signature as compared with circulating macrophages (11). Those differences between microglia and macrophages and other immune cells highlight that microglia are not classical immune cells (12). During neonatal development, myeloid precursors differentiate into microglia,

and various molecules control the developmental program. Interestingly, the transcription factor Myb, which is required for hematopoiesis and generation of hematopoietic stem cells HSCs), is not essential for the generation of microglia (13).

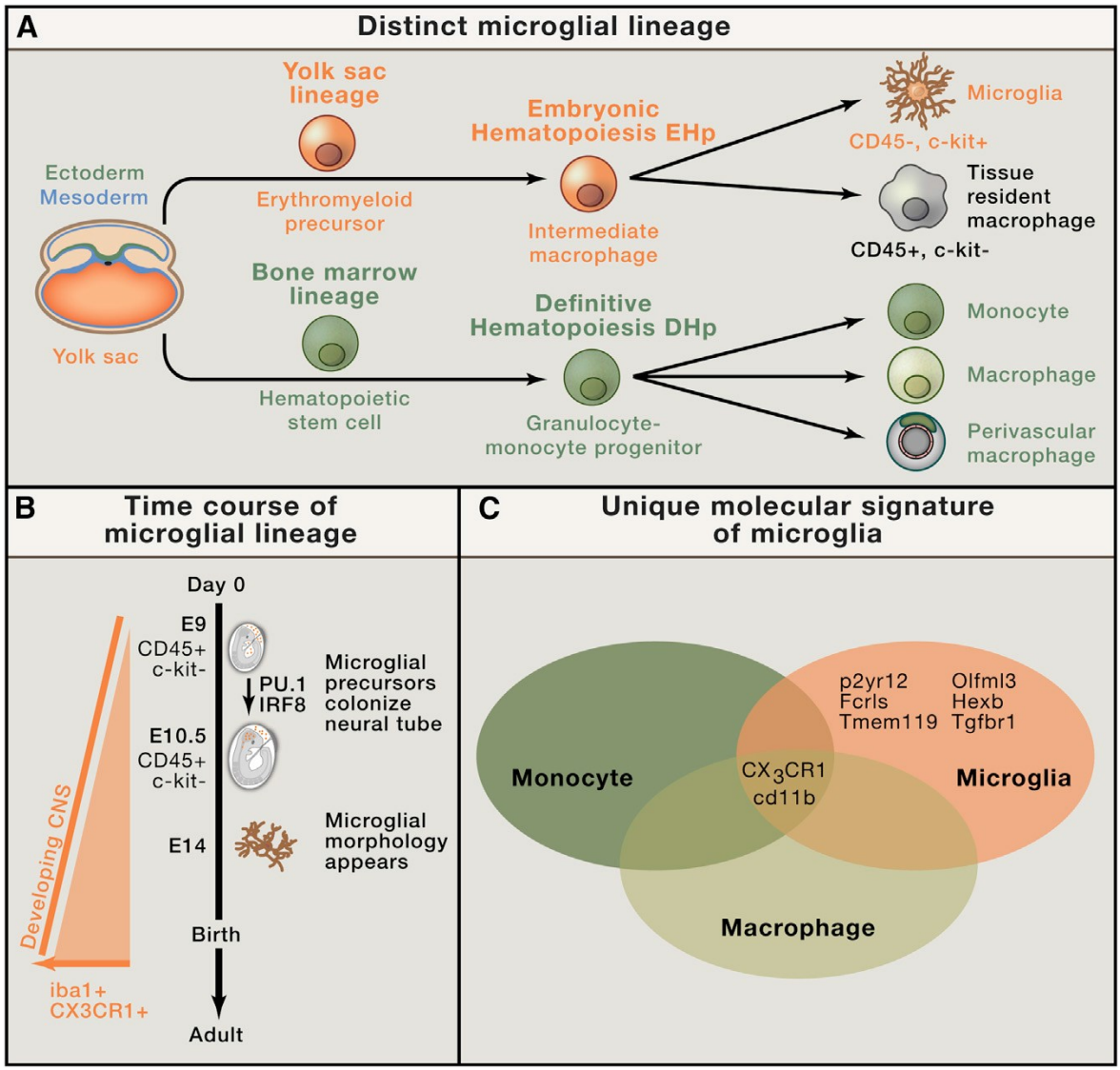

Figure 1. Microglia Have a Distinct Lineage and Molecular Signature

(A) Genesis and progression of yolk-sac-derived cell lineages. Microglia are derived from primitive erythromyeloid progenitors in the yolk sac (embryonic hematopoiesis, yellow), distinct from definitive hematopoiesis (green) from which the majority of macrophages is derived (11).

(B) Time course of microglial derivation and embryonic colonization as revealed by fate-mapping experiments. Microglia originate from PU.1-dependent precursors in the yolk sac that proliferate and invade the neuroectoderm-derived developing CNS, as indicated by an increase in the markers CX3CR1 and Iba1 (orange ramp) (11).

(C) The diagram presents the overlap in gene expression between microglia, macrophages, and monocytes. Two of the most widely used "markers," CX3CR1 and cd11b, are common to all three. Although there is molecular similarity between tissue-resident macrophages and microglia, a subset of microglial-specific genes has been identified, and the six genes with highest expression are displayed (11).

Analyses of YS progenitors revealed that microglia are derived from $CD45^-$ c-kit^+ erythromyeloid progenitor cells (10), which eventually convert to $CD45^+$ c-kit^- $CX3CR1^+$ microglia and invade the brain using matrix metalloproteinase (MMPs), such as MMP-8 and MMP-9.

The key factors that promote microglia development and homeostasis are presented below.

Runx1

Runx1 directly binds to the enhancer elements of many genes relating to hematopoietic development and interactions with other transcriptional elements are crucial for expression of genes that participate in lineage specific development of multipotent progenitors (14). The YS derived $Runx1^+$ precursors populate the CNS and develop into microglia during stages that precede brain development and vascularization (9). During development $Runx1^+$ microglia have an amoeboid morphology and undergo mitosis. Microglial morphological transformation from amoeboid to ramified, around postnatal day 10, coincides with loss of Runx1 expression. In the adult brain, Runx1 is reexpressed following traumatic nerve injury and this suggests an additional role for the transcription factor in the regulation of microglia activation (15).

PU.1

PU.1 is a transcription factor that is expressed by various cells, including macrophages, neutrophils, mast cells, B cells, and microglia. The PU.1 protein is constitutively expressed in both resting and activated microglia (rodent and human) (16, 17). PU.1 is a master regulator for myelomonocytic differentiation during embryonic development and PU.1 deficiency impedes the maturation of YS myeloid progenitors (18). It has been reported that PU.1 expression is regulated by other hematopoietic transcription factors including CSF1 (19).

CSF1R

CSF1R is a tyrosine kinase expressed on mononuclear myeloid cells throughout the body (3). It is a critical regulator of proliferation, survival, differentiation and chemotaxis of microglia and other mononuclear phagocytic cells (20).

IRF-8

Interferon regulatory factor 8 (IRF-8) is a transcriptional factor that participates in development of the immune system. It has a direct impact on CNS microglia and IRF-8

deficiency results in increased microglial abundance in the adult brain (21).IRF-8 deficient cells have also reduced branch complexity and morphological changes suggestive of activation. IRF-8 plays a key role in microglia homeostasis and development by regulating as well apoptosis related genes (22).

miR-124

MicroRNAs regulate gene expression through posttranscriptional modification of mRNAs by promoting their degradation. miR-124 is one of the most abundantly expressed mRNAs in the CNS and by altering gene expression in neurons, regulates neurogenesis and neuronal differentiation (23, 24). It is also highly expressed in microglia, which down regulate its expression following activation, suggesting a possible role for miR-124 in maintaining microglia quiescence (25).

PHYSIOLOGY AND FUNCTION

Microglia are indispensable for normal brain development and CNS homeostasis and there is mounting evidence for important roles (**Figure 2**) of these cells in the establishment of a healthy nervous system (20). Current research has established the importance of these multifunctional cells in numerous physiological processes (26).

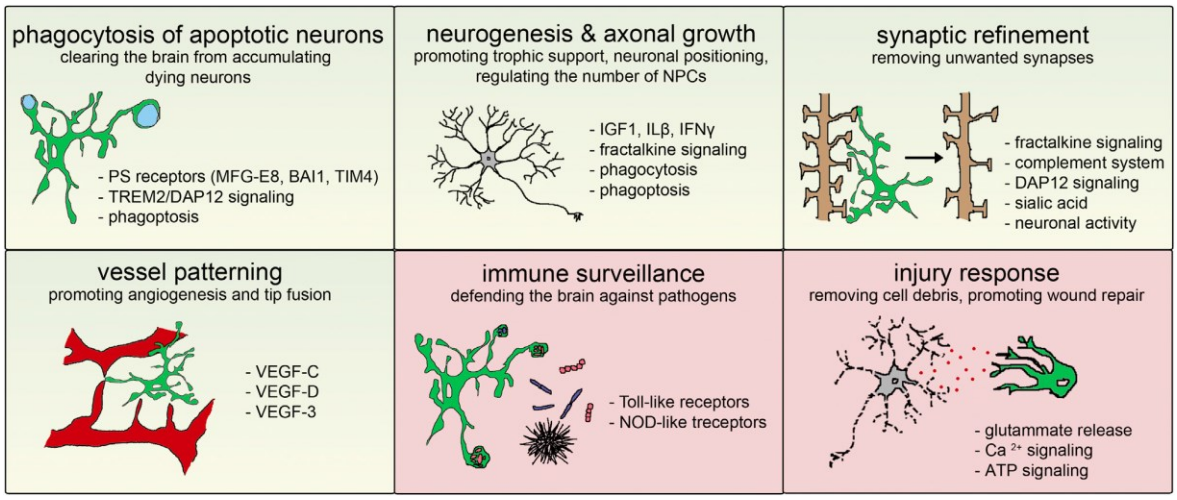

Figure 2. Schematic representation of microglial roles in the brain

Yellow and pink boxes indicate microglial roles during developmental stages and general immune-related functions, respectively (26).

1.1.1 Clearance of apoptotic cells

Microglia play critical role in removing accumulating apoptotic neurons, both during CNS development and later in the adult brain (26). They also efficiently discard cellular debris resulting from apoptosis, normal cell death or brain parenchyma lesions (damaged cells, plaques etc.) promoting the homeostatic maintenance of healthy CNS.

1.1.2 Neurogenesis

Microglia support neurogenesis during developmental stages and adulthood, by producing neurotrophic factors. They are necessary for proper assembly of neuronal networks (27). They create a favorable environment for neuronal development and regeneration by secretion of neurotrophins, and other neurotrophic or growth factors (26, 28). Moreover, they play active roles in the induction of neuronal cell death in the developing brain.

1.1.3 Synaptogenesis and Synaptic Plasticity

One of the most intriguing functions of microglia is 'synaptic pruning'. During CNS development, axonal connections with synapses exceed those required and are reduced during a process called pruning (7). Microglia shape neuronal synapses; they phagocytose dendritic spines that not receiving input from synaptic contacts (27). Microglia participate also in synaptic plasticity, a process of removing branches from damaged neurons in order to promote repair and regrowth (29) They secrete immune-related signaling molecules such as pro-inflammatory cytokines, NO, ROS, and neurotrophic factors that alter synapse strength and plasticity (27).

1.1.4 Vascular development

Microglia contribute to the construction and maintenance of the vascular system in the CNS. They facilitate angiogenic sprouting during development and promote the fusion of nearby blood vessel (7, 30).

1.1.5 Oligodendrocytes survival

Except for neuronal survival, microglia also promote oligodendrocytes survival and maturation. They inhibit apoptosis, secrete soluble factors, PDGF (platelet-derived growth factor), and induce the expression of transcription factor NF-kB p65 (nuclear factor kappa-light-chain-enhancer of activated B-cells) (28). Microglia are also considered potential stem cells that can differentiate into neurons, astrocytes and oligodendrocytes (31).

1.1.6 Immune surveillance

As already mentioned, microglia are the resident immune cells of the CNS. They defend the brain against pathogens holding a critical role in immune surveillance and control (32). They constantly monitor synaptic activity (each synapse is contacted about once per hour) and impact synaptic plasticity, remodeling functionally impaired synapses, by the release of neurotrophic factors and anti-inflammatory cytokines (33).

1.1.7 Injury response

Microglia respond rapidly to danger signals and migrate towards the sites of injury to remove cellular debris and promote tissue repair. They are the "scavenger" of the nervous tissue and therefore represent a key factor in the nervous parenchyma defense. They release immunoregulatory cytokines and growth factors in order to maintain CNS homeostasis (34).

1.2 Heterogeneous Activation States

There is constantly growing experimental evidence that the subdivision of microglia into resting and activated is an oversimplification (8, 35). Microglia are recognized as "active sensor and versatile effector cells in the normal and pathological brain" (33).

1.2.1 The activation process: from "resting" state to "activated" microglia

Microglia in the healthy CNS have a ramified morphology, a small soma with fine cellular processes. This appearance has been associated with microglial "resting" state. In reality, however, these cells constantly scan their environment and actively survey brain parenchyma, ready to transform to executive states of activity (36, 37).

In response to different signals and various micro environmental changes, these plastic cells can switch activity states and exist in multiple phenotypes (7, 38, 39). Real or potential danger to the CNS evokes profound changes in microglial cell shape, gene expression and functional behavior (36). Activated microglia may adopt not only an amoeboid morphology but also rod, epithelioid, or multinucleated morphology (40). They become motile, move to the site of injury following chemotactic gradients, and unfold their phagocytic activities to clear tissue debris, microbes, or damaged cells.

Microglial activation is a highly regulated process (**Figure 3**). These cells are part of a specialized tissue (brain parenchyma), which also has to protect itself from the damaging

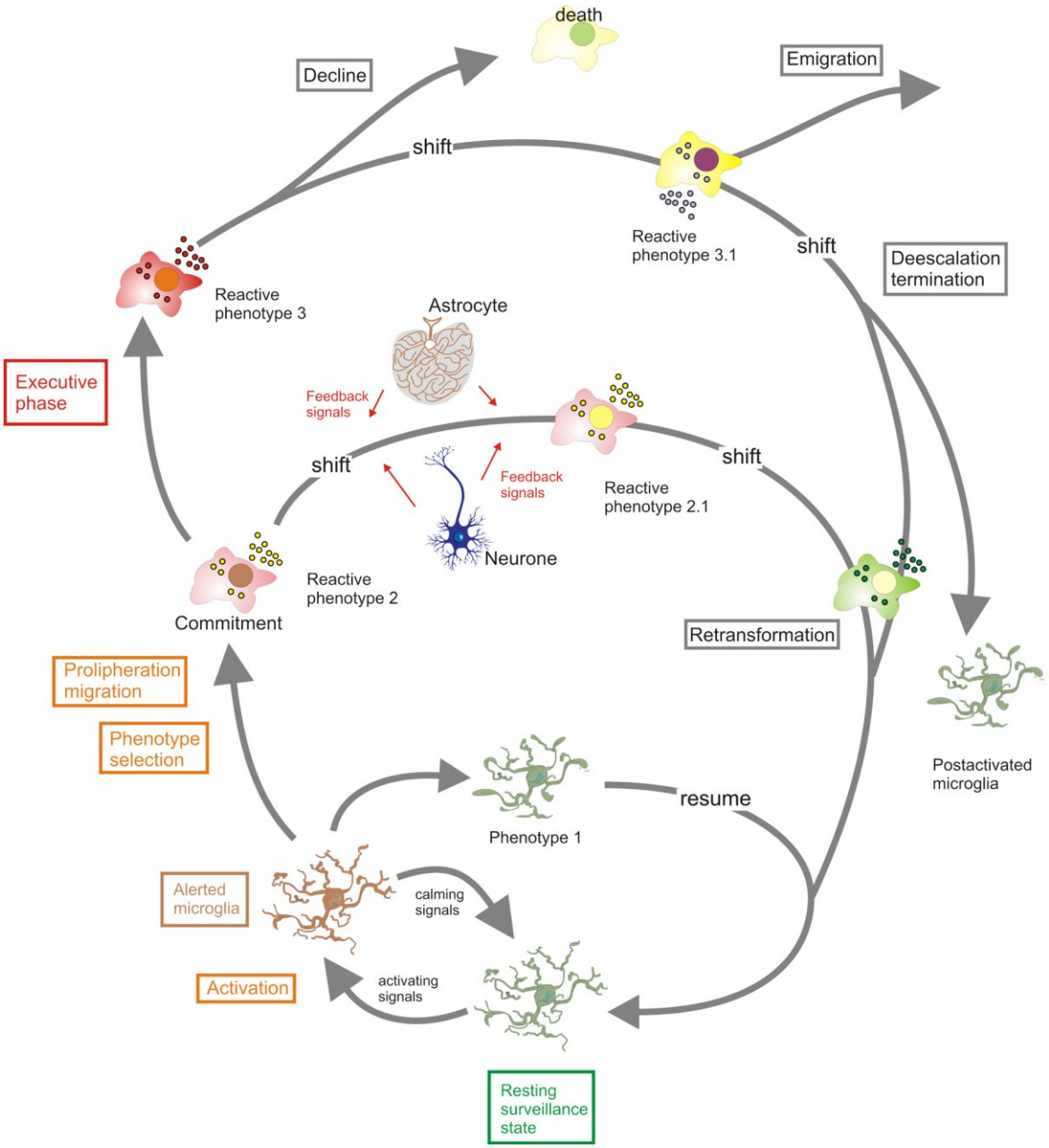

Figure 3. Microglial activity states throughout an activation process

The "resting" microglia constantly scan their environment for exogenous or endogenous signals that may oppose a threat to CNS homeostasis. The appearance of "activating" signals or a loss of constitutively "calming" inputs can trigger transitions to activated states.

Cells adopt distinct reactive phenotypes depending on the challenging stimuli and the situational context. Initial response profiles may further shift as instructed by concomitant cues (36). Except for the resident CNS cells, also infiltrating immune cells exert such modulating functions. Initial reactive phenotypes with defense orientation may convert to repair-orientated activity profiles (36).

Cells may eventually return to a resting state or stay "experienced." Experienced microglia could reveal altered responsiveness and exert distinct responses upon a new challenge (35).

consequences of an immune response (36). Thus, microglia may not necessarily represent a homogeneous population. The transition from the "resting" state to an executive one represents more of a shift in activities rather than "activation" per se.

Less is known about the period subsequent to the activation event. A terminated microglial response, even in the case that it was successful, may still leave traces (35). The post activated microglia may remain undistinguishable by the "resting" ones, yet may still bearing adjustments and could behave differently when being challenged again.

1.2.2 M1 vs M2 activation

In the context of activation, microglia can acquire different phenotypes (**Figure 4**), depending on the specific polarization conditions (28, 41). However, it needs to be highlighted that there is not a single phenotype for microglia activation but a broad spectrum of microglial activation states (42-44). Microglia can acquire intermediate phenotypes that display a combination of different markers (41, 45). Microglia are a non-homogeneous population and different cells in the same area may adopt different phenotypes. Hence, it will be more correct and accurate to speak for polarization towards a phenotype and not strictly about solely one activation state.

There are three distinct activated forms toward which microglia can be polarized: classical M1 (pro-inflammatory) activation, alternative M2 (anti-inflammatory) activation and acquired deactivation.

Classical M1 (pro-inflammatory) activation

During classical activation, in response to LPS or the proinflammatory cytokine IFN-γ, the innate immune system favors a T-helper cell type 1 (Th1) phenotype. Thus, during a Th1 response, microglia express CD86 and CD16/32, and produce high amounts of oxidative metabolites (NO and O2 •−), proteases, toxic mediators and proinflammatory cytokines and chemokines (TNF, IL-1, IL-2, IL-6). This phase plays a critical role in host defense against pathogens and tumor cells yet can also damage resident healthy cells (40, 41, 46).

Alternative M2 (anti-inflammatory) activation

In this form of activation, which can be induced by IL-4 and IL-13, the innate immune system favors a T-helper cell type 2 (Th2). During a Th2 response, activated microglia will express CD206 and arginase 1, secrete anti-inflammatory cytokines (IL-4, IL-5, IL-10, IL-13), transforming growth factor beta (TGF-β), and are characterized by the suppression of

Th1-proinflammatory cytokines (41). There is reduced NOS2 (nitric oxide synthase 2) expression, NOX2 (phagocyte NADPH oxidase) activation and induction of a transcriptional profile characteristic for this phenotype (47).

The conversion of microglia towards an alternative activation state appears to be coordinated by two members of the peroxisome proliferator-activated receptor (PPAR) family (superfamily of nuclear hormone receptors): PPAR-γ and PPAR-β/-δ (28). Recently, PPAR-γ has been recognized as a prime target for modulating inflammation, by inhibiting pro-inflammatory gene expression, a process termed PPAR-γ-mediated transcriptional trans-repression (48). During this phase microglia promote tissue repair and angiogenesis, by down-regulating the inflammation.

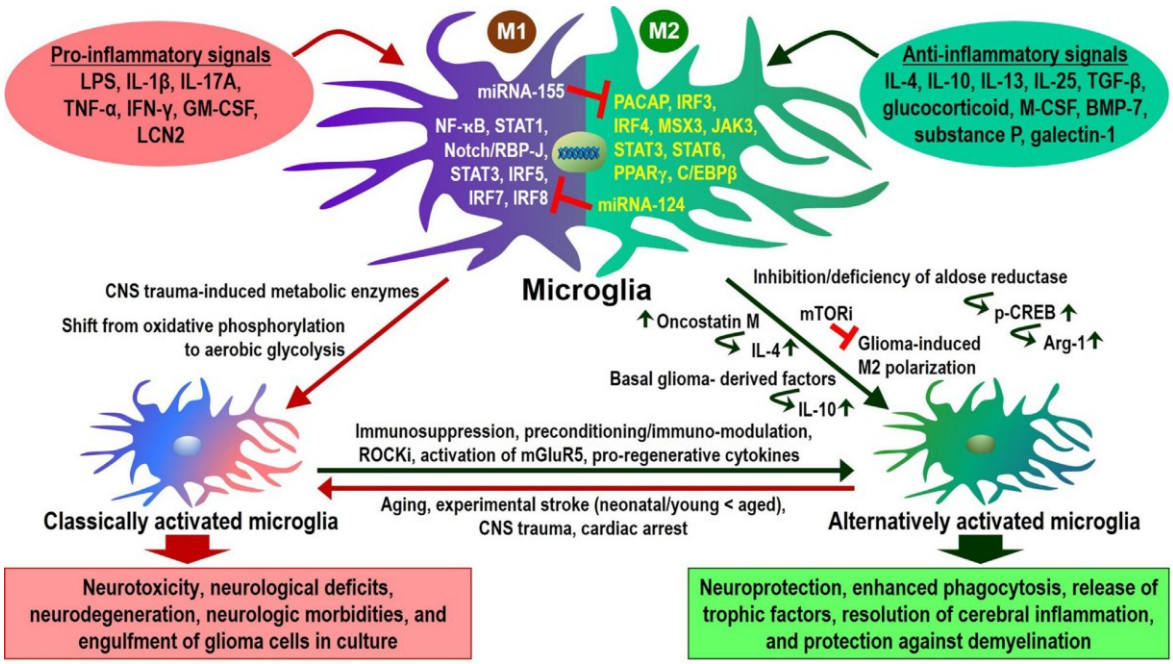

Figure 4. Phenotypic polarization of microglia

Microglia polarization and phenotype switching is under control of diverse intra- and extracellular cues. Microglia can develop into proinflammatory/classically activated (M1) or anti-inflammatory/alternatively activated (M2) phenotypes depending on the specific polarizing signals present at diverse stages after CNS injuries, and thereby revealing beneficial or detrimental responses for tissue protection and repair (41).

The M1 polarized microglia release proinflammatory mediators and free radicals to induce functional neurological deficits and neurodegeneration. This population also engulfs glioma cells in culture. On the contrary, the M2 polarized microglia support brain repair and regeneration by enhancing phagocytosis, releasing trophic factors, resolving inflammation, and protecting against demyelination. The functional polarization of microglia characterized by diverse transcription factors, acute phase proteins, receptors, pathological conditions, and metabolic states (41).

Acquired deactivation

The acquired deactivation state allows microglia to detect apoptotic cells and clear them in the absence of inflammation. This phase allows normal tissue maintenance and patterned cell death to be performed without setting off an inflammatory response and regulated by the secretion of anti-inflammatory cytokines such as IL-10 and TGF-β (48). The acquired deactivation phase, considered a distinct phase of alternative activation, and is associated with suppression of the innate immune response. It is characterized by down-regulation of molecules associated with antigen presentation and decreased production of pro-inflammatory cytokines, chemokines, NO and free radicals.

1.2.3 Microglial priming

Microglia priming is a condition characterized by exaggerated and heightened microglial response to a second inflammatory stimulus (49). Priming can induce apparent changes in microglial morphology, proliferation numbers and upregulation of cell surface antigens. The concept of this state provides a cellular and molecular pathway by which systemic inflammation (such as sepsis) might contribute to the progression of chronic neurodegenerative diseases.

Microglia priming is widely observed in aged brains (50). The age-related priming induces an exaggerated secondary inflammatory response (51). Elderly individuals are more susceptible to peripheral infections and neurodegeneration due to hyperactivation of microglia. This prolonged activation of microglia makes them resistant to regulation and impair their responses leading to disruption of the fine coordination between the nervous and the immune system (49).

1.2.4 Microglial ageing

Many phenotypic changes have been observed for microglia over the lifespan of the cell (52). Ageing affects microglia by altering their endogenous characteristics and inducing a less responsive (dystrophic) phenotype (53). Morphological and functional alterations are accompanied by changes in gene expression, reduced expression of quiescence molecules, and production of higher levels of NOS2, TNF, IL-1β, and IL-6 (34). Microglia appear to have decreased capacity to mount cellular responses to injury, reduced phagocytic capacity and reduced motility (54). In addition they are increased in numbers and are being less evenly distributed in the cerebral cortex (55, 56).

1.2.5 Microglial senescence

Like all cells, microglia are believed to enter "senescence", a phenomenon usually linked to the development of age-related pathologies (57). In this state microglia lose their ability to respond adequately to injury or external stimuli (a state similar to "ageing microglia"). Microglial senescence can contribute to the development of dystrophic microglia and this in turn contributes to the pathogenesis of neurodegenerative diseases. Selective removal of those cells has proved to successfully prevent age-related tissue deterioration and dysfunction (58).

1.2.6 Dark microglia

Dark microglia is a new microglial phenotype that was recently described (50, 59). Dark microglia exhibit signs of oxidative stress, mitochondrial dysfunction, and endoplasmic reticulum dilatation. This phenotype could be implicated in the loss of synapses, which correlates to several diseases of cognitive decline. Particularly, dark microglia are hyperactive cells that become stressed due to their hyperactivity, leading to dysregulated interactions with the synapses (60).

1.3 Microglia and Disease

Microglia play a critical role in many acute and chronic diseases such as stroke, neuropathic pain, traumatic brain injury, immunological diseases, neurological diseases and cancer. In the CNS, they have long been the center of attention due to their strong proliferative responses (microgliosis) and their distinct roles in determining progression of all CNS diseases (61).

1.3.1 Inflammation in Neurodegeneration

The immune system serves to protect from external and internal danger by using a network of immune sensors (62). The brain and the immune system were studied separately under the notion that these two systems are two isolated entities. Growing evidence though suggests that brain and immune system cooperate to maintain homeostasis (63).

The brain was considered for a long time an immune-privileged organ, where inflammation can occur only after breakdown of the BBB and infiltration of peripheral immune cells or through direct infection (64). It is well known now that there are cell types in the brain that can trigger inflammatory signaling pathways. Microglia are the major

cellular component of the innate immune system of the brain. They respond immediately in the presence of an internal danger or an injurious stimuli and initiate repair processes, thereby employing what is called an inflammatory response (65).

Under physiological conditions, once the infection has been eradicated or the damaged tissue has been repaired, microglia exhibit a deactivated phenotype and promote the production of anti-inflammatory and trophic factors (47, 66). However, in case that the trigger cannot be removed or the resolution mechanism fails, the immune response turn into chronic inflammation that cause neuronal dysfunction and cell death (65, 67, 68). Interaction between damaged neurons and over activated, dysregulated microglia create a vicious cycle of uncontrolled, prolonged inflammation (**Figure 5**) that results in the production of toxic factors, which amplify the underlying disease state (64, 69, 70).

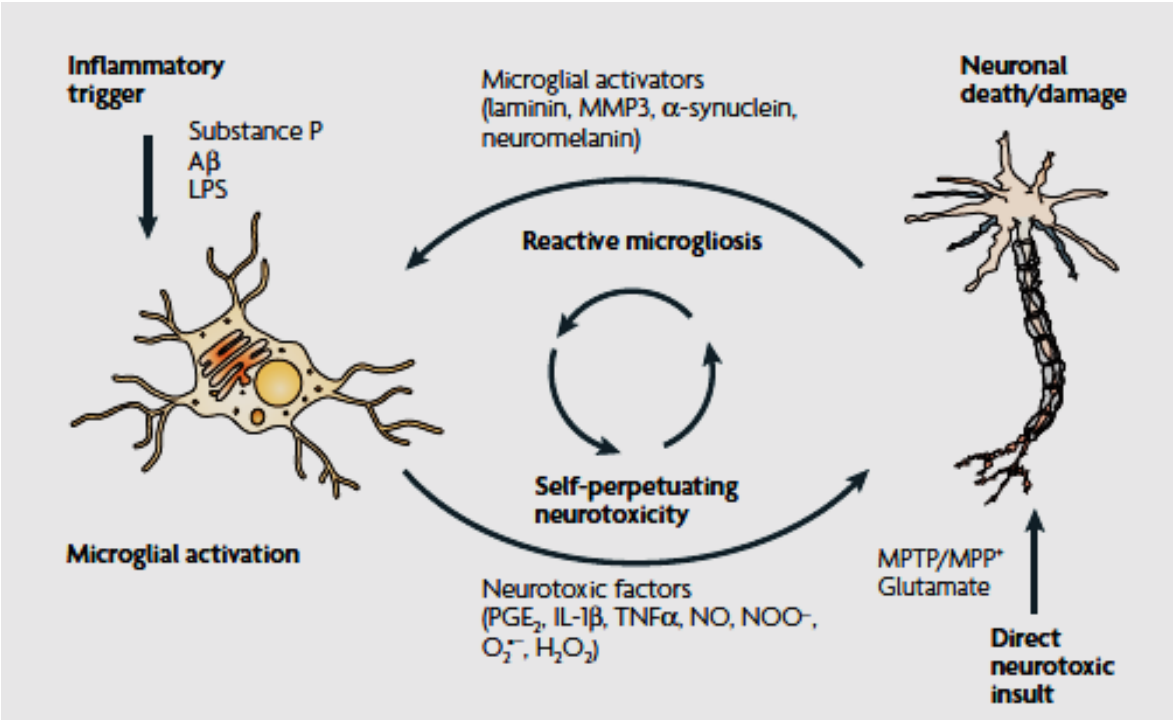

Figure 5. Reactive microgliosis during chronic neuroinflammation

Microglia can become over activated and induce neurotoxicity through two mechanisms. First, microglia can initiate neuronal damage by recognizing pro-inflammatory stimuli, such as lipopolysaccharide (LPS), becoming activated and producing neurotoxic pro-inflammatory factors. Second, microglia can become over activated in response to neuronal damage (reactive microgliosis), which is then toxic to neighboring neurons, resulting in a perpetuating neurotoxicity. Reactive microgliosis could be an underlying mechanism of progressive neuron damage across numerous neurodegenerative diseases, regardless of the initiating stimuli (70).

Neurodegenerative diseases are a group of chronic, progressive disorders that characterized by gradual loss of neurons in discrete areas of the CNS and lead to deficits in particular brain functions (67). Neuroinflammation is a feature shared by various neurodegenerative diseases and can have both detrimental and beneficial effects to neurons. It is still a topic of debate whether activated microglia exacerbate the pathology or aid in tissue repair and ameliorate the disease (71).

1.3.2 Microglia in Neurodegenerative Diseases

Each neurodegenerative disease has a disease-specific mechanism for induction of the inflammatory response (3, 64, 65). However, activation of the innate immune cells of the CNS is one of the common components that these diseases share. During the inflammatory process, microglia appear to be heterogeneous with diverse functional phenotypes, ranging from the pro-inflammatory M1 phenotype to immunosuppressive/anti-inflammatory M2 phenotype (72). They can exacerbate the disease process or promote neuronal survival depending on their activation profile, thus can influence disease progression (61).

In most of the cases, microglia are considered to become unable to perform some of their physiological processes, thus it was suggested that their deletion might be beneficial. The situation though is not clear-cut, since ablation of microglia couldn't block disease progression and in some cases even deteriorated disease pathology. Studies are currently performed in order to identify at which time point microglia become dysfunctional and if possible to find ways to manipulate microglia and change their current polarization state.

Below is briefly described how microglia respond and affect the most common neurodegenerative diseases.

Alzheimer's Disease (AD)

Alzheimer's disease is characterized by cognitive dysfunction and progressive memory decline. Histologically, AD is defined by parenchymal deposition of amyloid-β and the formation of neurofibrillary tangles (NFTs) that are composed of microtubule-associated protein tau (64, 73). Amyloid-β is constitutively generated from amyloid precursor protein (APP) (74); this overproduction can be caused by mutations in the genes encoding enzymes that contribute to the generation of the APP.

Neuroinflammation is an important contributor to Alzheimer's disease pathogenesis (27). Increased levels of pro-inflammatory mediators have been reported that impair microglial cell mediated clearance of amyloid-β and neuronal debris and induce NO production (75,

76). Aggregated amyloid-β also elicits an acute immune response by activating microglia via the cell surface receptor CD36, which subsequently triggers the formation of a TLR2–TLR6 heterodimer and results in augmented NF-κB signaling (77). CD33, a receptor that is expressed at the surface of myeloid cells and is involved in the inhibition of cellular responses, is highly upregulated in microglia and prevents cell-mediated clearance of amyloid-β (78). Moreover, a rare variant of the triggering receptor expressed on myeloid cells 2 (TREM2) in microglia has been associated with an increased risk for AD (79). Microglial driven neuroinflammation causes the formation of NFTs and their activation induces tau phosphorylation in primary mouse neurons (80).

Interestingly, it has been suggested that microglia initially have protective functions in the AD brain by phagocytizing Aβ. However, their chronic activation may lead to either loss and/or dysfunction, which can sustain a chronic inflammatory response (81).

Frontotemporal Dementia (FTD)

Frontotemporal Dementia is a form of progressive neuronal atrophy, characterized by the loss of cells from the frontal and temporal cortices (82).

Neuroinflammation is a major component of the disease, accompanied by increased microglial activation in the frontotemporal lobe of FTD patients (83). Mutations in the *GRN* gene that encodes the inflammation-related protein progranulin, lead to a tau-negative form of FTD (84). Progranulin-deficient microglia induce neuronal cell death and show a dysregulated inflammatory response that promotes the development of FTD (85).

Amylotrophic Lateral Sclerosis (ALS)

ALS is a fatal neurodegenerative disease, which primarily affects the upper and lower motor neurons. It causes corticospinal tract signs, atrophy of targeted muscles, and ultimately leads to complete paralysis (86, 87). Several pathological factors have been implicated in the pathogenesis of ALS. In most of the cases, ALS is caused by mutations in superoxide dismutase 1 (SOD1) (88, 89).

Microglia and astrocytes produce aggregates of mutant SOD1, which activate neighboring microglia by binding to TLR2, TLR4 and CD14, and subsequently promote neuronal cell death (90). Microglia appear to have impaired overall motility and reduced capacity to clear neuronal cell debris (91). They also release pro-inflammatory cytokines, ROS and RNS that may drive motor neuron damage. The extent of microglial activation positively correlated with the severity of clinical symptoms (92).

Parkinson's Disease (PD)

Parkinson's disease is characterized by the loss of dopaminergic neurons in the substantia nigra pars compacta within the mid-brain. This is associated with the activation of microglia and astrocytes (93, 94), increased cytokine levels (95), and the presence of intraneuronal aggregates (Lewy bodies) that mainly consist of α-synuclein.

Several polymorphisms in inflammatory genes (genes encoding TNF, TNFR1, IL-1β, IL-1 receptor antagonist, CD14 and, TREM2) have been associated with PD (96).

Microglia are activated by α-synuclein and this enhances neurotoxicity and induces the production of IL‑1β, superoxide and NO (97-99).

Huntington's Disease (HD)

Huntington's disease is an autosomal dominant neurodegenerative disease, caused by the expansion of a trinucleotide CAG (which codes for the amino acid glutamine) in the gene that encodes huntingtin (*HTT*). A mutant form of HTT (mHTT) contains a polyglutamine expansion at the amino terminus, which affects protein stability and leads to the formation of aggregates that adversely affect neuronal function (64). HD is characterized by the loss of medium spiny neurons within the striatum. Pathological iron accumulation in the striatum is a characteristic of HD. During early stages of the disease activated microglia contain ferritin, an iron-storage protein, which could reflect the attempt of microglia to dispose of the accumulating iron (100).

Generally, microglia induce an inflammatory response (101), increased levels of IL‑1β, and production of complement components (102, 103). Microglial cell migration and motility of cellular processes are compromised and increased microglial activation correlates with reduced neuronal activity (104, 105). Microglia may be altered by the expression of mHTT, are unable to perform neuroprotective functions, and induce neuronal cell death (106). Glutamate uptake, which is an important glial function that is involved in the control of excitotoxicity, is reduced and this probably contributes to neuronal dysfunction and death (107).

Multiple Sclerosis (MS)

Multiple sclerosis is a chronic inflammatory disease with an autoimmune component that leads to demyelination and progressive loss of functional neurons. Two phases can be recognized based on symptom progression: a *relapsing–remitting phase* in which damage

is associated with inflammatory infiltrates and a second *"progressive" phase* in which functional loss continues, sometimes without signs of inflammation (61).

Active lesions are associated with the presence of activated microglia (108). Prior to the development of severe symptoms and infiltration of peripheral immune cells, massive microgliosis is observed at lesion sites (109). Disruption of BBB plays a key role in activation of microglia through extravasation of serum components that have pro-inflammatory effects (110). Microglia attract inflammatory monocytes, express high levels of MHC-I and MHC-II against which T cells are capable of reacting, and this epitope spreading plays a role in exacerbating demyelination (111).

Whether microglia cause damage or actually limit disease progression, or perhaps both at different stages of the disease, is still unknown (112). Microglia have been also ascribed positive roles in experimental autoimmune encephalomyelitis (EAE), a murine model of MS, due to their ability to polarize to an M2 state in response to type-2 cytokines and remove myelin debris (113).

Other neurodegenerative diseases

Neuroinflammation is observed in the brains of patients who are affected by dementia with Lewy bodies (DLB), which is a neuropathology that shares disease characteristics with both AD and PD (114). Other neurodegenerative diseases, such as spinocerebellar ataxia type 3 (115), multiple system atrophy (93), and ataxia-telangiectasia (116), has not been yet profoundly studied. However, in all three cases there are evidences of elevated immune response in glial cells.

2. Lysophosphatidic Acid (LPA)

The brain is characterized by a high lipid context (117), which are important in cell signaling and tissue physiology (118) and divided into structural and signaling, and include well-known families such as cholesterol, sphingolipids, phospholipids as well as fatty acids, eicosanoids, endocannabinoids, and prostaglandins (119). Normal brain function depends on a balanced set of structurally diverse lipid species, which have structural as well as signaling roles. Structural lipids comprise cell membranes and their domain organized by proteins (120). Bioactive (signaling) lipids transmit their function through different receptors to activate downstream pathways (121). Lysophospholipids (LPs) are an important family of signaling lipid molecules, and lysophosphatidic acid (LPA) is a crucial subclass of this family (119).

2.1 Metabolism and Distribution

Lysophosphatidic acid (LPA) is a small glycerophospholipid (molecular mass: 430–480 Da) and is ubiquitously present in all examined tissues (122). It acts as an extracellular signaling molecule through at least six G protein-coupled receptors (GPCRs) in numerous processes (122). There is a range of structurally related LPA species present in various biological systems (123). An important aspect of LPA receptor biology is that different LPA species may activate different LPA receptor isoforms (124). All LPA species consist of a glycerol backbone connected to a phosphate head group and is linked to an acyl or alkyl residue of varied length and saturation (122). Thus, LPA does not refer to a single chemical entity but rather a family of structurally related forms (125). The various forms of LPA derive from many sources, such as membrane lipids (126). The term LPA (mono-acyl-sn-glycerol-3-phosphate) often refers to 18:1 oleoyl-LPA (1-acyl-2-hydroxy-sn-glycero-3-phosphate), and has a wide laboratory use (119).

There are two major synthetic pathways for LPA (122). In the first pathway, phospholipids (phosphatidylcholine, phosphatidylserine, or phosphatidylethanolamine) are converted to their corresponding lysophospholipids such as LPC, LPS, or LPE (122, 127). This occurs via phosphatidylserine-specific phospholipase A1 (PS-PLA1) or secretory phospholipase A2 (sPLA2) activity (122). Lysophospholipids are then converted to LPA via autotaxin (ATX) activity (**Figure 6**). In the second pathway, phosphatidic acid (PA) is produced from phospholipids (PLs) through phospholipase D activity or from diacylglycerol (DAG)

through diacylglycerol kinase (DGK) activity (122). Finally, PA is converted directly to LPA by the actions of either PLA1 or PLA2 (127).

Through a separate mechanism, LPA can be generated through the acylation of glycerol-3-phosphate by glycerophosphate acyltransferase and the phosphorylation of monoacylglycerol by monoacylglycerol kinase (122, 128) (**Figure 6**).

Several enzymes can degrade LPA, including three types of lipid phosphate phosphatases (LPPs) (129), LPA acyltransferase, and various phospholipases (e.g., PLA1 or PLA2) (122, 130). LPA can be converted back to PA by LPA acyltransferase, hydrolyzed by LPP (1–3), or converted by phospholipases into glycerol- 3-phosphate (122, 130).

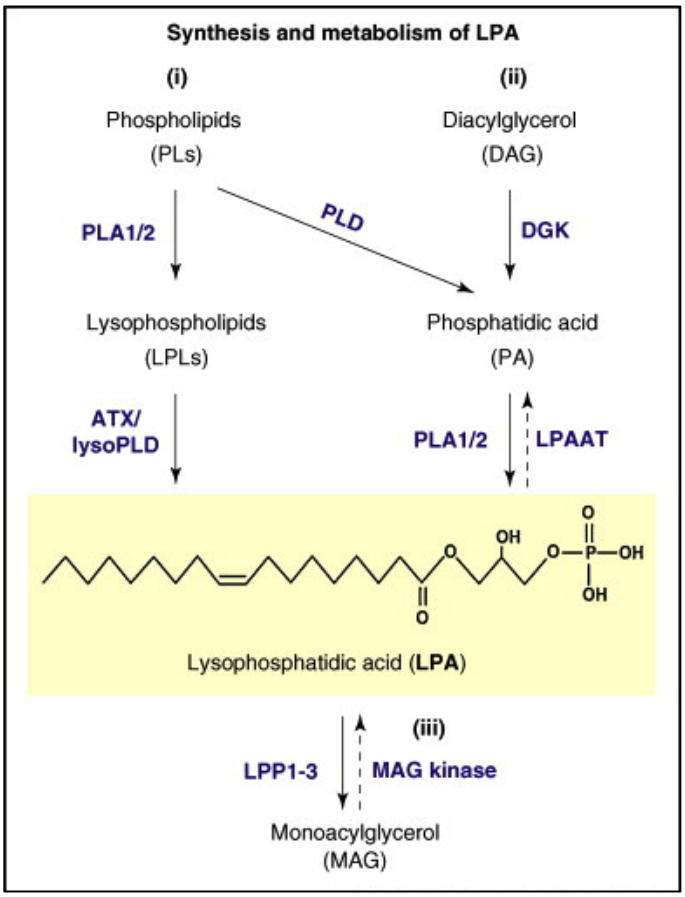

Figure 6. Two pathways of LPA production

(i) In the PLA1/2-ATX pathway, lysophospholipids (LPLs) generated by phospholipase A1 (PLA1) or PLA2 reaction are subsequently converted to LPA by ATX/lysophospholipase D (lysoPLD) reaction (127) (extracellular pathway).

(ii) In the PLD-PLA1/2 pathway, phosphatidic acid (PA) generated by phospholipase D (PLD) or diacylglycerol kinase (DGK) reaction is subsequently converted to LPA by PLA1 or PLA2 reaction (127) (intracellular pathway).

LPA can be generated from membrane phospholipids in both intracellular and extracellular ways (122, 130). *Intracellular LPA* is an intermediate for the de novo biosynthesis of complex glycerolipids, including mono-, di-, and triglycerides, as well as phospholipids (122, 130). *Extracellular LPA* mediates bioactive effects through the different LPA receptors (122, 131). Furthermore, it has been reported that LPA might be a ligand for the intracellular transcription factor PPARγ, and have an important regulatory role (132, 133).

As mentioned above, LPA has been found in all examined eukaryotic tissues. LPA is present in blood, where it ranges from 0.1 μM in plasma to 10 μM in serum (119), which is much over the apparent nanomolar Kd of LPAR1–6 (122, 134-136). The 18:2, 20:4, 16:1, 16:0, and 18:1 LPA forms are specifically abundant in plasma (122, 137). Except for blood, LPA has been quantified in a variety of species, tissues, and fluids (138-141). There are various methods to detect LPA including enzymatic assays (135), TLC-GC, LC-MS, and LC-MS/MS (142-145).

2.2 Autotaxin (ATX)

ATX or ectonucleotide pyrophosphatase/ phosphodiesterase family member 2 (*Enpp2*) is a secreted lysophospholipase D (lysoPLD), which hydrolyzes extracellular LPLs into LPA (146, 147). ATX was first identified as an "autocrine motility factor" from human melanoma cells and is one of the best-studied enzymes associated with LPA signaling (122). Although ATX is classified as a phospholipase D, it is distinct from classical PLDs. It doesn't possess homology to previously characterized phospholipases, as it lacks the HKD motifs, which form the catalytic center of PLDs (131). Also, it doesn't hydrolyze phosphatidylcholine (PC) with two long acyl chains and is selective for lysophospholipids (138, 148).

ATX has three splicing isoforms, ATX-β, -α and –γ (146, 149). ATX-β is abundantly expressed in plasma, melanoma cells secrete ATX-α, and ATX-γ (PD-1a) is mainly expressed in brain.

ATX is abundant in blood yet its origin is unknown. ATX is broadly expressed, but relatively high levels of ATX are detected in brain, kidney and lymphoid organs (122). In brain, ATX is highly expressed in the choroid plexus, which explains the high ATX levels found in cerebrospinal fluid (150). High levels of ATX are also found in lymph nodes, especially at the high endothelial venules (HEVs) (151, 152).

Genetic deletion of ATX in mice (Enpp2-/-) has contributed significantly in understanding this enzyme's physiological role (122). ATX is a vital enzyme for early embryological and vascular development. ATX knockout (KO) (Enpp2-/-) embryos die *in utero* at day 9.5 with vascular and neural tube defects (153-155). Malformations in the allantois, neural tube and headfold are detected by day 8.5, and by day 10.5 embryos become necrotic (156). Enpp2-/- embryos have increased expression of VEGF mRNA, consistent with hypoxic conditions in the absence of a functional vascular system (157).

ATX regulates oligodendrocyte differentiation (158) and the correct left–right asymmetry for normal organ morphogenesis through Wnt-dependent pathways (159). Enpp2+/- mice are viable, and express both half the levels of ATX and LPA compared to normal mice. However, they are hyper-responsive to hypoxia-induced vasoconstriction and remodeling and they develop pulmonary hypertension (160).

High ATX mRNA is found in adult neuronal tissues (161), which depicts the importance of this enzyme to proper neuronal function. ATX mRNA levels are also high in adipose tissues (162). The most important role of ATX after birth is probably in wound healing and tissue remodeling. LPA is a potent activator of platelet aggregation and it stimulates the growth and migration of fibroblasts, vascular smooth muscle cells, endothelial cells and keratinocytes (163). ATX expression is also upregulated in microglia in response to oxidative stress and this way protects microglia cells against damage from H_2O_2 (164). In order to maintain immune homeostasis, ATX mediates lymphocyte extravasation and T cell migration (165-167).

2.3 Signaling through LPARs

Currently there are six LPARs: protein names LPAR1–LPAR6 with gene names LPAR1-LPAR6 (human) and Lpar1-Lpar6 (non-human) (119, 122, 168). These 7-transmembrane GPCRs activate heterotrimeric G proteins defined in part by their Gα subunits ($G_{12/13}$, $G_{q/11}$, $G_{i/o}$, and G_s) to initiate various signaling cascades (122) (**Figure 7**). LPARs are expressed in varying spatiotemporal patterns from fetal through mature life and LPA signaling drives diverse physiological and pathophysiological processes (119, 122). The various physiological and pathophysiological roles of LPA signaling are presented in detail in appendix II.

2.3.1 LPAR1

LPAR1 was the first receptor identified (169) and is the most studied of the six LPA receptors (122). The LPAR1 gene (human chromosome locus 9q31.3) encodes a 41 kDa protein containing 364 amino acids with 7-TM domains (122). In mice, the Lpar1 gene (mouse chromosome locus 4, 32.2 cM) encodes five exons with a conserved intron (shared among Lpar1–3) interrupting TM domain 6 (122). LPAR1 shares with LPAR2 and LPAR3 approximately 50–60% amino acid sequence identity.

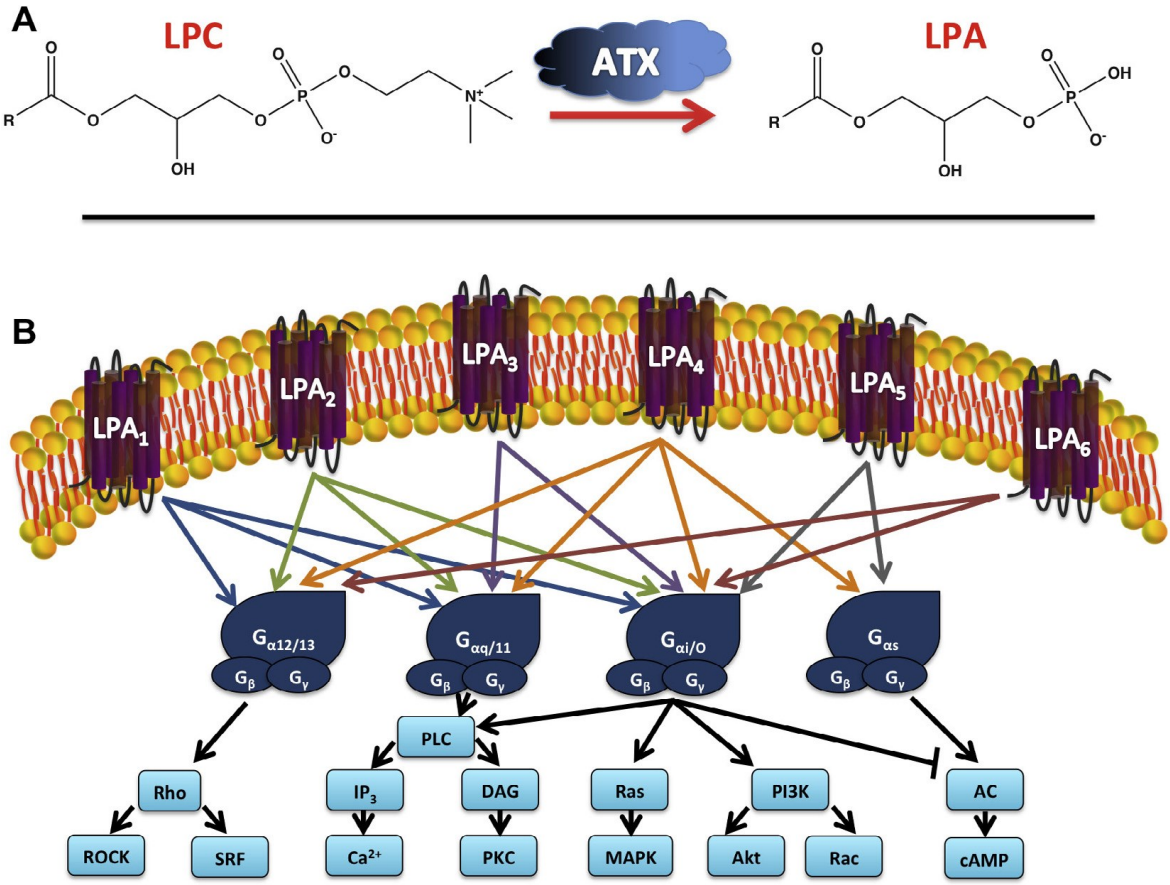

Figure 7. Overview of ATX/LPA signaling

(A) LPA is produced extracellular from lysophosphatidylcholine (LPC) via ATX catalytic activity.

(B) LPA signals through at least six G-protein coupled receptors (GPCR) to elicit a wide range of cellular responses. Signaling through some of these receptors may be antagonistic; depending on which heterotrimeric G-protein is coupled to the LPA receptor (170).

Mutagenesis studies have identified three important residues in LPAR1–3 signaling. R3.28A and K7.36A are important for the efficacy and potency of LPA, while Q3.29A decreases ligand interaction and activation (122, 171).

LPAR1 couples with three types of G_α proteins: $G_{i/o}$, $G_{q/11}$, and $G_{12/13}$ that initiate downstream signaling cascades though PLC, MAPK, Akt, and Rho. LPAR1 activation is responsible for a range of cellular responses (122), including cell proliferation and survival, cell-cell interactions, cell migration and cytoskeletal changes, Ca2+ mobilization, and adenylyl cyclase inhibition (172, 173). Lpar1/LPAR1 is widely expressed in both adult mice and humans, including the brain, uterus, testis, lung, small intestine, heart, stomach, kidney, spleen, thymus, placenta, and skeletal muscle (122, 173, 174). During development, Lpar1 expression is restricted, including parts of the brain, dorsal olfactory bulb, limb buds, craniofacial region, somites and genital tubercle (175, 176).

Phenotypically, Lpar1-/- mouse litters have 50% lethality (122) due to impaired suckling behavior (176), and defective olfaction. Surviving Lpar1-/- mice have a significantly reduced body size, craniofacial dysmorphism, and increased apoptosis in sciatic nerve Schwann cells (SCs) (122, 176).

2.3.2 LPAR2

LPAR2 shows 55% amino acid similarity to LPAR1 (122). LPAR2 (human chromosome 19p12) encodes a 39.1 kDa protein containing 351 amino acids (177), while mouse Lpar2 (mouse chromosome 8, 33.91 cM) encodes for a 38.9 kDa protein with 348 amino acids (122). Mutagenesis studies of LPAR2 have found two key residues (Q3.29E and R5.38A) that, when altered, decrease LPAR2 activation (122, 171).

LPAR2 couples with the $G_{i/o}$, $G_{q/11}$, and $G_{12/13}$ proteins, and initiate downstream signaling pathways through molecules such as Ras, Rac, PI3K, MAPK, PLC, DAG, and Rho (122). LPAR2 activation is associated with cell survival and migration (178). Compared to Lpar1 /LPAR1, Lpar2 /LPAR2 expression is more restricted in adult mice and humans (122), with high LPAR2 in leukocytes and the testis, and Lpar2 in the kidney, uterus, and testis (173). During development, Lpar2 expression is observed in the embryonic brain, limb buds, craniofacial region, and Rathke's pouch (179, 180).

Phenotypically, Lpar2-/- mice appear normal, with normal prenatal and postnatal viability (181). Like LPAR1, LPAR2 is involved in numerous aspects of nervous system function and development and signaling is important for immune system function as well (122). Lpar1-/- /Lpar2-/- mice have also been generated. Such mutants have body size reduction, craniofacial dysmorphism, and 50% perinatal lethality, and also exhibit an increased

incidence of frontal hematomas (122). Studies with these mice uncovered the importance of LPAR1 and LPAR2 signaling in distinct neural and vascular phenotypes (182, 183).

2.3.3 LPAR3

LPAR3/ Lpar3 (human chromosomal locus 1p22.3; mouse chromosome locus 3, 71.03 cM) encodes a 353 amino acid protein with a molecular mass of 40 kDa (122) that, in both humans and mice, is around 50% identical to LPAR1/Lpar1 and LPAR2/Lpar2 (184, 185). Mutagenesis studies identified two residues involved in LPAR3 activation (W4.64A and R5.38N), as well as a residue that increased the EC50 of LPAR3 by a factor of 10 (K7.35A) (122, 171).

LPAR3 couples with $G_{i/o}$ and $G_{q/11}$ to initiate LPA induced Ca2+ mobilization, adenylyl cyclase inhibition and activation, PLC activation, and MAPK activation (185, 186). LPAR3 has been reported to prefer 2-acyl-LPA containing unsaturated fatty acids (122, 187). In adults, LPAR3 /Lpar3 expression is most prominent in the human heart, testis, prostate, and pancreas (184), and in mouse lung, kidney, uterus, and testis (122). Lower LPAR3 /Lpar3 expression observed in the human lung, ovary, and brain, as well as mouse small intestine, brain, heart, stomach, placenta, spleen, and thymus (185). During development, Lpar3 expression observed in the heart, mesonephros, and in three spots in the otic vesicle (122, 175).

Lpar3-/- mice are viable and appear normal, with no reported neural deficits, even though this receptor is found in the frontal cortex, hippocampus, and amygdala (122, 184). LPAR3 appears to be involved in determining vertebrate left-right patterning during embryogenesis, a crucial process for proper organ formation and function (122, 159).

2.3.4 LPAR4

LPAR4 shows a dissimilar amino acid sequence from the LPAR1–3. It shares only 20% homology with LPAR1 (185) and slightly greater homology to the other LPA receptors (188). LPAR4 was previously known as the orphan GPCR P2Y9 (122), and is more closely related to P2Y purinergic receptors (185). LPAR4 /Lpar4 (human chromosome Xq21.1, mouse chromosome X region D) encodes a 370 amino acid protein with molecular mass of 41.9 kDa (122).

LPAR4 couples with $G_{12/13}$, $G_{q/11}$, $G_{i/o}$, and G_s proteins (189). This receptor induces neurite retraction and stress fiber formation through $G_{12/13}$ and subsequent Rho/ROCK pathway activation (122, 189, 190). It facilitates both ROCK-dependent cell aggregation and N-

cadherin-dependent cell adhesion (190), induces intracellular cAMP accumulation through G_s activation and influences the differentiation of immortalized hippocampal progenitor cells (191). Interestingly, LPA-induced cell migration is inhibited by activation of LPAR4 (192). In adults, LPAR4 is prominently found in the human ovary, while less prominent expression observed in the thymus, pancreas, brain, heart, small intestine, testis, prostate, colon, and spleen. Lpar4 is present in mouse heart, ovary, skin, thymus, and bone marrow (185). During development, Lpar4 is found in the mouse embryonic brain, brachial arches, limb buds, maxillary processes, liver, and somites (122, 175).

Lpar4-/- mice appear normal but exhibit increased bone volume, number, and thickness (185), suggesting that LPAR4 negatively regulates osteogenesis (193). During embryonic development, there is decreased prenatal survival for Lpar4-/- mutants (122). Phenotypes in these mice include pericardial effusions, edema and hemorrhage, abnormally dilated blood and lymphatic vessels, and impaired pericyte recruitment (194). This indicates important roles for LPAR4 in circulatory and lymphatic system development (122).

2.3.5 LPAR5

LPAR5 identification has led to the deorphanization of GPR92 (195). LPAR5 shares 35% homology with LPAR4, however only 22% homology to LPAR1–3 (122, 196). LPAR5 /Lpar5 (human chromosome 12p13.31; mouse chromosome 6, 59.21 cM) encodes a 372 amino acid protein (122). Mutagenesis studies revealed that several residues are involved in the binding of LPA to LPAR5, including one mutant that abolished receptor activation (R2.60N) and three other mutants that significantly reduced receptor activation (H4.64E, R6.62A, and R7.32A) (122, 197).

LPAR5 couples to $G_{12/13}$ and $G_{q/11}$ (122). Signaling through the $G_{12/13}$ pathway induces neurite retraction, stress fiber formation, and receptor internalization in vitro, while activation of G_q increases intracellular calcium levels and induce cAMP accumulation (185, 196). In melanoma cells, LPAR5 signaling acts as a chemo repellent pathway by inhibiting migration and the cAMP-protein kinase A pathway (122). Moreover, LPAR5 has demonstrated a 10-fold preference for alkyl, rather than acyl, 18:1 LPA (122, 198).

LPAR5 is highly expressed in spleen, and to a lesser extent in heart, small intestine, placenta, colon, and liver (122). Lpar5 in murine tissues is broadly expressed in small intestine, and more moderately in lung, heart, stomach, colon, spleen, thymus, skin, liver, platelets, mast cells, gastrointestinal lymphocytes, and dorsal root ganglia (122, 199, 200).

During development, Lpar5 was found in the early embryonic mouse forebrain, midbrain, and hindbrain. This expression pattern becomes more ubiquitous from E9.5–E12.5, showing diffuse patterns in the developing brain and choroid plexus (122). This suggests a possible role for LPAR5 in brain development (175).

2.3.6 LPAR6

The most recently identified receptor is LPAR6. In 1993, the 6H1 receptor was isolated from a chicken T cell library (201) and then renamed to p2y5 due to sequence homology with P2Y receptors (202). The p2y5 has been reclassified as an LPA receptor (203) and renamed LPAR6 (122). LPAR6 appears to show preference to 2-acyl- than 1-acyl-LPA.

Recent studies indicated multiple effects for LPAR6, including cAMP accumulation, Rho-dependent changes in cell morphology, [^{3}H] LPA binding, and [^{35}S] guanosine 5′ -3-O -(thio) triphosphate binding (122, 204). When LPAR6 was co expressed with a G_{α} protein, LPAR6 signaling resulted in increased intracellular Ca2+, reduced forskolin-stimulated [$cAMP_i$], and ERK1/2 activation (122, 205).

Interestingly, many of the performed assays require surprisingly high concentrations of LPA (up to 10 μM) to show an effect, compared with the nanomolar concentrations needed for activating LPAR1–5 (122). Genetic studies indicated a role for LPAR6 in hypotrichosis simplex (122), a complex of diseases involving familial hair loss (203) and several recent studies have identified LPAR6 mutations in hypotrichosis patients (206, 207).

2.4 LPA in Nervous System

In the CNS, LPA is found in the embryonic brain, choroid plexus, meninges, neural tube, blood vessels, spinal cord, and cerebrospinal fluid (CSF) at low nanomolar to micromolar concentrations (119).

Many roles for LPA signaling have been elucidated, including effects on neuroprogenitor cell (NPC) function (208), myelination (209), synaptic transmission (210), and brain immune responses (211), which influence neural development, function, and behavior (119) (**Figure 8**). In addition, LPA signaling is important in neurovascular and endothelial cell function (212). Below I will briefly review the importance and functions of LPA signaling in the nervous system.

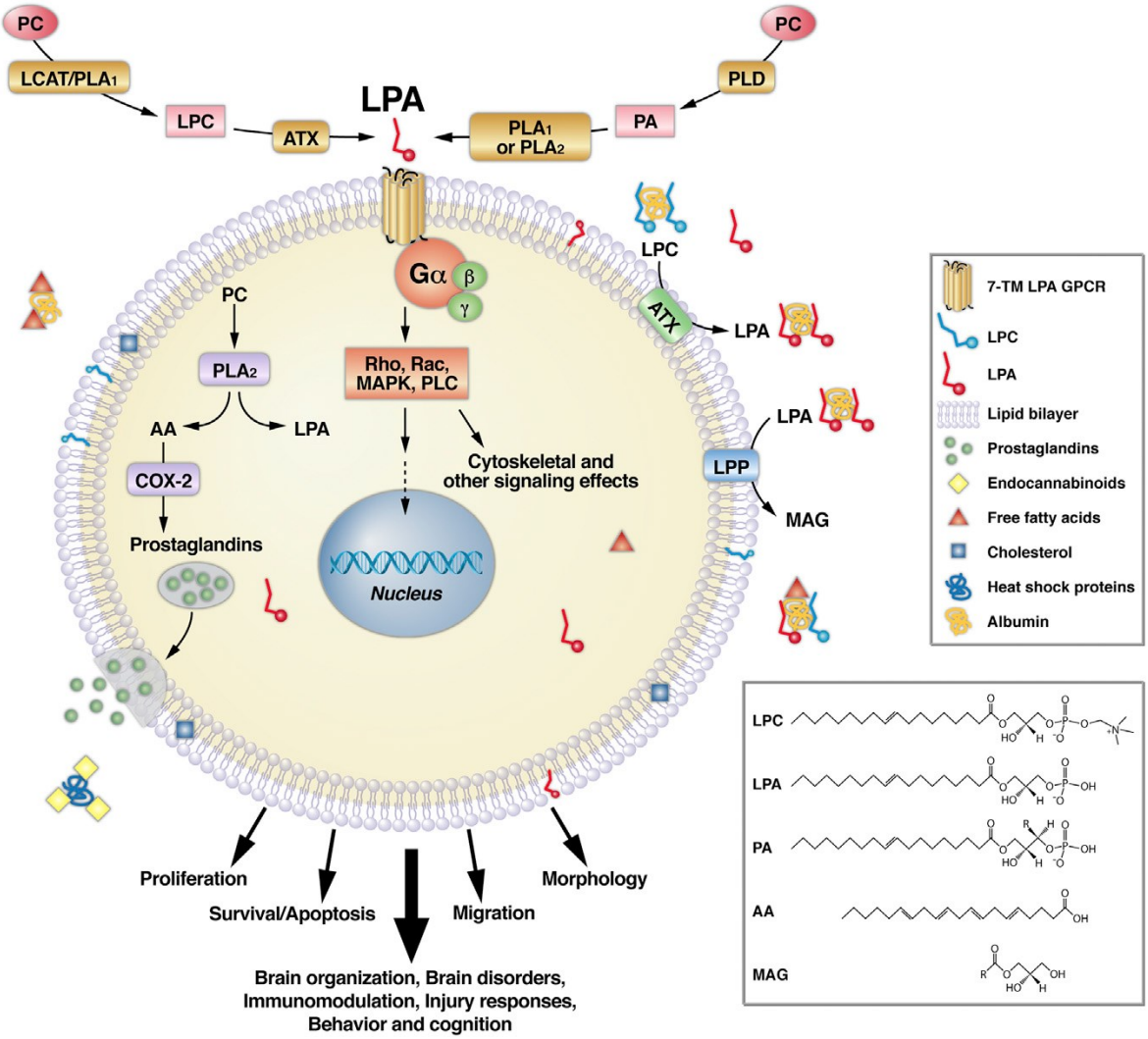

Figure 8. LPA Signals through Defined GPCRs within the Nervous System

Lipids are highly produced in CNS where they have different structural, energetic, and bioactive signaling properties. Signaling lipids are often bound to carrier proteins such as albumin or heat shock proteins (119).

LPA activates members of a family of G protein-coupled receptors (GPCRs) and influences multiple cellular processes including proliferation, survival, apoptosis, morphological change, and migration, as well as the production of other lipids such as prostaglandins through arachidonic acid (AA) conversion by cyclooxygenase-2 (COX-2).

The synthetic pathways for LPA have already been discussed in 2.1

The nervous system is a major locus of LPA receptor expression, and LPA exists in the brain at relatively high concentrations (143, 185). The restricted expression of LPAR1 within the proliferative cortical VZ of the embryonic brain (169, 213) indicated an important role for LPA signaling in the development of VZ cells. LPA receptors are expressed in most cell types of the nervous system, including neural progenitors, primary

neurons, astrocytes, microglia, oligodendrocytes, and Schwann cells (185). Studies have revealed that LPA signaling influences several developmental processes within the nervous system, including cortical development and function (214, 215), growth and folding of the cerebral cortex (182), growth cone and process retraction (216, 217), survival (182), migration (218), adhesion (219), and proliferation (182). In addition, LPA signaling may be involved in many neurological disorders (119, 176, 215, 220).

2.4.1 Neuroprogenitor Cells

LPA signaling has significant influence on *neuroprogenitor cells (NPCs)*. LPA affects cellular morphology, proliferation and differentiation of primary NPCs (185), and neurosphere cultures (221) via LPAR1 and differentiation of immortalized hippocampal progenitor cells via LPAR4 (191). LPA signaling also has impact on the morphology of NPCs, such as induction of neurite retraction and compaction in the VZ (217).

There are studies that provide evidence for a significant role of LPA signaling in controlling the organization of the ***developing cortex*** (182). Recently, the characterization of a Lpar1-/- variant revealed new in vivo roles for LPAR1. The Malaga variant demonstrated that LPAR1 deficiency resulted in defects in cortical development (185), including reduced proliferative populations and increased cortical apoptosis (214), with similar effects on hippocampal neurogenesis (222).

2.4.2 Neurons

Many studies have unraveled the effects of LPA on *neurons*. In embryonic murine cortical neurons, LPA signaling inhibits migration by inducing neurite retraction and growth cone collapse (185, 218). LPA-mediated morphological changes are present even in neurons derived from Lpar1-/- animals (218), so it is likely that these effects are mediated by other LPARs. Additionally, LPA signaling has been reported to influence survival (223), synapse formation (224), and synaptic transmission (210) of post mitotic neurons, indicating possible roles of LPA signaling in learning and memory (185).

2.4.3 Astrocytes

Astrocytes are the most abundant glial cell type and play an important role in many neurodevelopmental and neurodegenerative processes (185). In vivo, they appear to express mainly LPAR1, whereas in culture LPAR1-5 were identified (119). During development, LPA signaling in astrocytes results in generation of ROS and actin cytoskeletal rearrangement (225). A study using LPAR1-null astrocytes identified the

involvement of this receptor in LPA-mediated astrocyte proliferation (226). LPA signaling also regulates morphological changes of astrocytes via the Rho-cAMP pathway and stabilization of stress fibers (227). In vivo LPA injection into the striatum resulted in astrogliosis (228), although the receptors that mediate this response have not been identified (probably Lpar1-3).

2.4.4 Microglia

Microglia are the CNS resident macrophages and have a variety of functions in the inflammation challenged nervous system (185). LPARs expression (211, 229, 230), and LPA-dependant signaling cascades impact microglia functions, including proliferation, cell membrane hyperpolarization, enhanced chemokinesis, membrane ruffling, and growth factor upregulation (211, 231, 232). LPAR responses probably vary with microglia maturation and activation state. It is interesting that LPAR3 is upregulated in lipopolysaccharide-stimulated microglia (229), suggesting a role for LPA signaling in activated microglia during neuroinflammation. Other important functions, especially those that are of potential relevance to pathophysiological conditions, remain to be identified in future studies.

2.4.5 Oligodendrocytes

Oligodendrocytes, the myelin-forming glial cells in the CNS, express LPAR1 and LPAR3 during differentiation (233-235). Lpar1 gene expression pattern was spatially and temporally correlated with oligodendrocytes maturation and myelination (236). Recently, an in vitro study revealed that LPA has positive effect on process formation and myelin protein production as they switch from premyelinating to myelinating forms (237).

2.4.6 Schwann Cells

Schwann cells (SCs) are the myelinating cells of the peripheral nervous system (185). SCs express LPAR1 and LPAR2 (219, 238), activation of which is known to affect processes associated with myelination. LPA induced SC survival in vivo, as mice deficient for LPAR1 showed increased apoptosis of SCs in the sciatic nerves (176). In addition to promote survival, LPAR2 signaling may contribute to SC differentiation (239). LPA also induced dynamic regulation of the actin cytoskeleton and cellular adhesion (219), which suggests a key role for LPA signaling in SC motility and myelination. In addition to this, evidence suggests a potential role for LPA signaling in remyelination after neuropathic pain (220) and nerve transection where LPAR1 and LPAR2 are upregulated (240).

2.5 LPA in Disease

Aberrant LPA signaling may contribute to a range of diseases, including neuropathic pain, neurodevelopmental and neuropsychiatric disorders, cardiovascular disease, bone disorders, fibrosis, cancer, infertility, and obesity (122). Due to the nature of this study, I will briefly describe the role of LPA only in neurological diseases and inflammation.

2.5.1 Neurological Disorders

CNS Injury

Beyond development and normal function of the nervous system, LPAR signaling is also important during CNS stress or damage (119). During injury, LPA concentrations in brain and CSF are significantly elevated (241) and can reach thousands of times the apparent Kd of LPA receptors (119, 208). After traumatic injury, Lpar1 expression is increased in reactive murine spinal cord astrocytes, and Lpar3 in cortical and spinal cord neurons (241). Moreover, high ATX levels are reported in white matter adjacent to injury lesions in the rat cortex (242), suggesting possible aberrant LPA signaling.

Alzheimer's Disease (AD)

One of the main pathologies in AD is the abundance of senile plaques and tangles composed of beta-amyloid (Aβ) and tau aggregates (119). Increased ATX expression found in the frontal cortex of Alzheimer's patients (243) suggests that altered LPAR signaling might contribute to the pathology of the disease (119). LPA increases β-secretase activity, leading to elevated Aβ production (244), and enhances pathogenic tau phosphorylation, leading to GSK3-mediated growth cone collapse in neurons (245).

Gintonin is a bioactive fraction isolated from ginseng and composed of protein-bound LPA that can activate LPAR1-5. Treatment of transgenic mouse AD models with gintonin has been reported to improve cognition in AD, attenuate amyloid plaque deposition and prevent long-term memory impairment (246).

Nerve Injury and Pain

LPA signaling through different LPARs is involved in nerve injury and pain responses (119, 247). Intrathecal LPA injection initiates neuropathic pain in mice (220), while synthesis of LPA through ATX and PLA2 mediate the initial phases of pain (140). Using Rho pathway inhibitors, allodynia and demyelination are reduced, implicating LPAR1-mediated Rho activation (220). Lipids, including LPA, can indirectly activate or sensitize

nociceptors by interacting with TRP or sodium channel families, or by recruiting immune cells to the site of inflammation (119).

Brain Cancer

LPA signaling may be relevant to cancer by promoting tumor growth, neovascularization, survival, and metastasis (119, 248). Aberrant LPAR expression and signaling have been reported in CNS glioblastomas and neuroblastomas (119, 249). Moreover, in malignant glioblastoma multiforme (GBM), ATX and LPAR1 are overexpressed (250).

Dysregulated Rho and Rac signaling correlates with neural tumor proliferation and invasiveness (119, 251). Downstream Rho/ROCK activation through LPAR1 and LPAR2 signaling promotes stress fiber formation, cytoskeletal rearrangement, and cell migration in GBM cells (252). LPA-induced migration mechanisms may also involve Ras-MAP kinase signaling and matrix metalloproteinases (119, 253). Inhibition of ROCK activation in LPAR-expressing tumor cells reported to abrogate motility and invasion (254).

Hypoxia

Ischemia is a major cause of hypoxia, which results in decreased synaptic transmission, inflammation, and neuronal death (119, 255). LPAR1 signaling has been connected to hypoxia through several mechanisms. It has been reported that hypoxia enhances LPA-induced hypoxia inducible factor-1 alpha (HIF-1α) expression in cancer cells and VEGF expression in the vasculature (256, 257). Hypoxia can also alter brain development and result in neurological disability or psychiatric disease (119, 258). Stroke or trauma may cause hypoxia in postnatal brains (255). Under hypoxic conditions, increased LPA signaling promotes retinal cell survival through upregulation of Lpar1 and Lpar2 expression in ganglion cells and the inner retinal layers (119, 259).

Neuropsychiatric Disorders

Lpar1 null mice display numerous negative behavioral signs and cognitive deficits, suggesting that LPAR1 signaling is essential in normal cognition (119). Neonatal Lpar1 null mice display problems in olfaction related to suckling, and pronounced craniofacial dysmorphism (119, 176), a trait that commonly observed in autism (260).

LPA signaling has also been linked to many molecular and neurotransmitter pathways involved in both genetic and environmental risk factors for neuropsychiatric disorders (119). Many environmental risk factors for neuropsychiatric diseases, such as bleeding,

infection, and hypoxia, can over activate LPA signaling (258). Additionally, cortical LPA administration reported to induce increased anxiety, and depression-associated immobility in adult mice (119, 261).

Hydrocephalus

Several neurological disorders are strongly correlated with a preceding hemorrhagic event during development, possibly resulting in enhanced LPA signaling through blood exposure (119). Fetal hydrocephalus, which is one of the most common neurological diseases of perinatal life, has been linked to aberrant LPA signaling in an embryonic mouse model of disease (208).

2.5.2 Inflammation and autoimmunity

ATX/LPA signaling is implicated in many inflammatory diseases (170, 262, 263). When the acute inflammation become chronic, ATX/LPA signaling fuels additional cytokine production and recruitment into the local tissue environment, which can aggravate the course of disease (170, 264, 265). LPA is a potent mediator of the immune response and can contribute to improper immune activation (122), up regulating the production of several inflammatory cytokines such as IL-2 and IL-6 (185). LPAR1 and LPAR2 signaling can activate microglial cells in the brain, triggering immune invasion. LPA has been also linked to several inflammatory and autoimmune disorders, including systemic sclerosis, asthma, and arthritis (122).

Abnormally high levels of LPA have been detected in fibroblasts from systemic sclerosis patients (266), and the bronchoalveolar fluids of allergen-provoked asthmatic patients showed an increase in ATX levels and LPA concentrations (267). The blockade of ATX activity and LPAR2 expression in a mouse model of allergic asthma attenuated the Th2 cytokines and allergic lung inflammation (122, 267).

Increased ATX concentrations have been identified in synovial fluid of rheumatoid arthritis patients, and elevated cytokine production was found in patient fibroblast-like synoviocytes treated with LPA (122, 268). Studies have also demonstrated that LPA signaling through LPAR1 contributes to the development of rheumatoid arthritis via cellular infiltration (269), underlining the effect of LPA on inflammation and immune regulation (122). Moreover, functional single-nucleotide polymorphism in the promoter region of LPAR1 increased susceptibility to knee osteoarthritis (122), possibly through LPAR1 upregulation (270).

3. Hypothesis and Objectives

Extrinsic signals determine whether microglia acquire - depending on disease context - a beneficial or detrimental phenotype. Their crucial role in brain homeostasis makes these cells potential therapeutic targets, which necessitate a thorough understanding of polarization cascades, and pathways that modulate their function.

There is growing appreciation that many human disease mechanisms are linked to altered LPA signaling. LPA is a mixture of saturated or unsaturated acyl/alkyl residues esterified at the sn-1 or sn-2 position that are present in biological fluids including CSF. The majority of LPA is produced through autotaxin (ATX)-dependent cleavage of lysophosphatidylcholine and LPA signaling is mediated via six LPA receptors (LPAR1-6) that are all expressed in the brain.

LPA has diverse biological functions mediated by downstream signaling through the different receptors. These receptors play prominent role in the central nervous system, and signaling is amplified at sites of inflammation where LPA concentrations are increased.

The main hypothesis of the present study is that inflammatory levels of LPA can induce changes in microglia biology and function.

To pursue this hypothesis an experimental plan was set up in order to:

- Study the impact of increased LPA levels on microglia morphology and cytoskeletal alteration
- Unravel the effect of LPA on microglial migration and get insights into potential underlying mediators
- Examine how LPA affects the inflammatory response of microglia cells, e.g. microglial polarization, phagocytosis and neurotoxicity
- Which inflammatory mediators are secreted after exposure of microglia to increased LPA concentrations
- Clarify which LPA receptors and which signaling pathways are responsible for these phenotypic changes

1. Materials

Complete lists of all the materials, reagents, antibodies, and primers that have been used during the study are presented in the appendix I.

2. Methods

2.1 Cell cultures

2.1.1 BV-2 microglia culture

The murine microglial cell line BV-2 was from Banca Biologica e Cell Factory (Genova, Italy). Cells were grown and maintained in RPMI1640 medium supplemented with 10% FCS, 100 U/ml penicillin, 100 mg/ml streptomycin, and 5 ml L-glutamine (100 mM) at 37°C in a humified incubator under 5% CO_2 and 95% air. The culture medium was changed to fresh medium every two or three days. When cells reached confluence, they were splitted into new flasks or used immediately for the experiments (1).

2.1.2 Primary microglia culture

PMM were isolated and purified from the cortices of neonatal (P0-P4) mice as previously described (1, 271). In brief, the brain cortices were isolated from the whole brain, stripped from their meninges and minced with scissors into small pieces. Glial cells were separated by trypsinization (0.1% trypsin, 20 min, 37°C/5%CO_2) and the cell suspension was cultured in 75 cm^2 tissue culture flasks precoated with 5 mg/ml poly-D-lysine (PDL) in DMEM containing 15% FCS, 100 U/ml penicillin, 100 mg/ml streptomycin, and 5 ml L-glutamine. After 3 days in culture, the medium was changed to fresh DMEM containing 10% FCS and the cells were cultured for another 10 to 14 days. Microglia were removed from the mixed glial cell cultures by smacking the culture flasks 10-20 times and seeded onto PDL precoated cell culture plates for future use. The purity of primary murine microglia was determined by immunocytochemistry using CD11b immunostaining or tomato lectin staining and was > 95%.

2.1.3 CATHa neurons culture

The murine neuronal cell line CATH.a was from ATCC Cells were grown and maintained in RPMI1640 medium supplemented 10% horse serum, 5% FCS, 1% penicillin-streptomycin, 0,4 % HEPES, and 0,2% sodium pyruvate at 37°C in a humified incubator under 5% CO_2 and 95% air. The culture was maintained by transferring floating cells to additional flasks. When cells reached confluence, they were splitted into new flasks (subcultivation ratio of 1:4) using 0.12% trypsin without EDTA or used immediately for the experiments.

2.2 Animals

Primary microglia cultures were prepared from pooled male and female C57BL/6 mice. Mice were housed under the 12/12 h light–dark cycle in the specific pathogen-free animal facility. All animal care and procedures were followed and approved by the Medical University of Graz Animal Care and Use Committee.

2.3 Cell treatments

2.3.1 LPA treatment

Cells were plated in 6, 12 or 24-well plates (PDL-coated in case of primary microglia) and allowed to adhere for 2-3 days. Cells were always incubated in serum free medium overnight before the beginning of each experiment. The following day, medium was changed to serum-free RPMI (BV-2) or DMEM (primary microglia) containing 0.1% bovine serum albumin (BSA; control) or medium containing 0.1% BSA and LPA (1 μM). BSA was used as LPA carrier. For inhibitor studies, cells were incubated in serum-free medium containing 0.1% BSA, LPA (1 μM) and each inhibitor accordingly (1). Aqueous LPA stock solutions (10 mM) were stored at -70 °C. Only freshly thawed stocks were used for the experiments. LPA solutions, culture medium, BSA, and PBS that were used during the experiments, were tested for endotoxin content using the Limulus amebocyte lysate test. Endotoxin content was always < 0.5 EU/ml.

2.3.2 Treatments with pharmacological inhibitors

For inhibitor studies BrP-LPA, a pan LPA receptor/ATX inhibitor (122), TCLPA5, a specific inhibitor for LPA5 (272), CRT0066101 (273), a pan PKD inhibitor and SP600125 (274), a selective inhibitor of c-Jun N-terminal kinase (JNK), were used. BrP-LPA was diluted in distilled water (stock concentration of 2 mM), aliquoted and kept at -20°C. TCLPA5 and SP600125 were diluted in DMSO (stock concentration 100 mM) and kept at -20°C. TCLPA5 solutions are stated to be stable at -20°C for maximum 40 days. CRT0066101 was also diluted in DMSO (stock concentration 10 mM) and kept at -20°C. During the experiments, TCLPA5 and CRT0066101 were used at a final concentration of 2 μM and 1 μM, respectively, while BrP-LPA and SP600125 at a final concentration of 5 μM. Cells were preincubated overnight with the antagonists before each experiment.

2.4 Immunoblotting

BV-2 cells (seeded onto 6-well plates at a density of $1x10^5$ cells/well) or PMM (cultured on PDL-coated 12-well plates at a density of $5x10^5$ cells/well) were used in Western blotting experiments for the detection of different proteins' expression. Prior to experiments cells were cultured in serum-free medium (o/n) and then incubated in presence of the desired substances (according to each experiment). After the indicated time periods, culture medium was removed and cells were washed twice with ice-cold PBS. The cells were lysed in RIPA buffer (50 mM Tris-HCl pH 7.4, 1% NP-40, 150 mM NaCl, 1 mM Na_3VO_4, 1 mM NaF, 1 mM EDTA) containing protease inhibitors (Sigma; aprotinin, leupeptin, pepstatin: 1 μg/ml each), 10 μM PMSF and phosphatase inhibitors cocktail (Thermo Scientific, Waltham, MA, USA), scraped and centrifuged at 13,000 rpm for 10 min. Protein content was determined using the BCA kit (Thermo Scientific) and BSA as standard. Equal amounts of protein samples in 2x Lämmli buffer were separated on 10% SDS-PAGE gels and transferred to polyvinylidene difluoride membranes (PVDF). Membranes were blocked with 5% low-fat milk in Tris-buffered saline containing Tween 20 (TBST) for 2 h at RT and incubated with the primary antibodies, overnight with gentle shaking at 4°C. After removal of primary antibodies, the membranes were washed for 30 min in TBST and incubated for 2 h at RT with HRP-conjugated secondary antibodies (anti-rabbit 1:10000; anti-mouse 1:5000). Following washes with TBST for 1 h, immunoreactive bands were visualized using ECL or ECL plus reagents and detected with a

chemiluminescence detection system (ChemiDoc Bio-Rad, Berkeley, CA, USA). Where indicated, the membranes were stripped using a stripping buffer (140 µl β-mercaptoethanol in 20 ml buffer 60mM Tris/ 2% SDS, pH 6.8) under gentle shaking for 30 min at 50°C in a water bath, washed for 1 h in TBST, blocked with 5 % low-fat milk in TBST for 1 h at room temperature and probed again with the desired primary antibodies. Anti-β-actin (1:5,000) and anti-β-tubulin (1:2,000) were used as loading controls.

2.5 Immunofluorescence

Double and/or triple immunofluorescence staining was carried out in BV-2 and PMM. Cells were seeded in chamber slides (PDL-coated in case of primary cells) at a density of $1.5x10^4$ and $3x10^4$ cells/well, respectively. Cells were serum-starved overnight and incubated in the presence of the desired (according to each experiment) solutions for 24 h. Cells were washed with pre-warmed PBS, fixed with 4% paraformaldehyde in 0.1 M PBS for 15 min and permeabilized with 0.5% TritonX-100/PBS for 10 min at 25°C. Following three washing steps with PBS, cells were incubated with blocking buffer (Thermo Scientific, Waltham, MA, USA) for 1 h at 4°C and incubated with primary antibodies for 1 h or over-night at 4°C. The slides were washed three times with PBS and incubated with fluorescently labeled secondary antibodies (1:200) for 30 min. Following washes with PBS, BV-2 and PMM were incubated with a second primary antibody for 1h at 4°C. In cases where the primary antibody was not already fluorescently labeled, cells were incubated again with a conjugated secondary antibody (1:200) for 30 min. Finally, all slides were washed 3 times with PBS, stained with Hoechst 33342 (Invitrogen, Waltham, MA, USA) and mounted using mounting medium (Dako, Vienna, Austria). Confocal fluorescence microscopy imaging was performed using a Leitz/Leica TCSSP2 microscope (Leica Lasertechnik GmbH, Heidelberg, Germany). Quantitation of fluorescence intensity and morphological analysis were performed with ImageJ. At least 50 cells out of 3 different areas per chamber were analyzed.

2.6 qPCR analysis

BV-2 (24-well plates, $5x10^4$ cells/well) or PMM (PDL-coated 24-well plate, $2.5x10^5$ cells/well) were incubated in serum-free medium overnight and then treated with the

desired solutions for the indicated time periods. Culture medium was removed; cells were washed twice with ice-cold PBS, and lysed in lysis buffer (included in the RNA isolation kit).

Total RNA was extracted from BV-2 or primary microglia cells using the RNeasy Mini or RNeasy Micro kit (Qiagen, Hilden, Germany) and quantified using NanoDrop (Thermo Fisher Scientific, Waltham, Massachusetts, USA). RNA was reverse-transcribed by using the high capacity cDNA reverse transcription kit (Applied Biosystems, Foster City, CA) or by using the SuperScript® III reverse transcription kit (Invitrogen, Waltham, Massachusetts, USA). Quantitative real time PCR (qPCR) was performed on an Applied Biosystems 7900HT Fast Real Time PCR System using the QuantiTect SYBR® Green PCR kit (Qiagen, Hilden, Germany). Amplification of murine hypoxanthine-guanine phosphoribosyltransferase (HPRT) as housekeeping gene was performed on all samples as internal controls for variations in mRNA levels. Expression profiles and associated statistical parameters were analyzed by the 2^{-ddCt} method (275) or with the relative expression software tool (REST©, http://www.gene-quantification.de/rest.html) using a pair-wise fixed reallocation test. Gene specific primers were purchased from Qiagen (LPA receptors, PKD isoforms, and migratory genes) and Invitrogen (cytokines and chemokines). Primer sequences are listed in tables 1,3, and 4 in the appendix. In case of non-detects we discriminate between undetermined values (that do not exceed the Ct threshold) and absent values (no reaction occurred) (276).

2.7 Customized qPCR arrays

Primary microglia cells were seeded on PDL-coated 24-well plates at a density of $2.5x10^5$ cells/well. Cells were cultured in DMEM without FCS overnight and then treated with 1 µM LPA for 2, 8 and 24 h. Untreated cells were used as negative controls. Total RNA was extracted with the RNeasy Micro kit (Qiagen, Hilden, Germany) and quantified using Nanodrop (Thermo Fisher Scientific, Waltham, Massachusetts, USA). Aliquots of 1 µg of total RNA were reverse transcribed using SuperScript III Reverse Transcriptase and random hexamer primers according to the manufacturer's protocol (Invitrogen, Waltham, Massachusetts, USA). Real-time qPCR was performed with an Applied Biosystems 7900HT Fast Real Time PCR System. Gene expressions were normalized to housekeeping gene murine HPRT. Customized qPCR arrays containing primers for the detection of the

gene products listed in table 2 in the appendix were purchased from GeneCopoeia (Rockville, MD, USA).

2.8 Lentiviral transduction (shRNA)

PMM were cultured on PDL-coated 24-well plates at a density of $1.2x10^5$ cells/well. Polybrene (8 µg/ml) and viral particles (multiplicity of infection = 2) were added onto cultured microglia. We used shRNA control transduction lentiviral particles (sh-scrambled) and PKD1 (shPKD1 NM_008858, clone ID: TRCN0000024007, *Sequence: CCGGCCTTCAGCTTTAACTCCCGTTCTCGAGAACGGGAGTTAAAGCTGAAGGTTTTT)* and PKD2 (shPKD2 NM_178900, clone ID: TRCN0000322346, *Sequence: CCGGGTACGACAAGATCCTGCTCTTCTCGAGAAGAGCAGGATCTTGTCGTACTTTTT G*) specific constructs. After 12 h treatment with the shRNA control transduction particles and the PKD1 and PKD2 silencing constructs medium was replaced by pre-warmed conditioned medium that was prepared from mixed glial cultures after centrifugation and filtration through a 0.45 µm filter. Cells were kept at 37°C/5% CO_2 for 72 h and collected to validate silencing efficacy by qPCR or to proceed with the different experiments.

2.9 Time-lapse microscopy

BV-2 cells and PMM were seeded onto 24-well plates at a density of $2x10^4$ and $5x10^4$ cells/well, respectively. Cells were cultured in serum-free medium overnight. The next day cells were treated with the indicated concentrations of LPA, with LPA plus DMSO (to account for vehicle effects), or with 1 µM LPA in the absence or presence of inhibitors (TCLPA5, 2 µM; CRT0066101, 1 µM). Control cells were incubated in serum-free medium in the absence or presence of DMSO (negative controls) or treated with N-arachidonylglycine (NAGly; Sigma; 1 µM; positive migration control).

For silencing experiments PMM (non-transduced or transduced with lentiviral particles containing sh-scrambled, or shPKD1 or shPKD2) were cultured on PDL-coated 24-well plates at a density of $1.2x10^5$ cells/well. After transduction, the cells were incubated in serum-free medium in the absence or presence of LPA (1 µM).

Images were acquired every 20 min for 24 h at five different positions of each well using a Zeiss Cell Observer microscope. Data analysis was carried out using ImageJ. Image

intensity correction was achieved by correcting each image median value to 125 (8 bit images have a resolution of 255 grey levels). Image stabilization was achieved using the Lucas-Kanade method with a macro for ImageJ (K. Li, "The image stabilizer plugin for ImageJ"; http://www.cs.cmu.edu/~kangli/code/Image_Stabilizer.html; ®Kang Li) to correct for changes in position due to mechanical tolerances in the microscope stage. Equalization of low-frequency variations in the background signal of the image using an FFT band pass filtering and reducing low and high frequency changes in the images (low frequency filter set to 40 pixels and high frequency filter set to 6 pixels) enabled simple thresholding of the images. After thresholding, which allowed object selection, a Gaussian blur was applied. The resulting TIFF images were analyzed using ImageJ inherent functions. The Image J 'Manual tracking' plug-in was used to manually track the cells. The following image shows an example of different cell movements and the terms of accumulated and Euclidean distance are explained.

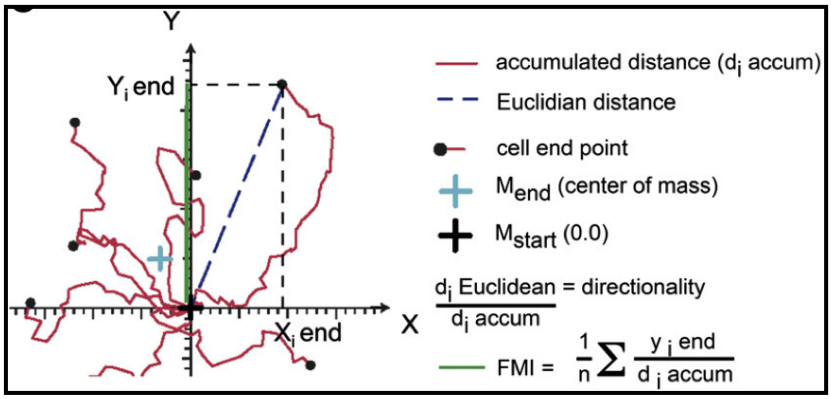

In random, a minimum of 20 viable cells per condition was selected and followed. Using the Image J 'Chemotaxis and Migration Tool' plug-in the accumulated distance (the total cell path traveled by the cell), the Euclidean distance (the distance between start and end point), and cell velocity were calculated. Experiments were repeated at least two times.

2.10 xCELLigence migration assay

BV-2 microglia cells were cultured in 6-well plates at a density of $3x10^5$ cells/well. Before the experiment, cells were incubated in serum-free RPMI medium or pretreated with TCLPA5 (2 µM) or CRT0066101 (1 µM) for 3 h. Chemotaxis assays were carried out using CIM-16 well plates and an xCELLigence RTCA-DP instrument (Roche Diagnostics,

West Sussex, UK). LPA solutions were prepared at the desired concentrations and 160 µl of them were loaded in the lower wells of the CIM-16 plate. NAGly was used as a positive chemotaxis control and serum-free medium served as negative control.

Following upper chamber attachment, the upper wells were first filled with 50 µl of pre-warmed serum-free medium and the plate was left at RT for 30 min to pre-equilibrate. Cultured cells were trypsinized and re-suspended in serum-free medium in the absence or presence of TCLPA5 (2 µM) or CRT0066101 (1 µM). Fifty µl of the cell suspensions (containing $3x10^4$ cells) were placed into the upper wells. The plate was transferred to the RTCA-DP instrument and data were collected every 5 min over 24 h. As cells pass through the pores of the filter with an embedded gold microelectrode, an increase in electrical impedance corresponds to increased numbers of migrating cells ('cell index'). The image below presents a CIM-16 plate (**A**) and the structure of each well of the plate (**B**).

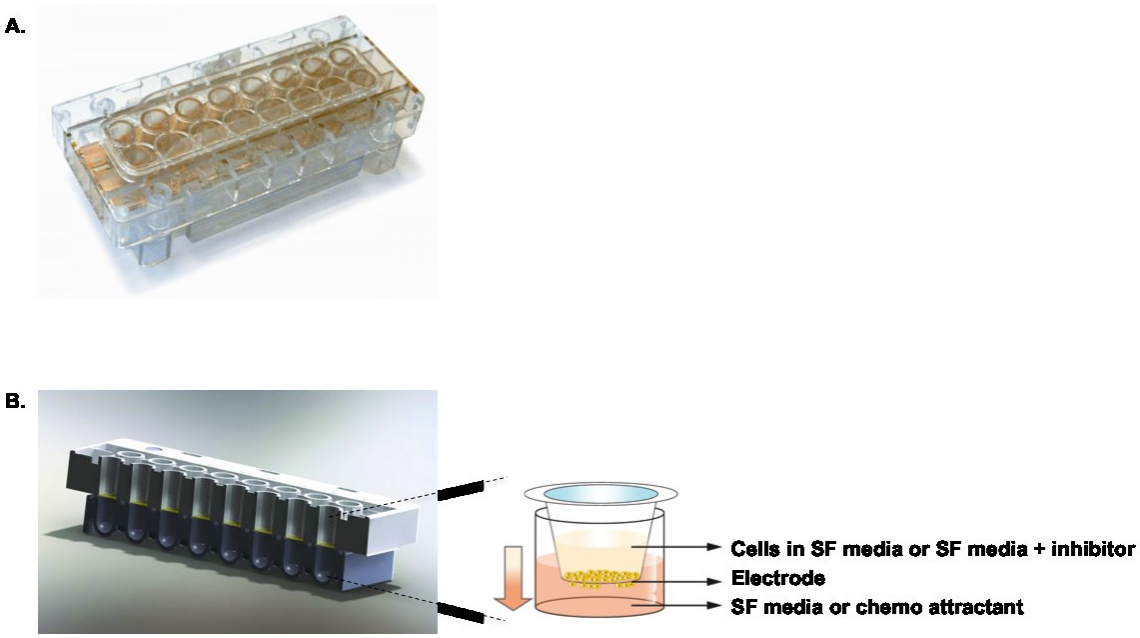

Data were normalized and analyzed using the RTCA Software 1.2.1. Experiments were performed at least three times in triplicate.

2.11 Flow Cytometry

Flow cytometry was used in order to assess the expression of CD40, CD86, and CD206 in microglia cells. BV-2 and PMM were seeded in triplicate onto 6-well and poly-D-lysine coated 24-well plates at a density of $1x10^5$ and $1.5x10^5$ cells per well, respectively (1). After 24 h serum-starvation, cells were incubated in the presence of 1 μM LPA for 12, 24, and 48 h. BV-2 cells were also used to test effects of the inhibitors on surface marker expression. Serum-starved cells were incubated with vehicle controls, LPA or LPA plus the antagonists for the above-mentioned time periods. Cells were then collected, blocked using the Ultra V blocker (Thermo Scientific) and incubated with PE anti-CD40, APC anti-CD86, or PE anti-CD206 antibody (1:50). Finally cells were fixed and measured using a Guava easyCyte 8 Millipore flow cytometer.

2.12 ELISA

IL-1β, TNFα, IL-6, CCL5 (RANTES), CXCL2 (MIP-2), and CXCL10 (IP-10) concentrations in the cellular supernatant were quantitated using the murine ELISA development kits (Peprotech, NJ, USA) (1). Briefly, BV-2 and PMM were seeded in triplicate onto 12-well and poly-D-lysine coated 24-well plates at a density of $5x10^4$ and $2.5x10^5$ cells per well, respectively. After serum-starvation (o/n), cells were incubated in serum-free medium, containing LPA in the absence or presence of the antagonists for the indicated time periods. For each time point, the supernatants were collected and kept at -70 °C until further use. The assays were performed according to manufacturer's instructions. The standard curve for each ELISA was performed in triplicate. The concentrations of the cytokines and chemokines were determined using the external standard curve.

2.13 Total NO assay

iNOS activity was assessed indirectly using the total nitric oxide assay kit (ENZO Life Sciences, Switzerland). The accumulated total nitrate levels were measured in the supernatant of cells that were incubated in serum-free medium, containing LPA in the absence or presence of the antagonists after 12, 24, and 48 h in the case of BV-2 cells and 2, 8, 24, and 48 h in the case of primary microglia cells. In this Griess assay nitrate is reduced to nitrite by means of nitrate reductase. Fifty μl of supernatant from each sample

was processed according to manufacturer's protocol. A standard curve was generated in the range between 0-100 μM using nitrate as standard. The total nitrate concentration per sample was determined using the external calibration curve.

2.14 Measurement of carboxy-H2DCFDA oxidation

Intracellular reactive oxygen species (ROS) levels were measured using the DCFDA cellular ROS detection kit (Abcam, Cambridge, UK). After internalization and subsequent hydrolysis, the redox indicator probe carboxy-H_2DCFDA is converted to carboxy-H_2DCF, which in the presence of oxidant species is oxidized to fluorescent carboxy-DCF (277). BV-2 and PMM were seeded in black clear bottom 96-well plates at a density of $5x10^4$ cells per well (1). Cells were allowed to adhere overnight and then incubated with 20 μM DCFDA for 40 min at 37^{o}C in the dark. The solution was removed and the cells were incubated in serum-free medium, containing LPA in the absence or presence of the antagonists for 0.5, 1, 3, and 6 h. Fluorescence intensity was measured with excitation and emission wavelengths of 485 nm and 535 nm, respectively.

2.15 LDH Assay

Lactate dehydrogenase is a soluble enzyme located in the cytosol and released into the culture medium upon cell lysis or damage. LDH activity can therefore be used as an indicator of membrane integrity and thus a measurement of cytotoxicity (Cayman Chemical, Ann Arbor, MI, USA). For the experiment we use BV-2 microglia cells and the CATH.a neuronal cell line.

BV-2 cells were seeded in triplicate onto 12-well plates at a density of $5x10^4$ cells per well. After serum-starvation (o/n), cells were incubated in serum-free medium, containing LPA in the absence or presence of the antagonists for the indicated time periods. For each time point, the supernatants were collected and kept at -70 °C until further use.

The CATH.a neurons were seeded in a 96 well plate at a concentration of $1x10^5$ cells per well and allowed to adhere. Following overnight serum-starvation, the cells were incubated in the presence of the supernatants collected from the above-mentioned BV-2 cells. Three wells containing only medium without cells were used for background control. For a positive control, cells were incubated with the LDH positive control solution. In order to

measure maximum and spontaneous release, cells were incubated with 10% Triton X-100 and assay buffer, respectively. Cells were kept at 37°C/5% CO_2 for 24 hours and then the plate was centrifuged at 1,300 rpm for 5 min. 100µl of the supernatants were transferred to a new 96 well plate and 100µl of LDH reaction solution were added to each well. The plate was incubated at 37°C/5% CO_2 for 30 min under gentle shaking and the absorbance at 490nm was measured using a plate reader.

The % cytotoxicity was calculated using the following equation:

$$\%\text{Cytotoxicity} = \left[\frac{experimental\ value - spontaneous\ release}{maximum\ release - spontaneous\ release}\right] \text{x}100$$

2.16 Phagocytosis Assay

Latex beads coated with fluorescently labeled IgG (IgG PE) were used as a probe for the measurement of the phagocytic process (Cayman Chemical, Ann Arbor, MI, USA). BV-2 and PMM cells were plated in 96-well plates at a concentration of $5x10^4$ cells per well and allowed to adhere. Cells were serum starved overnight and then incubated in the presence of the desired solutions, containing the latex beads to a final concentration of 1:100, for 24 hours. Following centrifugation at 1,300 rpm for 5 min, medium was removed carefully and cells were incubated in trypan blue solution (1:50 in assay buffer) for 4 min. After a second centrifugation at 1,300 rpm for 5 min and removal of the trypan blue solution, the fluorescence intensity was measured with excitation and emission wavelengths of 494 nm and 575 nm, respectively.

2.17 Statistical analysis

All experiments were performed in triplicate and repeated at least three times. For statistical analysis, data obtained from independent measurements are presented as mean+SD, unless otherwise stated. Statistical tests were performed using the GraphPad Prism version 5.0a for Mac (GraphPad Software, Inc., San Diego, CA). Data were analyzed by one-way ANOVA followed by Bonferroni's post hoc test. Values of $p \leq 0.05$ were considered significantly different.

Results

1. Effects of LPA on the Microglial Cytoskeletal Architecture

Microglia are able to change their morphology in response to extracellular stimuli. In response to brain damage, injury, or changes in their environment microglia reorganize their structure in order to directly reach the site of stress with their cellular processes. Microglia undergo structural transformation, which is a surrogate index of the microglia activation process (278).

During this study, the first question that was addressed is whether LPA can induce changes in microglial cytoskeleton. From a pharmacological point of view it was of interest to determine which LPA receptor(s) is/are responsible for these changes and whether members of the PKD family, which regulate numerous (immune) cell functions can play a role in this structural reorganization.

1.1 LPAR and PKD isoform expression in BV-2 and PMM

During these experiments both, the BV-2 microglia cell line and primary murine microglia were used. As a first step, LPA receptor expression in BV-2 and PMM was analyzed using qPCR analysis. LPAR2, LPAR3, LPAR5, and LPAR6 were detected in BV-2 cells. LPAR1 and 4 were undetectable, whereas LPAR3 was detected at very low copy numbers. In PMM all of the LPARs (with the exception of LPAR3) were detected (**Fig. 1A**). LPAR6 expression was arbitrarily set to 1 (1).

To test whether LPA-receptor expression changes upon cell activation BV-2 and primary cells were incubated in the presence of LPA (1 μM). After 24 h LPA receptor expression was analyzed by qPCR. The experiments (**Fig. 1B**) revealed that LPA has no effect on LPA receptor mRNA expression in BV-2 cells. LPA tended to decrease LPAR mRNA in PMM; however, these effects were statistically not significant (1).

PKD expression in BV-2 and PMM was characterized by qPCR and Western blot analysis. BV-2 cells express PKD2 and PKD3 mRNA (**Fig. 1C**), while PMM express all three members of the PKD family (**Fig. 1D**). PKD1-3 protein expression was detected in total mouse brain lysates, the cortex, and in PMM. In line with the mRNA data, only PKD2 and PKD3 protein expression was detectable in BV-2 cells (**Fig. 1E**).

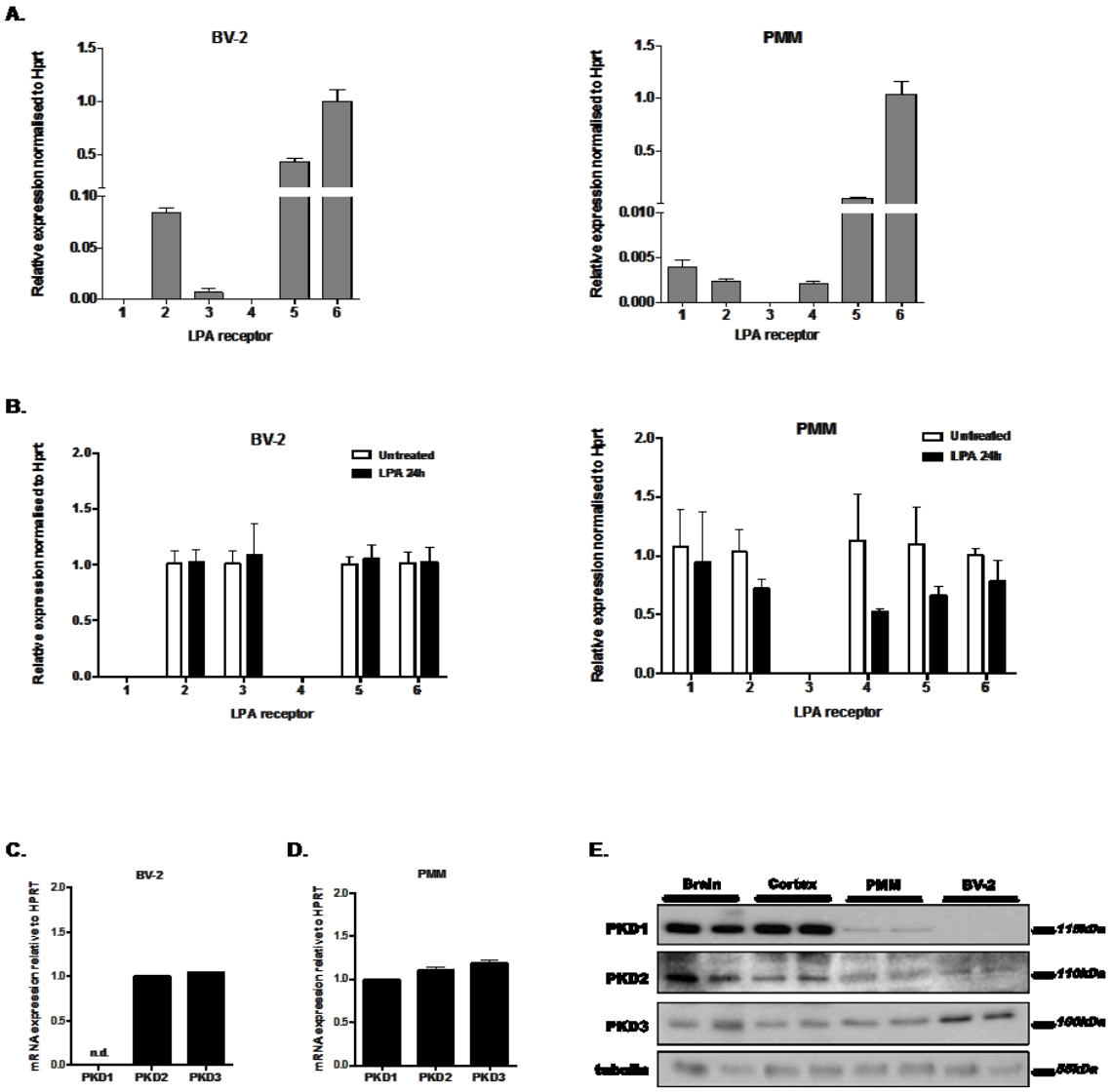

Fig 1. Analysis of LPA receptor and PKD isoform expression in BV-2 and PMM

(**A**) Gene expression was monitored by qPCR and normalized to the housekeeping gene Hprt in BV-2 and PMM. Values are expressed as mean + SD (n=6-9). LPAR6 expression was arbitrarily set to 1 (1).

n.d. = not detected.

(**B**) LPA receptor expression after treatment with 1 µM LPA for 24 h. Results are expressed as mean + SD from three independent experiments (1).

Gene expression of PKD1-3 in (**C**) BV-2 and (**D**) PMM was analyzed by qPCR and normalized to HPRT. Values are expressed as mean +SD. PKD2 expression in BV-2 and PKD1 in primary microglia was arbitrarily set to 1. (n.d.: not detectable). (**E**) Protein expression of PKD isoforms was determined by Western blotting. Samples from whole brain and cortex were used as controls. One representative blot out of three separate experiments is shown.

1.2 LPA induces changes in microglia morphology

Quantification of morphological features of non-stimulated and LPA-stimulated cells revealed profound changes in both BV-2 and primary cells. In BV-2 cells, light microscopy indicated that the majority of cells (**Fig. 2A**, upper panel) transformed to a spindle-like cell type in response to LPA. Here, I observed the formation of a leading edge followed by an elongated tail. LPA stimulation resulted in increased immunoreactivity for Iba-1 being indicative of microglia activation (Fig. 2A; lower panel). LPA treatment also induced a larger cell area, and cell perimeter (Fig. 2A; bar graphs in the right panel). Quantitative evaluation of Iba1 fluorescence is also shown in the right bar graphs.

Treatment of PMM with LPA induced structural transformation from an elongated to a more condensed phenotype and increased Iba-1 fluorescence (**Fig. 2B**). Comparable to BV-2 cells, LPA induced an increase in cell area and perimeter (Fig. 2B; bar graphs in the right panel). Iba1 fluorescence intensity of control and LPA-treated cells is shown in the right bar graphs.

In addition to Iba-1 analysis, we performed F-actin and tubulin staining, in order to further characterize changes in microglial architecture (1). Immunofluorescence studies revealed significant rearrangements of the cytoskeleton in both BV-2 (**Fig. 3A**) and PMM (**Fig. 3B**). F-actin staining indicated that untreated cells were unipolar with one or more processes. After LPA treatment the cells increased their surface area and acquired a flat morphology with more condensed actin labelling.

Moreover tubulin staining indicated an increase in cell area in response to LPA treatment and formation of thin protrusions. Tubulin labelling changed from a diffuse pattern in untreated BV-2 cells to a more dense network in response to LPA (Fig. 3A; lower panels). In primary cells F-acting staining revealed that LPA treated cells had increased body size adopting an amoeboid morphology. Tubulin staining was also more condensed and occupied a larger area after LPA treatment (Fig. 3B, lower panels).

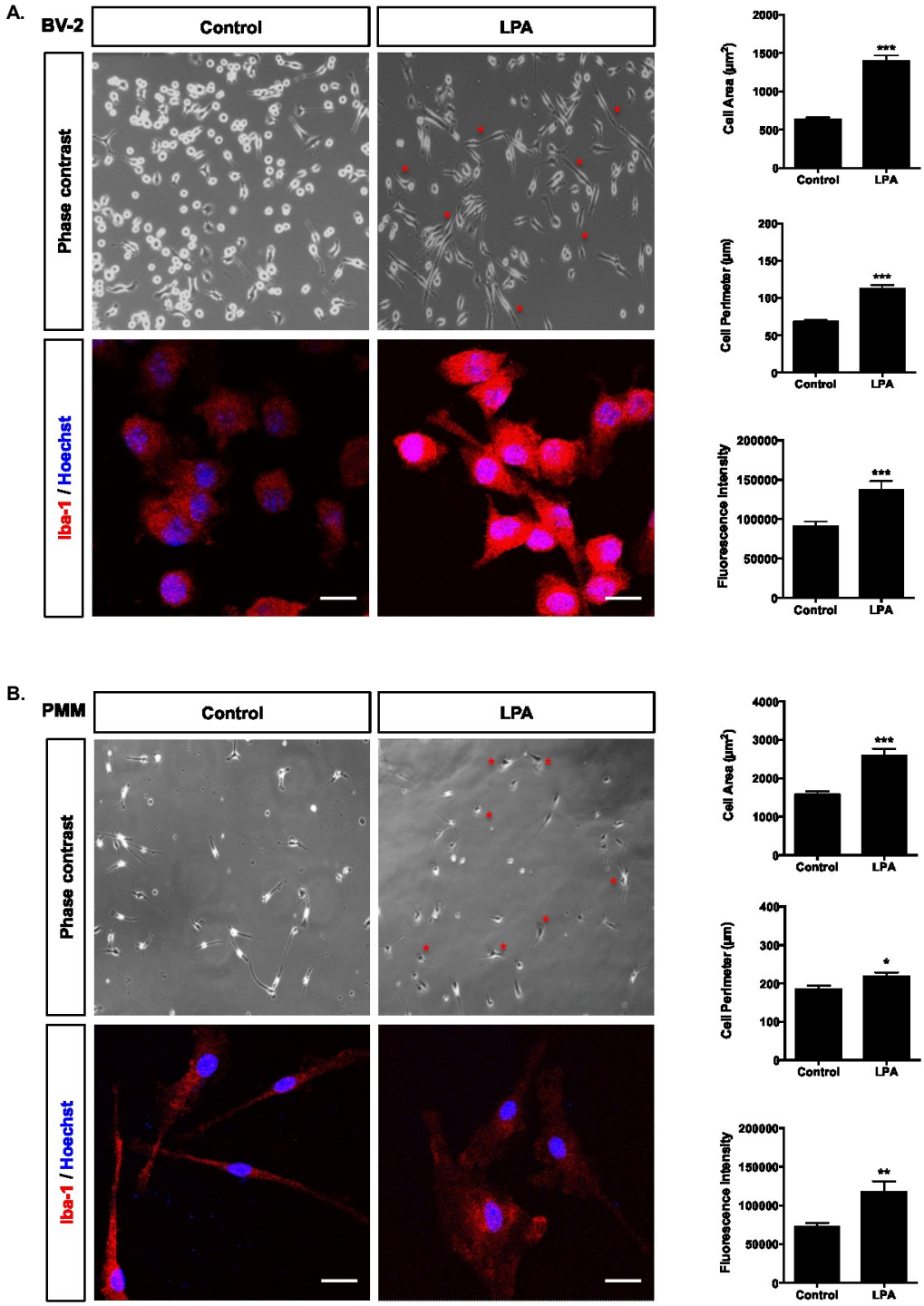

Fig 2. LPA alters the morphology of BV-2 and PMM

(**A**) BV-2 and (**B**) PMM were cultured in 24-well plates and serum-starved overnight prior LPA treatment (1 µM; 24 h). Cells were incubated with rabbit anti-mouse Iba-1 (1:200) antibody and Cy-3-labeled secondary goat anti-rabbit antibody (1:300), mounted and examined using a Leica confocal microscope. Representative micrographs depict morphological changes upon LPA treatment. Morphological analysis (cell area and perimeter) and analysis of Iba-1 fluorescence intensity was performed using ImageJ. At least 50 cells out of 3 different areas per chamber were measured in two independent experiments. Scale bar = 20 µm. The results are presented as mean +SD (*p<0.05, **p<0.01, ***p<0.001; one-way ANOVA with Bonferroni correction).

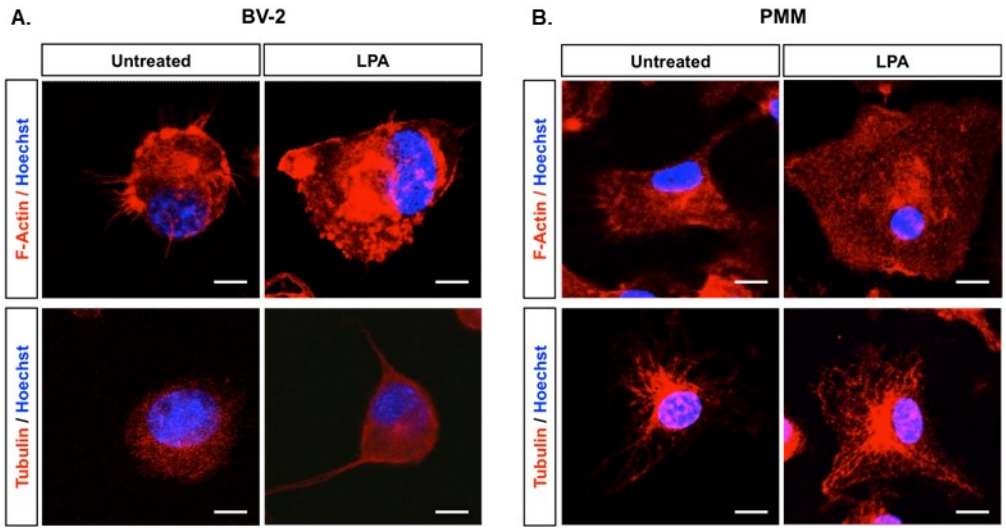

Fig 3. **LPA induces significant rearrangements in microglia cytoskeleton**

Staining for F-actin and β-tubulin in **(A)** BV-2 cells and (**B**) PMM**.** Cells on chamber slides were serum starved (o/n) and then incubated in the absence or presence of LPA (1 µM, 24 h). After washing, incubation with primary and secondary antibodies, cells were analyzed by confocal microscopy. Nuclei were stained with DAPI. Representative images reveal rearrangement of the cytoskeleton following LPA treatment (1). Scale bar = 40 µm. Results from one representative experiment (out of two) are shown.

LPAR5 is highly expressed in both BV-2 and PMM cells and was identified as a member of the microglia sensome (279). In order to unravel whether this receptor and the PKD family members are involved in these morphological alterations, I inhibited LPAR5 and PKD1-3 using specific pharmacological inhibitors.

In BV-2 cells and PMM, LPAR5 (TCLPA5; 2 µM) and PKD1-3 (CRT0066101; 1 µM) antagonism significantly attenuated LPA-mediated Iba-1 staining (**Fig. 4A,B;** upper panels), and suppressed LPA-mediated increase in cell area, cell perimeter, and fluorescence intensity (Fig. 4A,B; lower panels). These data indicate that LPAR5 acts as a sensor and at least one member of the PKD family acts as transducer of LPA-mediated signal(s) that impact on cell morphology.

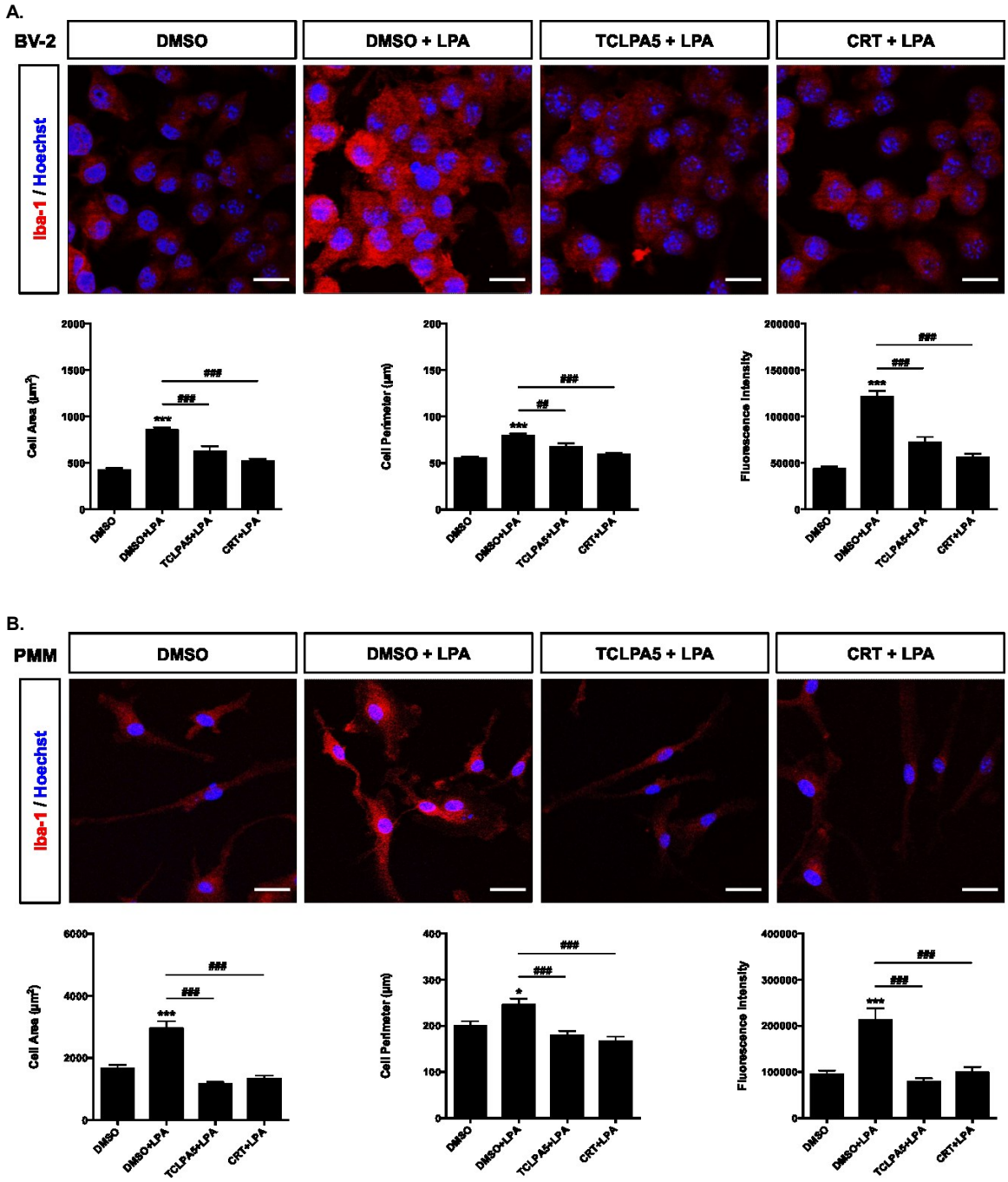

Fig 4. Inhibition of LPAR5 and PKD isoforms reverses LPA-induced morphological changes

(**A**) BV-2 and (**B**) PMM were cultured on chamber slides, serum-starved overnight, and treated with 1 µM LPA plus DMSO or LPA plus TCLPA5 (2 µM) or CRT0066101 (1 µM) for 24 hours. Cells were fixed, permeabilized, blocked, and incubated with rabbit anti-mouse Iba-1 antibody (1:200) and subsequently Cy-3-labeled secondary goat anti-rabbit antibody (1:300). A Leica confocal microscope was used to acquire images. Morphological analysis and analysis of Iba-1 fluorescence intensity was performed using ImageJ. At least 50 cells out of 3 different areas per chamber were measured (two independent experiments).

Scale bar = 20 µm. The results are presented as mean +SD (*$p<0.05$; ***$p<0.001$ compared to DMSO-treated cells; $^{\#\#}p<0.01$; $^{\#\#\#}p<0.001$ LPA plus TCLPA5 or CRT0066101 versus LPA only; one-way ANOVA with Bonferroni correction).

2. LPA increases the Microglial Migrational Response

Cell migration is a complex and highly regulated process in which extracellular and intracellular signals produce a coordinated response (280, 281). The PKD family members are implicated in the regulation of many fundamental biological processes, including signal transduction, membrane trafficking, and cell survival, differentiation, proliferation, and also migration (282). Other studies have demonstrated that mitogen-activated protein kinases (MAPKs), including Jun N-terminus kinase (JNK), p38 and ERK, play crucial roles in cell migration (283).

Before we examined the microglia migration in response to LPA treatment, we analyzed LPA-mediated downstream signaling pathways, and studied whether and which PKD isoforms and MAP kinase members are activated by LPA and whether LPAR5 plays a role in the activation state of these kinases.

2.1 LPA-mediated signaling events in BV-2 and PMM

LPA induced phosphorylation of PKD2 (these cells do not express PKD1; Fig. 1A), JNK, AKT, ERK1/2, and p38 MAPK in BV-2 cells (**Fig. 5A**). Preincubation with TCLPA5 (for 0.5-8 h prior to LPA addition) and subsequent activation with LPA (1 μM) revealed that the antagonist time-dependently inhibited activation of downstream signaling modules. CRT0066101 suppressed PKD2, JNK, AKT, ERK1/2 and p38 MAPK activation even after 30 min inhibitor pre-treatment (**Fig. 5B**).

In PMM, an activation pattern comparable to BV-2 cells was observed in response to LPA. Activation of PKD1 and PKD2 was observed after 5 min, reached a maximum after 10 min and then gradually decreased. This activation pattern correlated with the time course of JNK, AKT, ERK1/2, and p38 phosphorylation (**Fig. 5C**). In the presence of CRT0066101 or TCLPA5 phosphorylation of PKD1 and -2, JNK, AKT, and ERK1/2 was attenuated, was however, less pronounced for the MAP kinases compared to the one observed for PKD1 and PKD2 (**Fig. 5D**).

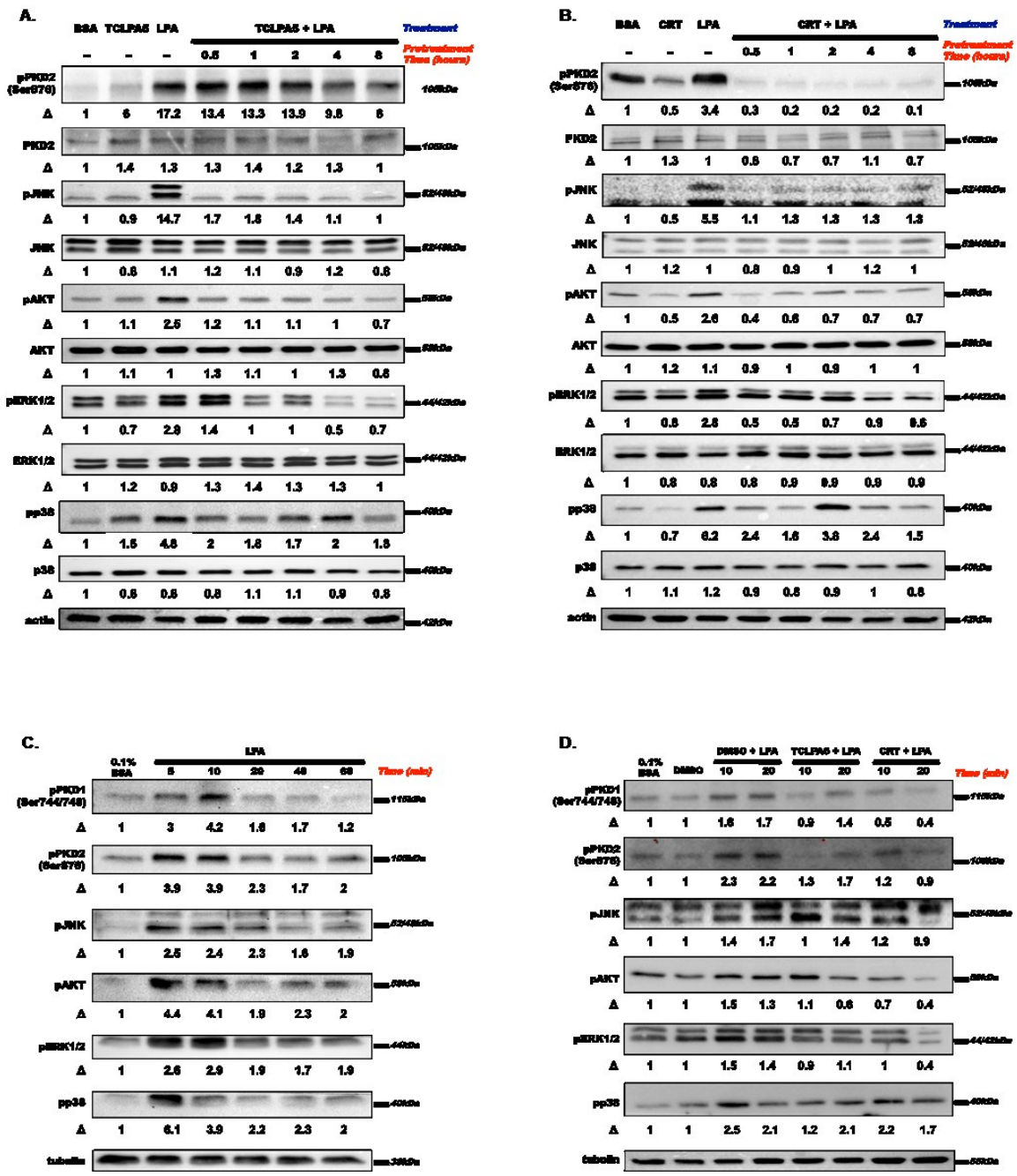

Fig 5. TCLPA5 and CRT0066101 inhibit LPA downstream signaling

BV-2 microglia cells were cultured in 6-well plates and serum starved overnight. The cells were preincubated for different time periods with (**A**) TCLPA5 (2 µM) or (**B**) CRT0066101 (1 µM) as indicated and then incubated with LPA (1 µM). Cells incubated with 0.1 % BSA were used as controls.

(**C**) PMM were cultured in 12-well PDL-coated plates, serum-starved overnight, and treated with 0.1 % BSA or 1 µM LPA. (**D**) PMM were pre-incubated overnight with TCLPA5 (2 µM) or CRT0066101 (1 µM) before treatment with 1 µM LPA. Cells incubated only with 0.1 % BSA or DMSO were used as negative control.

The phosphorylation states of PKDs, JNK, AKT, ERK1/2, and p38 were detected by Western blotting. Protein/loading control ratios were normalized to the ratio of unstimulated microglia. One representative blot out of three is shown.

Activation of microglia involves a migrational response to the site of injury (35). A crucial component of this migratory response is the formation of lamellipodia at the leading edge of migrating cells (284). PKD1 and PKD2 were shown to rapidly translocate between different cellular compartments depending on the stimulus and the cellular context (285).

Therefore confocal laser scanning microscopy analyzed subcellular trafficking of endogenous PKD1 and PKD2 in response to LPA activation.

It has been already mentioned that BV-2 microglia cells do not express the PKD1 isoform. Immunofluorescence staining for PKD2 only was performed in theses cells. The cytoskeleton was visualized using tubulin staining. Primary microglia express all the three isoforms of PKD family. Separate staining for PKD1 and PKD2 was performed while tomato lectin was used to visualize the cytoskeleton of primary microglia.

In unstimulated BV-2 cells, PKD2 was detected mainly at perinuclear areas (**Fig. 6A**, upper panel). After LPA stimulation (Fig. 6A, lower panel), cell size increased and induced the formation of new plasma membrane protrusions containing tubulin, likely lamellipodia. In LPA-stimulated BV-2 cells PKD2 underwent translocation with a distribution that was almost exclusively detected in newly formed tubulin-positive membrane projections (Fig. 6A).

In untreated PMM, PKD1 shows some nuclear and cytosolic (in cellular protrusions/extensions) staining (**Fig. 6B**, upper panel). In response to LPA, PMM changed from a spindle shaped to a more flattened morphology (Fig. 6B, tomato lectin staining). The major part of cytosolic PKD1 in unstimulated cells undergoes translocation to the nuclear compartment upon LPA treatment (Fig. 6B, lower panel).

In contrast to PKD1, PKD2 translocation in response to LPA is less clear-cut in PMM (**Fig. 6C**). No nuclear PKD2 staining was observed in untreated or LPA-treated cells. In the absence of LPA, the majority of PKD2 was detected in membrane protrusions and as a more diffuse staining in the cytosol (Fig. 6C, upper panel). In response to LPA, PKD2 is mainly located at perinuclear areas. Also PKD2 staining was observed in membrane ruffles, and cellular protrusions (Fig. 6C, lower panel).

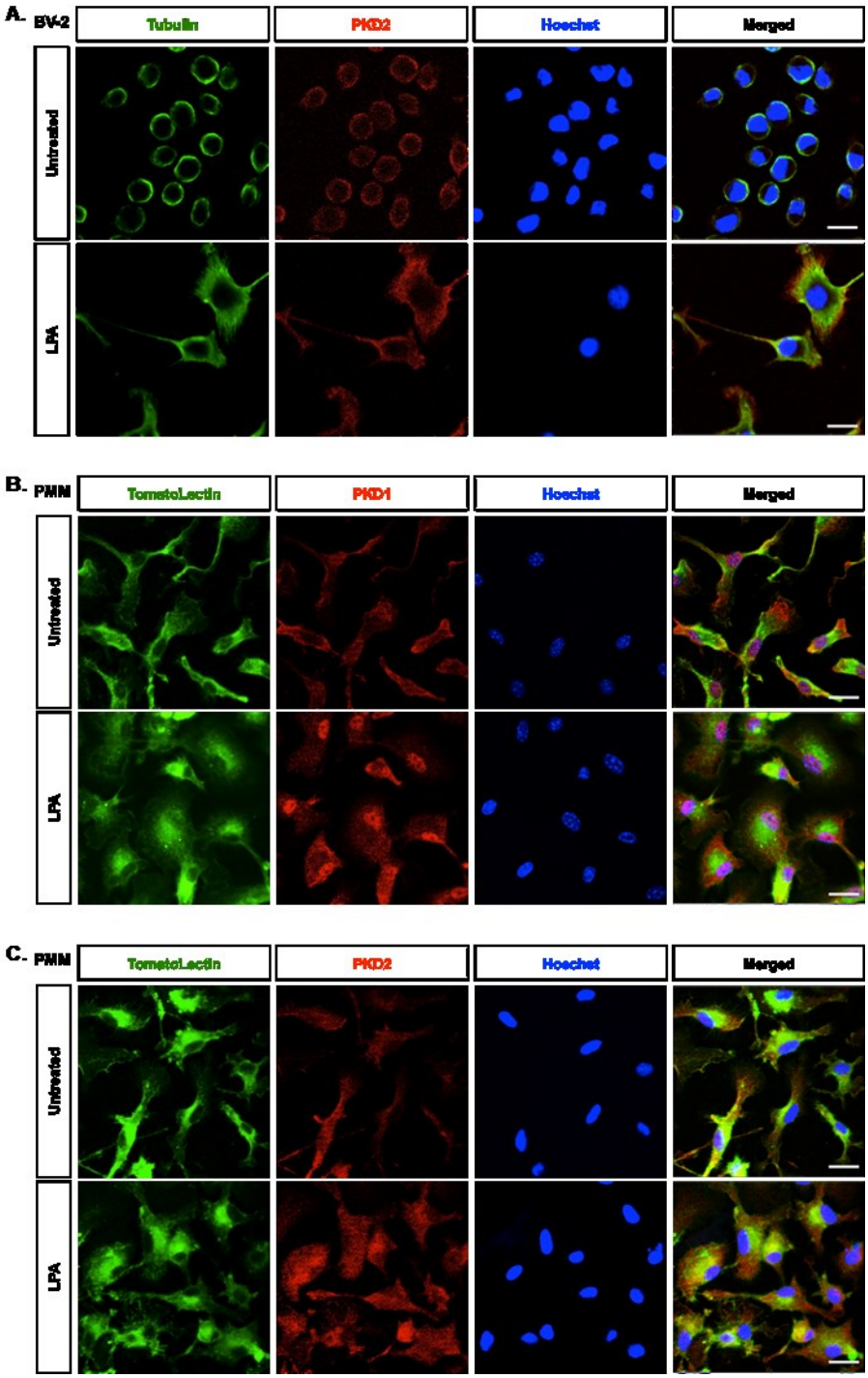

Fig 6. Intracellular trafficking of PKD1 and PKD2 in response to LPA

(**A**) BV-2 cells were cultured on chamber slides, serum-starved and incubated in the presence of 0.1 % BSA ('untreated') or 1 μM LPA for 24 h. Cells were fixed, permeabilized, blocked and stained for tubulin, PKD2 and nuclei (Hoechst). Scale bar = 20 μm.

(**B, C**) PMM were cultured on chamber slides and serum-starved overnight. Cells were incubated in the presence of 0.1 % BSA ('untreated') or 1 μM LPA overnight, stained with tomato lectin, (**B**) PKD1 or (**C**) PKD2 and for DNA (Hoechst), and examined using a Leica confocal microscope. Scale bar = 20 μm.

2.2 LPA induces chemokinesis and chemotaxis

In order to analyze microglia migration in response to LPA treatment, we used two different methods. Firstly we used time-lapse microscopy in order to examine microglia migration in 2 dimensions. Sequential images were collected (the time between two images was 20 min), stabilized and using the chemotaxis tool in ImageJ, the cells were manually tracked. In order to support our results, we utilized also a second experimental approach for studying cell migration that provides the opportunity to follow chemotaxis in real time. Experiments were performed using Transwell plates. Interdigitated gold microelectrodes on the bottom side of a filter membrane (CIM plates) detect impedance changes, caused by the presence of transmigrated cells and is expressed as 'Cell Index' as indicated by the manufacturer (xCELLigence).

The impact of LPA on microglia chemokinesis was examined using time-lapse video microscopy and the tracks of individual cells were analyzed. The trajectory plots (**Fig. 7A**) for unstimulated and LPA-treated cells revealed profound changes in microglial response after treatment with LPA. Using the ImageJ software we calculated velocity, accumulated distance (the total distance covered by the migrating cell), and Euclidian distance (defining the final relative distance to origin) of cell migration. As shown in **Fig. 7B,** the migrational response of BV-2 cells to increasing LPA concentrations is reaching a maximum at 1 μM and returning almost to baseline at 5 μM LPA. The mean velocity of unstimulated cells increased 2-fold in response to 1 μM LPA (**Fig. 7B**). The total accumulated migration distance increased 2-fold (**Fig. 7C,** control vs. 1 μM LPA) and the euclidian distance increased 3-fold (**Fig. 7D,** control vs. 1 μM LPA).

During the second experimental approach, utilizing the xCELLigence system, we studied real time directional migration. Migration of serum-starved cells across uncoated CIM plates was analyzed in the absence or presence of increasing LPA concentrations or NAGly (that drives migration through GPR18 (286) and was used as a positive control) in the lower chamber of the Transwell inserts. LPA induced a statistically significant increase of directional migration at 0.5 and 1 μM compared to control conditions (**Fig. 8A**). LPA at 2 μM was without effect on directional migration paralleling findings shown in Fig. 7B-D. Statistical evaluation of results gathered from three independent experiments in triplicate is presented in **Fig. 8B** and these data are expressed as relative impedance values.

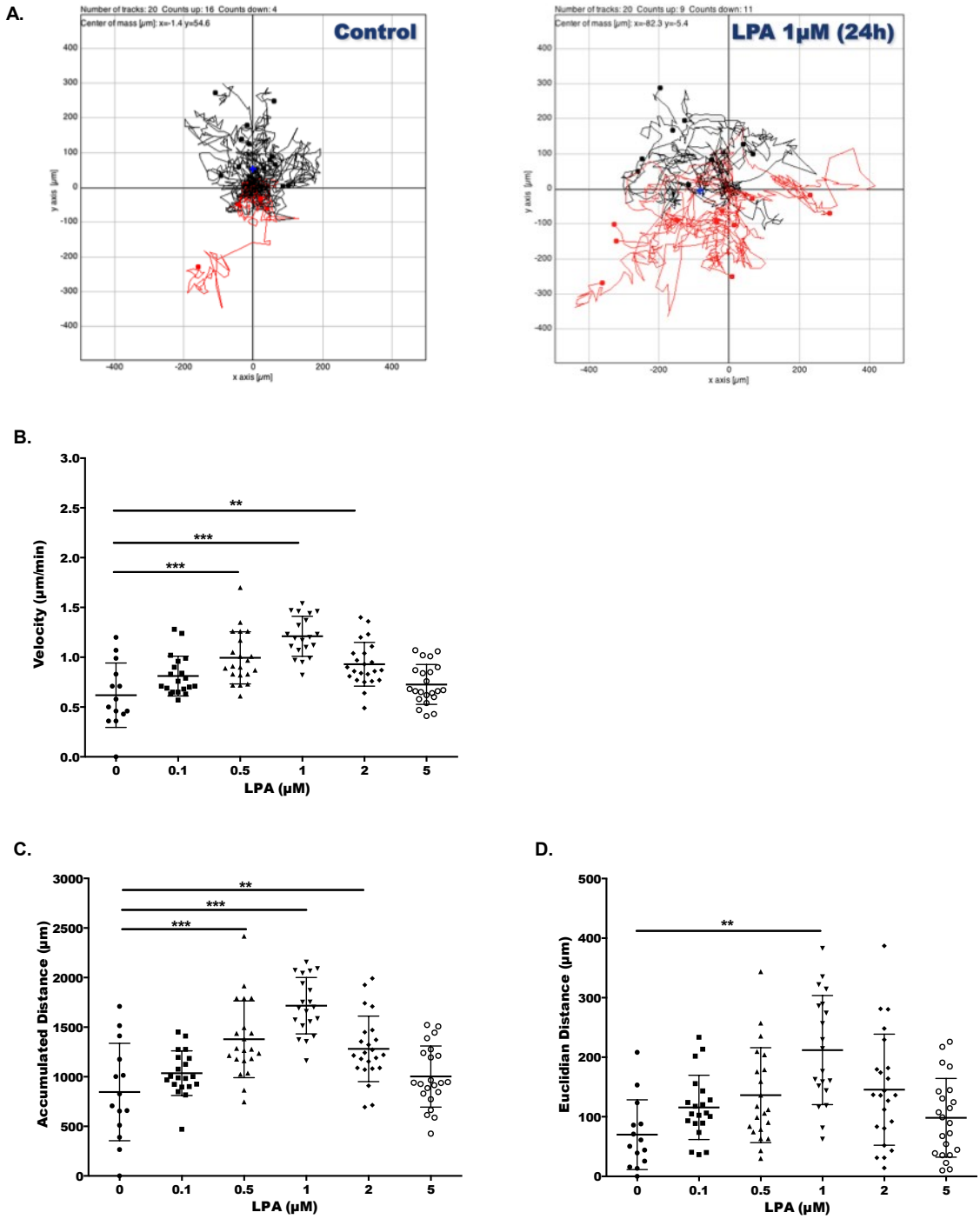

Fig 7. LPA induces chemokinesis of BV-2 microglia cells

(**A**) BV-2 microglia cells were cultured in 24-well plates, serum starved overnight and treated with LPA for 24 h. Time-lapse microscopy was used to analyze migration in 2-D. (**B**) Velocity, (**C**) accumulated distance, and (**D**) euclidian distance of at least twenty viable cells was determined by ImageJ. Results of three separate experiments in triplicate were combined and expressed as mean ± SD (**p<0.01, ***p<0.001; one-way ANOVA with Bonferroni correction LPA-treated versus untreated).

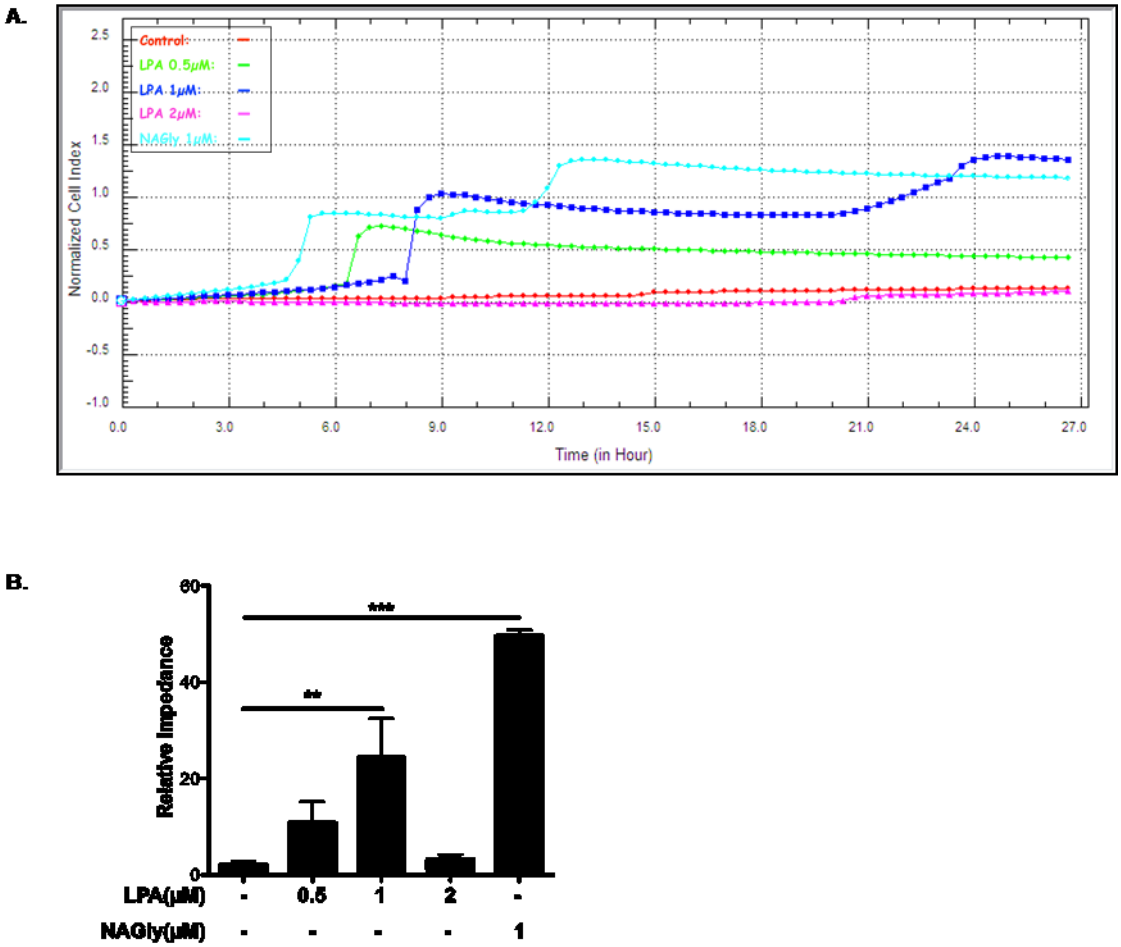

Fig 8. LPA induces chemotaxis of BV-2 microglia cells

(**A-B**) Chemotaxis was analyzed using the xCELLigence system. Serum-starved cells were incubated with different LPA concentrations and allowed to migrate across uncoated Transwell inserts (CIM plates) for 24 h. Chemotaxis (LPA added to lower compartment) was followed in real time by continuous electrical impedance measurement. NAGly was used as positive control. Results of four experiments in triplicate were combined and expressed as mean + SD (**p<0.01, ***p<0.001; one-way ANOVA with Bonferroni correction LPA-treated versus untreated).

In the case of primary microglia, we studied the effect of 1 µM LPA since this was the concentration that induced the most pronounced migrational response for the BV-2 cells. PMM also responded to LPA with increased chemokinesis. Tracks of PMM observed in the absence (left panel) or presence of LPA (right panel) is shown in **Fig. 9A**. LPA treatment increased cell velocity (2-fold) and significantly augmented accumulated (1.8-fold) and euclidian (1.5-fold) distance (**Figs. 9B-D**).

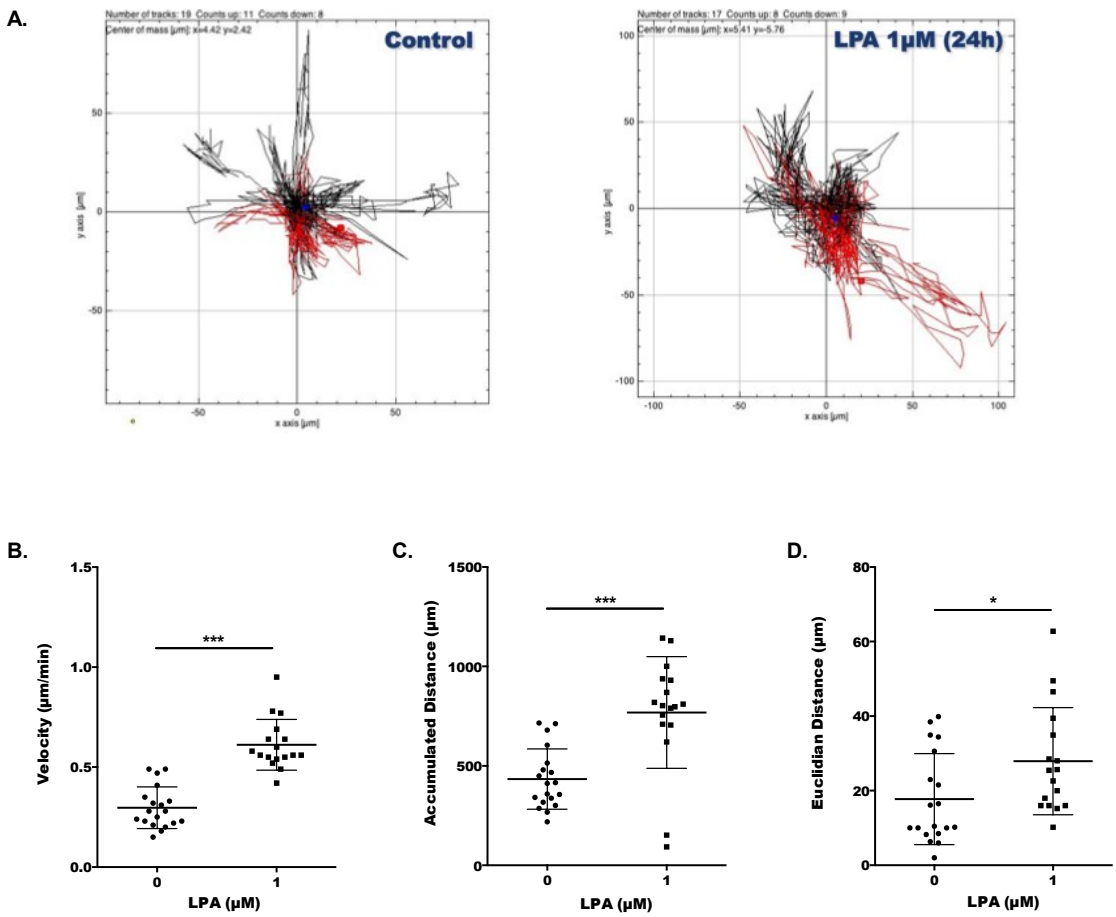

Fig 9. LPA induces chemokinesis of primary microglia

(**A**) PMM were cultured on PDL-coated 24-well plates, serum-starved overnight and treated with 0.1 % BSA or 1 µM LPA. Time-lapse microscopy was used to analyze 2-D migration of at least 20 viable cells per condition. (**B**) Velocity, (**C**) accumulated distance, and (**D**) euclidian distance was determined using ImageJ. Results of two independent experiments (performed in triplicate) were combined and expressed as mean ± SD (*p<0.05, ***p<0.001; one-way ANOVA with Bonferroni correction LPA-treated versus untreated).

2.3 TCLPA5 and CRT inhibit microglia chemokinesis and chemotaxis

Pharmacological antagonism of LPAR5 and PKDs with TCLPA5 and CRT0066101 respectively, effectively diminished chemokinetic parameters (velocity, accumulated and euclidian distance) of BV-2 cells back to baseline levels (**Fig. 10A-C**). Chemotaxis experiments using the xCELLigence system (**Fig. 10D**) revealed that both inhibitors decreased directed cell migration. Statistical evaluation of four independent chemotaxis experiments is shown in **Fig. 10E**. From these data it is evident that LPAR5 and the PKD family control the chemokinetic and chemotactic response of BV-2 cells.

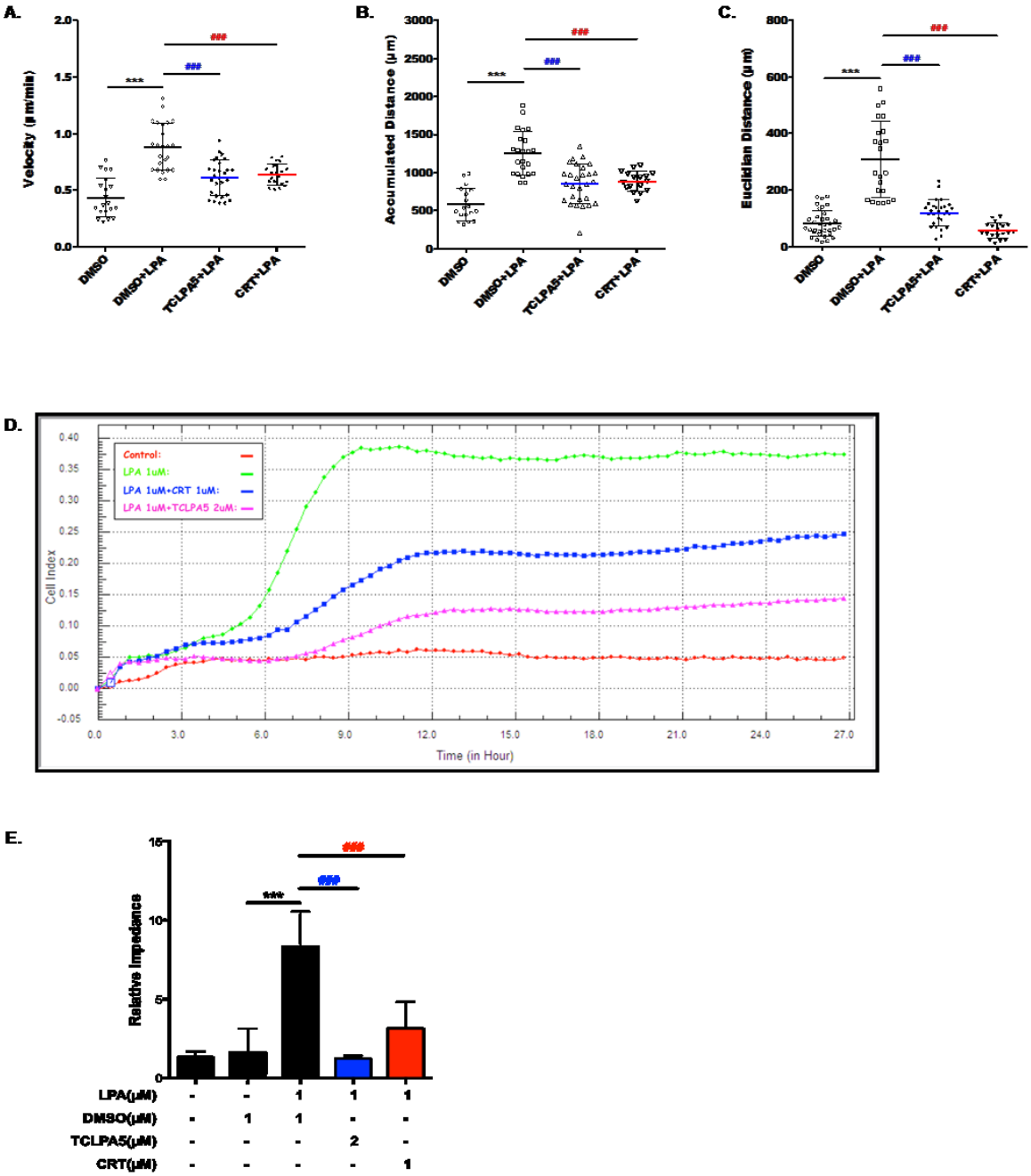

Fig 10. LPAR5 and PKD isoforms control the migrational response of BV-2 cells

BV-2 microglia were cultured in a 24-well plate, serum-starved overnight and treated with DMSO, DMSO plus 1 µM LPA and 1 µM LPA plus TCLPA5 (2 µM) or CRT0066101 (1 µM). Time-lapse microscopy was used to elucidate the effect of the inhibitors on (**A**) velocity, (**B**) accumulated distance, and (**C**) euclidian distance.

(**D, E**) Serum-starved cells were incubated with LPA in the absence or presence of the indicated antagonists and allowed to migrate across Transwell inserts (CIM plates) for 24 h. Real-time cell migration was monitored using the xCELLigence system. Results of four experiments in triplicate are presented as mean +SD (***$p<0.001$ compared to DMSO; $^{###}p<0.001$ cells treated with the inhibitor plus LPA compared to LPA-treated cells; one-way ANOVA with Bonferroni correction).

In line with the results of the experiments with BV-2 cells, both TCLPA5 and CRT0066101 decreased velocity, accumulated and euclidian distance of LPA-stimulated PMM back to values observed under control conditions (**Fig. 11A-C**).

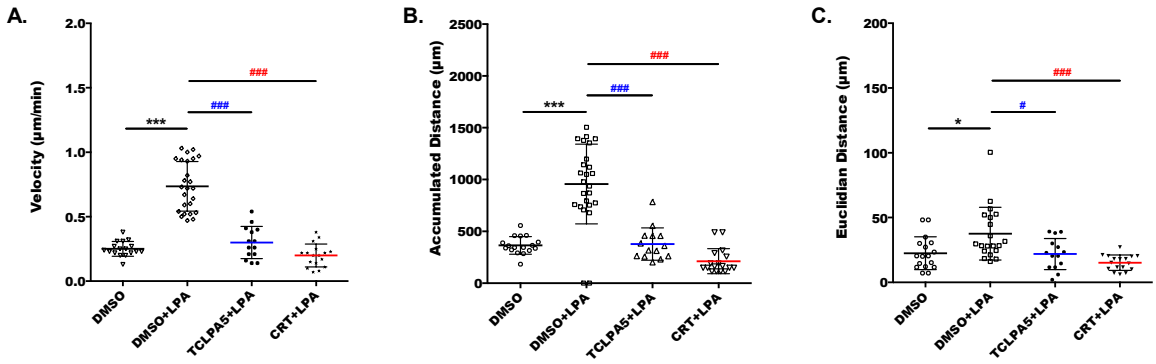

Fig 11. LPAR5 and PKD isoforms control the migrational response of PMM

PMM were cultured in PDL-coated 24-well plates, serum-starved overnight and treated with DMSO, DMSO plus 1 µM LPA or 1 µM LPA plus TCLPA5 (2 µM) or CRT0066101 (1 µM). Time-lapse microscopy was used to analyze 2-D migration. (**A**) Velocity, (**B**) accumulated distance, and (**C**) euclidian distance was determined.

Results of two separate experiments in triplicate are presented as mean +SD (*$p<0.05$; ***$p<0.001$ compared to DMSO; $^{\#}p<0.05$; $^{\#\#\#}p<0.001$ cells treated with the inhibitor plus LPA compared to LPA-treated cells; one-way ANOVA with Bonferroni correction).

In order to distinguish between the contributions of PKD1 and/or PKD2 to PMM chemokinesis a silencing approach using lentiviral shRNA constructs was adopted. During these experiments, cells transduced with lentiviral expressing non-targeting (scr)-shRNA were used as control. Assessment of the transduction efficacy (**Fig. 12A**) revealed that PKD1 and PKD2 silencing was efficient and was diminished by 80 and 60 %, respectively. Stimulation of (scr)-shRNA transduced cells with LPA (1 µM) resulted in significantly increased velocity, accumulated and euclidian distance (**Fig. 12B-D**). Silencing of PKD1 had no effect on the migrational response of microglia, while silencing of PKD2 reduced all migrational parameters back to baseline levels indicating that this S/T kinase takes a key role in LPA-mediated PMM migration.

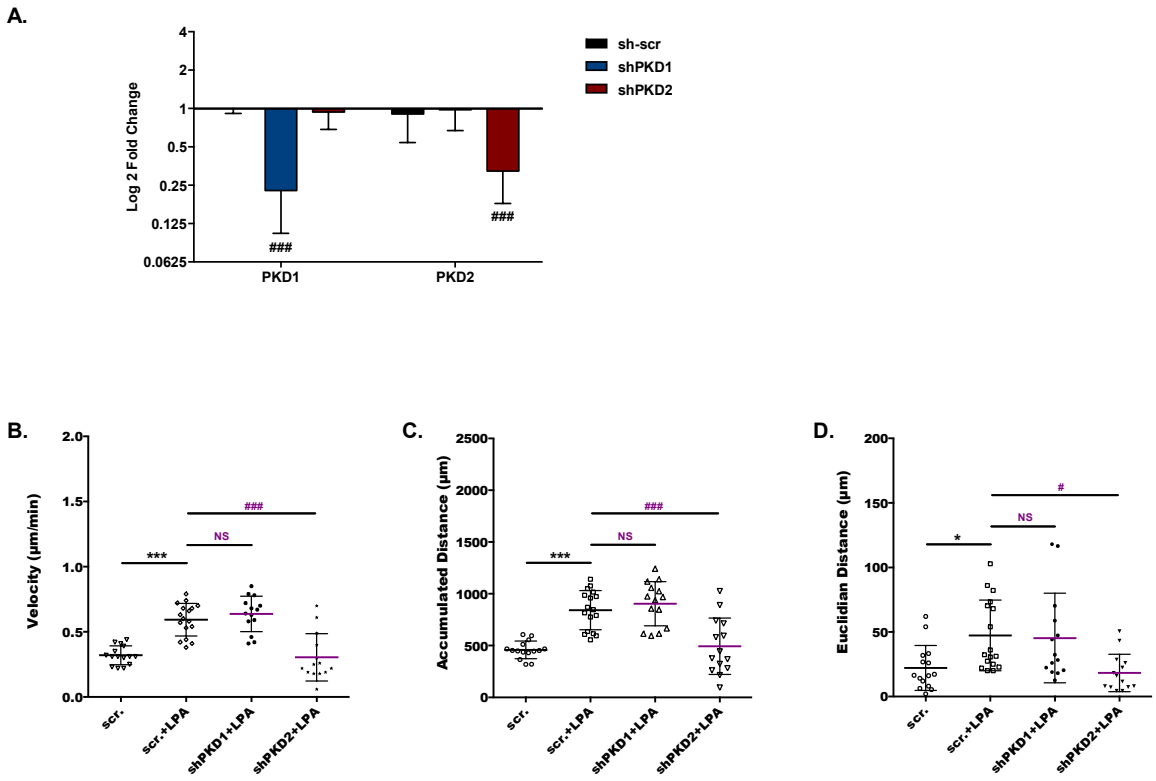

Fig 12. PKD2 is mainly responsible for the migrational response of PMM

PMM were cultured in PDL-coated 24-well plates, and transduced using shPKD1 and shPKD2. Control vectors were used as negative control. (**A**) The silencing efficacy was assessed 72 hours post transduction. The cells were serum-starved overnight and treated with 0.1 % BSA or 1 µM LPA and (**B**) Velocity, (**C**) accumulated distance, and (**D**) euclidian distance were analysed.

Results of two separate experiments in triplicate are presented as mean ±SD (*$p<0.05$; ***$p<0.001$ compared to DMSO; $^{\#}p<0.05$; $^{\#\#\#}p<0.001$ cells treated with the inhibitor plus LPA compared to LPA-treated cells; one-way ANOVA with Bonferroni correction).

2.4 Transcriptional regulation of potential migratory factors by LPA

Several potential targets that may control the microglial chemotactic response were chosen on basis of a literature search to identify genes (listed in Table 3 in the appendix) that support microglia migration and/or invasion and were shown to be under PKD control in other cellular systems. Using customized qPCR arrays for these genes we analyzed the effect of LPA (1 µM) on PMM compared to untreated cells (**Fig. 13**), after a 2, 8, and 24 h incubation. Results of these analyses indicated that the expression of 8 (list genes here) out of 17 spotted genes was significantly increased after LPA treatment. Based on these results, we performed RT-qPCR analysis using primers for each gene, for both BV-2 and primary cells.

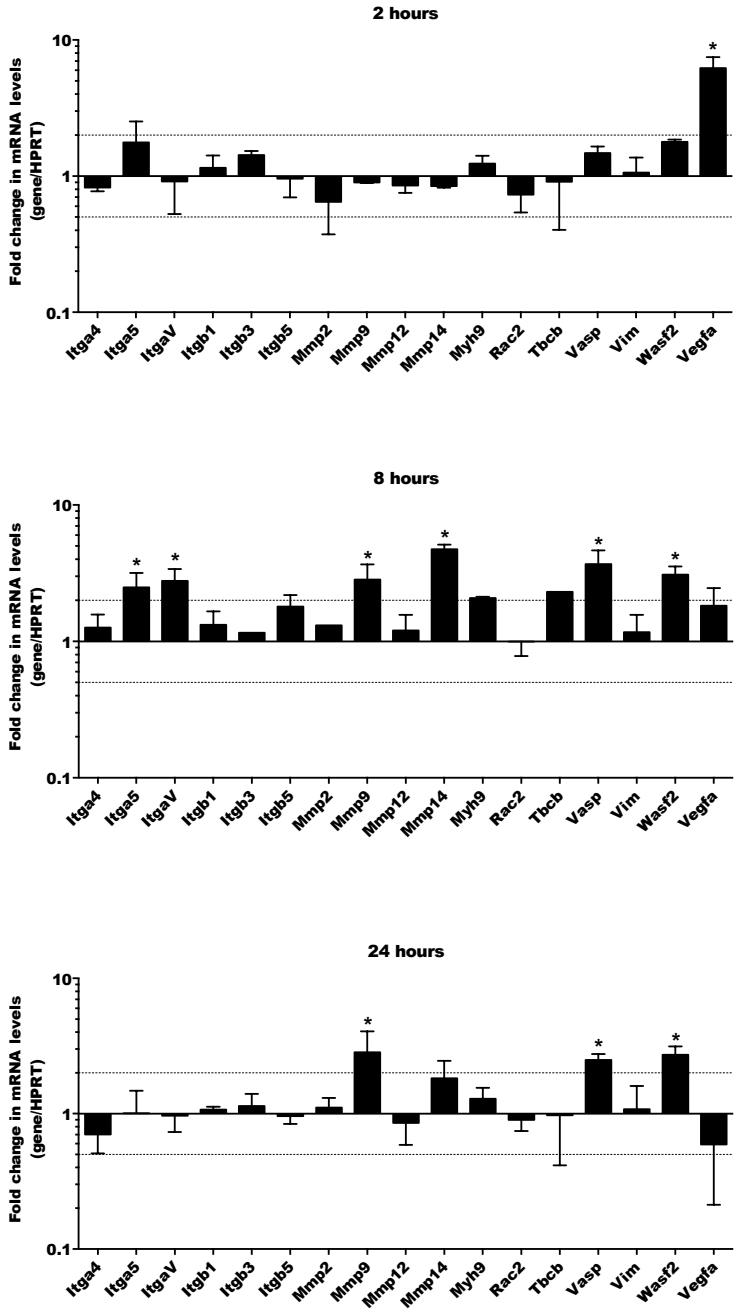

Fig 13. Expression profile of target genes in response to LPA treatment

The effect of LPA on 17 genes in primary microglia was analyzed using customized PCR arrays. Differences in gene expression higher that 2 fold were considered significant (*). The most prominently regulated genes were consequently analyzed by qPCR for both BV-2 and primary microglia cells.

In BV-2 cells qPCR analyses revealed upregulation of Itga5, Itgav, Mmp9, Mmp14, Vasp, and Wasf2 2 h and remained over baseline after 8 h of LPA treatment (except Itgav). At 24 h, Mmp9 and Wasf2 were still significantly higher as compared to untreated cells (**Fig.**

14A). In PMM, LPA treatment (1 µM, 2 h) resulted in upregulation of Itga4, Mmp9, Mmp14, Wasf2 and Vegfa. At 8 h mRNA levels of Itga4, Itga5, Vasp, Wasf2, and Vegfa were still increased >2-fold (**Fig. 14B**) and returned to baseline at 24 h.

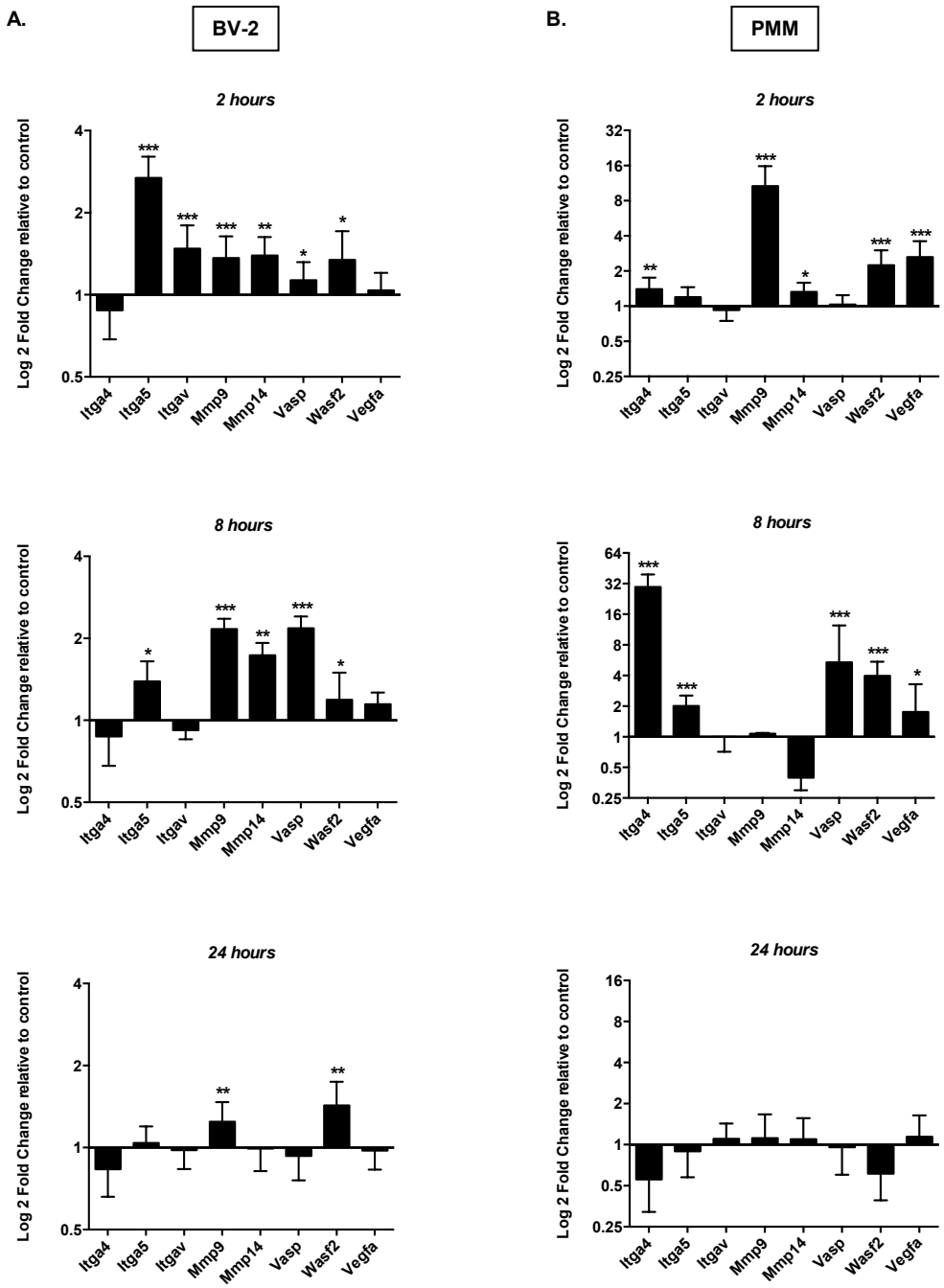

Fig 14. Effect of LPA treatment on expression of potential pro-migratory genes in microglia

(**A**) BV2 cells and (**B**) PMM were seeded onto 24-well plates, serum-starved overnight and treated with LPA (1 µM). At the indicated time points RNA was isolated, reverse transcribed and analyzed by qPCR. Expression ratios were normalized to HPRT. Results of two separate experiments in triplicate were expressed as mean +SD (*p<0.05, **p<0.01, ***p<0.001; one-way ANOVA with Bonferroni correction).

Finally we studied the impact of LPAR5 and PKD family inhibition, on the expression patterns of these eight genes in LPA-stimulated BV-2 and PMM. Inhibitor studies revealed that both antagonists reversed the effects of LPA on Mmp9, Mmp14, Wasf2, Vegfa, Itgav, Itga4, and Itga5 in BV-2 cells (**Fig. 15A**). Comparable results obtained in PMM where LPA-mediated induction of these genes suppressed by both TCLPA5 and CRT (**Fig. 15B**).

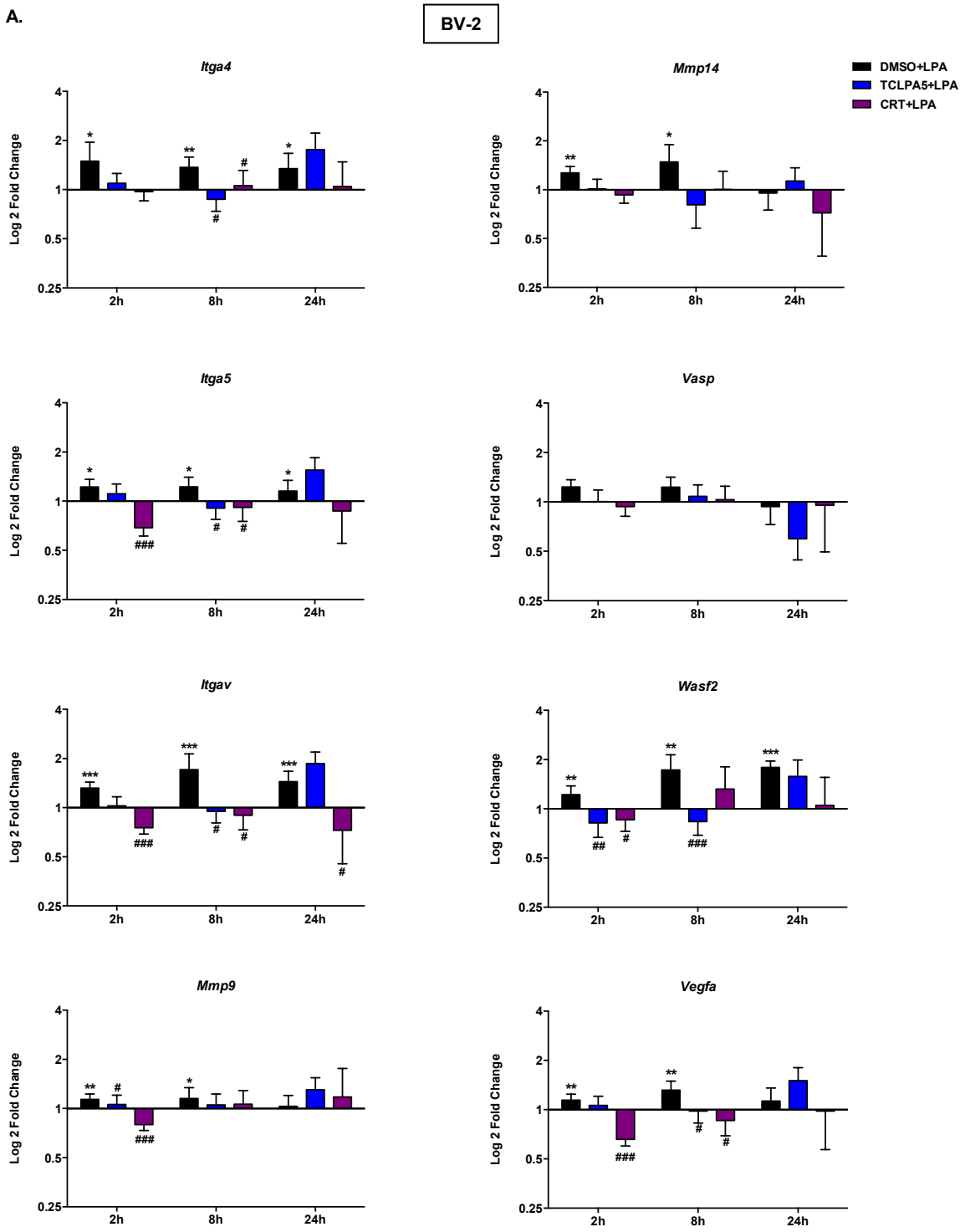

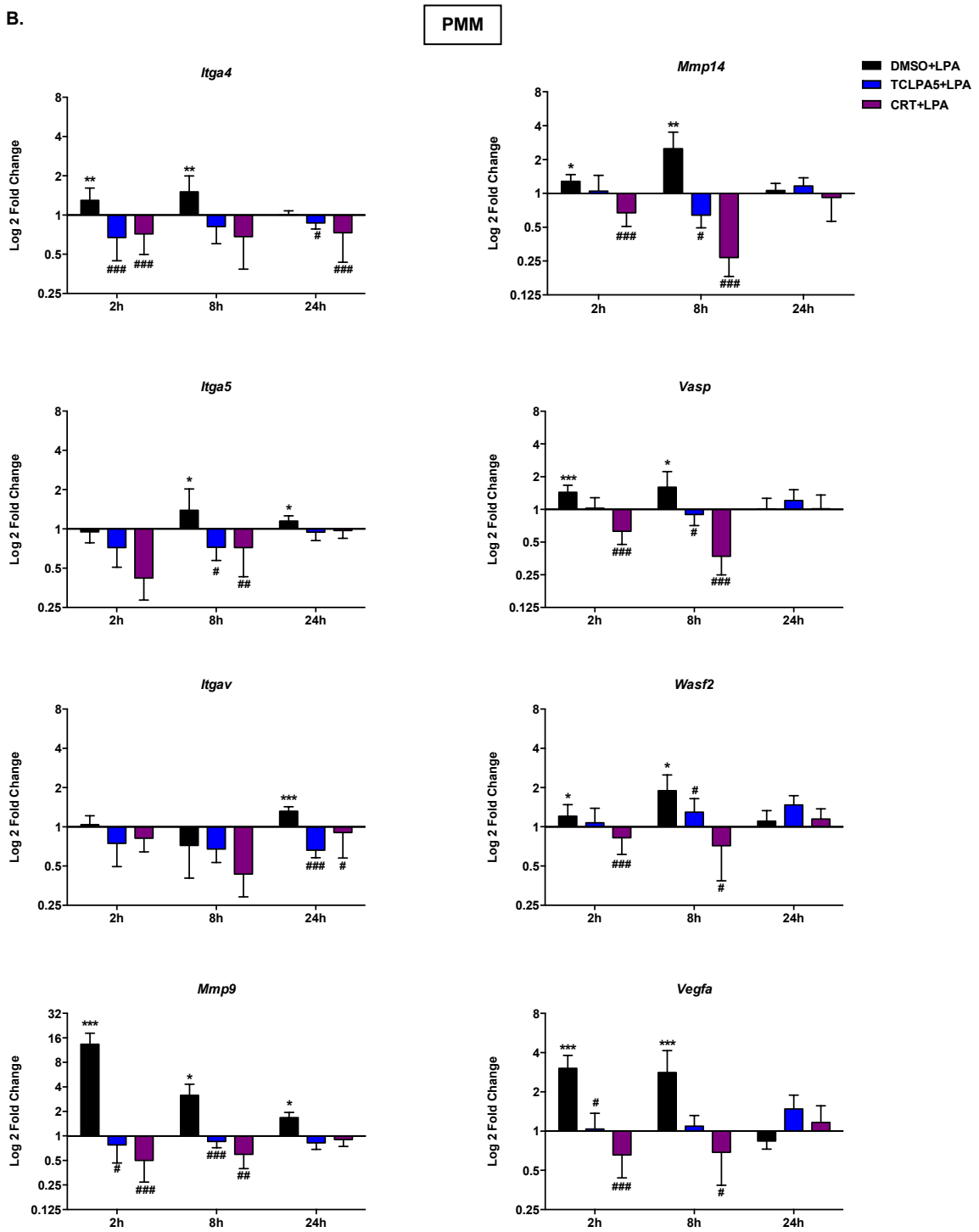

Fig 15. The LPA/LPA5/PKD axis controls expression of migration related genes in microglia

(**A**) BV-2 cells and (**B**) PMM were cultured in 24-well plates, serum-starved overnight and treated with DMSO, DMSO plus 1 μM LPA, and 1 μM LPA plus TCLPA5 (2 μM) or CRT0066101 (1 μM). At the indicated time points cells were scraped, RNA was isolated, reverse transcribed and the gene products indicated were analyzed by qPCR. Expression ratios are normalized to HPRT expression.

Results of two separate experiments performed in triplicate are expressed as mean + SD (*$p<0.05$; **$p<0.01$; ***$p<0.001$ compared to vehicle control; $^{\#}p<0.05$, $^{\#\#}p<0.01$; $^{\#\#\#}p<0.001$ cells treated with each inhibitor plus LPA compared to LPA-treated cells; one-way ANOVA with Bonferroni correction).

3. Effects of LPA on the Inflammatory Response of microglia

During transition from the surveillance-to-effector function in response to external stimuli or injury microglia can (up) regulate a variety of surface receptors and produce multiple secreted factors including pro- and anti-inflammatory cytokines, nitric oxide, reactive oxygen species (ROS), glutamate, and growth factors. In addition, microglia can induce apoptosis and phagocytosis of injured cells and cell debris in order to sustain homeostasis. However, in other circumstances, microglia may phagocytose stressed but still viable neurons or produce toxic substances that may lead to neuronal death. These differential responses are indicative of the dichotomy of microglia reactivity in promoting neuronal survival or degeneration (287). As already mentioned in the introduction, LPA plays an important role during (neuro) inflammatory diseases. However the effects of LPA on the microglial inflammatory response were never addressed before. In order to unravel the role of LPA on the activation state of microglia, we analyzed different M1 and M2 markers using various complementary techniques.

3.1 LPA induces the expression of different M1 markers

As the first step, we evaluated the effects of LPA on BV-2 polarization by Western blot analyses to get an indication about time-dependent changes of M1/M2 marker expression. These analyses revealed that LPA increased the expression of iNOS and COX-2, but did not affect significantly the M2 marker Arg-1 (**Fig. 16A**) (1). As expected, stimulation of BV-2 cells with LPS (20 ng/ml) profoundly increased iNOS and COX-2 levels. In contrast, IL-4 (a polarization signal towards M2) induced Arg-1 without affecting iNOS and COX-2 levels. IL-10 was without effect on iNOS and COX-2 levels but slightly decreased Arg-1 levels. The bar graphs in the right panel represent densitometric evaluation of the indicated protein bands after 3 separate experiments.

Primary microglia were treated with LPA, LPS or IL-4 and analyzed using confocal microscopy for COX-2 and Arg-1 immunoreactivity (1). LPA treatment (1 µM, 24 h) led to increased COX-2 immunofluorescence that was mainly detected in cellular processes (**Fig. 16B,** upper panel). LPS induced a more rounded cell shape of PMM and COX-2 staining was observed along the cell periphery. COX-2 expression was unaffected by IL-4. Both LPA and LPS treatment decreased Arg-1 staining, which was increased in response to IL-4 (**Fig. 16B**, lower panel). The bar graphs in the right panel show the quantification of the fluorescence intensities of 50 cells per condition.

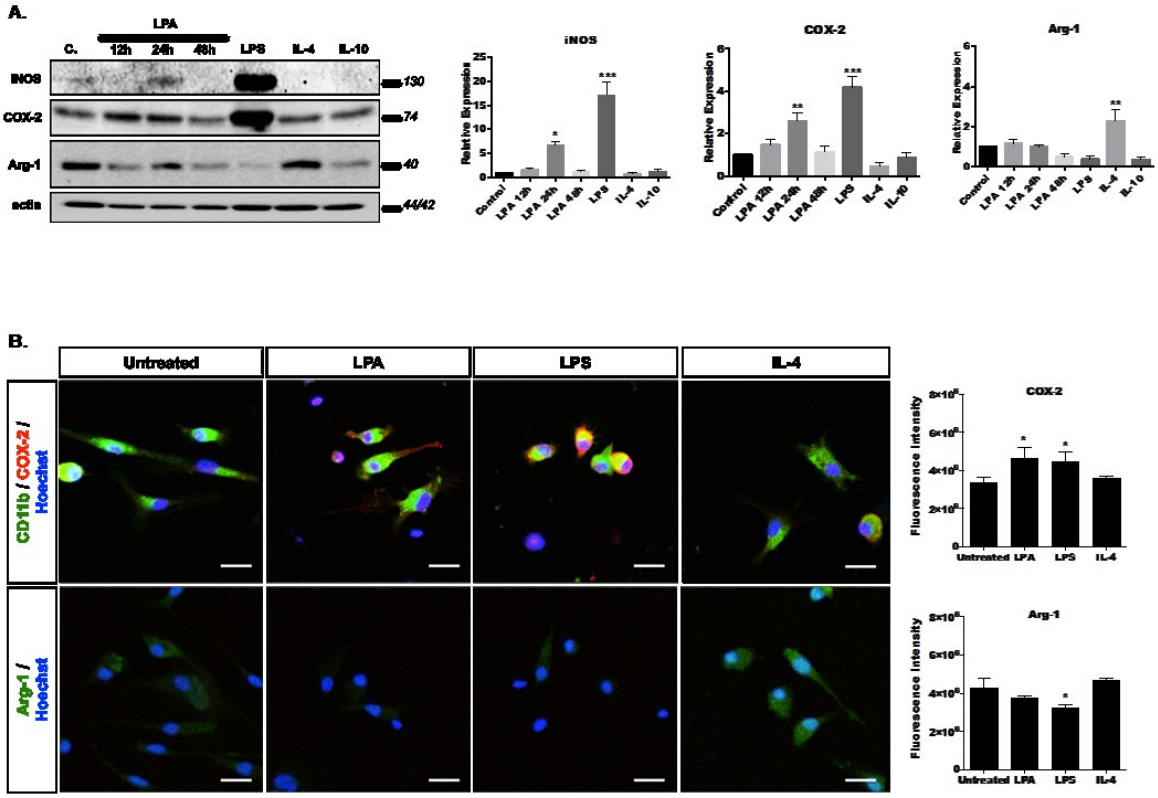

Fig 16. LPA promotes classical activation of BV-2 and primary microglia

(A) Serum-starved BV-2 cells were treated with BSA (0.1%; 'c.'), LPA (1 µM), LPS (20 ng/ml), IL-4 (40 ng/ml) or IL-10 (40 ng/ml)], and cellular protein lysates were analysed by Western blotting. LPS, IL-4, and IL-10 were used to polarize cells to an M1- or M2-like phenotype, respectively (1). One representative plot for each protein and the densitometric analysis (mean + SD; normalized to actin) from four independent experiments is presented. Control = 0.1% BSA.

(**B**) Confocal immunofluorescence microscopy of PMM in the absence or presence of LPA (1 µM, 24 h). LPS (20 ng/ml) and IL-4 (40 ng/ml) were used to induce an M1- or M2-like phenotype, respectively. Cells were stained for CD11b (microglia marker) and COX-2 or Arg-1. Nuclei were counterstained with Hoechst. Scale bars = 20 µm. Results from one representative experiment (out of two) are shown (1).

The results are presented as mean + SD (*p<0.05, **p<0.01, ***p<0.001; one-way ANOVA with Bonferroni correction).

In time-dependent studies, LPA increased iNOS fluorescence intensity in PMM (**Fig. 17**) by 1.6-fold (24 h). Using a double M1/M2 immunofluorescence staining for COX-2 and RELMα, we detected 2.3-fold increased fluorescence intensity for COX-2 (at 48 h), while RELMα fluorescence was reduced by 22 % (48 h). Arg-1 expression was also reduced in response to LPA treatment (by 35%). The right panel shows the quantification of the fluorescence intensities.

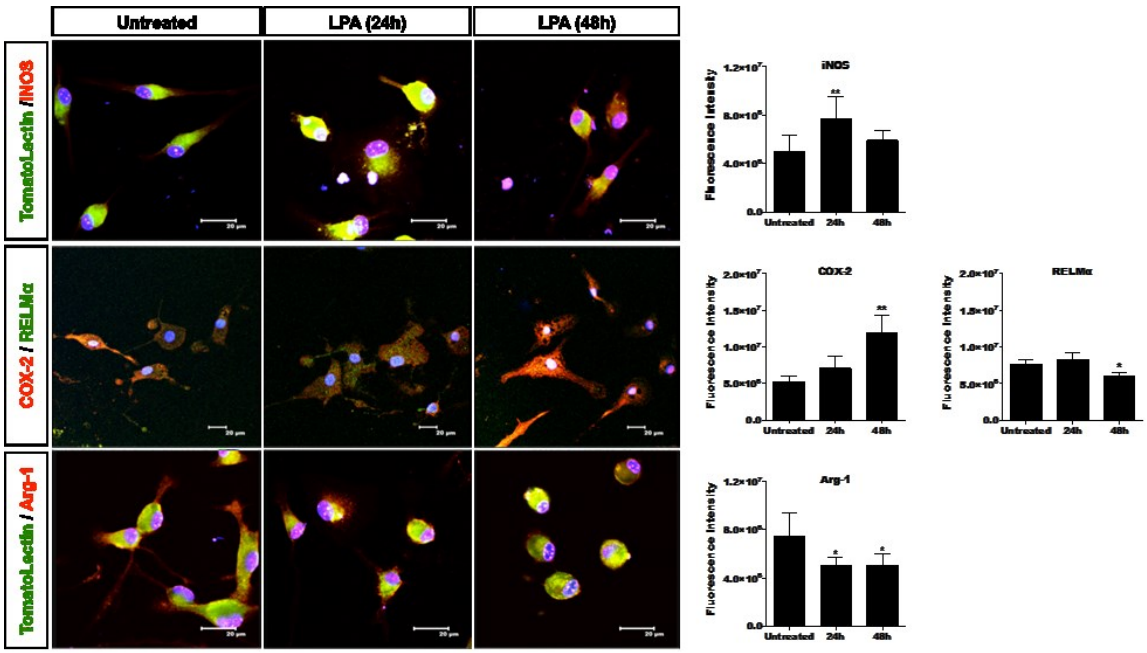

Fig 17. Increased levels of M1 markers in LPA-treated microglia

PMM cultured on chamber slides were incubated in the absence or presence of LPA (1 µM) for 24 and 48 h. Cells were stained for specific inflammatory markers and nuclei were counterstained with Hoechst (1). The fluorescence intensity for each marker was quantitated with ImageJ. At least 50 cells out of 3 different areas per chamber were measured in two independent experiments. Scale bar = 20 µm.

The results are presented as mean + SD (*p<0.05, **p<0.01; one-way ANOVA with Bonferroni correction).

Microglia express different surface receptors some of which are significantly up regulated during an inflammatory response. CD40 (a member of the TNF receptor superfamily) and CD86 (T-Lymphocyte Activation Antigen CD86) are two receptors highly induced in macrophages and microglia under pro-inflammatory conditions. In contrast, the mannose receptor CD206 is connected to an M2 anti-inflammatory phenotype.

Analysis of these surface markers was performed in LPA-treated BV-2 and primary cells using flow cytometry (1). LPA increased the percentage of CD40+ BV-2 cells up to 20% (**Fig. 18A**). LPS (20 ng/ml) induced an increase of CD40+ population from 7 to 29%. CD86 expression was elevated approximately 2-fold in response to LPA (12 and 24 h) while CD206+ cells were reduced from 35 to 22% (24 h). Primary microglia (**Fig. 18B**) showed a comparable though more pronounced response. LPA increased the percentage of CD40+ cells from 6 to 39% (48 h), while LPS increased CD40+ cells up to 67%. The CD86+ cell population reached the 29% (12 h) and then decreased to ≈ 12% (48 h). On the contrary, the CD206+ population was decreased from 17 to 6% (48 h).

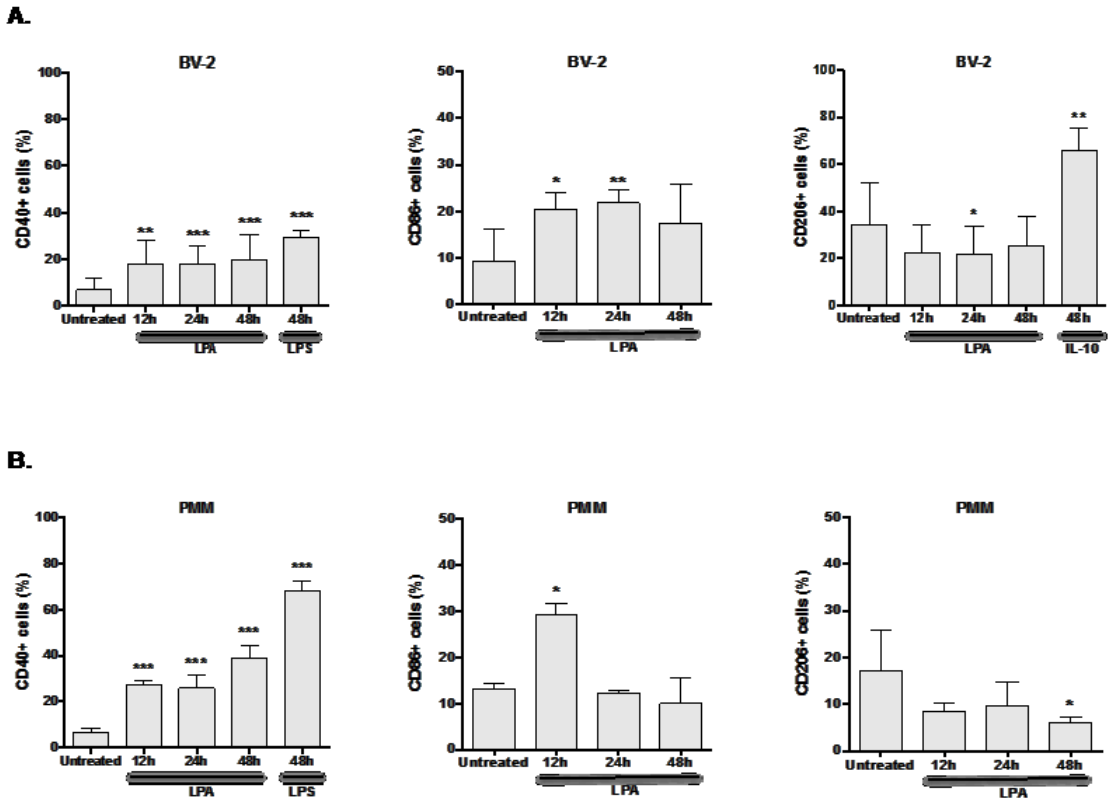

Fig. 18. **LPA induces a pro-inflammatory microglia phenotype**

(A) Serum-starved BV-2 cells (o/n) were treated with 1 µM LPA for the indicated time points. LPS (20 ng/ml) and IL-10 (40 ng/ml) were used as positive controls to induce M1- and M2-like phenotypes, respectively. Cells were stained with PE anti-CD40, APC anti-CD86 or PE anti-CD206 and analyzed using a FACSCalibur Flow Cytometer (1). Results (6 separate experiments in triplicate) are expressed as mean + SD (*p<0.05, **p<0.01, *** p<0.001; one-way ANOVA with Bonferroni correction).

(B) Serum-starved PMM (o/n) were cultivated in the presence of LPA (1 µM) for the indicted times. LPS was used as a positive control. Cells were stained with PE-conjugated anti-CD40, APC-conjugated anti-CD86, or PE-conjugated anti-CD206 antibodies and analyzed using a Guava easyCyte 8 Millipore Flow Cytometer (1). Results from three individual preparations (measurements performed in duplicate) are shown as mean values + SD. (*p<0.05, *** p<0.001 compared to untreated cells; one-way ANOVA with Bonferroni correction).

3.2 Elevated expression and secretion of pro-inflammatory cytokines / chemokines in LPA-treated microglia cells

Next, we determined the effect of LPA treatment on gene expression and secretion of selected pro-inflammatory cytokines and chemokines that are associated with an M1-like microglia phenotype (288). qPCR analyses revealed that LPA increased transcription of Il1β, Tnfα, and Ccl5 in BV-2 cells. The Cxcl2 transcript was not significantly up regulated,

while Cxcl10 was undetectable at mRNA level. In primary cells, LPA induced a time-dependent transcription of Il1β, Tnfα, Il-6, Ccl5 and Cxcl2 (Cxcl10 levels were undetectable) (**Fig. 19**) (1).

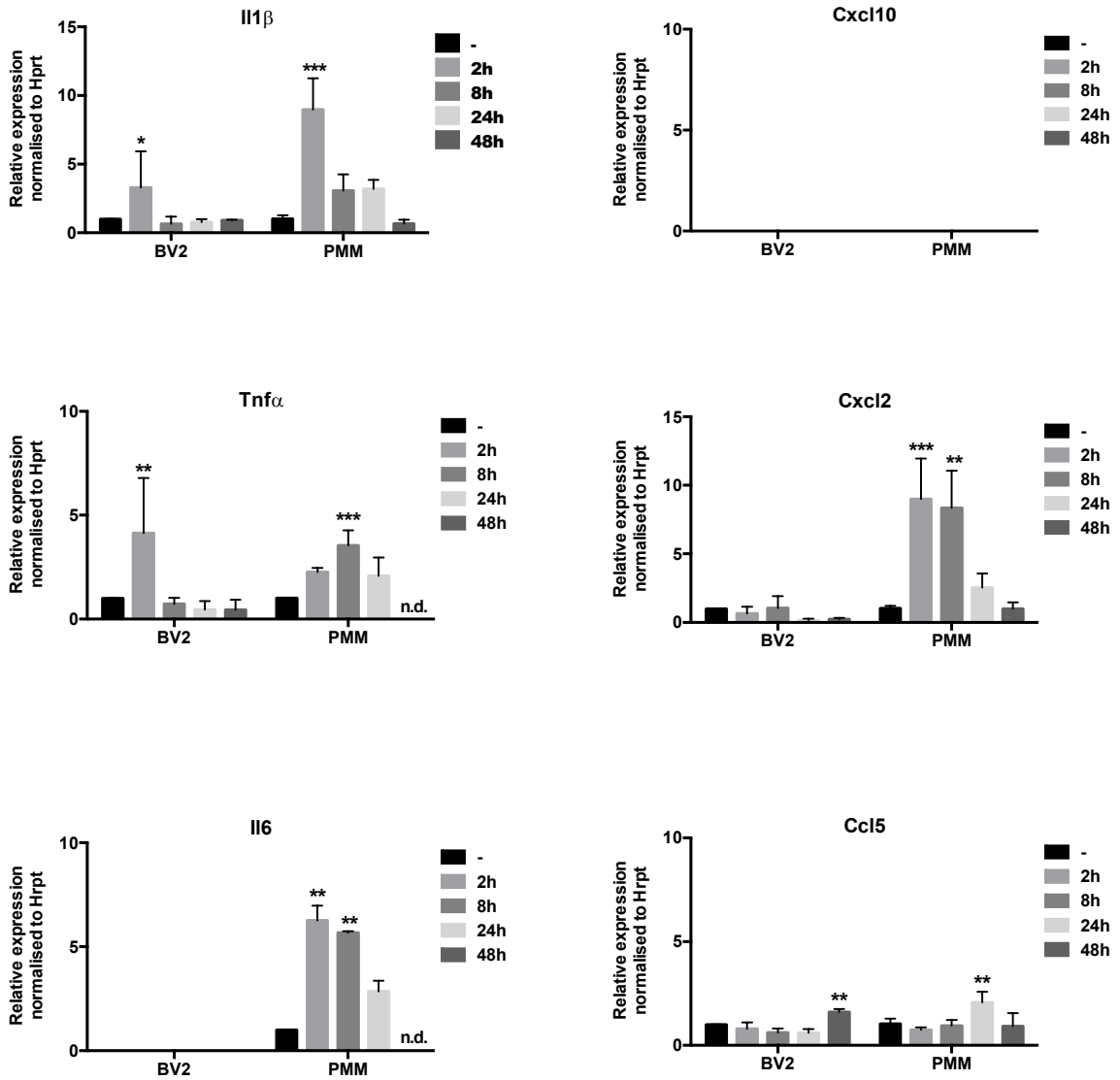

Fig. 19. LPA induces expression of pro-inflammatory cytokines and chemokines

BV-2 and PMM were cultured on 24-well plates and serum-starved (untreated) or incubated in the presence of 1 μM LPA for the indicated times. The expression of different inflammatory cytokines and chemokines was monitored by qPCR and mRNA expression was normalized to Hprt (1). Data are shown as mean + SD from 3 independent experiments performed in triplicate. Expression profiles were determined using the 2^{-ddCt} method.

Data are expressed as mean values + SD (*p<0.05; **p<0.01; ***p<0.001; one-way ANOVA with Bonferroni correction).

In addition we quantitated cytokine/chemokine concentrations in the cellular supernatants using ELISA (1). In both BV-2 and primary cells LPA augmented secretion of IL-1β, TNFα, IL-6, CCL5, CXCL2, and CXCL10 (**Fig. 20**). In BV-2 cells, the analytes were maximally induced at 2 or 8 h post activation. In PMM maximum concentrations were observed between 24 (IL-1β, TNFα, IL-6, CCL5) and 48 h (CXCL2 and CXCL10).

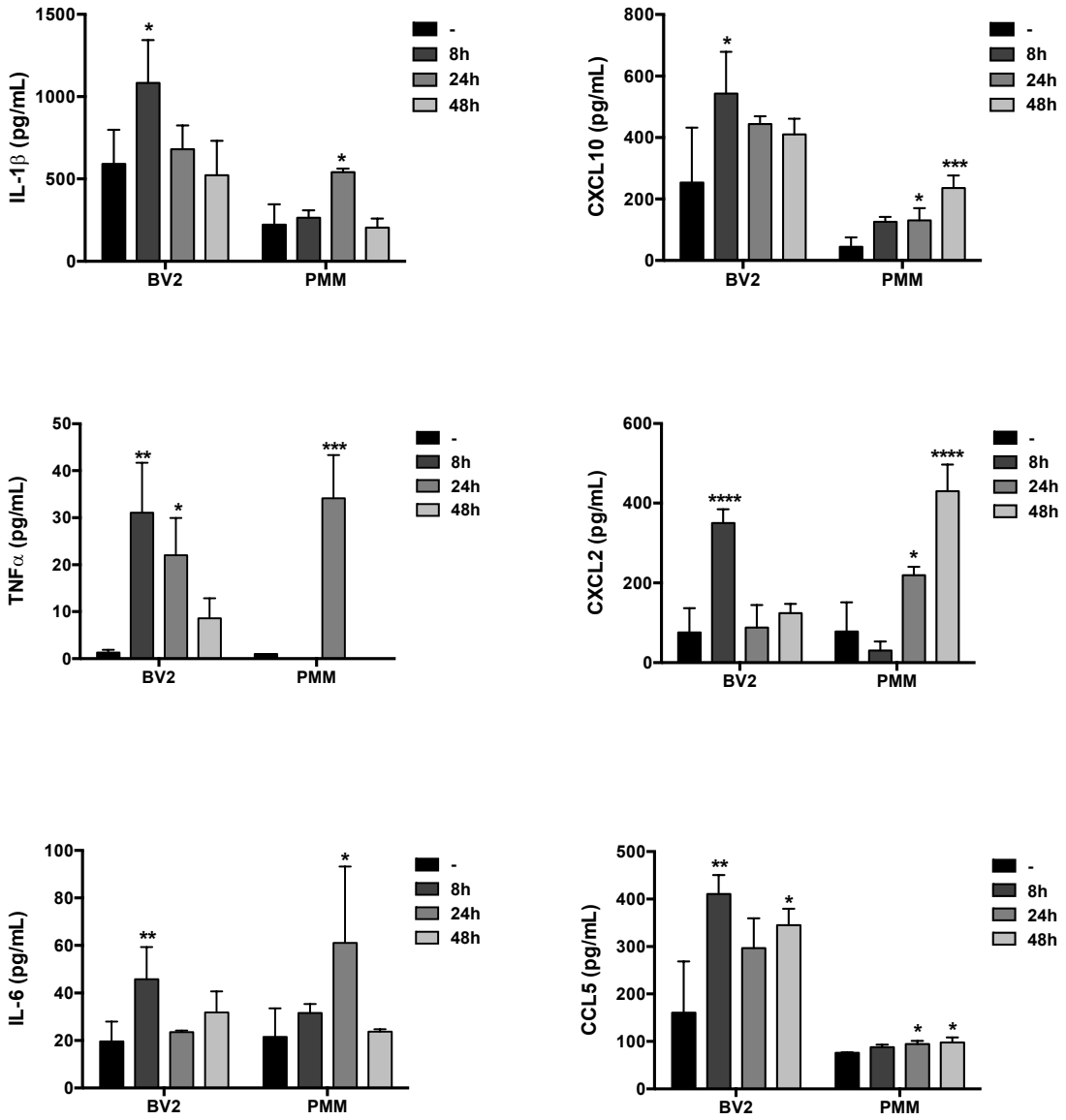

Fig. 20. Increased secretion of pro-inflammatory cytokines and chemokines in response to LPA

Serum-starved microglia cells were treated with LPA (1 μM) for the indicated times. Murine ELISA kits were used to quantitate the concentrations of IL-1β, TNFα, IL-6, CCL5 (RANTES), CXCL10 (IP-10), and CXCL2 (MIP-2) in the cellular supernatants (1). Results shown represent mean + SD from two independent experiments performed in triplicate. Data are expressed as mean values + SD (*p<0.05; **p<0.01; ***p<0.001; one-way ANOVA with Bonferroni correction).

3.3 NO and ROS levels are increased upon LPA treatment

Microglia function normally under basal NO and intracellular ROS levels. In response to increasing concentrations of these mediators the pro-inflammatory function is amplified and microglia can become over activated and contribute to neurotoxicity.

To analyze the intracellular redox status, we measured DCF fluorescence (1). These experiments revealed a 2-fold increase of fluorescence 3 h post LPA addition (**Fig. 21A,** left panel). *tert*-Butyl hydroperoxide (tBHP; an inducer of intracellular ROS formation) was used as positive control (50 μM, 6 h). The DCF response was more pronounced in PMM and time-dependently increased (3.3-fold). In these cells tBHP increased DCF fluorescence by 5.7-fold (Fig. 21A, right panel).

Nitrate concentrations, (a surrogate marker for NO production via iNOS), in LPA-treated BV-2 and primary cells showed a significant yet quantitatively less pronounced increase. Compared to unstimulated cells, LPA treatment induced an increase of 1.3- and 1.2-fold, in BV-2 and PMM, respectively (**Fig. 21B**) (1).

Having clarified that LPA induces a proinflammatory microglia phenotype; I used the murine neuronal cell line CATH.a in order to examine the impact of microglia-secreted factors on neuronal viability. The supernatants from untreated and LPA-treated (concentrations between 0.5 – 10 μM) BV-2 cells were collected after 24 and 48 h and the plated neurons were then incubated for 24 h in the presence of these supernatants.

The percentage of cytotoxicity was calculated based on a given formula (presented in detail in the 2.1 Methods section). These experiments revealed a more than 2-fold increase in cytotoxicity for all LPA concentrations (24 h LPA treated microglia) yet due to the high variance only the 1μM LPA treatment resulted in a statistically significant increase (**Fig. 22A)**. Incubation with the supernatants of LPA treated microglia for 48h revealed a significantly increase in cytotoxicity (at least 2.5-fold) for concentrations between 0.5 and 5μM (**Fig. 22B)**.

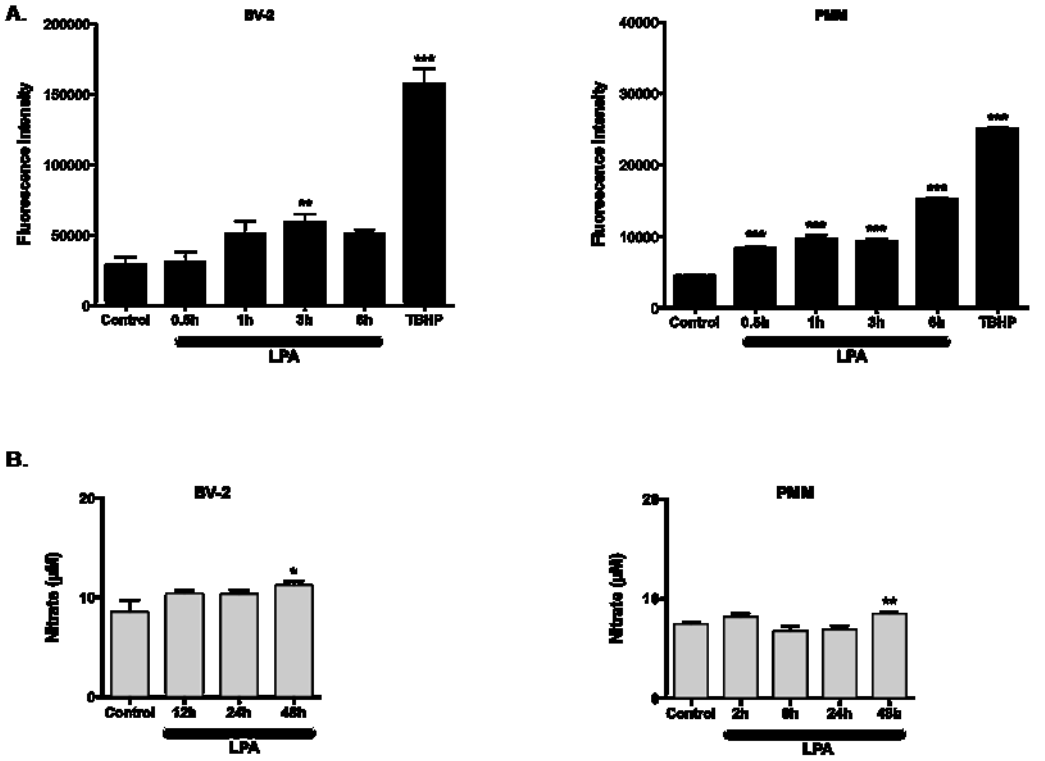

Fig. 21. LPA increases NO and ROS production in BV-2 and primary murine microglia

(A) The cellular redox status was determined using carboxy-H_2DCFDA (1). Serum-starved BV-2 cells and PMM were incubated with carboxy-H_2DCFDA, treated with LPA (1 µM) and the fluorescence intensity was quantitated. Results (4 independent experiments performed in triplicate) are expressed as mean values + SD. (**p ≤ 0.01; ***p<0.001; one-way ANOVA with Bonferroni correction).

(B) Serum-starved cells were treated with LPA (1 µM) for the indicated time periods. The production of NO was determined by measuring nitrate concentrations (1). Data (3 experiments performed in triplicate) are presented as mean values + SD. (*p<0.05; **p<0.01; one-way ANOVA with Bonferroni correction).

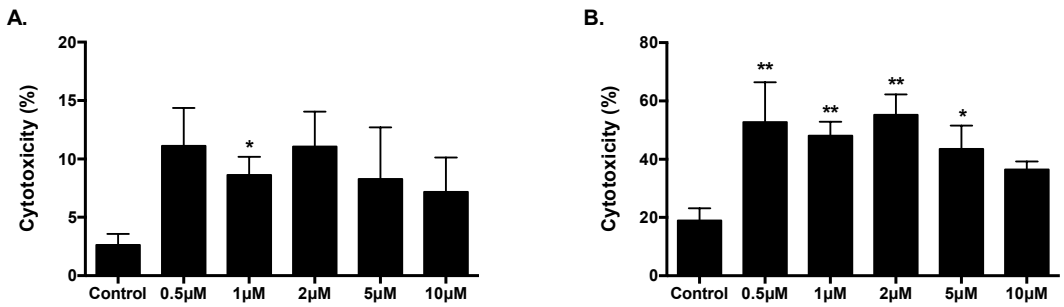

Fig. 22. Conditioned medium from LPA-treated BV-2 cells promotes microglia neurotoxicity

LDH activity was used as a measurement of cytotoxicity. CATH.a neurons were incubated for 24h in the presence of different supernatants collected from LPA-treated BV-2 cells after **(A)** 24h and **(B)** 48h. Results of 2 independent experiments in triplicate are presented as mean values + SD. (*p<0.05; **p<0.01; one-way ANOVA with Bonferroni correction).

3.4 LPAR5 controls the LPA-induced pro-inflammatory phenotype

To get a more detailed picture regarding which member(s) of the LPA receptor family is/are responsible for signal transmission in BV-2 and primary microglia we used the pan LPA receptor inhibitor BrP-LPA and the LPAR5 inhibitor TCLPA5 (1). To the best of our knowledge no LPAR6 inhibitor is currently commercially available. In BV-2 cells, BrP-LPA reduced LPA-induced COX2 expression (statistically not significant) and increased Arg-1 expression levels (**Fig. 23,** upper left panel). COX-2 activation by LPA was reduced by TCLPA5 at both time points analyzed (**Fig. 23;** lower panel**)**. During the experiments where the LPAR5 antagonist was studied, LPA activation was performed in the presence of DMSO to account for potential inadvertent effects mediated by the vehicle. Bar graphs present the densitometric analysis of immunoreactive bands (3 separate experiments).

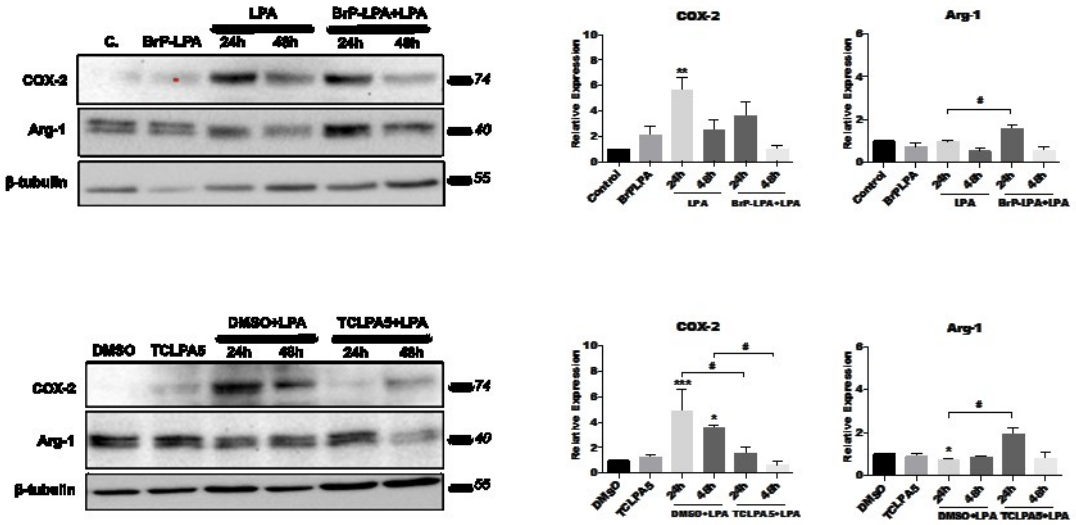

Fig. 23. Inhibition of LPAR5 suppresses the LPA-induced pro-inflammatory phenotype in BV-2 cells
Serum-starved BV-2 cells were treated with LPA in the absence or presence of BrP-LPA (5 μM; upper panel) or TCLPA5 (5 μM; lower panel) added 2 h prior to LPA addition. COX-2 and Arg-1 response was monitored using Western blotting (1). One representative plot for each protein and the densitometric analysis (mean + SD) from four independent experiments is presented. (**p<0.01; ***p<0.001; $^{\#}$p<0.05, inhibitor compared to LPA-treated cells; one-way ANOVA with Bonferroni correction).

To confirm the involvement of LPAR5 in primary cells as well, we performed immunofluorescence staining and analyses using confocal microscopy (**Fig. 24**). These experiments revealed the expected induction of iNOS and COX-2 in response to LPA (1 μM; 24h), while the M2 markers Arg-1 and RELMα were decreased. In response to

TCLPA5, iNOS and COX-2 expression was significantly reduced with Arg-1 and RELMα being unaffected (slightly yet not significantly increased). The right panel shows the quantification of the fluorescence intensities for the corresponding micrographs (1).

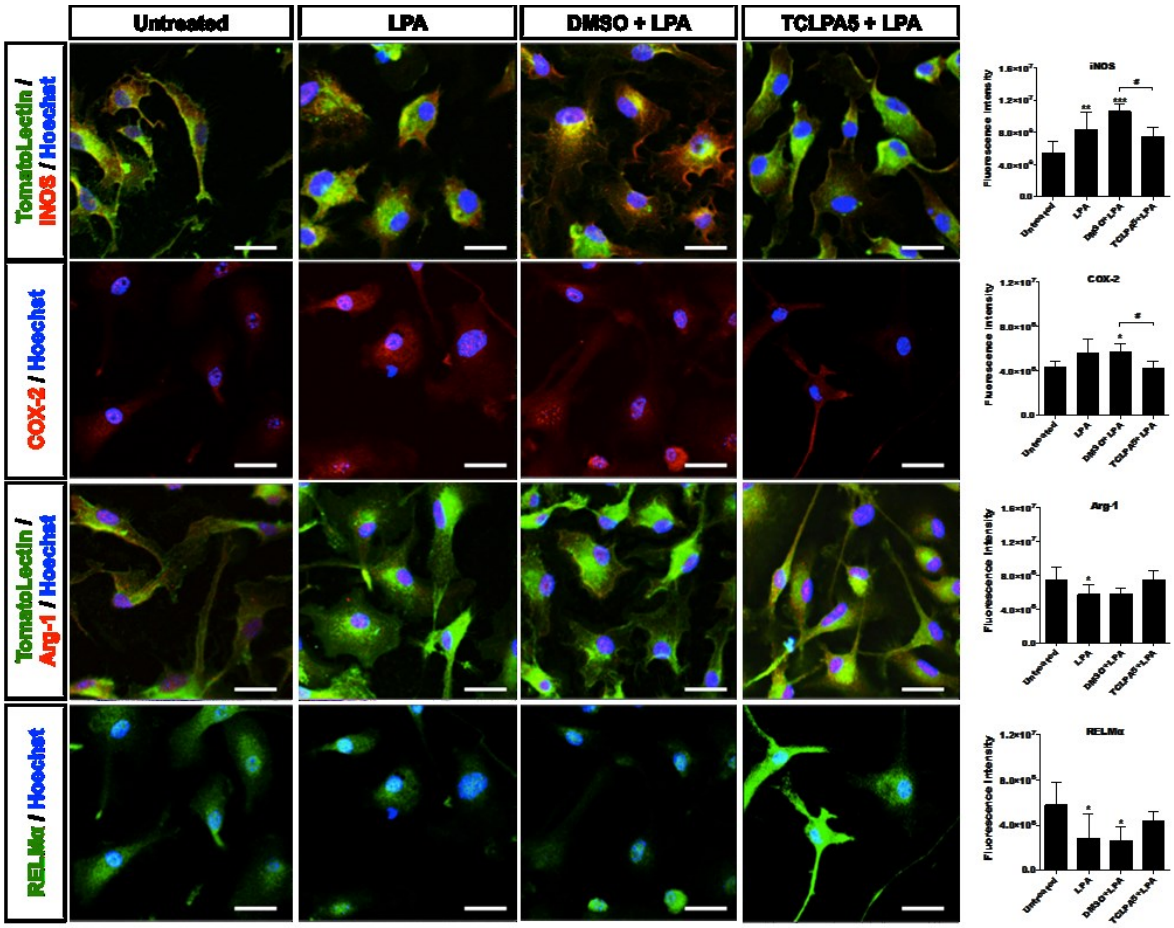

Fig. 24. LPAR5 controls the LPA-induced pro-inflammatory phenotype in primary microglia
PMM were incubated in the presence of vehicle (DMSO), LPA (1 µM) or LPA plus TCLPA5 (5 µM; added 2 h prior to LPA addition) for 24 h. Cells were stained for iNOS, COX-2, Arg-1 or RELMα and visualized using confocal microscopy (1). Fluorescence intensity was quantitated with ImageJ. At least 50 cells out of 3 different areas per chamber were measured. Scale bar = 20 µm. Results (three independent experiments) are presented as mean + SD (*p<0.05; ***p<0.001; $^{\#}$p<0.05 inhibitor compared to LPA-treated cells; one-way ANOVA with Bonferroni correction).

Surface marker expression analyses in LPA-stimulated BV-2 in the absence or presence of BrP-LPA and TCLPA5 is shown in **Fig. 25** (1). CD40 expression was lower in the presence of BrP-LPA (though not significant) whereas CD86 levels were significantly decreased at all time points analyzed (**Fig. 25A**). The percentage of CD206+ cells was unaffected by BrP-LPA. The presence of TCLPA5 during LPA activation significantly

reduced both CD40 and CD86 positive cell populations to baseline levels at all time points analyzed while CD206 was unaffected (**Fig. 25B**).

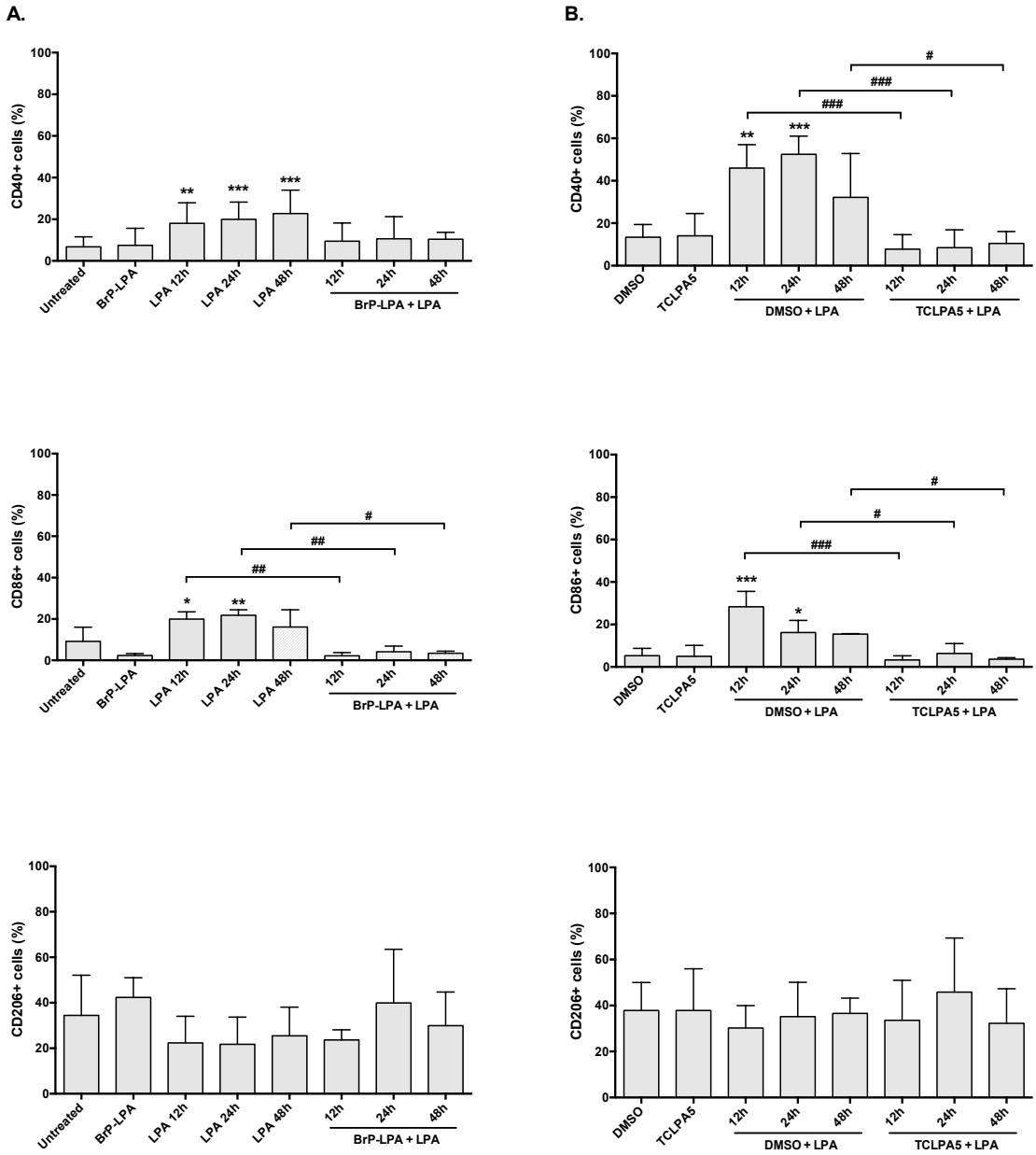

Fig. 25. LPA receptor antagonists attenuate M1 surface markers' expression in BV-2 cells

Serum-starved (o/n) cells were cultivated in the presence of vehicle, LPA (1 μM) or LPA plus (**A**) BrP-LPA (5 μM) and (**B**) TCLPA5 (5 μM) for the indicated times. Inhibitors were added 2 h prior LPA addition. Cells were stained with PE-conjugated anti-CD40, APC-conjugated anti-CD86 or PE-conjugated anti-CD206 antibodies and analyzed using flow cytometry (1). Results from four individual experiments in triplicate are shown as mean values + SD. (*$p<0.05$; **$p<0.01$; ***$p<0.001$ compared to untreated or DMSO-treated cells; $^{\#}p<0.05$; $^{\#\#}p<0.01$; $^{\#\#\#}p<0.001$ inhibitor compared to LPA-treated cells; one-way ANOVA with Bonferroni correction).

Cytokine secretion in response to LPA in BV-2 cells and PMM showed a general tendency to be reduced when TCLPA5 was present (**Fig. 26**). Secretion of all cytokines/chemokines was significantly reduced in BV-2 at one (IL-1β, and CXCL2) or two (TNFα, IL-6, CXCL10, and CCL5) time points (**Fig. 26A**). In line with these results, in primary cells, TCLPA5 inhibited secretion of all the six analytes (**Fig. 26B**).

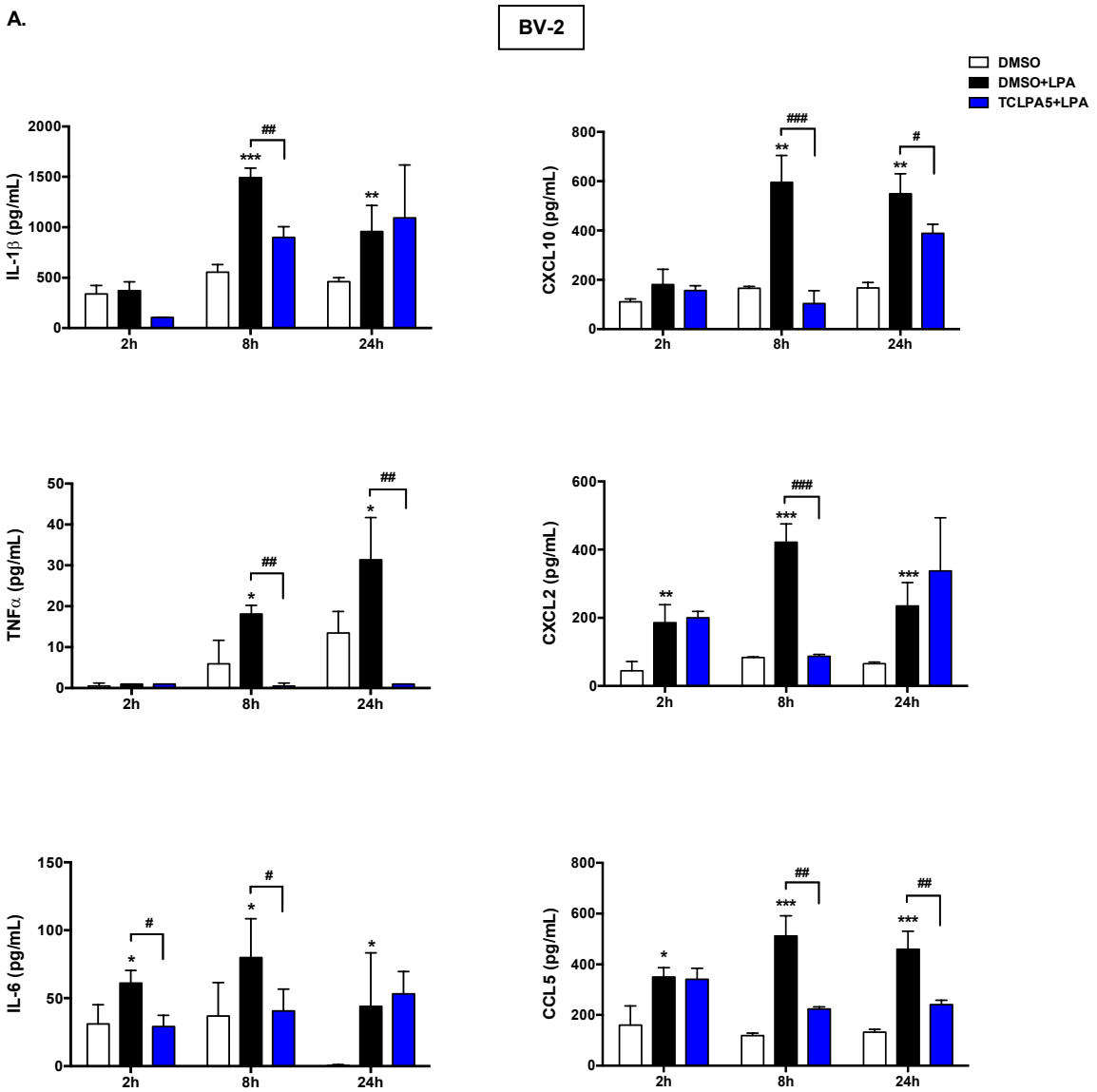

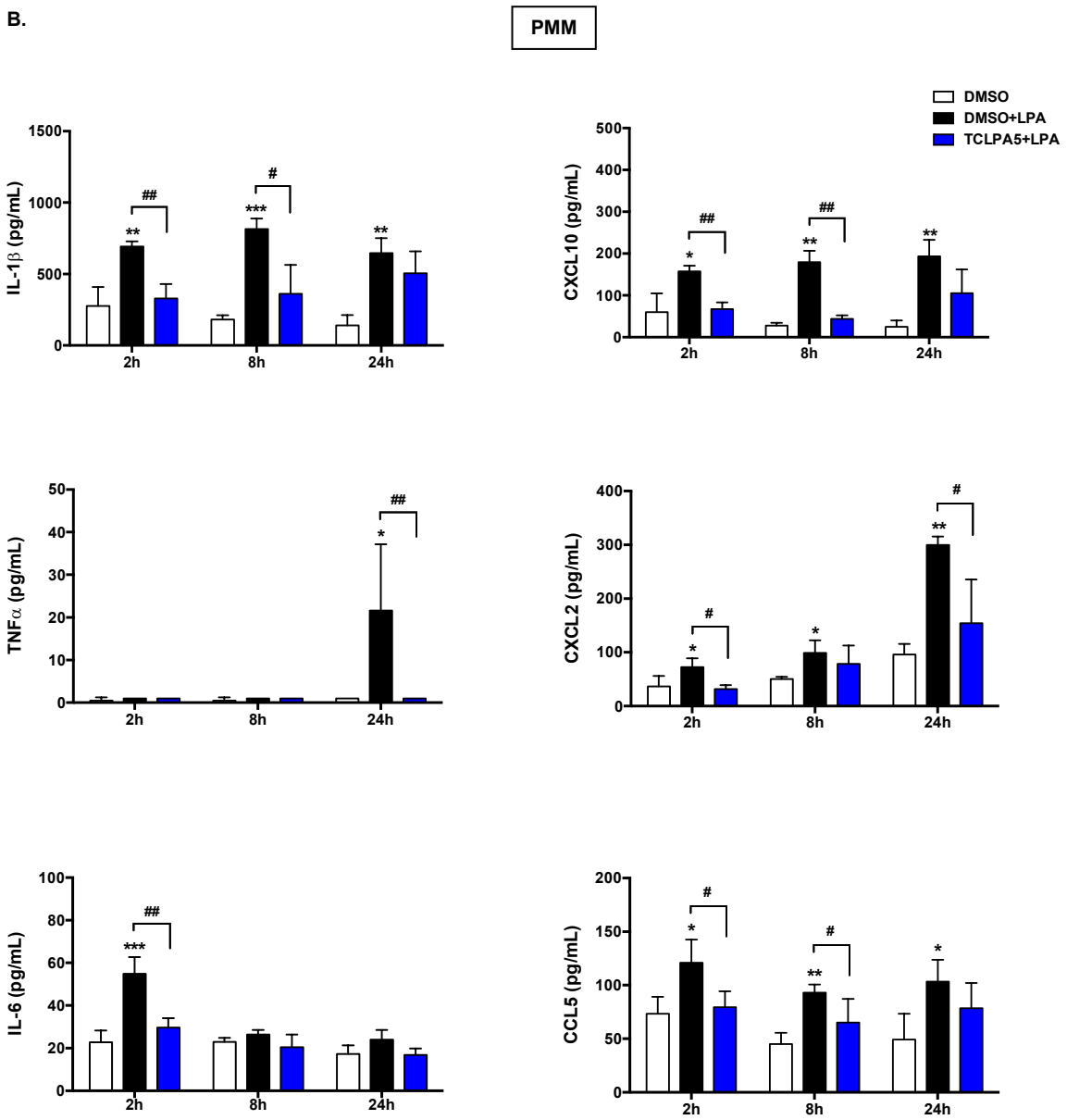

Fig. 26. TCLPA5 inhibits the secretion of pro-inflammatory cytokines and chemokines

(**A**) BV-2 and (**B**) primary murine microglia were cultured on 24-well plates and serum-starved o/n. The supernatants were collected after incubation with vehicle, 1 μM LPA or LPA plus TCLPA5 (5 μM) for the indicated times. ELISA was used to quantitate the concentrations of IL-1β, TNFα, IL-6, CXCL10 (IP-10), CXCL2 (MIP-2), and CCL5 (RANTES) (1).

Results shown represent mean + SD from three independent experiments performed in triplicate (*$p<0.05$; **$p<0.01$; ***$p<0.001$ compared to vehicle control; $^{\#}p<0.05$, $^{\#\#}p<0.01$; $^{\#\#\#}p<0.001$ TCLPA5 compared to LPA treated cells; one-way ANOVA with Bonferroni correction).

Furthermore, we examined the impact of TCLPA5 treatment on ROS and NO formation in both cell types (1). TCLPA5 significantly reduced LPA-mediated DCF fluorescence at 6 h in BV-2 and primary microglia (**Fig. 27A**). Nitrate concentrations were reduced at 48 (BV-2) and 24 h (PMM) by TCLPA5 (**Fig. 27B**).

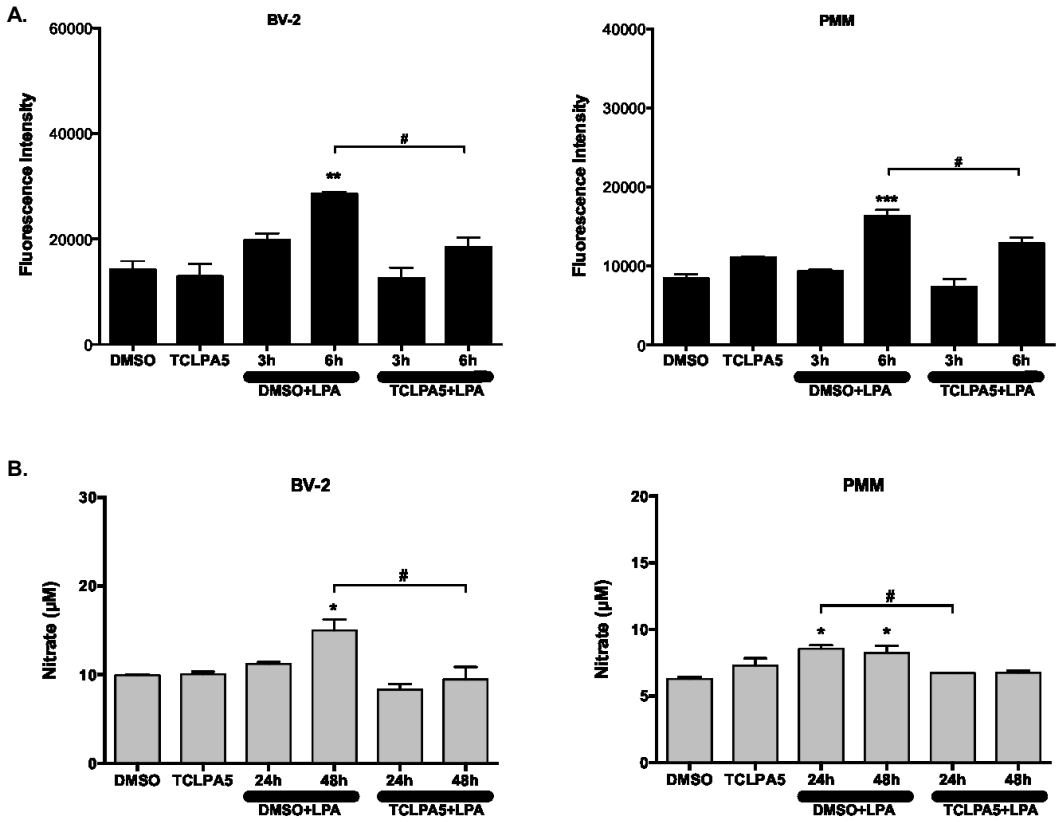

Fig. 27. TCLPA5 suppresses ROS and NO production

(A) The intracellular ROS levels generated by BV-2 and PMM were determined using carboxy-H_2DCFDA. Serum-starved BV-2 and primary murine microglia were incubated with carboxy-H_2DCFDA, treated with vehicle control, LPA (1µM) or LPA plus TCLPA5 (5 µM) for the indicated time periods and the fluorescence intensity was evaluated (1). Results (3 independent experiments performed in triplicate) are presented as mean values + SD. (**p<0.01; ***p<0.001 compared to vehicle; $^{\#}$p<0.05 compared to LPA treated cells; one-way ANOVA with Bonferroni correction).

(B) Serum-starved BV-2 and PMM were incubated with vehicle (DMSO), LPA (1 µM) or LPA plus TCLPA5 (5 µM) for the indicated times and the production of NO was determined by measuring the total nitrate concentration in the supernatants (1). Data (3 independent experiments performed in triplicate) are presented as mean values + SD. (*p<0.05; compared to untreated cells; $^{\#}$p<0.05 compared to LPA treated cells; one-way ANOVA with Bonferroni correction).

Finally, we analyze whether LPAR5 plays a critical role in LPA-induced neurotoxicity and phagocytosis. In BV-2 cells, BrP-LPA could slightly affect but not significantly reduce neuronal toxicity of conditioned medium collected from LPA-treated (1 μM) BV-2 cells (**Fig. 28A**). On the contrary, pharmacological inhibition with TCLPA5 decreased the levels of microglial neurotoxicity from 22% to less than 10% (**Fig. 28B**). In primary cells, BrP-LPA had no effect on increased phagocytosis in response to LPA (1 μM) (**Fig. 28C**). However, LPAR5 inhibition slightly but significantly reduced LPA-induced phagocytosis (**Fig. 28D**).

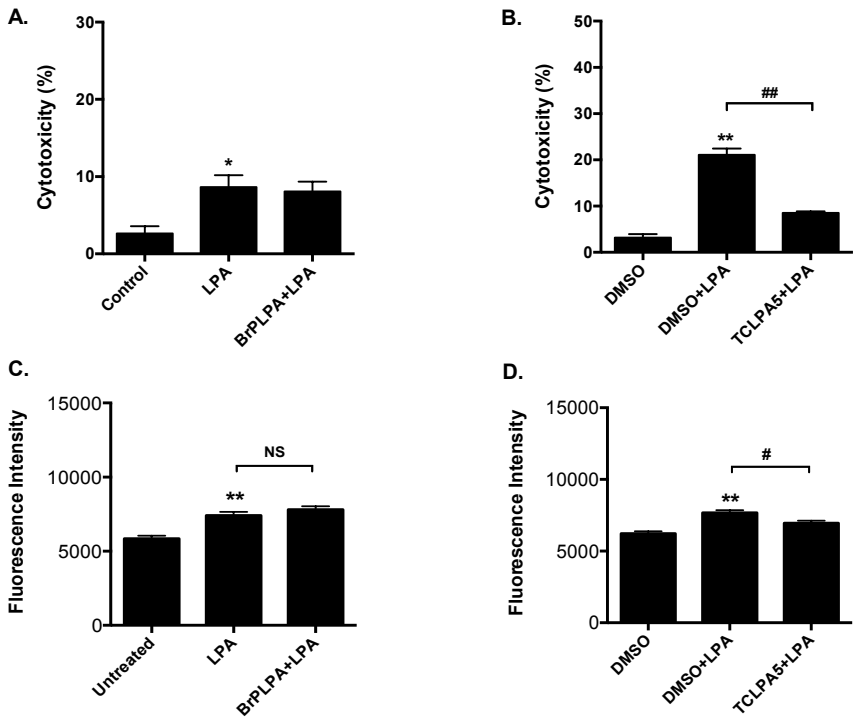

Fig. 28. LPAR5 regulates LPA-induced microglia neurotoxicity and phagocytosis

CATH.a neurons were incubated for 24h with supernatants collected from LPA-treated BV-2 cells in the presence or absence of BrP-LPA **(A)** and TCLPA5 **(B)**. The LDH levels for each sample were measured and cytotoxicity was calculated according to the manufacturer's suggestions.

(C-D) Latex beads coated with fluorescently labeled IgG (IgG PE) were used as a probe for the measurement of the phagocytic process. Serum-starved BV-2 cells incubated with LPA (1 μM) in the presence or absence of the inhibitors for 24h and the fluorescence intensity was measured using a plate reader.

Results of 2 independent experiments in triplicate are presented as mean values + SD. (*$p<0.05$; **$p<0.01$; $^{\#}p<0.05$, $^{\#\#}p<0.01$; compared to LPA treated cells; one-way ANOVA with Bonferroni correction).

4. Signaling Pathways that control the Microglial Inflammatory Response

Inflammation is a multicomponent response to tissue stress, injury and infection, and a crucial point of control is at the level of gene transcription (289). The inducible inflammatory gene expression program is comprised of several regulated sets of genes that encode key functional programs. Three common transcription factors that serve as modulators of the inflammatory response pathway(s) are the NF-κB, AP-1, and STAT.

NF-κB functions as a regulator of the acute phase of inflammation. NF-κB upregulates the expression of cytokines that are considered proinflammatory mediators. These cytokines include IL-1, IL-6, TNF-α, lymphotoxin and IFN-γ. Moreover, IL-1 and TNF-α can activate NF-κB, thereby creating a feedback loop (290). c-Jun, a component of the AP-1 transcription factor complex, regulates the expression of many genes, including inflammatory and cytokine genes. c-Jun/AP-1 proteins can damage the nervous system by upregulation of harmful programs in microglia and are associated with the release of neurodegenerative molecules (291). The STAT family of proteins has multiple functions during inflammation depending on the type of inflammatory inducer. The type of inducer determines which cytokines are synthesized. Those cytokines activate a STAT protein, which either increases or decreases inflammation (292).

4.1 LPA promotes NF-kB, c-Jun and STAT activation in microglia cells

During the previous experiments, we examined the effect of LPA on microglial inflammatory response and we unraveled LPAR5 as a critical receptor that controls the LPA-induced pro-inflammatory phenotype. However, it is unknown the downstream signaling pathway via which LPAR5 excerpts this response. In 2.1 we analyzed the impact of LPA on PKDs and MAPK activation. Inhibition of LPAR5 and the PKD family down-regulated the activation of JNK, AKT, ERK1/2, and p38 MAPK. For the first time in the case of microglia cells, we reported a direct connection between PKDs and MAPK signaling. The MAPKs are implicated in many pathological conditions, however their function in microglia inflammatory response is mainly unknown.

Based on these findings we hypothesized that LPA via the LPAR5-PKD-JNK axis may regulate different transcription factors that lead in production of pro-inflammatory genes, NO, ROS and induce neuronal toxicity.

In the first set of experiments during this part of my thesis I examined the expression of different transcription factors in BV-2 cells after LPA (1 µM) treatment by Western blot analysis. Cells were time-dependently incubated to determine the time course of transcription factor expression/activation. Results of these experiments indicated that LPA induced the activation of p65-NF-kB, c-Jun, and STAT1 and -3 (**Fig. 29**) reaching maximum levels of phosphorylation between 6 and 24h.

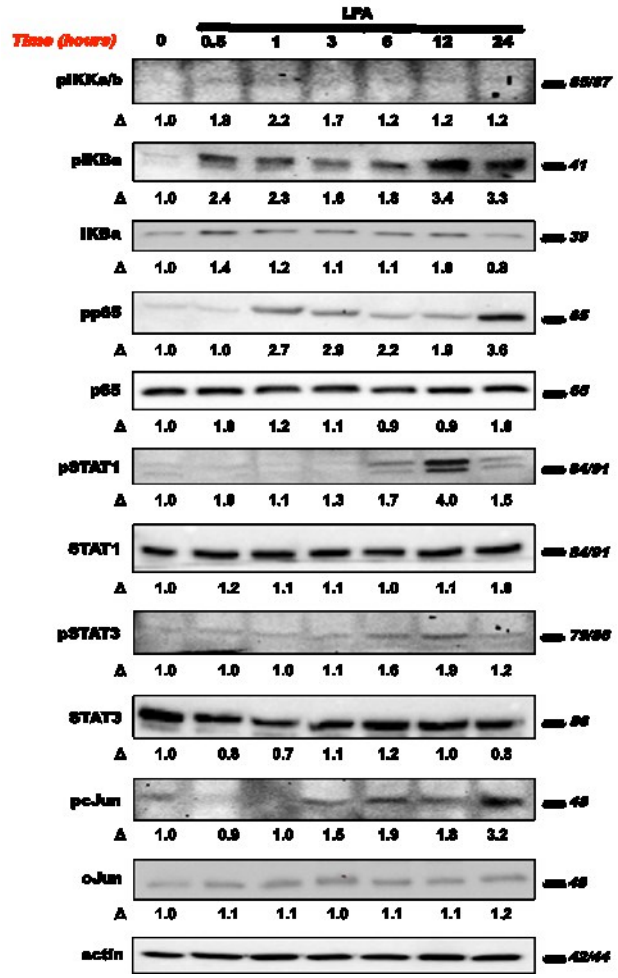

Fig 29. LPA induces the activation of pro-inflammatory transcription factors

Serum-starved BV-2 cells were treated with BSA (0.1%), or LPA (1 µM) for the indicated periods of time and cellular protein lysates were collected. Phosphorylation of p65-NF-kB, c-Jun, STAT1 and STAT3 was analyzed by Western blotting. Protein/loading control ratios were normalized to the ratio of unstimulated microglia. One representative blot out of three independent experiments is shown.

Pharmacologically inhibition of LPAR5 (TCLPA5; 5 µM), PKD1-3 (CRT0066101; 1 µM), and JNK (SP600125; 5 µM) clearly suppressed LPA-induced phosphorylation of all four transcription factors (**Fig. 30A-C**).

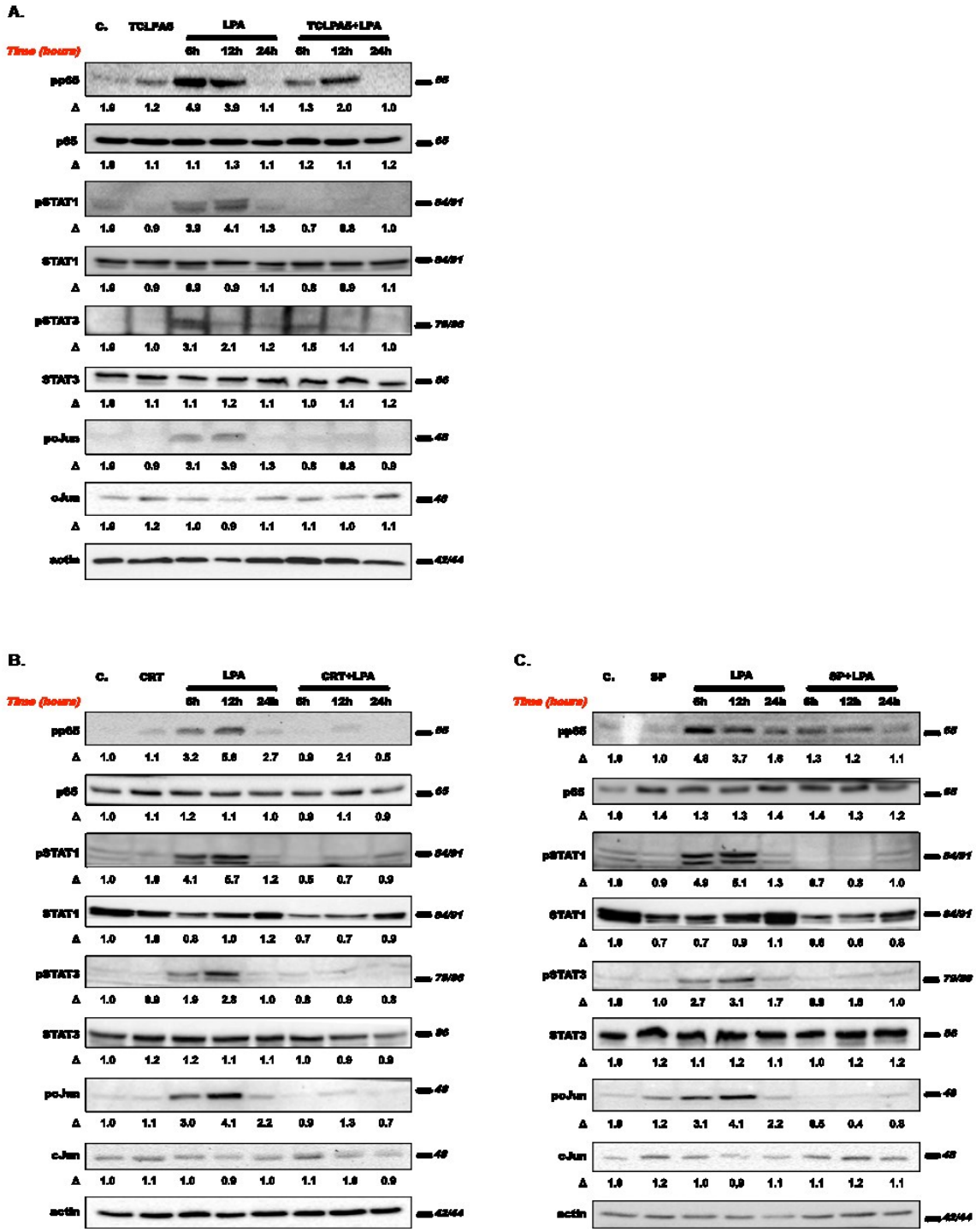

Fig 30. The LPAR5-PKD-JNK axis controls the LPA-induced pro-inflammatory response

BV-2 microglia cells were cultured in 6-well plates and serum starved overnight. Cells were treated with 0.1% BSA, LPA (1 μM), or LPA (1μM) in the presence of (**A**) TCLPA5 (5 μM), (**B**) CRT0066101 (1 μM), or **(C)** SP600125 (5 μM) for the indicated time periods and cell protein lysates collected. The phosphorylation states of p65-NF-kB, c-Jun, STAT1, and STAT3 were detected by Western blotting. Protein/loading control ratios were normalized to the ratio of unstimulated microglia. One representative blot out of three is presented.

In PMM, the response to LPA treatment was more rapid as compared to BV-2 cells. Phosphorylation of p65-NF-kB, c-Jun, STAT1 and STAT3 was detectable already after 2h and started gradually to decline at 24 h (**Fig. 31A**). The phosphorylation of p65-NF-kB remained up until 24 h post LPA-treatment. Inhibition of LPAR5 and PKD1-3 effectively diminished the phosphorylation state of the transcription factors in both analyzed time points (2 and 8h) (**Fig. 31B**).

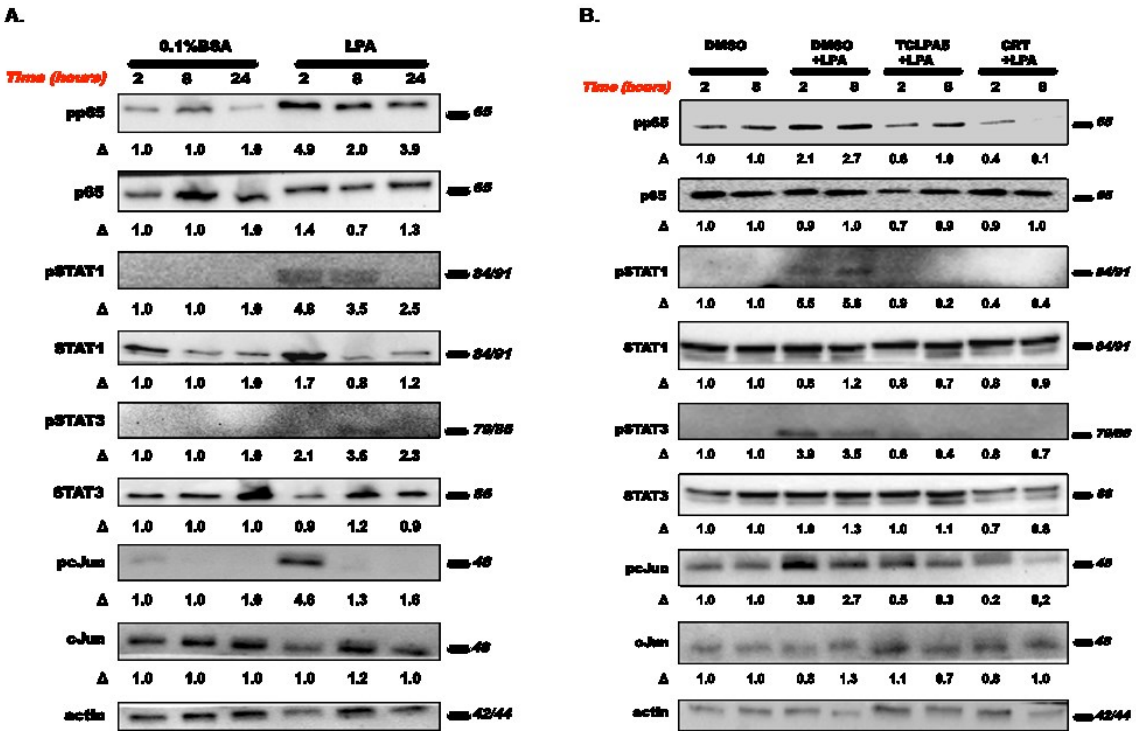

Fig 31. TCLPA5 and CRT abrogate the LPA-induced activation of transcription factors

(A) PMM were cultured in 12-well PDL-coated plates, serum-starved overnight, and treated with 0.1 % BSA or 1 µM LPA for 2, 8, and 24h. (**B**) Cells were treated with DMSO plus LPA (1 µM) in the absence or presence of TCLPA5 (5 µM) or CRT0066101 (1 µM) for the indicated time periods and cellular protein lysates were collected. Cells incubated only with 0.1 % BSA or DMSO were used as negative control.

The phosphorylation state of p65-NF-kB, c-Jun, STAT1, and STAT3 was detected by Western blotting. Protein/loading control ratios were normalized to the ratio of unstimulated microglia. One representative blot out of three separate experiments is shown.

4.2 CRT and SP600125 decreases the LPA-induced expression of M1 markers

In BV-2 cells, treatment with CRT significantly reduced LPA-dependent COX2 expression and increased the levels of Arg-1 expression (**Fig. 32**; upper left panel). SP600125 could

also inhibit COX-2 activation at both time points analyzed and slightly increased Arg-1 expression (**Fig. 32**; lower panel**)**. Bar graphs at the right side of each panel, present the densitometric analysis of immunoreactive bands out of 3 separate experiments.

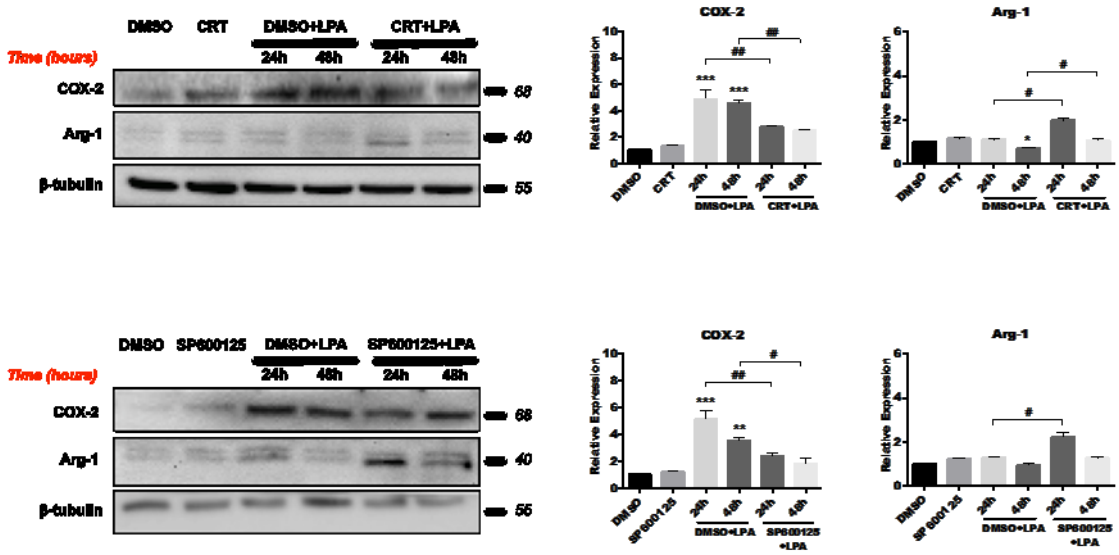

Fig. 32. Inhibition of PKD1-3 or JNK suppresses the LPA-induced pro-inflammatory phenotype

Serum-starved BV-2 cells were treated with DMSO plus LPA (1 µM) in the absence or presence of TCLPA5 (5 µM; upper panel) or SP600125 (5 µM; lower panel) for 24 and 48h. Cell lysates were collected and the expression of COX-2 and Arg-1 was monitored using Western blotting.

One representative plot for each protein and the densitometric analysis (mean + SD) from three independent experiments is presented. (**p<0.01; ***p<0.001; $^{\#}$p<0.05; $^{\#\#}$p<0.01, each inhibitor compared to LPA-treated cells; one-way ANOVA with Bonferroni correction).

In parallel, we also performed immunofluorescence staining and analysis using confocal microscopy (**Fig. 33**). The experiments revealed the expected induction of iNOS and COX-2 in response to DMSO plus LPA (1 µM; 24h), while the M2 markers Arg-1 and RELMα were decreased. In response to CRT and SP600125 inhibition, iNOS and COX-2 expression was profoundly attenuated with Arg-1 and RELMα levels being slightly increased. The right panel shows the quantification of the fluorescence intensities for the corresponding micrographs. The fluorescence intensities were quantitated using the software ImageJ. At least 50 cells out of 3 different areas per chamber were measured.

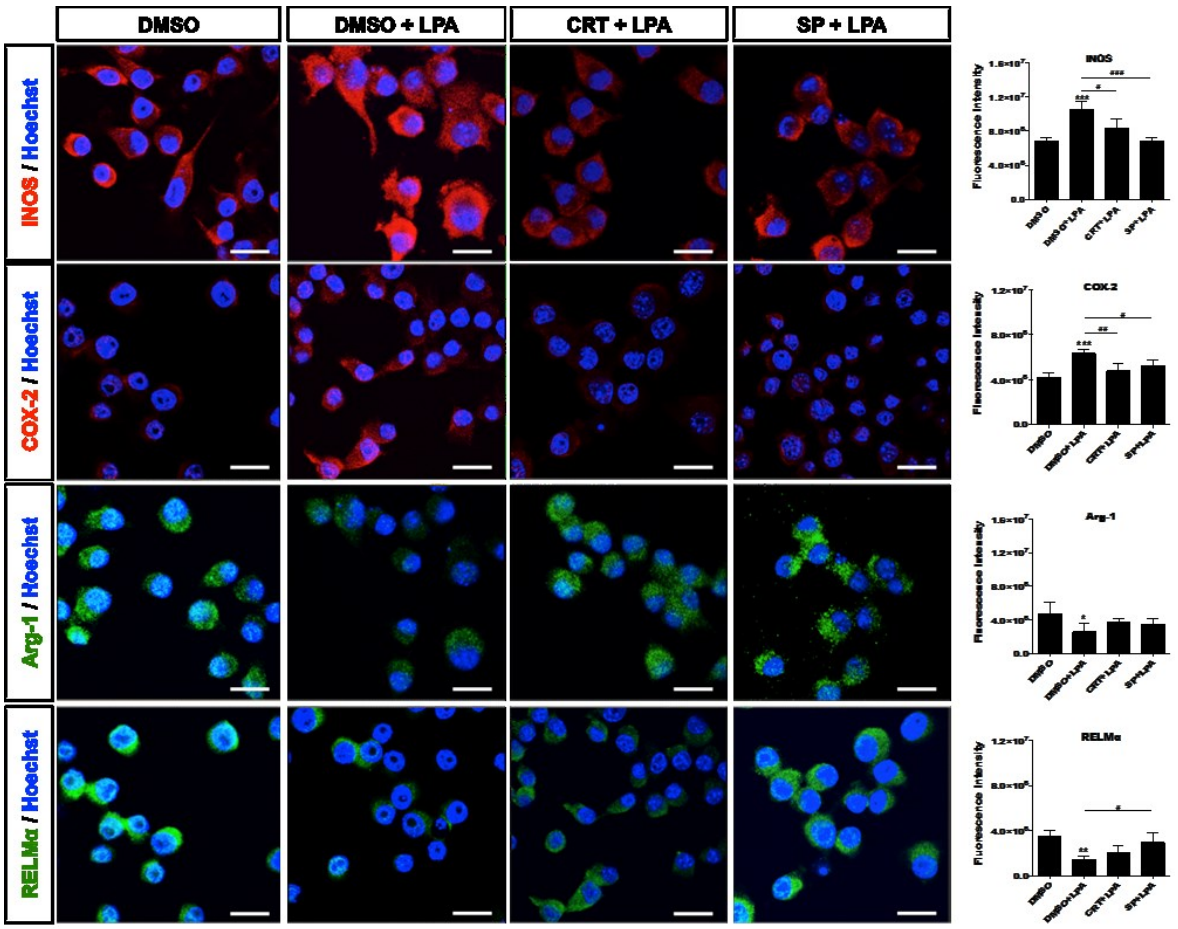

Fig. 33. CRT and SP600125 reduce the expression of M1 markers that are upregulated in response to LPA treatment

PMM were incubated in the presence of vehicle (DMSO), LPA (1 µM) or LPA plus TCLPA5 (5 µM; added 2 h prior to LPA addition) for 24 h. Cells were stained for iNOS, COX-2, Arg-1 or RELMα and visualized using confocal microscopy. Fluorescence intensity was quantitated with ImageJ. At least 50 cells out of 3 different areas per chamber were measured. Scale bar = 20 µm. Results (three independent experiments) are presented as mean + SD (*p<0.05; ***p<0.001; $^{\#}$p<0.05 inhibitor compared to LPA-treated cells; one-way ANOVA with Bonferroni correction).

Using flow cytometry we then analyzed the expression pattern of different surface markers in LPA-stimulated BV-2 cells in the absence or presence of CRT and SP600125 (**Fig. 34**). CD40 and CD86 expression was dramatically decreased in the presence of CRT, whereas CD206 levels were unaffected at all time points analyzed (**Fig. 34A**). The presence of SP600125 during LPA activation significantly reduced CD40+ cells to baseline levels at all time points analyzed. However, in contrast to CRT, JNK inhibition had no effect on CD86+ cell populations. CD206 levels were also unaffected (**Fig. 34B**).

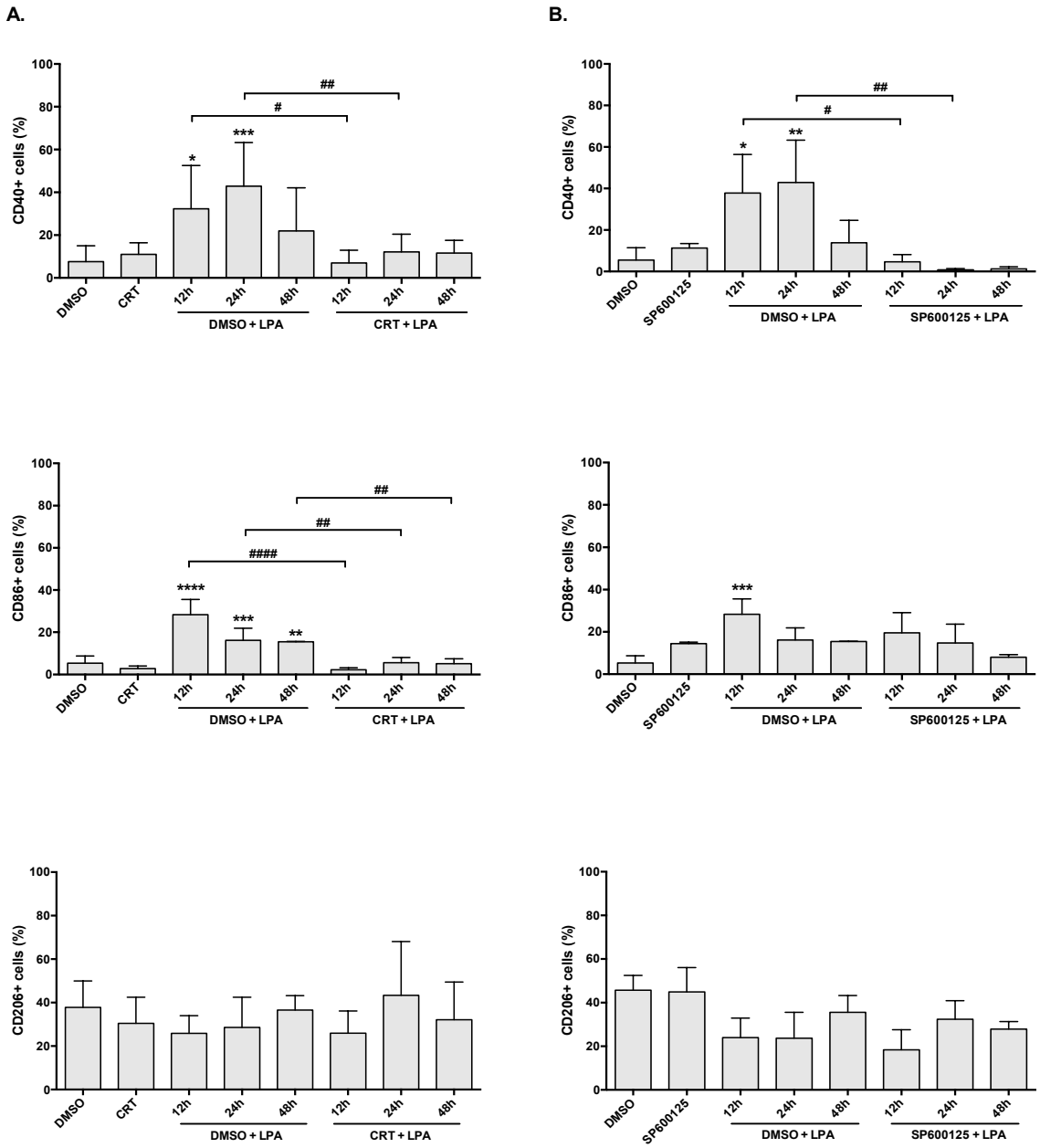

Fig. 34. PKD and JNK antagonists attenuate the expression of M1 surface marker in BV-2 cells

Serum-starved (o/n) BV-2 cells were cultivated in the presence of DMSO, DMSO plus LPA (1 µM) or LPA plus (**A**) CRT0066101 (1 µM) and (**B**) SP600125 (5 µM) for the indicated times. Cells were stained with PE-conjugated anti-CD40, APC-conjugated anti-CD86 or PE-conjugated anti-CD206 antibodies and analyzed using a Guava easyCyte 8 Millipore flow cytometer. Results from four individual experiments in triplicate are shown as mean values + SD. (*$p<0.05$; **$p<0.01$; ***$p<0.001$ compared to DMSO-treated cells; $^{\#}p<0.05$; $^{\#\#}p<0.01$; $^{\#\#\#}p<0.001$ each inhibitor compared to LPA-treated cells; one-way ANOVA with Bonferroni correction).

4.3 The PKD - JNK axis controls the production of pro-inflammatory factors, neurotoxicity and phagocytosis in LPA-treated microglia

Cytokine and chemokine secretions in response to LPA treatment in BV-2 cells showed significant reduction after CRT treatment (**Fig. 35A**). JNK inhibition profoundly decreased the secretion of TNFα, IL-6, CXCL10, CXCL2, and CCL5 at almost all time points yet it had no effect on IL-1β levels. In line with the results of BV-2 cells, CRT inhibited LPA-dependent secretion of all six analytes in primary cells (**Fig. 35B**).

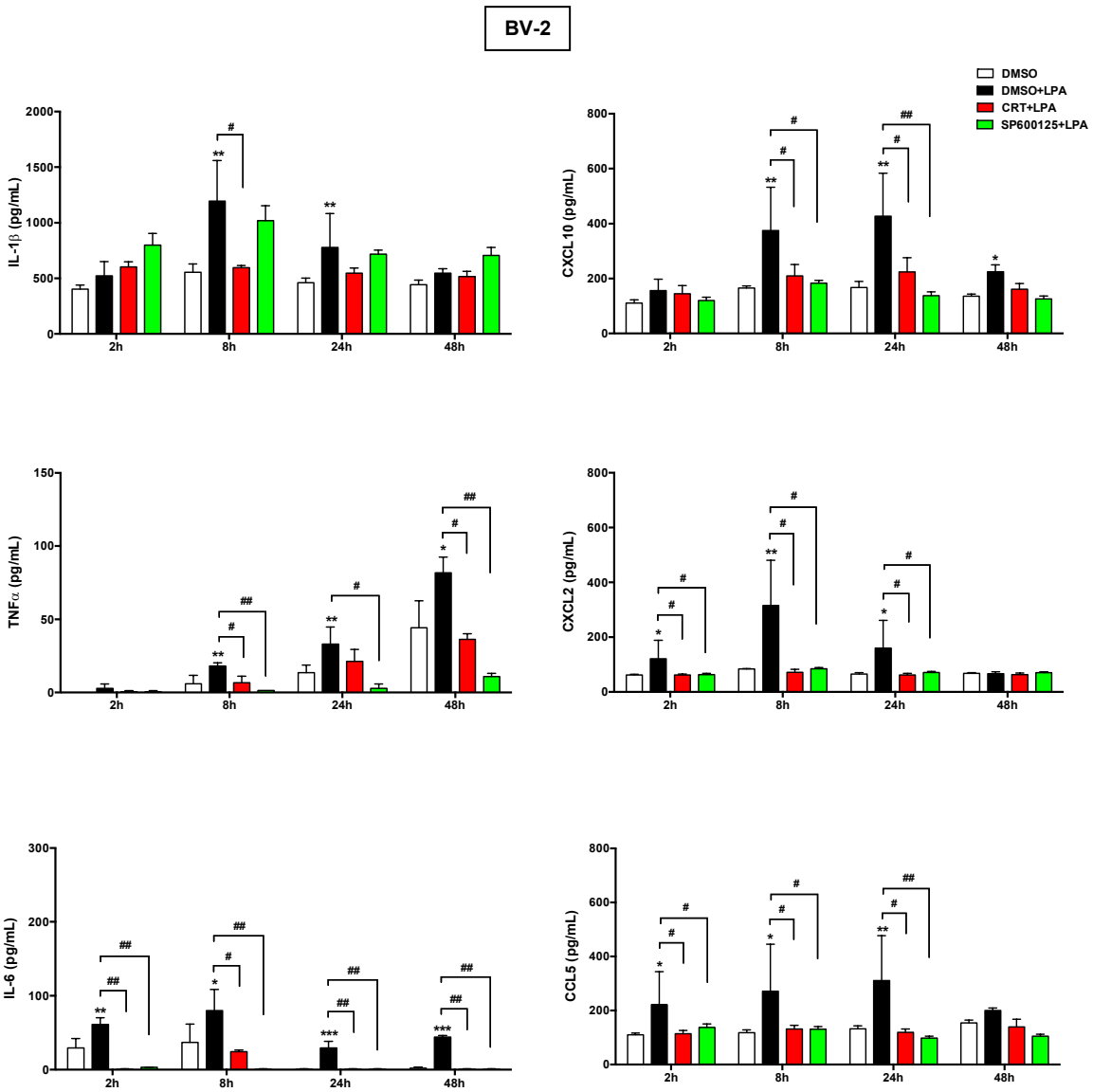

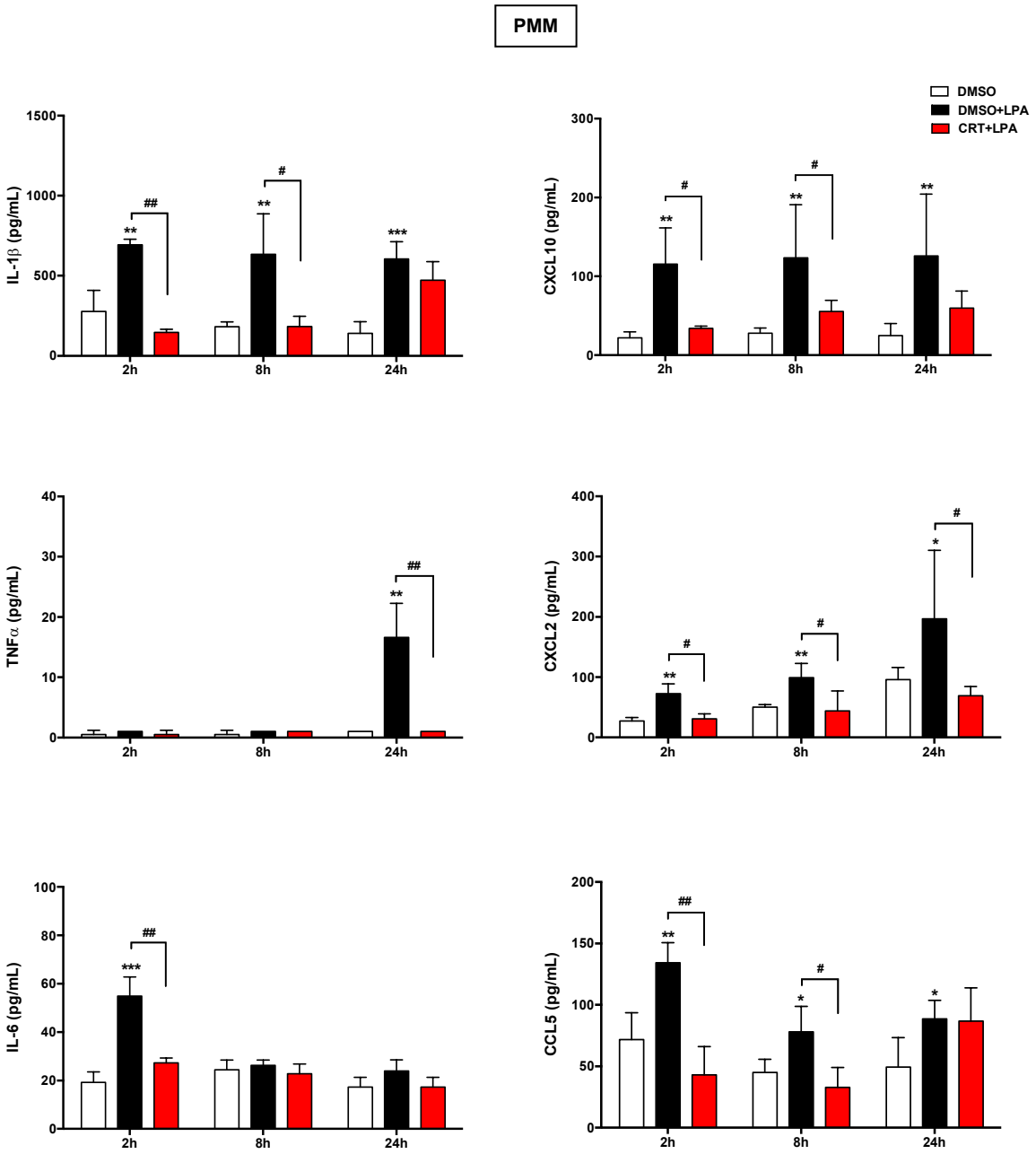

Fig. 35. CRT and SP600125 inhibit the secretion of pro-inflammatory cytokines and chemokines

(**A**) BV-2 and (**B**) primary murine microglia were cultured on 12- and 24-well plates, respectively and serum-starved o/n. The supernatants were collected after incubation with vehicle control (DMSO), DMSO plus LPA (1 μM) or LPA plus CRT0066101 (1 μM) (for both BV-2 and primary microglia) and SP600125 (5 μM) (only for BV-2 microglia cells) for the indicated time periods. ELISA was used to quantitate the concentrations of IL-1β, TNFα, IL-6, CXCL10 (IP-10), CXCL2 (MIP-2), and CCL5 (RANTES). Results shown represent mean + SD from two independent experiments performed in triplicate (*p<0.05; **p<0.01; ***p<0.001 compared to vehicle control; $^{\#}$p<0.05, $^{\#\#}$p<0.01; each inhibitor compared to LPA treated cells; one-way ANOVA with Bonferroni correction).

In addition, we examined the impact of CRT and SP600125 on ROS and NO formation in BV-2 cells. CRT (left panel) significantly decreased LPA-mediated DCF fluorescence at 6 h. On the contrary, SP600125 (right panel) could not inhibit ROS formation at any time point (**Fig. 36A**). Nitrate concentrations reached a maximum after 48h LPA treatment. Both CRT (left panel) and SP600125 (right panel) profoundly reduced the nitrate levels at 48h (**Fig. 36B**).

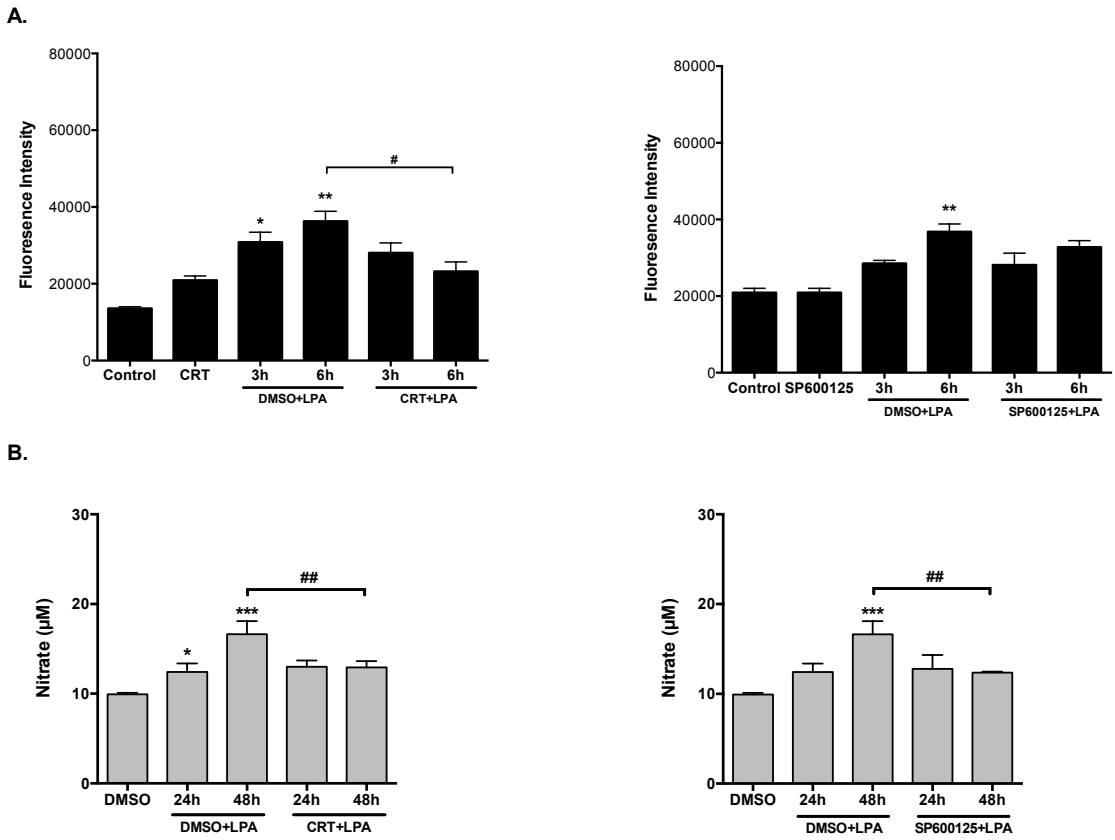

Fig. 36. CRT and SP600125 differentially control ROS and NO production

(A) The intracellular ROS levels generated by BV-2 cells were determined using carboxy-H_2DCFDA. Serum-starved cells were incubated with carboxy-H_2DCFDA, treated with DMSO, DMSO plus LPA (1µM) or LPA plus CRT0066101 (1 µM; left panel) and SP600125 (5 µM; right panel). After the indicated time periods the fluorescence intensity was evaluated. Results (2 independent experiments performed in triplicate) are presented as mean values + SD. (*$p<0.05$; **; $p<0.01$ compared to vehicle; $^{\#}p<0.05$ compared to LPA treated cells; one-way ANOVA with Bonferroni correction).

(B) Serum-starved BV-2 cells were incubated with vehicle (DMSO), DMSO plus LPA (1 µM) or LPA plus each inhibitor for the indicated times and the production of NO was determined by measuring the total nitrate concentration in the supernatants. Data (2 separate experiments performed in triplicate) are presented as mean values + SD. (*$p<0.05$; ***$p<0.001$ compared to untreated cells; $^{\#\#}p<0.01$ compared to LPA treated cells; one-way ANOVA with Bonferroni correction).

We finally analyzed the impact of PKD1-3 and JNK inhibition on LPA-induced neurotoxicity and phagocytosis. In BV-2 cells, CRT could dramatically reduce LPA-induced neurotoxicity (**Fig. 37A**). Also SP600125 reduced the neurotoxic potential of conditioned medium collected from LPA-treated BV-2 cells, yet to a lesser extent as compared to CRT0066 (**Fig. 37B**). In both BV-2 (**Fig. 37C**) and primary cells (**Fig. 37D**), phagocytosis of latex beads was slightly yet significantly increased in response to LPA (1 μM). Pharmacological inhibition using CRT and SP600125 effectively decreased this LPA-induced phagocytosis back to baseline levels.

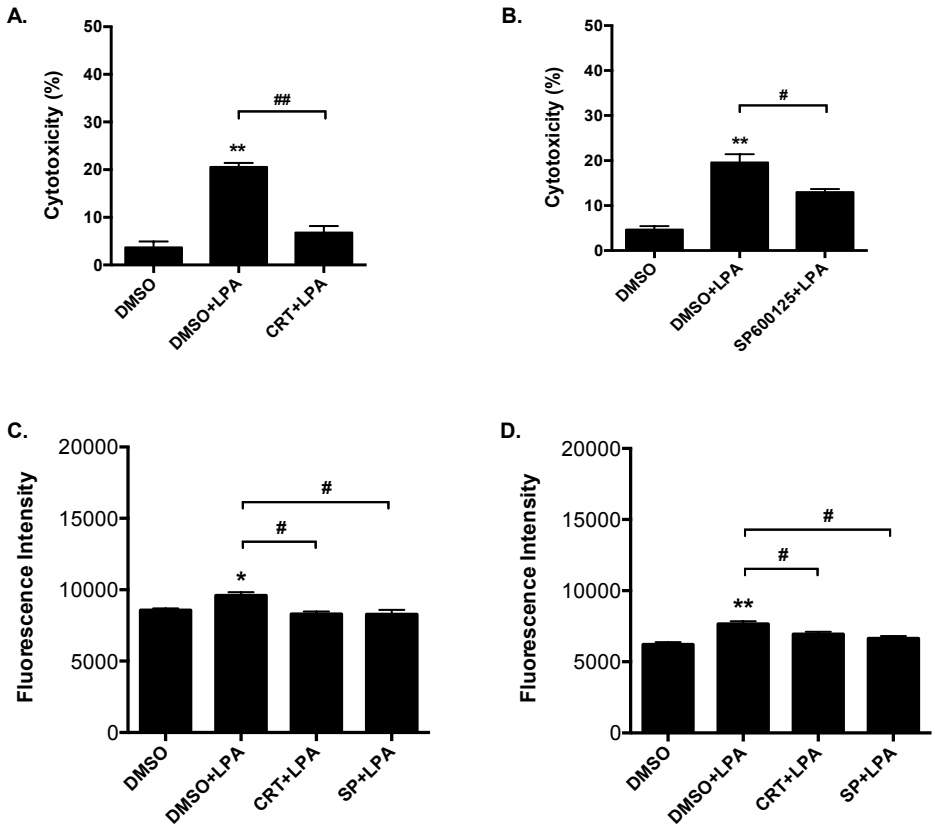

Fig. 37. PKDs and JNK inhibition suppress the LPA-induced microglia neurotoxicity and phagocytosis

CATH.a neurons were incubated for 24h with conditioned media collected from LPA-treated BV-2 cells in the presence or absence of CRT0066101 (1 μM) **(A)** and SP600125 (5 μM) **(B)** for 24h. The LDH levels were detected and cytotoxicity was calculated according to the manufacturer's directions.

(C-D) Fluorescently labeled latex beads were used as a probe for the measurement of the phagocytic process. Serum-starved BV-2 **(C)** and PMM **(D)** cells incubated with DMSO, DMSO plus LPA (1μM) or LPA plus each inhibitor for 24h and the fluorescence intensity was measured using a plate reader. Results of 2 independent experiments in triplicate are presented as mean values + SD. (*$p<0.05$; **$p<0.01$; $^{\#}p<0.05$, $^{\#\#}p<0.01$; compared to LPA treated cells; one-way ANOVA with Bonferroni correction).

The results of this thesis are summarized in the following two graphs.

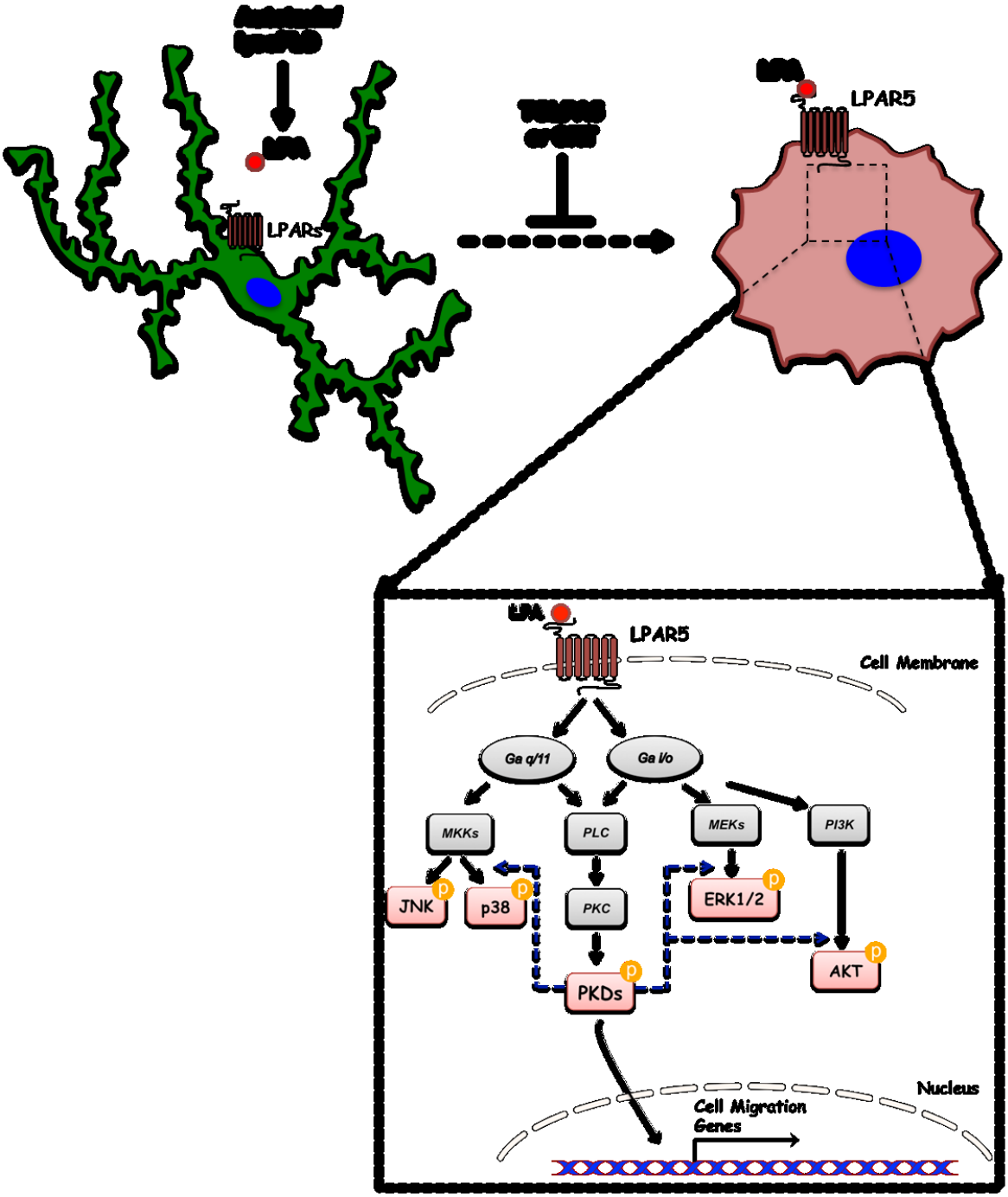

Fig. 38. Effect of LPA on microglial migrational response

LPA treatment induces a migratory signature in BV-2 and primary murine microglia that is controlled by the LPAR5 – PKD2 axis. Data of the present study provide insights on a new role of LPAR5 and PKD family in microglia function.

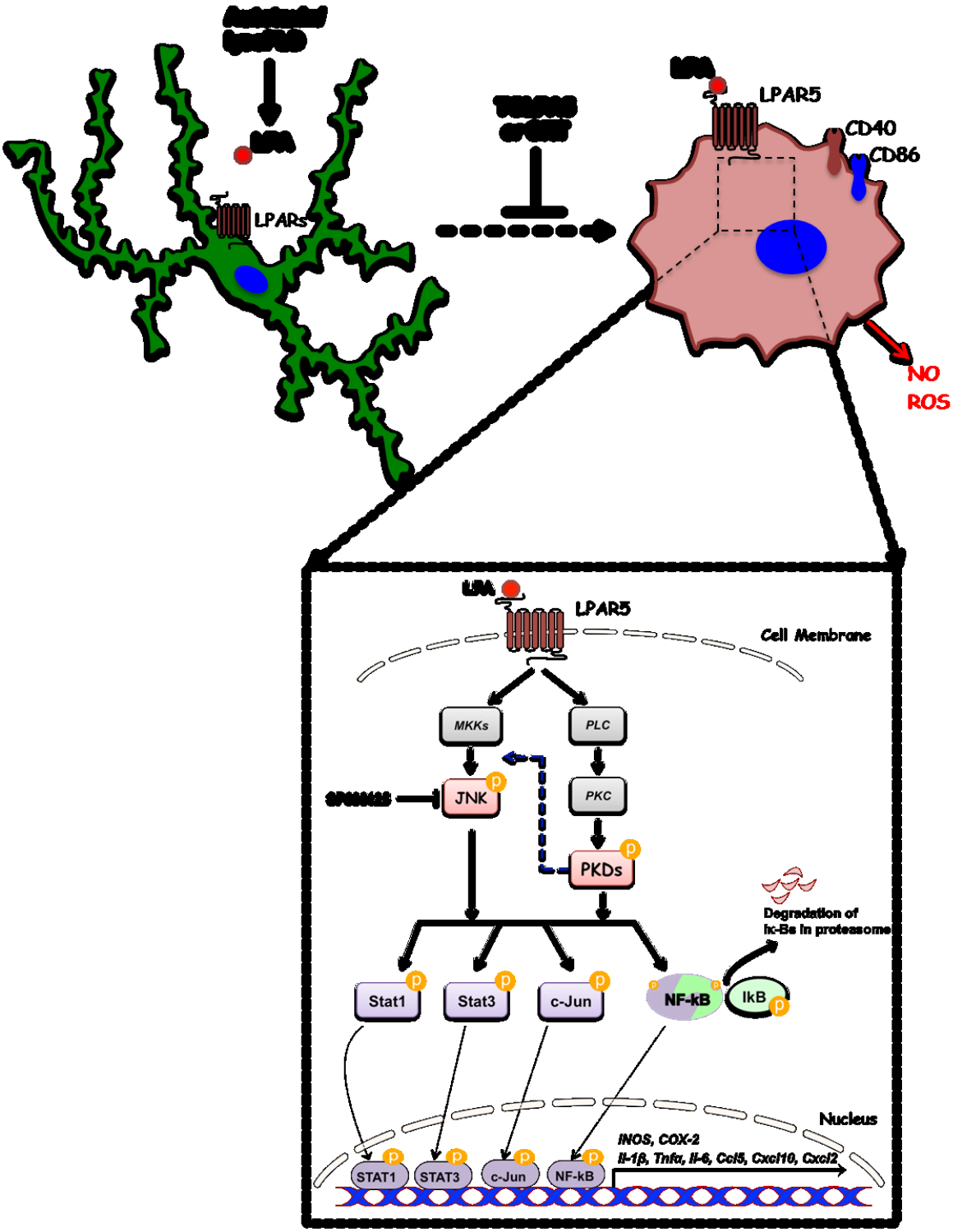

Fig. 39. Effect of LPA on microglial inflammatory response

LPA treatment induces a unique pro-inflammatory M1-like signature in BV-2 and primary mouse microglia that is completely or partially controlled by the LPAR5 – PKDs – JNK axis.

Discussion

In the present research study we tried to unravel the effects of increased LPA levels on microglia function using both the BV-2 cell line and primary murine microglia cells. The study is mainly divided into two directions, which are inter- connected. On the one hand, we examined the impact of LPA on microglial morphological alterations and migrational response. On the other hand, we investigated how LPA affects the inflammatory response of the CNS immune cells and which signaling pathway(s) may control this response.

As far as the first part of this study in concerned, I manipulated LPAR5 and PKD activity and present first evidence that LPA affects the microglial cytoskeleton and chemotactic response via PKD signaling. LPA receptor profiling in the present study confirmed low expression of the classical LPAR1-3 receptors (211) (and LPAR4) but revealed high expression of LPAR5 and LPAR6. All of the LPA receptors are expressed in the developing brain and expression levels vary with developmental age (119). LPA-mediated processes regulate proliferation, microtubule-dependent interkinetic nuclear migration, neurite retraction, cell survival, morphological changes, and cell migration (119). The cell line BV-2 expresses PKD2 and PKD3 while PMM express all of the PKD family members, namely PKD1-3.

LPA levels in brain and cerebrospinal fluid significantly increase in response to injury (140, 208, 242, 293, 294), traumatic brain injury (295), and glioblastoma multiforme (GBM) (296-298). Thus, overshooting LPA synthesis (probably by autotaxin overexpression in response-to-injury) (242) could provide an 'on' signal (36) for microglia migration that is detected by one or more of the LPA receptors expressed by microglia (1). These GPCRs couple (among others) to $G\alpha_{12/13}$ subunits, which stimulate activation of the small G protein RhoA (299). Some of the enzymes located downstream of RhoA are regulated by PKD family members and affect cell migration and gene expression (299).

Microglia are unique cells and remodeling is required for all the activities that they are involved in (278). Especially in the case of injury, microglia can adopt at least four different morphologies (e.g. giant multinucleated cells, phagocytic, motile/locomotory, and hypertrophied or bushy) and re-orientate their processes towards the site of damage. They can undergo full or partial de-ramification and develop filopodia-like structures that allow them to become motile (278). In response to LPA we observed an increase in cell area, cellular perimeter, and Iba-1 fluorescence. Many studies have documented that in response

to injury and adoption of an M1 phenotype, microglia undergo soma enlargement and transformation to an amoeboid morphology (300, 301). Iba-1 is a macrophage/microglia marker upregulated in response to activation (302) and was implicated in PDGF and M-CSF membrane ruffling and cell locomotion (303). In addition, Iba-1 couples to morphological changes mediated by Rac (another small G protein) and migration via a PLCγ-dependent pathway (304). Morphometric analysis of Iba-1 positive microglia in grey and white matter of the human dorsal anterior cingulate cortex demonstrated that primed microglia have an average 2-fold increase in cell surface area (305). This is reminiscent of what we observed here, namely increased cell area (approx. 2-fold) and cell perimeter (1.7- and 1.2-fold, for BV-2 and PMM respectively). There is less information available regarding morphological changes associated with the M2 phenotype. Some cell culture-based studies indicated though that treatment with IL-4 or IL-10 could trigger amoeboid microglia to adopt a ramified morphology (306). Interestingly, we observed that LPA-induced morphological changes were reversed to baseline, when BV-2 cells and PMM were incubated with TCLPA5 or CRT0066101 prior to LPA treatment.

At this point it is important to refer to the use of DMSO as a vehicle during my inhibition experiments. DMSO is a near-perfect polar aprotic solvent (dissolving polar and apolar compounds) but has a wide range of biological actions. Its effects have been studied in many pathological conditions including cardiac disease, traumatic brain injury, pain, cancer, stroke, spinal cord injury, and Alzheimer's disease. Its chemical structure reacts and deactivates toxic molecules generated by DNA damage, free radical formation, inflammation, oxidation, and infection (307). DMSO has been suggested to play and anti-inflammatory and protective role in many cases (308). However, in a recent study DMSO appeared to induce high nitrite production in N9 microglia cells (309). Moreover DMSO was found to block mouse macrophages from polarizing to either an M1- or an M2-phenotype. Hence, it is not clear-cut that it has anti-inflammatory effects on those cells. On the other hand, DMSO suppressed *E. coli*-induced ERK1/2, p38, JNK and Akt phosphorylation in human monocytes, suggesting that it can inhibit inflammatory cytokine/chemokine production (310). In our study, all the inhibitors that have been used (except for BrP-LPA) were dissolved in DMSO. The role of DMSO on microglia biology and function is not clear. Preliminary experiments revealed that there are slight differences in migrational response of microglia cells where only 0.1% BSA was added to the cells compared to cells that were treated with DMSO although qPCR analysis of pro-migratory

genes between those two conditions revealed pronounced changes (results are not presented here). In order to assure the accuracy of our results, during the experiments where the effect of these inhibitors on microglial morphology, migration and inflammatory response was studied, DMSO was used as a negative control and DMSO was also added together with LPA before each treatment to account for potential vehicle effects.

PKD members are recruited to different subcellular compartments in response to stimulation. LPA treatment of BV-2 cells and PMM induced altered intracellular trafficking of PKD2 and/or PKD1. In BV-2 cells, LPA induced a pronounced relocation of PKD2 from perinuclear localization to newly formed membrane protrusions. Whether this is an indication for PKD-dependent actin remodeling as reported for PKD1 (311) is currently unclear. However, it is been reported that PKD2 undergoes reversible translocation from the cytosol to the plasma membrane when stimulated via GPCRs (312). In PMM, a major part of originally cytosolic PKD1 undergoes translocation to the nuclear compartment in response to LPA. This is in line with results reported for fibroblasts and epithelial cells, where cell stimulation with GPCR agonists resulted in nuclear accumulation of PKD1 that was prevented by inhibiting PKC activation (313). This nuclear translocation step of PKD1 might be important to induce PKD1-mediated phosphorylation of HDAC5/7 resulting in cytoplasmic sequestration, thereby relieving transcriptional repression of specific target genes (314).

LPA treatment promoted activation of PKD-downstream signaling cascades in microglia cells. ERK1/2 activation (regulating fMLP-induced neutrophil chemotaxis) (315) proceeds via PKD-mediated phosphorylation of Ras and Rab interactor 1 (RIN1) that (in its non-phosphorylated state) prevents ERK1/2 activation by inhibiting Ras/Raf interaction (316). Also the MAPK members, p38 and JNK are downstream of PKDs since PKD1 silencing attenuates p38 and JNK activation (317). Moreover AKT might be under control of PKD and along this line our group previously demonstrated that in glioblastoma cells PKD2 co-immunoprecipitates with AKT indicating physical interaction (318).

A motile cycle of a cell induces the formation of lamellipodia, which mediate cellular locomotion and directed cell movement. Here I observed that LPA induces chemokinetic and chemotactic microglia migration. LPA-induced migration of BV-2 cells was concentration-dependent with a maximum at 1 μM. At LPA concentrations >1 μM migration tended to decrease again, an observation consistently made during time-lapse video microscopy or impedance measurements. This finding is indicative of LPA receptor

desensitization probably in a similar manner as described for hepatic epithelial cells, where this process was coupled to phosphorylation and subsequent internalization of LPA receptors (319).

All three PKD members play prominent roles during cell motility. They promote integrin recruitment to newly formed adhesions and regulate the invasiveness of cancer cells (282). PKD1 activation regulates directed cell movement. In general, PKD1 appears to reduce directed cell migration via phosphorylation of protein phosphatase Slingshot homolog 1 (SSH1L) an enzyme de-phosphorylating cofilin in lamellipodia (320). PKD1 catalyzes direct phosphorylation of SSH1L in the actin-binding domain. This generates a 14-3-3 binding motif separating the phosphatase from actin filaments at the leading edge of the cell (321, 322). Besides SSH1L, PKD1 also phosphorylates cortactin and blocks cell migration by attenuating Arp complex-driven actin polymerization (323). In contrast to PKD1, PKD2 and PKD3 appear to be pro-migratory kinases. E.g. silencing of PKD2 resulted in significantly reduced migration of doxorubicin-resistant breast cancer (324), glioblastoma (325), prostate cancer (326), and endothelial cells (327). In HeLa cells PKD2 and PKD3 form a complex that - depending on the activation state - can either increase or decrease cell migration via cofilin-mediated pathways (328). Silencing experiments with shRNA performed during the present study suggest that PKD2-dependent pathways primarily drive LPA-mediated migration of PMM while silencing of PKD1 had no effect. The role of PKD3 was not experimentally addressed during the present study. LPA-mediated nuclear translocation of PKD1 in PMM could indicate that the kinase might act as a transcriptional regulator probably via HDAC phosphorylation (329).

Except for the important role of PKD family in cell's chemotactic response, it is worth mentioning that also the members of MAPK family that are activated through PKDs, play crucial roles in migration (283). Briefly, activation of JNK, p38 and ERK1/2 correlates with an increased migrational response in several cells types and also signaling molecules that activate these kinases are essential for cell migration. However, different cell types may employ different MAPKs to control their migrational response (283).

LPA treatment promoted an upregulated transcription of gene products that are under regulation of PKD isoforms and LPAR5 (as confirmed by inhibition with CRT0066101 and TCLPA5). Along this line it is worth mentioning that we specifically address the role of PKD1 and PKD2 (but not PKD3) by an shRNA silencing approach. qPCR analyses performed during this study revealed upregulation of Itga5, Itgav, Mmp9, Mmp14, Vasp,

and Wasf2 in BV-2 cells. In PMM, LPA induced upregulation of Vegfa, Itga4, Itga5, Mmp9, Mmp14, Vasp, and Wasf2. These genes play an important role in cell migration, invasion, and angiogenesis, and are potent regulators of microglia function in the healthy and diseased CNS.

The connection between integrins and actin regulates adhesion organization and provides traction for migration (330). The recycling of integrins is critical for the migration response. Along this line it was shown that PKD1 phosphorylates Rabaptin-5, a posttranslational event controlling α5β1 and αvβ3 recycling, thereby regulating cell migration (331). The pre-proteins encoded by Itgα5 and Itgαv are proteolytically processed to generate light and heavy chains that comprise the α5 and v subunit of the fibronectin and vitronectin receptors, respectively. During the pathogenesis of multiple sclerosis the blood-brain barrier is compromised, which leads to influx of plasma fibronectin and vitronectin into the brain. In a murine experimental autoimmune encephalomyelitis model brain levels of fibronectin and vitronectin are increased and promote microglia activation via α5β1 and αvβ3 signaling (332). In addition, integrin play crucial roles in glioma cells migration, promoting the invasiveness of these cells (333, 334)

PKDs regulate also the expression of MMPs (314), which are important regulators of cellular functions including migration (335). In cancer cells, PKD2 represents a core factor in the formation of a multiprotein complex that controls secretion of MMPs from the trans Golgi network (336). Accumulated evidence suggests that MMPs (mainly MMP2 and MMP9) contribute to glioma cell migration and invasion (337, 338). MMP9 secretion by microglia (and other immune cells) appears to play a detrimental role in neuroinflammatory conditions and in gliomas (339, 340). MMP14 (also termed MT1-MMP) expression in microglia is low under normal conditions; however, it is upregulated under pathophysiological conditions, e.g. when microglia are exposed to glioma cells (339) in a similar manner as observed here in response to LPA.

Vegfα expression/secretion by gastrointestinal tumor cells and Vegf-stimulated blood vessel formation is upregulated by PKD2 (314, 341). Signaling through VEGFR-1 was reported to induce chemotaxis in BV-2 and rat microglia cells (342). Liu and colleagues reported that Vegf and Vegf receptor 1 (Flt-1) play important roles in A$_{1-42}$ induced microglia chemotaxis (343) and Vegf (receptor) signaling resembles an integral chemotactic component of microglia in Alzheimer's disease (344).

Vasp is an actin-associated protein that regulates cell migration. Doppler and colleagues identified Vasp as a PKD1 substrate: PKD1-mediated phosphorylation of Vasp induces re-localization to the leading edge and increases filopodia formation although persistent activation can decrease motility (311). In microglia, ADP-mediated Vasp phosphorylation induced membrane ruffling and chemotaxis in a PKA-dependent manner (345).

Wasf-2 is involved in the transmission of signals from tyrosine kinase receptors and small GTPases to the actin cytoskeleton. There, the Wasf-2 complex regulates lamellipodia formation where Wasf-2, Arp and cortactin have been reported to interact in pancreatic and breast cancer cells (323). This group demonstrated that PKD1 phosphorylates cortactin at Ser^{298} thereby generating a 14-3-3 binding site similar as shown for SSHL1. Mutation of the regulatory serine residue synergistically accelerates Wasf-2-Arp-driven actin polymerization, lamellipodia formation, and chemotaxis (323).

Summarizing the data from this part of the study, we provide strong evidence that the LPA/LPAR5/PKDs axis affects microglial cytoskeletal architecture, promotes chemotaxis, and controls the expression of pro-migratory genes that are upregulated in neurodegenerative diseases. In order to move one step forward and translate these findings into new pharmacological opportunities, the role (and complexities) of LPA signaling pathways in the healthy and diseased CNS should be carefully also studied *in vivo*.

During the second part of my thesis, I addressed the effect of inflammatory levels of LPA on microglia polarization state. We successfully provided the first evidence that LPA polarizes BV-2 and PMM cells towards an M1-like pro-inflammatory phenotype (1). Of note, the responses in BV-2 and primary microglia were qualitatively comparable, indicating that BV-2 cells represent a suitable prescreening model for such studies. Our findings might have bearings in neurological disease settings where LPA levels are increased, e.g. in spinal cord injury, traumatic brain injury, or multiple sclerosis (119).

Generally, under physiological conditions LPA-mediated signaling contributes to normal development and function of the CNS. However, in response to injury LPA levels can rise significantly in brain and CSF (140, 208, 242, 293, 294). LPA levels are elevated in human (0.05 controls vs. 0.27 µM post injury) and mouse (0.8 and 2 µM, prior vs. post injury) CSF in response to traumatic brain injury (295). In this context it is of importance that exogenous LPA can fuel endogenous LPA production via an LPAR3-dependent pathway (346). Increased LPA signaling has been linked to the development of fetal hydrocephalus

in embryonic mice, a pathophysiological process that is ameliorated in LPAR1/LPAR2 double knockout animals (208). LPA signaling is also involved in nerve injury-triggered pain responses (247), where LPAR1 (220) and LPAR5 (347) contribute via independent mechanisms. Findings that LPAR5 is activated during nerve injury (but not under basal conditions) are consistent with the fact that LPA levels rise significantly in response to spinal cord injury (140, 294). In the contused spinal cord parenchymal LPA concentrations increase nearly ten-fold (from 75 to 725 pmol/mg protein; naive vs. 3 d post injury) and contribute to secondary injury manifested as demyelination (294). Demyelination in the injured spinal cord was (at least in part) ascribed to LPA-activated microglia (294). Lysophosphatidylcholine injected intrathecally is converted to LPA via ATX-mediated pathways and, in an LPAR3-dependent feed-forward loop induces further endogenous synthesis of LPA (346). It was suggested that within this setting microglia activation is responsible for de novo LPA synthesis and concomitant development of neuropathic pain (348). Thus, findings of the present study that LPA induces an M1-like microglial phenotype are relevant to the pathophysiology of the injured/diseased CNS.

As already mentioned above, microglia undergo morphological transformation and become motile in response to a transformation from the surveillance to the activated phenotype. Activated microglia, can also, depending on the particular stimuli, adopt different activation states. Each state is characterized by the expression of different markers, proteins, cytokines, chemokine, and other mediators. Here I present evidence that LPA induces an M1-like signature in BV-2 and primary microglia (1), in line with a previous study (288), where LPS promoted increased iNOS, COX-2, CD40, and CD86 expression. LPA treatment resulted in upregulation of the M1 markers iNOS, COX-2, CD40, and CD86 and down regulation of the M2 markers CD206 (MRC1), Arg-1, and RELMα□□□□BV-2 and primary microglia. Increased cytokine/chemokine mRNA and protein levels as well as ROS and NO production in BV-2 and PMM accompanied classical M1 marker expression. In PMM LPS increased iNOS and COX-2 expression as well as IL-6 release (288) in a similar manner as observed here for LPA-treated BV-2 cells and PMM. Also the temporal expression profiles are in agreement to what was reported for M1 marker expression in LPS-treated PMM. Gene expression of iNOS and COX-2 was significantly elevated between 4 and 72 h, and protein levels of IL-6 were significantly elevated over baseline up to 72 h (288). The 2.5-fold increase in IL-6 secretion of primary microglia in response to LPA observed here is in a comparable range reported for LPA-

stimulated fibroblast-like synoviocytes (268), which play an active role in synovial inflammation and damage via ATX/LPA-mediated pathways.

Time-dependent gene and protein expression of cytokines and chemokines have specific profiles for an M1 or M2 microglia phenotype (288). In response to LPA treatment we observed upregulated secretion of IL-1β, IL-6, TNFα, and the immunomodulatory chemokines CCL5, CXCL10, and CXCL2 (1), findings reminiscent of what was reported for LPS-activated PMM (288). In particular, increased IL-1β, IL-6 and TNFα concentrations were linked to a poor prognosis in infants suffering from ischemic encephalopathy (349). In addition, IL-1β, IL-6, TNFα and the chemokines CCL5, CXCL10, and CXCL2 (which were all upregulated in LPA-treated primary microglia cells) are implicated as modulators of the neuroinflammatory response during traumatic brain injury (350) where LPA levels are increased (295).

Over activated microglia can result in progressive neuronal damage and contribute to the process of neuroinflammation in many neurodegenerative diseases (70). Microglia-induced neurotoxicity may be mediated by the constant increased production of pro-inflammatory cytokines and chemokines, NO (351), and ROS (352). iNOS is not expressed in the healthy brain, but expression is induced in response to inflammatory mediators like LPS or cytokines. In microglia, upregulation of iNOS is proposed to be the leading source of NO production (353). Increased ROS and NO concentrations make it reasonable to assume that, in response to iNOS upregulation, excess NO reacts with NADPH oxidase derived O_2^- . This reaction results in the formation of the highly neurotoxic mediator peroxynitrite ($ONOO^-$) in BV-2 microglia (354). It is important to note that DCF (used during the present study to detect alterations in cellular redox balance) is not a species-specific probe but is, in addition to H_2O_2, also oxidized by hypochlorous acid (generated via the myeloperoxidase/H_2O_2/chloride system), other peroxidases, and $ONOO^-$ (355). $ONOO^-$ was shown to induce mitochondrial dysfunction in neurons (356), to damage oligodendrocytes (357), and to compromise blood-brain barrier function (358). During the present study, we observed increased NO and ROS production in response to LPA treatment. Low concentrations of ROS and RNS are essential for many physiological functions like e.g. cell physiology, regulation of vascular tone, killing of invading bacteria, modulation of synaptic plasticity and communication between glia and neurons) (359) However, increased expression of these oxidative stressors has been suggested to have deleterious effects (e.g. cell membrane damage, lipids denaturation, changes in the inner

proteins, diminished antioxidant capacity of neurons etc.), and promote the pathogenesis of many diseases (352, 360). In line with this, I observed that treatment of CATH.a neurons with supernatants that were collected from LPA-treated BV-2 cells induced a 5-fold increase in cytotoxicity. Although our results suggest that LPA stimulation leads to ROS and NO production and is potentially neurotoxic, Awada and colleagues (164) have shown that overexpression of ATX in BV-2 microglia protects cells against H_2O_2-induced cell damage and oxidative stress. The same group (361) demonstrated ATX-mediated down regulation of cytokine production (mRNA and protein) in LPS-stimulated BV-2 cells. These seemingly contradictory results to the present study might be simply due to different incubation/culture conditions: In the ATX overexpression model (164) BV-2 cells are continuously exposed to LPA concentrations that are approx. 4-fold elevated over the vector controls in contrast to the single addition used in the present study (1). Although we here show that exposure to a single LPA bolus does not change LPA receptor expression in BV-2 cells and PMM, the situation might be different in ATX-overexpressing microglia. In terms of downregulated cytokine production in ATX-overexpressing BV-2 cells Awada et al. (361) used LPS-stimulated cells while we studied effects of LPA on BV-2 and PMM that were exposed only to LPA (in the absence of a co-agonist). This is reminiscent of what was reported for peritoneal macrophages (362): In that study LPA induced IL-6 but not TNF secretion in unstimulated macrophages while in LPS-stimulated cells LPA downregulated TNF but not IL-6 production. Thus it appears that LPA-mediated effects depend on the cellular preactivation experience resulting in altered responsiveness upon rechallenge probably related to the intrinsic immune memory of microglia (36).

Another aspect of microglia activation that plays a prominent role during inflammation is phagocytosis. So far it is not clear whether microglia phagocytosis is detrimental or beneficial in tissue repair, since this process differentially affects the context of each disease (363). In cases where it eliminates dead cells, clears cells debris and induces an anti-inflammatory response, it is considered beneficial. However, microglia may execute and eliminate stressed yet viable neurons (364) or the process itself may activate a respiratory burst that produces increased levels of ROS (365). Here, we observed that LPA treatment induced a minor (1.2-fold) yet statistically significant increase in microglia phagocytosis. This result is comparable to *in vitro* studies where stimulation of microglia with TLR ligands resulted in elevated phagocytosis during inflammation (366-368).

To get indications regarding the LPA receptors that are responsible for signal transmission in microglia we have performed pharmacological inhibitor studies. BrP-LPA is a pan LPA receptor/ATX inhibitor (369) while TCLPA5 is a specific antagonist of LPAR5 (272). Of note, both inhibitors suppressed M1 marker expression in BV-2 and PMM (1). BrP-LPA was without effect on LPA-induced phagocytosis and neurotoxicity. However, inhibition of LPAR5 (1) blunted the production of pro-inflammatory mediators (iNOS, COX-2), the secretion of pro-inflammatory cytokines and chemokines and the release of toxic factors (NO and ROS) leading to decreased neurotoxicity and phagocytosis. Hence, it is conceivable that LPAR5 is a major player in LPA-dependent M1 polarization of microglia. Our findings are in line with LPAR5-mediated signaling cascades in immunocompetent cells including a sensome function in microglia (279). Using a novel chemical probe acting as specific antagonist for LPAR5 it was shown that this receptor induces Ca^{2+} release from LPA-stimulated BV-2 cells in response to hexadecyl-LPA (370). In line with results of the present study, Kozian and colleagues (370) demonstrated highest expression for LPAR5 in BV-2 cells (LPAR6 is not mentioned in this article) and reported a sub μM IC50 (730 nM) for this novel LPAR5 antagonist for Ca^{2+} release in 16:0 alkyl-LPA stimulated BV-2 cells. Currently no published data are available whether commercially available TCLPA5 or the LPAR5 antagonist described in (370) crosses the blood-brain or blood-cerebrospinal fluid barriers to foster application in CNS disease models. In human mast cells, LPAR5 is essential for conveying signals leading to MIP-1β (CCL4) generation and secretion underlining the importance of this signaling route as regulator of cytokines and/or chemokines production (200).

This part of the study indicated that interference with the LPA signaling axis either at the level of LPA synthesis (using e.g. ATX inhibitors) or at the level of signal transmission (LPA receptor antagonists) could offer new means to modulate the microglia polarization status. These *in vitro* results (1) can provide valuable knowledge for follow up *in vivo* studies where the usefulness of such an approach can be carefully evaluated depending on the specific pathological context of each disease.

Since we identified that LPAR5 can potently control and drive a pro-inflammatory phenotype in microglia cells, we sought to unravel the signaling pathway that regulates this response. The signaling cascade and the transcriptional programs that drive an LPA-mediated M1-like signature in microglia are currently unknown. As it has been already stated, the PKD family induces activation of the MAPK family members. Inhibition using

CRT0066101 could abrogate the phosphorylation of ERK1/2, p38, and JNK. For the first time, we reported that in microglia cells there is a direct connection between PKDs and MAPKs. Also inhibition of LPAR5 decreased the LPA-induced activation of ERK1/2, p38, and JNK. Based on these results we examined whether the LPAR5/PKD/JNK axis could control different transcriptional programs and promote the M1-like phenotype in microglia. For the pharmacological inhibitor studies except for TCLPA5 and CRT, we used SP600125, which is a reversible ATP-competitive inhibitor of JNK (371).

The PKD family plays a crucial role in cell migration as already outlined above. In addition, PKD which isoform holds an important role in inflammatory responses (372). In a variety of cells, PKD induces NF-kB activation via GPCR agonists or oxidative stress (373-375). LPA led to a rapid activation of human colonic endothelial cells followed by NF-kB activation and IL-8 production (373). PKD2 has also been implicated in NF-kB activation of myeloid leukemia cells (376). Studies demonstrated that in colonic myofibroblasts, knockdown of PKD1 prevented the increase in COX-2 levels by pro-inflammatory mediators such as TNFα (377). Moreover, PKD1 has been reported to mediate hyperalgesia and maintain inflammatory heat hypersensitivity (378). In line with these observations, we reported that inhibition of PKD family using CRT could abolish the LPA-induced secretion of pro-inflammatory cytokines and chemokines, the production of iNOS and COX-2, and the release of ROS and NO. It could also reduce the levels of microglia-mediated neurotoxicity and inhibit phagocytosis.

MAPK signaling has been also connected with brain inflammation and gliosis and increased activity was observed in both astrocytes and microglia followed by synthesis of inflammatory mediators (379). Upon activation, MAP kinases can promote phosphorylation of transcription factors such as STAT1, STAT3, NF-kB, c-Jun and ATF2 and thereby controls expression of numerous target genes like e.g. iNOS, MMPs, COX-2, IL-1β, IL-6 etc.) (380). In the current study, LPA treatment of both BV-2 and PMM induced activation of these pathways. As already mentioned above, ERK1/2, p38 and JNK phosphorylation is under LPAR5 and PKD control. The ERK pathway is mainly involved and studied in tumorigenesis, while p38 and JNK were reported to be highly activated in neurodegenerative diseases where they promote neuronal apoptosis (381). In AD all of the three kinases mediated tau hyper phosphorylation (382). p38 and JNK also contributed to neuronal apoptosis (383, 384), activation of β- and γ- secretases (385), and phosphorylation of APP (386, 387). In PD, α-synuclein activated the MAP kinases

pathways in microglia cells resulting in production of TNFα and IL-1β (388). A role for JNK in neuronal apoptosis has also been investigated in PD models (389). Aberrant activation of p38 is reported in microglia and motor neurons in ALS (390). Moreover, both p38 and JNK are involved in cytoskeletal abnormalities of spinal motor neurons through phosphorylation and consequent aggregation of neurofilaments (391, 392).

The JNK pathway is activated by stress stimuli and plays crucial roles in development, cell growth, inflammatory and immune responses (393, 394). JNK activity has shown to be upregulated in many neuronal diseases (395-397). Several studies using JNK inhibitors unraveled that inhibition of this pathway can prevent cytokines production from macrophages and endothelial cells, and enhance recovery from ischemia (398-400). Also *in vivo* studies supported that JNK inhibition decreased cytokines production and neuronal death in brain injury, cerebral ischemia, and PD (401-403). The JNK pathway was reported to be involved in regulation of microglia immune responses (404-407). In LPS triggered microglia, inhibition of JNK using SP600125 reduced the induction of AP-1 genes, such as COX-2, TNFα, IL-6 and MCP-1 (274). Here, in LPA treated BV-2 and PMM we observed a similar pattern. Inhibition of JNK activity followed by reduced levels of iNOS, COX2, CD40, and decreased secretion of the cytokines IL-6, TNFα and the chemokines CCL5, CXCL10, and CXCL2. In addition, SP600125 treatment abolished the LPA-induced increase in NO levels, microglia toxicity and phagocytosis. Interestingly, JNK inhibition did not affect IL-1β secretion, CD86 expression and ROS release. One possible explanation for these observations id the fact that the JNK/c-Jun axis is not involved in the expression of these mediators in response to LPA-mediated downstream cascades.

Inhibition of JNK may exert positive results due to subsequent inhibition of c-Jun activation. The JNK/c-Jun axis in microglia cells may upregulate programs in similar ways as described for immune cells that lead to neuronal death and release of neurodegenerative molecules (291). c-Jun is a component of AP-1 transcription factors and regulates the expression of many inflammatory and cytokines genes, which are involved in brain inflammation (408). Except for SP600125, inhibition of LPAR5 and the PKD isoforms inhibited LPA-induced phosphorylation of c-Jun in both BV-2 and PMM.

Another transcription factor that exerts effects on almost all cell types and is constitutively activated and critical in chronic inflammatory diseases is NF-kB (290, 409). Studies have reported the involvement of NF-kB in both onset and resolution of inflammation (410). In brain the basal levels are relatively high compared to other tissues. Constitutive and

inducible activation in glial cells regulates inflammatory processes that exacerbate various diseases (411). Specifically in microglia, NF-kB activation regulated microglia activation, induced the release of pro-inflammatory cytokines and caused neurotoxicity (70, 412-415). In the present study we observed activation of p65-NF-kB that was detectable up to 24h post LPA addition. Inhibition of LPAR5/PKD/JNK axis abolished NF-kB phosphorylation at all time points tested.

The STAT proteins in the CNS are associated with development, hormone release, tumorigenesis, and inflammation (416). STATs are mediators of immunity and play important roles in inflammatory disease (417). Depending on which isoform will be activated, they may exert different effects on inflammation, survival, and proliferation (416). In brain tumors, STAT3 is highly upregulated (418, 419). The role of STAT3 in brain inflammation is not entirely clear, since both anti-inflammatory and pro-inflammatory mediators can activate it. In microglia it was reported that the JAK2-STAT3 pathway induces pro-inflammatory responses (420, 421). On the contrary the role of STAT1 is more clear and usually promotes inflammation, expression of different cytokines, and production of NO and ROS (422-425). Different expression levels has been detected in glial cells (426) and associated with CNS pathological conditions such as brain inflammation (427), traumatic brain injury (428), and cerebral ischemia (429, 430). Oxidative stress and some cytokines can activate both STAT1 and STAT3 in a JAK2 dependent manner (431). In the present study LPA treatment promoted activation of both STAT1 and STAT3. However, for the same amount of protein loaded for Western blot analysis, it is clear that phosphorylation of STAT1 was more pronounced as compared to STAT3. LPA-mediated activation of these transcription factors was also controlled by the LPAR5/PKD/JNK axis. All three inhibitors reversed STAT1 and STAT3 phosphorylation back to basal levels.

To conclude and summarize the findings of the present study, I am providing first evidence that LPA is a potent regulator of microglia biology and function. Increased LPA levels, as observed under inflammatory conditions, affected microglial morphology and promoted the migrational response. The LPA/LPAR5/PKD axis regulated the expression of migratory genes indicating possible downstream targets via which LPA signaling controls microglia chemotaxis. In addition, LPA promoted an M1 pro-inflammatory phenotype (with a distinct signature) in microglia under the control of LPAR5/PKD/JNK axis. Pharmacological inhibition of this axis abolished the activation of three major pro-

inflammatory transcription factors, unraveling possible transcription programs that are involved in LPA-induced inflammatory response of microglia cells.

The results that obtained during my PhD thesis are a step towards a better understanding of LPA-mediated effects on the immune cells of the CNS. The outcome of these experimental approaches should foster the study of LPA signaling and its impact on microglia function in the diseased brain. Interference with different members of the LPA pathway, depending on the context of disease, may unravel possible new targets for modulating neuroinflammation that, until now, were not considered.

Bibliography

1. Plastira I, Bernhart E, Goeritzer M, Reicher H, Kumble VB, Kogelnik N, et al. 1-Oleyl-lysophosphatidic acid (LPA) promotes polarization of BV-2 and primary murine microglia towards an M1-like phenotype. Journal of neuroinflammation. 2016;13(1):205. Epub 2016/08/28.
2. Galea I, Bechmann I, Perry VH. What is immune privilege (not)? Trends in immunology. 2007;28(1):12-8. Epub 2006/11/30.
3. Nayak D, Roth TL, McGavern DB. Microglia development and function. Annual review of immunology. 2014;32:367-402. Epub 2014/01/30.
4. Monteiro MA, Rasko D, Taylor DE, Perry MB. Glucosylated N-acetyllactosamine O-antigen chain in the lipopolysaccharide from Helicobacter pylori strain UA861. Glycobiology. 1998;8(1):107-12. Epub 1998/05/28.
5. Ginhoux F, Prinz M. Origin of microglia: current concepts and past controversies. Cold Spring Harbor perspectives in biology. 2015;7(8):a020537. Epub 2015/07/03.
6. Mittelbronn M, Dietz K, Schluesener HJ, Meyermann R. Local distribution of microglia in the normal adult human central nervous system differs by up to one order of magnitude. Acta neuropathologica. 2001;101(3):249-55. Epub 2001/04/20.
7. Ransohoff RM, Perry VH. Microglial physiology: unique stimuli, specialized responses. Annual review of immunology. 2009;27:119-45. Epub 2009/03/24.
8. Ransohoff RM, Cardona AE. The myeloid cells of the central nervous system parenchyma. Nature. 2010;468(7321):253-62. Epub 2010/11/12.
9. Ginhoux F, Greter M, Leboeuf M, Nandi S, See P, Gokhan S, et al. Fate mapping analysis reveals that adult microglia derive from primitive macrophages. Science. 2010;330(6005):841-5. Epub 2010/10/23.
10. Kierdorf K, Erny D, Goldmann T, Sander V, Schulz C, Perdiguero EG, et al. Microglia emerge from erythromyeloid precursors via Pu.1- and Irf8-dependent pathways. Nat Neurosci. 2013;16(3):273-80. Epub 2013/01/22.
11. Butovsky O, Jedrychowski MP, Moore CS, Cialic R, Lanser AJ, Gabriely G, et al. Identification of a unique TGF-beta-dependent molecular and functional signature in microglia. Nat Neurosci. 2014;17(1):131-43. Epub 2013/12/10.
12. Salter MW, Beggs S. Sublime microglia: expanding roles for the guardians of the CNS. Cell. 2014;158(1):15-24. Epub 2014/07/06.

13. Schulz C, Gomez Perdiguero E, Chorro L, Szabo-Rogers H, Cagnard N, Kierdorf K, et al. A lineage of myeloid cells independent of Myb and hematopoietic stem cells. Science. 2012;336(6077):86-90. Epub 2012/03/24.

14. Huang G, Zhang P, Hirai H, Elf S, Yan X, Chen Z, et al. PU.1 is a major downstream target of AML1 (RUNX1) in adult mouse hematopoiesis. Nature genetics. 2008;40(1):51-60. Epub 2007/11/13.

15. Zusso M, Methot L, Lo R, Greenhalgh AD, David S, Stifani S. Regulation of postnatal forebrain amoeboid microglial cell proliferation and development by the transcription factor Runx1. J Neurosci. 2012;32(33):11285-98. Epub 2012/08/17.

16. Walton MR, Gibbons H, MacGibbon GA, Sirimanne E, Saura J, Gluckman PD, et al. PU.1 expression in microglia. J Neuroimmunol. 2000;104(2):109-15. Epub 2000/03/14.

17. Smith AM, Gibbons HM, Oldfield RL, Bergin PM, Mee EW, Faull RL, et al. The transcription factor PU.1 is critical for viability and function of human brain microglia. Glia. 2013;61(6):929-42. Epub 2013/03/14.

18. Olson MC, Scott EW, Hack AA, Su GH, Tenen DG, Singh H, et al. PU. 1 is not essential for early myeloid gene expression but is required for terminal myeloid differentiation. Immunity. 1995;3(6):703-14. Epub 1995/12/01.

19. Mossadegh-Keller N, Sarrazin S, Kandalla PK, Espinosa L, Stanley ER, Nutt SL, et al. M-CSF instructs myeloid lineage fate in single haematopoietic stem cells. Nature. 2013;497(7448):239-43. Epub 2013/04/12.

20. Kierdorf K, Prinz M. Factors regulating microglia activation. Frontiers in cellular neuroscience. 2013;7:44. Epub 2013/05/01.

21. Minten C, Terry R, Deffrasnes C, King NJ, Campbell IL. IFN regulatory factor 8 is a key constitutive determinant of the morphological and molecular properties of microglia in the CNS. PloS one. 2012;7(11):e49851. Epub 2012/11/21.

22. Gabriele L, Phung J, Fukumoto J, Segal D, Wang IM, Giannakakou P, et al. Regulation of apoptosis in myeloid cells by interferon consensus sequence-binding protein. The Journal of experimental medicine. 1999;190(3):411-21. Epub 1999/08/03.

23. Yu JY, Chung KH, Deo M, Thompson RC, Turner DL. MicroRNA miR-124 regulates neurite outgrowth during neuronal differentiation. Experimental cell research. 2008;314(14):2618-33. Epub 2008/07/16.

24. Cheng LC, Pastrana E, Tavazoie M, Doetsch F. miR-124 regulates adult neurogenesis in the subventricular zone stem cell niche. Nat Neurosci. 2009;12(4):399-408. Epub 2009/03/17.

25. Ponomarev ED, Veremeyko T, Barteneva N, Krichevsky AM, Weiner HL. MicroRNA-124 promotes microglia quiescence and suppresses EAE by deactivating macrophages via the C/EBP-alpha-PU.1 pathway. Nat Med. 2011;17(1):64-70. Epub 2010/12/07.

26. Casano AM, Peri F. Microglia: multitasking specialists of the brain. Dev Cell. 2015;32(4):469-77.

27. Colonna M, Butovsky O. Microglia Function in the Central Nervous System During Health and Neurodegeneration. Annual review of immunology. 2017. Epub 2017/02/23.

28. Atallah N, Vasiu R, Bosca AB, Cretu DI, Georgiu C, Constantin AM, et al. Microglia--performers of the 21st century. Romanian journal of morphology and embryology = Revue roumaine de morphologie et embryologie. 2014;55(3):745-65. Epub 2014/10/21.

29. Wu Y, Dissing-Olesen L, MacVicar BA, Stevens B. Microglia: Dynamic Mediators of Synapse Development and Plasticity. Trends Immunol. 2015;36(10):605-13. Epub 2015/10/04.

30. Streit WJ. Microglia and macrophages in the developing CNS. Neurotoxicology. 2001;22(5):619-24. Epub 2002/01/05.

31. Yokoyama A, Yang L, Itoh S, Mori K, Tanaka J. Microglia, a potential source of neurons, astrocytes, and oligodendrocytes. Glia. 2004;45(1):96-104. Epub 2003/12/04.

32. Shemer A, Erny D, Jung S, Prinz M. Microglia Plasticity During Health and Disease: An Immunological Perspective. Trends Immunol. 2015;36(10):614-24. Epub 2015/10/04.

33. Benarroch EE. Microglia: Multiple roles in surveillance, circuit shaping, and response to injury. Neurology. 2013;81(12):1079-88. Epub 2013/08/16.

34. Michell-Robinson MA, Touil H, Healy LM, Owen DR, Durafourt BA, Bar-Or A, et al. Roles of microglia in brain development, tissue maintenance and repair. Brain. 2015;138(Pt 5):1138-59. Epub 2015/04/01.

35. Hanisch UK, Kettenmann H. Microglia: active sensor and versatile effector cells in the normal and pathologic brain. Nat Neurosci. 2007;10(11):1387-94. Epub 2007/10/30.

36. Kettenmann H, Hanisch UK, Noda M, Verkhratsky A. Physiology of microglia. Physiological reviews. 2011;91(2):461-553. Epub 2011/04/30.

37. Nimmerjahn A, Kirchhoff F, Helmchen F. Resting microglial cells are highly dynamic surveillants of brain parenchyma in vivo. Science. 2005;308(5726):1314-8. Epub 2005/04/16.

38. Mosser DM, Edwards JP. Exploring the full spectrum of macrophage activation. Nat Rev Immunol. 2008;8(12):958-69. Epub 2008/11/26.

39. Saijo K, Glass CK. Microglial cell origin and phenotypes in health and disease. Nat Rev Immunol. 2011;11(11):775-87. Epub 2011/10/26.

40. Yamasaki R, Lu H, Butovsky O, Ohno N, Rietsch AM, Cialic R, et al. Differential roles of microglia and monocytes in the inflamed central nervous system. The Journal of experimental medicine. 2014;211(8):1533-49. Epub 2014/07/09.

41. Jha MK, Lee WH, Suk K. Functional polarization of neuroglia: Implications in neuroinflammation and neurological disorders. Biochemical pharmacology. 2016;103:1-16. Epub 2015/11/12.

42. Wang N, Liang H, Zen K. Molecular mechanisms that influence the macrophage m1-m2 polarization balance. Frontiers in immunology. 2014;5:614. Epub 2014/12/17.

43. Hu X, Leak RK, Shi Y, Suenaga J, Gao Y, Zheng P, et al. Microglial and macrophage polarization-new prospects for brain repair. Nature reviews Neurology. 2015;11(1):56-64. Epub 2014/11/12.

44. Gertig U, Hanisch UK. Microglial diversity by responses and responders. Frontiers in cellular neuroscience. 2014;8:101. Epub 2014/04/20.

45. Lampron A, Elali A, Rivest S. Innate immunity in the CNS: redefining the relationship between the CNS and Its environment. Neuron. 2013;78(2):214-32. Epub 2013/04/30.

46. Colton C, Wilcock DM. Assessing activation states in microglia. CNS & neurological disorders drug targets. 2010;9(2):174-91. Epub 2010/03/09.

47. Cherry JD, Olschowka JA, O'Banion MK. Neuroinflammation and M2 microglia: the good, the bad, and the inflamed. J Neuroinflammation. 2014;11:98. Epub 2014/06/04.

48. Cameron B, Landreth GE. Inflammation, microglia, and Alzheimer's disease. Neurobiology of disease. 2010;37(3):503-9. Epub 2009/10/17.

49. Perry VH, Holmes C. Microglial priming in neurodegenerative disease. Nature reviews Neurology. 2014;10(4):217-24. Epub 2014/03/19.

50. Tay TL, Savage J, Hui CW, Bisht K, Tremblay ME. Microglia across the lifespan: from origin to function in brain development, plasticity and cognition. The Journal of physiology. 2016. Epub 2016/04/23.

51. Cunningham C. Microglia and neurodegeneration: the role of systemic inflammation. Glia. 2013;61(1):71-90. Epub 2012/06/08.

52. Harry GJ. Microglia during development and aging. Pharmacology & therapeutics. 2013;139(3):313-26. Epub 2013/05/07.

53. Rawji KS, Mishra MK, Michaels NJ, Rivest S, Stys PK, Yong VW. Immunosenescence of microglia and macrophages: impact on the ageing central nervous system. Brain. 2016;139(Pt 3):653-61. Epub 2016/02/26.

54. Streit WJ, Braak H, Xue QS, Bechmann I. Dystrophic (senescent) rather than activated microglial cells are associated with tau pathology and likely precede neurodegeneration in Alzheimer's disease. Acta neuropathologica. 2009;118(4):475-85. Epub 2009/06/11.

55. Tremblay ME, Zettel ML, Ison JR, Allen PD, Majewska AK. Effects of aging and sensory loss on glial cells in mouse visual and auditory cortices. Glia. 2012;60(4):541-58. Epub 2012/01/10.

56. Hefendehl JK, Neher JJ, Suhs RB, Kohsaka S, Skodras A, Jucker M. Homeostatic and injury-induced microglia behavior in the aging brain. Aging cell. 2014;13(1):60-9. Epub 2013/08/21.

57. Flanary BE, Sammons NW, Nguyen C, Walker D, Streit WJ. Evidence that aging and amyloid promote microglial cell senescence. Rejuvenation research. 2007;10(1):61-74. Epub 2007/03/24.

58. Naylor RM, Baker DJ, van Deursen JM. Senescent cells: a novel therapeutic target for aging and age-related diseases. Clinical pharmacology and therapeutics. 2013;93(1):105-16. Epub 2012/12/06.

59. Bisht K, Sharma K, Lacoste B, Tremblay ME. Dark microglia: Why are they dark? Communicative & integrative biology. 2016;9(6):e1230575. Epub 2017/01/04.

60. Bisht K, Sharma KP, Lecours C, Sanchez MG, El Hajj H, Milior G, et al. Dark microglia: A new phenotype predominantly associated with pathological states. Glia. 2016;64(5):826-39. Epub 2016/02/06.

61. Cartier N, Lewis CA, Zhang R, Rossi FM. The role of microglia in human disease: therapeutic tool or target? Acta neuropathologica. 2014;128(3):363-80. Epub 2014/08/12.

62. Czirr E, Wyss-Coray T. The immunology of neurodegeneration. The Journal of clinical investigation. 2012;122(4):1156-63. Epub 2012/04/03.

63. Lucin KM, Wyss-Coray T. Immune activation in brain aging and neurodegeneration: too much or too little? Neuron. 2009;64(1):110-22. Epub 2009/10/21.

64. Heneka MT, Kummer MP, Latz E. Innate immune activation in neurodegenerative disease. Nat Rev Immunol. 2014;14(7):463-77. Epub 2014/06/26.

65. Glass CK, Saijo K, Winner B, Marchetto MC, Gage FH. Mechanisms underlying inflammation in neurodegeneration. Cell. 2010;140(6):918-34. Epub 2010/03/23.

66. Chen Z, Trapp BD. Microglia and neuroprotection. J Neurochem. 2016;136 Suppl 1:10-7. Epub 2015/02/19.

67. Gao HM, Hong JS. Why neurodegenerative diseases are progressive: uncontrolled inflammation drives disease progression. Trends Immunol. 2008;29(8):357-65. Epub 2008/07/05.

68. Kettenmann H, Kirchhoff F, Verkhratsky A. Microglia: new roles for the synaptic stripper. Neuron. 2013;77(1):10-8. Epub 2013/01/15.

69. Wu W, Shao J, Lu H, Xu J, Zhu A, Fang W, et al. Guard of delinquency? A role of microglia in inflammatory neurodegenerative diseases of the CNS. Cell biochemistry and biophysics. 2014;70(1):1-8. Epub 2014/03/19.

70. Block ML, Zecca L, Hong JS. Microglia-mediated neurotoxicity: uncovering the molecular mechanisms. Nat Rev Neurosci. 2007;8(1):57-69. Epub 2006/12/21.

71. Perry VH, Nicoll JA, Holmes C. Microglia in neurodegenerative disease. Nature reviews Neurology. 2010;6(4):193-201. Epub 2010/03/18.

72. Tang Y, Le W. Differential Roles of M1 and M2 Microglia in Neurodegenerative Diseases. Molecular neurobiology. 2016;53(2):1181-94. Epub 2015/01/20.

73. Jack CR, Jr., Knopman DS, Jagust WJ, Petersen RC, Weiner MW, Aisen PS, et al. Tracking pathophysiological processes in Alzheimer's disease: an updated hypothetical model of dynamic biomarkers. The Lancet Neurology. 2013;12(2):207-16. Epub 2013/01/22.

74. Querfurth HW, LaFerla FM. Alzheimer's disease. The New England journal of medicine. 2010;362(4):329-44. Epub 2010/01/29.

75. Mawuenyega KG, Sigurdson W, Ovod V, Munsell L, Kasten T, Morris JC, et al. Decreased clearance of CNS beta-amyloid in Alzheimer's disease. Science. 2010;330(6012):1774. Epub 2010/12/15.

76. Wu Z, Sun L, Hashioka S, Yu S, Schwab C, Okada R, et al. Differential pathways for interleukin-1beta production activated by chromogranin A and amyloid beta in microglia. Neurobiology of aging. 2013;34(12):2715-25. Epub 2013/07/09.

77. Stewart CR, Stuart LM, Wilkinson K, van Gils JM, Deng J, Halle A, et al. CD36 ligands promote sterile inflammation through assembly of a Toll-like receptor 4 and 6 heterodimer. Nat Immunol. 2010;11(2):155-61. Epub 2009/12/29.

78. Bradshaw EM, Chibnik LB, Keenan BT, Ottoboni L, Raj T, Tang A, et al. CD33 Alzheimer's disease locus: altered monocyte function and amyloid biology. Nat Neurosci. 2013;16(7):848-50. Epub 2013/05/28.

79. Guerreiro R, Wojtas A, Bras J, Carrasquillo M, Rogaeva E, Majounie E, et al. TREM2 variants in Alzheimer's disease. The New England journal of medicine. 2013;368(2):117-27. Epub 2012/11/16.

80. Bhaskar K, Konerth M, Kokiko-Cochran ON, Cardona A, Ransohoff RM, Lamb BT. Regulation of tau pathology by the microglial fractalkine receptor. Neuron. 2010;68(1):19-31. Epub 2010/10/06.

81. Hickman SE, Allison EK, El Khoury J. Microglial dysfunction and defective beta-amyloid clearance pathways in aging Alzheimer's disease mice. J Neurosci. 2008;28(33):8354-60. Epub 2008/08/15.

82. Van Langenhove T, van der Zee J, Van Broeckhoven C. The molecular basis of the frontotemporal lobar degeneration-amyotrophic lateral sclerosis spectrum. Annals of medicine. 2012;44(8):817-28. Epub 2012/03/17.

83. Cagnin A, Rossor M, Sampson EL, Mackinnon T, Banati RB. In vivo detection of microglial activation in frontotemporal dementia. Annals of neurology. 2004;56(6):894-7. Epub 2004/11/25.

84. Baker M, Mackenzie IR, Pickering-Brown SM, Gass J, Rademakers R, Lindholm C, et al. Mutations in progranulin cause tau-negative frontotemporal dementia linked to chromosome 17. Nature. 2006;442(7105):916-9. Epub 2006/07/25.

85. Martens LH, Zhang J, Barmada SJ, Zhou P, Kamiya S, Sun B, et al. Progranulin deficiency promotes neuroinflammation and neuron loss following toxin-induced injury. The Journal of clinical investigation. 2012;122(11):3955-9. Epub 2012/10/09.

86. Talbot K. Motor neurone disease. Postgraduate medical journal. 2002;78(923):513-9. Epub 2002/10/03.

87. Ludolph AC, Brettschneider J, Weishaupt JH. Amyotrophic lateral sclerosis. Current opinion in neurology. 2012;25(5):530-5. Epub 2012/08/25.

88. Kawamata T, Akiyama H, Yamada T, McGeer PL. Immunologic reactions in amyotrophic lateral sclerosis brain and spinal cord tissue. The American journal of pathology. 1992;140(3):691-707. Epub 1992/03/01.

89. Frakes AE, Ferraiuolo L, Haidet-Phillips AM, Schmelzer L, Braun L, Miranda CJ, et al. Microglia induce motor neuron death via the classical NF-kappaB pathway in amyotrophic lateral sclerosis. Neuron. 2014;81(5):1009-23. Epub 2014/03/13.

90. Zhao W, Beers DR, Henkel JS, Zhang W, Urushitani M, Julien JP, et al. Extracellular mutant SOD1 induces microglial-mediated motoneuron injury. Glia. 2010;58(2):231-43. Epub 2009/08/13.

91. Sargsyan SA, Blackburn DJ, Barber SC, Grosskreutz J, De Vos KJ, Monk PN, et al. A comparison of in vitro properties of resting SOD1 transgenic microglia reveals evidence of reduced neuroprotective function. BMC neuroscience. 2011;12:91. Epub 2011/09/29.

92. Brettschneider J, Toledo JB, Van Deerlin VM, Elman L, McCluskey L, Lee VM, et al. Microglial activation correlates with disease progression and upper motor neuron clinical symptoms in amyotrophic lateral sclerosis. PloS one. 2012;7(6):e39216. Epub 2012/06/22.

93. Gerhard A, Banati RB, Goerres GB, Cagnin A, Myers R, Gunn RN, et al. [11C](R)-PK11195 PET imaging of microglial activation in multiple system atrophy. Neurology. 2003;61(5):686-9. Epub 2003/09/10.

94. Damier P, Hirsch EC, Zhang P, Agid Y, Javoy-Agid F. Glutathione peroxidase, glial cells and Parkinson's disease. Neuroscience. 1993;52(1):1-6. Epub 1993/01/01.

95. Mogi M, Harada M, Kondo T, Riederer P, Inagaki H, Minami M, et al. Interleukin-1 beta, interleukin-6, epidermal growth factor and transforming growth factor-alpha are elevated in the brain from parkinsonian patients. Neuroscience letters. 1994;180(2):147-50. Epub 1994/10/24.

96. Hirsch EC, Hunot S. Neuroinflammation in Parkinson's disease: a target for neuroprotection? The Lancet Neurology. 2009;8(4):382-97. Epub 2009/03/20.

97. Zhang W, Wang T, Pei Z, Miller DS, Wu X, Block ML, et al. Aggregated alpha-synuclein activates microglia: a process leading to disease progression in Parkinson's disease. FASEB J. 2005;19(6):533-42. Epub 2005/03/26.

98. Shavali S, Combs CK, Ebadi M. Reactive macrophages increase oxidative stress and alpha-synuclein nitration during death of dopaminergic neuronal cells in co-culture: relevance to Parkinson's disease. Neurochemical research. 2006;31(1):85-94. Epub 2006/02/14.

99. Theodore S, Cao S, McLean PJ, Standaert DG. Targeted overexpression of human alpha-synuclein triggers microglial activation and an adaptive immune response in a mouse

model of Parkinson disease. Journal of neuropathology and experimental neurology. 2008;67(12):1149-58. Epub 2008/11/20.

100. Simmons DA, Casale M, Alcon B, Pham N, Narayan N, Lynch G. Ferritin accumulation in dystrophic microglia is an early event in the development of Huntington's disease. Glia. 2007;55(10):1074-84. Epub 2007/06/07.

101. Silvestroni A, Faull RL, Strand AD, Moller T. Distinct neuroinflammatory profile in post-mortem human Huntington's disease. Neuroreport. 2009;20(12):1098-103. Epub 2009/07/11.

102. Singhrao SK, Neal JW, Morgan BP, Gasque P. Increased complement biosynthesis by microglia and complement activation on neurons in Huntington's disease. Experimental neurology. 1999;159(2):362-76. Epub 1999/10/03.

103. Ona VO, Li M, Vonsattel JP, Andrews LJ, Khan SQ, Chung WM, et al. Inhibition of caspase-1 slows disease progression in a mouse model of Huntington's disease. Nature. 1999;399(6733):263-7. Epub 1999/06/03.

104. Kwan W, Trager U, Davalos D, Chou A, Bouchard J, Andre R, et al. Mutant huntingtin impairs immune cell migration in Huntington disease. The Journal of clinical investigation. 2012;122(12):4737-47. Epub 2012/11/20.

105. Tai YF, Pavese N, Gerhard A, Tabrizi SJ, Barker RA, Brooks DJ, et al. Microglial activation in presymptomatic Huntington's disease gene carriers. Brain. 2007;130(Pt 7):1759-66. Epub 2007/04/03.

106. Crotti A, Benner C, Kerman BE, Gosselin D, Lagier-Tourenne C, Zuccato C, et al. Mutant Huntingtin promotes autonomous microglia activation via myeloid lineage-determining factors. Nat Neurosci. 2014;17(4):513-21. Epub 2014/03/04.

107. Shin JY, Fang ZH, Yu ZX, Wang CE, Li SH, Li XJ. Expression of mutant huntingtin in glial cells contributes to neuronal excitotoxicity. The Journal of cell biology. 2005;171(6):1001-12. Epub 2005/12/21.

108. Lassmann H, Bruck W, Lucchinetti CF. The immunopathology of multiple sclerosis: an overview. Brain Pathol. 2007;17(2):210-8. Epub 2007/03/29.

109. Ajami B, Bennett JL, Krieger C, McNagny KM, Rossi FM. Infiltrating monocytes trigger EAE progression, but do not contribute to the resident microglia pool. Nat Neurosci. 2011;14(9):1142-9. Epub 2011/08/02.

110. Ramaglia V, Hughes TR, Donev RM, Ruseva MM, Wu X, Huitinga I, et al. C3-dependent mechanism of microglial priming relevant to multiple sclerosis. Proc Natl Acad Sci U S A. 2012;109(3):965-70. Epub 2012/01/06.

111. Satoh J, Lee YB, Kim SU. T-cell costimulatory molecules B7-1 (CD80) and B7-2 (CD86) are expressed in human microglia but not in astrocytes in culture. Brain research. 1995;704(1):92-6. Epub 1995/12/15.

112. Jack C, Ruffini F, Bar-Or A, Antel JP. Microglia and multiple sclerosis. J Neurosci Res. 2005;81(3):363-73. Epub 2005/06/11.

113. Butovsky O, Landa G, Kunis G, Ziv Y, Avidan H, Greenberg N, et al. Induction and blockage of oligodendrogenesis by differently activated microglia in an animal model of multiple sclerosis. The Journal of clinical investigation. 2006;116(4):905-15. Epub 2006/03/25.

114. Mackenzie IR. Activated microglia in dementia with Lewy bodies. Neurology. 2000;55(1):132-4. Epub 2000/07/13.

115. Rub U, Brunt ER, Gierga K, Schultz C, Paulson H, de Vos RA, et al. The nucleus raphe interpositus in spinocerebellar ataxia type 3 (Machado-Joseph disease). Journal of chemical neuroanatomy. 2003;25(2):115-27. Epub 2003/03/29.

116. Petersen AJ, Katzenberger RJ, Wassarman DA. The innate immune response transcription factor relish is necessary for neurodegeneration in a Drosophila model of ataxia-telangiectasia. Genetics. 2013;194(1):133-42. Epub 2013/03/19.

117. Svennerholm L, Bostrom K, Jungbjer B, Olsson L. Membrane lipids of adult human brain: lipid composition of frontal and temporal lobe in subjects of age 20 to 100 years. J Neurochem. 1994;63(5):1802-11. Epub 1994/11/01.

118. Adibhatla RM, Hatcher JF. Role of Lipids in Brain Injury and Diseases. Future Lipidol. 2007;2(4):403-22. Epub 2008/01/08.

119. Yung YC, Stoddard NC, Mirendil H, Chun J. Lysophosphatidic Acid signaling in the nervous system. Neuron. 2015;85(4):669-82. Epub 2015/02/20.

120. Rossy J, Ma Y, Gaus K. The organisation of the cell membrane: do proteins rule lipids? Current opinion in chemical biology. 2014;20:54-9. Epub 2014/05/13.

121. Bieberich E. It's a lipid's world: bioactive lipid metabolism and signaling in neural stem cell differentiation. Neurochemical research. 2012;37(6):1208-29. Epub 2012/01/17.

122. Yung YC, Stoddard NC, Chun J. LPA receptor signaling: pharmacology, physiology, and pathophysiology. J Lipid Res. 2014;55(7):1192-214. Epub 2014/03/20.

123. Aoki J. Mechanisms of lysophosphatidic acid production. Seminars in cell & developmental biology. 2004;15(5):477-89. Epub 2004/07/24.

124. Kano K, Arima N, Ohgami M, Aoki J. LPA and its analogs-attractive tools for elucidation of LPA biology and drug development. Current medicinal chemistry. 2008;15(21):2122-31. Epub 2008/09/11.

125. Tokumura A. A family of phospholipid autacoids: Occurrence, metabolism and bioactions. Progress in Lipid Research. 1995;34(2):151-84.

126. van Meer G, Voelker DR, Feigenson GW. Membrane lipids: where they are and how they behave. Nat Rev Mol Cell Biol. 2008;9(2):112-24. Epub 2008/01/25.

127. Aoki J, Inoue A, Okudaira S. Two pathways for lysophosphatidic acid production. Biochim Biophys Acta. 2008;1781(9):513-8. Epub 2008/07/16.

128. Bektas M, Payne SG, Liu H, Goparaju S, Milstien S, Spiegel S. A novel acylglycerol kinase that produces lysophosphatidic acid modulates cross talk with EGFR in prostate cancer cells. The Journal of cell biology. 2005;169(5):801-11. Epub 2005/06/09.

129. Brindley DN, Pilquil C. Lipid phosphate phosphatases and signaling. J Lipid Res. 2009;50 Suppl:S225-30. Epub 2008/12/11.

130. Pages C, Simon MF, Valet P, Saulnier-Blache JS. Lysophosphatidic acid synthesis and release. Prostaglandins Other Lipid Mediat. 2001;64(1-4):1-10. Epub 2001/04/28.

131. Okudaira S, Yukiura H, Aoki J. Biological roles of lysophosphatidic acid signaling through its production by autotaxin. Biochimie. 2010;92(6):698-706. Epub 2010/04/27.

132. McIntyre TM, Pontsler AV, Silva AR, St Hilaire A, Xu Y, Hinshaw JC, et al. Identification of an intracellular receptor for lysophosphatidic acid (LPA): LPA is a transcellular PPARgamma agonist. Proc Natl Acad Sci U S A. 2003;100(1):131-6. Epub 2002/12/28.

133. Tigyi G. Aiming drug discovery at lysophosphatidic acid targets. Br J Pharmacol. 2010;161(2):241-70. Epub 2010/08/26.

134. Aoki J, Taira A, Takanezawa Y, Kishi Y, Hama K, Kishimoto T, et al. Serum lysophosphatidic acid is produced through diverse phospholipase pathways. J Biol Chem. 2002;277(50):48737-44. Epub 2002/10/02.

135. Hosogaya S, Yatomi Y, Nakamura K, Ohkawa R, Okubo S, Yokota H, et al. Measurement of plasma lysophosphatidic acid concentration in healthy subjects: strong correlation with lysophospholipase D activity. Annals of clinical biochemistry. 2008;45(Pt 4):364-8. Epub 2008/06/28.

136. Watanabe N, Ikeda H, Nakamura K, Ohkawa R, Kume Y, Aoki J, et al. Both plasma lysophosphatidic acid and serum autotaxin levels are increased in chronic hepatitis C. Journal of clinical gastroenterology. 2007;41(6):616-23. Epub 2007/06/20.

137. Scherer M, Schmitz G, Liebisch G. High-throughput analysis of sphingosine 1-phosphate, sphinganine 1-phosphate, and lysophosphatidic acid in plasma samples by liquid chromatography-tandem mass spectrometry. Clinical chemistry. 2009;55(6):1218-22. Epub 2009/03/28.

138. Tokumura A, Harada K, Fukuzawa K, Tsukatani H. Involvement of lysophospholipase D in the production of lysophosphatidic acid in rat plasma. Biochim Biophys Acta. 1986;875(1):31-8. Epub 1986/01/03.

139. Eichholtz T, Jalink K, Fahrenfort I, Moolenaar WH. The bioactive phospholipid lysophosphatidic acid is released from activated platelets. Biochem J. 1993;291 (Pt 3):677-80. Epub 1993/05/01.

140. Ma L, Uchida H, Nagai J, Inoue M, Aoki J, Ueda H. Evidence for de novo synthesis of lysophosphatidic acid in the spinal cord through phospholipase A2 and autotaxin in nerve injury-induced neuropathic pain. J Pharmacol Exp Ther. 2010;333(2):540-6. Epub 2010/02/04.

141. Tokumura A, Taira S, Kikuchi M, Tsutsumi T, Shimizu Y, Watsky MA. Lysophospholipids and lysophospholipase D in rabbit aqueous humor following corneal injury. Prostaglandins Other Lipid Mediat. 2012;97(3-4):83-9. Epub 2012/01/28.

142. Smyth SS, Cheng HY, Miriyala S, Panchatcharam M, Morris AJ. Roles of lysophosphatidic acid in cardiovascular physiology and disease. Biochim Biophys Acta. 2008;1781(9):563-70. Epub 2008/07/01.

143. Aaltonen N, Laitinen JT, Lehtonen M. Quantification of lysophosphatidic acids in rat brain tissue by liquid chromatography-electrospray tandem mass spectrometry. J Chromatogr B Analyt Technol Biomed Life Sci. 2010;878(15-16):1145-52. Epub 2010/04/13.

144. Lee JW, Nishiumi S, Yoshida M, Fukusaki E, Bamba T. Simultaneous profiling of polar lipids by supercritical fluid chromatography/tandem mass spectrometry with methylation. Journal of chromatography A. 2013;1279:98-107. Epub 2013/02/06.

145. Triebl A, Trotzmuller M, Eberl A, Hanel P, Hartler J, Kofeler HC. Quantitation of phosphatidic acid and lysophosphatidic acid molecular species using hydrophilic interaction liquid chromatography coupled to electrospray ionization high resolution mass spectrometry. Journal of chromatography A. 2014;1347:104-10. Epub 2014/05/13.

146. Perrakis A, Moolenaar WH. Autotaxin: structure-function and signaling. J Lipid Res. 2014;55(6):1010-8. Epub 2014/02/20.

147. Moolenaar WH, Perrakis A. Insights into autotaxin: how to produce and present a lipid mediator. Nat Rev Mol Cell Biol. 2011;12(10):674-9. Epub 2011/09/15.
148. Umezu-Goto M, Kishi Y, Taira A, Hama K, Dohmae N, Takio K, et al. Autotaxin has lysophospholipase D activity leading to tumor cell growth and motility by lysophosphatidic acid production. The Journal of cell biology. 2002;158(2):227-33. Epub 2002/07/18.
149. Giganti A, Rodriguez M, Fould B, Moulharat N, Coge F, Chomarat P, et al. Murine and human autotaxin alpha, beta, and gamma isoforms: gene organization, tissue distribution, and biochemical characterization. J Biol Chem. 2008;283(12):7776-89. Epub 2008/01/08.
150. Nakamura K, Ohkawa R, Okubo S, Yokota H, Ikeda H, Yatomi Y, et al. Autotaxin enzyme immunoassay in human cerebrospinal fluid samples. Clinica chimica acta; international journal of clinical chemistry. 2009;405(1-2):160-2. Epub 2009/05/06.
151. Nakasaki T, Tanaka T, Okudaira S, Hirosawa M, Umemoto E, Otani K, et al. Involvement of the lysophosphatidic acid-generating enzyme autotaxin in lymphocyte-endothelial cell interactions. The American journal of pathology. 2008;173(5):1566-76. Epub 2008/09/27.
152. Kanda H, Newton R, Klein R, Morita Y, Gunn MD, Rosen SD. Autotaxin, an ectoenzyme that produces lysophosphatidic acid, promotes the entry of lymphocytes into secondary lymphoid organs. Nature immunology. 2008;9(4):415-23. Epub 2008/03/11.
153. van Meeteren LA, Ruurs P, Stortelers C, Bouwman P, van Rooijen MA, Pradere JP, et al. Autotaxin, a secreted lysophospholipase D, is essential for blood vessel formation during development. Molecular and cellular biology. 2006;26(13):5015-22. Epub 2006/06/20.
154. Koike S, Keino-Masu K, Masu M. Deficiency of autotaxin/lysophospholipase D results in head cavity formation in mouse embryos through the LPA receptor-Rho-ROCK pathway. Biochem Biophys Res Commun. 2010;400(1):66-71. Epub 2010/08/10.
155. Koike S, Yutoh Y, Keino-Masu K, Noji S, Masu M, Ohuchi H. Autotaxin is required for the cranial neural tube closure and establishment of the midbrain-hindbrain boundary during mouse development. Developmental dynamics : an official publication of the American Association of Anatomists. 2011;240(2):413-21. Epub 2011/01/20.
156. Moolenaar WH, Houben AJ, Lee SJ, van Meeteren LA. Autotaxin in embryonic development. Biochim Biophys Acta. 2013;1831(1):13-9. Epub 2012/10/02.

157. Tanaka M, Okudaira S, Kishi Y, Ohkawa R, Iseki S, Ota M, et al. Autotaxin stabilizes blood vessels and is required for embryonic vasculature by producing lysophosphatidic acid. J Biol Chem. 2006;281(35):25822-30. Epub 2006/07/11.

158. Yuelling LW, Waggener CT, Afshari FS, Lister JA, Fuss B. Autotaxin/ENPP2 regulates oligodendrocyte differentiation in vivo in the developing zebrafish hindbrain. Glia. 2012;60(10):1605-18. Epub 2012/07/24.

159. Lai SL, Yao WL, Tsao KC, Houben AJ, Albers HM, Ovaa H, et al. Autotaxin/Lpar3 signaling regulates Kupffer's vesicle formation and left-right asymmetry in zebrafish. Development. 2012;139(23):4439-48. Epub 2012/10/26.

160. Cheng HY, Dong A, Panchatcharam M, Mueller P, Yang F, Li Z, et al. Lysophosphatidic acid signaling protects pulmonary vasculature from hypoxia-induced remodeling. Arteriosclerosis, thrombosis, and vascular biology. 2012;32(1):24-32. Epub 2011/10/22.

161. Fotopoulou S, Oikonomou N, Grigorieva E, Nikitopoulou I, Paparountas T, Thanassopoulou A, et al. ATX expression and LPA signalling are vital for the development of the nervous system. Developmental biology. 2010;339(2):451-64. Epub 2010/01/19.

162. Dusaulcy R, Rancoule C, Gres S, Wanecq E, Colom A, Guigne C, et al. Adipose-specific disruption of autotaxin enhances nutritional fattening and reduces plasma lysophosphatidic acid. J Lipid Res. 2011;52(6):1247-55. Epub 2011/03/23.

163. Brindley DN. Lipid phosphate phosphatases and related proteins: signaling functions in development, cell division, and cancer. Journal of cellular biochemistry. 2004;92(5):900-12. Epub 2004/07/20.

164. Awada R, Rondeau P, Gres S, Saulnier-Blache JS, Lefebvre d'Hellencourt C, Bourdon E. Autotaxin protects microglial cells against oxidative stress. Free radical biology & medicine. 2012;52(2):516-26. Epub 2011/12/14.

165. Umemoto E, Hayasaka H, Bai Z, Cai L, Yonekura S, Peng X, et al. Novel regulators of lymphocyte trafficking across high endothelial venules. Critical reviews in immunology. 2011;31(2):147-69. Epub 2011/05/06.

166. Bai Z, Cai L, Umemoto E, Takeda A, Tohya K, Komai Y, et al. Constitutive lymphocyte transmigration across the basal lamina of high endothelial venules is regulated by the autotaxin/lysophosphatidic acid axis. J Immunol. 2013;190(5):2036-48. Epub 2013/02/01.

167. Zhang Y, Chen YC, Krummel MF, Rosen SD. Autotaxin through lysophosphatidic acid stimulates polarization, motility, and transendothelial migration of naive T cells. J Immunol. 2012;189(8):3914-24. Epub 2012/09/11.

168. Chun J, Hla T, Lynch KR, Spiegel S, Moolenaar WH. International Union of Basic and Clinical Pharmacology. LXXVIII. Lysophospholipid receptor nomenclature. Pharmacol Rev. 2010;62(4):579-87. Epub 2010/11/17.

169. Hecht JH, Weiner JA, Post SR, Chun J. Ventricular zone gene-1 (vzg-1) encodes a lysophosphatidic acid receptor expressed in neurogenic regions of the developing cerebral cortex. The Journal of cell biology. 1996;135(4):1071-83. Epub 1996/11/01.

170. Benesch MG, Ko YM, McMullen TP, Brindley DN. Autotaxin in the crosshairs: taking aim at cancer and other inflammatory conditions. FEBS Lett. 2014;588(16):2712-27.

171. Valentine WJ, Fells JI, Perygin DH, Mujahid S, Yokoyama K, Fujiwara Y, et al. Subtype-specific residues involved in ligand activation of the endothelial differentiation gene family lysophosphatidic acid receptors. J Biol Chem. 2008;283(18):12175-87. Epub 2008/03/05.

172. Ishii I, Fukushima N, Ye X, Chun J. Lysophospholipid receptors: signaling and biology. Annual review of biochemistry. 2004;73:321-54. Epub 2004/06/11.

173. Contos JJ, Ishii I, Chun J. Lysophosphatidic acid receptors. Molecular pharmacology. 2000;58(6):1188-96. Epub 2000/11/28.

174. An S, Bleu T, Hallmark OG, Goetzl EJ. Characterization of a novel subtype of human G protein-coupled receptor for lysophosphatidic acid. J Biol Chem. 1998;273(14):7906-10. Epub 1998/05/09.

175. Ohuchi H, Hamada A, Matsuda H, Takagi A, Tanaka M, Aoki J, et al. Expression patterns of the lysophospholipid receptor genes during mouse early development. Developmental dynamics : an official publication of the American Association of Anatomists. 2008;237(11):3280-94. Epub 2008/10/17.

176. Contos JJ, Fukushima N, Weiner JA, Kaushal D, Chun J. Requirement for the lpA1 lysophosphatidic acid receptor gene in normal suckling behavior. Proc Natl Acad Sci U S A. 2000;97(24):13384-9. Epub 2000/11/23.

177. Contos JJ, Chun J. Genomic characterization of the lysophosphatidic acid receptor gene, lp(A2)/Edg4, and identification of a frameshift mutation in a previously characterized cDNA. Genomics. 2000;64(2):155-69. Epub 2000/03/24.

178. Lai YJ, Lin WC, Lin FT. PTPL1/FAP-1 negatively regulates TRIP6 function in lysophosphatidic acid-induced cell migration. J Biol Chem. 2007;282(33):24381-7. Epub 2007/06/27.

179. Diez-Roux G, Banfi S, Sultan M, Geffers L, Anand S, Rozado D, et al. A high-resolution anatomical atlas of the transcriptome in the mouse embryo. PLoS biology. 2011;9(1):e1000582. Epub 2011/01/27.

180. Dubin AE, Herr DR, Chun J. Diversity of lysophosphatidic acid receptor-mediated intracellular calcium signaling in early cortical neurogenesis. J Neurosci. 2010;30(21):7300-9. Epub 2010/05/28.

181. Yang AH, Ishii I, Chun J. In vivo roles of lysophospholipid receptors revealed by gene targeting studies in mice. Biochim Biophys Acta. 2002;1582(1-3):197-203. Epub 2002/06/19.

182. Kingsbury MA, Rehen SK, Contos JJ, Higgins CM, Chun J. Non-proliferative effects of lysophosphatidic acid enhance cortical growth and folding. Nat Neurosci. 2003;6(12):1292-9. Epub 2003/11/20.

183. Panchatcharam M, Miriyala S, Yang F, Rojas M, End C, Vallant C, et al. Lysophosphatidic acid receptors 1 and 2 play roles in regulation of vascular injury responses but not blood pressure. Circ Res. 2008;103(6):662-70. Epub 2008/08/16.

184. Bandoh K, Aoki J, Hosono H, Kobayashi S, Kobayashi T, Murakami-Murofushi K, et al. Molecular cloning and characterization of a novel human G-protein-coupled receptor, EDG7, for lysophosphatidic acid. J Biol Chem. 1999;274(39):27776-85. Epub 1999/09/17.

185. Choi JW, Herr DR, Noguchi K, Yung YC, Lee CW, Mutoh T, et al. LPA receptors: subtypes and biological actions. Annual review of pharmacology and toxicology. 2010;50:157-86. Epub 2010/01/09.

186. Ishii I, Contos JJ, Fukushima N, Chun J. Functional comparisons of the lysophosphatidic acid receptors, LP(A1)/VZG-1/EDG-2, LP(A2)/EDG-4, and LP(A3)/EDG-7 in neuronal cell lines using a retrovirus expression system. Molecular pharmacology. 2000;58(5):895-902. Epub 2000/10/20.

187. Sonoda H, Aoki J, Hiramatsu T, Ishida M, Bandoh K, Nagai Y, et al. A novel phosphatidic acid-selective phospholipase A1 that produces lysophosphatidic acid. J Biol Chem. 2002;277(37):34254-63. Epub 2002/06/14.

188. Noguchi K, Ishii S, Shimizu T. Identification of p2y9/GPR23 as a novel G protein-coupled receptor for lysophosphatidic acid, structurally distant from the Edg family. J Biol Chem. 2003;278(28):25600-6. Epub 2003/05/02.

189. Lee CW, Rivera R, Dubin AE, Chun J. LPA(4)/GPR23 is a lysophosphatidic acid (LPA) receptor utilizing G(s)-, G(q)/G(i)-mediated calcium signaling and G(12/13)-mediated Rho activation. J Biol Chem. 2007;282(7):4310-7. Epub 2006/12/15.

190. Yanagida K, Ishii S, Hamano F, Noguchi K, Shimizu T. LPA4/p2y9/GPR23 mediates rho-dependent morphological changes in a rat neuronal cell line. J Biol Chem. 2007;282(8):5814-24. Epub 2006/12/19.

191. Rhee HJ, Nam JS, Sun Y, Kim MJ, Choi HK, Han DH, et al. Lysophosphatidic acid stimulates cAMP accumulation and cAMP response element-binding protein phosphorylation in immortalized hippocampal progenitor cells. Neuroreport. 2006;17(5):523-6. Epub 2006/03/18.

192. Lee Z, Cheng CT, Zhang H, Subler MA, Wu J, Mukherjee A, et al. Role of LPA4/p2y9/GPR23 in negative regulation of cell motility. Molecular biology of the cell. 2008;19(12):5435-45. Epub 2008/10/10.

193. Liu YB, Kharode Y, Bodine PV, Yaworsky PJ, Robinson JA, Billiard J. LPA induces osteoblast differentiation through interplay of two receptors: LPA1 and LPA4. Journal of cellular biochemistry. 2010;109(4):794-800. Epub 2010/01/14.

194. Sumida H, Noguchi K, Kihara Y, Abe M, Yanagida K, Hamano F, et al. LPA4 regulates blood and lymphatic vessel formation during mouse embryogenesis. Blood. 2010;116(23):5060-70. Epub 2010/08/18.

195. Kotarsky K, Boketoft A, Bristulf J, Nilsson NE, Norberg A, Hansson S, et al. Lysophosphatidic acid binds to and activates GPR92, a G protein-coupled receptor highly expressed in gastrointestinal lymphocytes. J Pharmacol Exp Ther. 2006;318(2):619-28. Epub 2006/05/03.

196. Lee CW, Rivera R, Gardell S, Dubin AE, Chun J. GPR92 as a new G12/13- and Gq-coupled lysophosphatidic acid receptor that increases cAMP, LPA5. J Biol Chem. 2006;281(33):23589-97. Epub 2006/06/16.

197. Williams JR, Khandoga AL, Goyal P, Fells JI, Perygin DH, Siess W, et al. Unique ligand selectivity of the GPR92/LPA5 lysophosphatidate receptor indicates role in human platelet activation. J Biol Chem. 2009;284(25):17304-19. Epub 2009/04/16.

198. Jongsma M, Matas-Rico E, Rzadkowski A, Jalink K, Moolenaar WH. LPA is a chemorepellent for B16 melanoma cells: action through the cAMP-elevating LPA5 receptor. PloS one. 2011;6(12):e29260. Epub 2011/12/24.

199. Amisten S, Braun OO, Bengtsson A, Erlinge D. Gene expression profiling for the identification of G-protein coupled receptors in human platelets. Thrombosis research. 2008;122(1):47-57. Epub 2007/10/09.

200. Lundequist A, Boyce JA. LPA5 is abundantly expressed by human mast cells and important for lysophosphatidic acid induced MIP-1beta release. PloS one. 2011;6(3):e18192. Epub 2011/04/06.

201. Kaplan MH, Smith DI, Sundick RS. Identification of a G protein coupled receptor induced in activated T cells. J Immunol. 1993;151(2):628-36. Epub 1993/07/15.

202. Webb TE, Kaplan MG, Barnard EA. Identification of 6H1 as a P2Y purinoceptor: P2Y5. Biochem Biophys Res Commun. 1996;219(1):105-10. Epub 1996/02/06.

203. Pasternack SM, von Kugelgen I, Al Aboud K, Lee YA, Ruschendorf F, Voss K, et al. G protein-coupled receptor P2Y5 and its ligand LPA are involved in maintenance of human hair growth. Nature genetics. 2008;40(3):329-34. Epub 2008/02/26.

204. Yanagida K, Masago K, Nakanishi H, Kihara Y, Hamano F, Tajima Y, et al. Identification and characterization of a novel lysophosphatidic acid receptor, p2y5/LPA6. J Biol Chem. 2009;284(26):17731-41. Epub 2009/04/24.

205. Lee M, Choi S, Hallden G, Yo SJ, Schichnes D, Aponte GW. P2Y5 is a G(alpha)i, G(alpha)12/13 G protein-coupled receptor activated by lysophosphatidic acid that reduces intestinal cell adhesion. American journal of physiology Gastrointestinal and liver physiology. 2009;297(4):G641-54. Epub 2009/08/15.

206. Shimomura Y, Garzon MC, Kristal L, Shapiro L, Christiano AM. Autosomal recessive woolly hair with hypotrichosis caused by a novel homozygous mutation in the P2RY5 gene. Experimental dermatology. 2009;18(3):218-21. Epub 2008/09/23.

207. Nahum S, Morice-Picard F, Taieb A, Sprecher E. A novel mutation in LPAR6 causes autosomal recessive hypotrichosis of the scalp. Clinical and experimental dermatology. 2011;36(2):188-94. Epub 2010/11/13.

208. Yung YC, Mutoh T, Lin ME, Noguchi K, Rivera RR, Choi JW, et al. Lysophosphatidic acid signaling may initiate fetal hydrocephalus. Sci Transl Med. 2011;3(99):99ra87. Epub 2011/09/09.

209. Anliker B, Choi JW, Lin ME, Gardell SE, Rivera RR, Kennedy G, et al. Lysophosphatidic acid (LPA) and its receptor, LPA1 , influence embryonic schwann cell migration, myelination, and cell-to-axon segregation. Glia. 2013;61(12):2009-22. Epub 2013/10/12.

210. Trimbuch T, Beed P, Vogt J, Schuchmann S, Maier N, Kintscher M, et al. Synaptic PRG-1 modulates excitatory transmission via lipid phosphate-mediated signaling. Cell. 2009;138(6):1222-35. Epub 2009/09/22.

211. Moller T, Contos JJ, Musante DB, Chun J, Ransom BR. Expression and function of lysophosphatidic acid receptors in cultured rodent microglial cells. J Biol Chem. 2001;276(28):25946-52. Epub 2001/05/08.

212. Teo ST, Yung YC, Herr DR, Chun J. Lysophosphatidic acid in vascular development and disease. IUBMB Life. 2009;61(8):791-9. Epub 2009/07/22.

213. Fukushima N, Kimura Y, Chun J. A single receptor encoded by vzg-1/lpA1/edg-2 couples to G proteins and mediates multiple cellular responses to lysophosphatidic acid. Proc Natl Acad Sci U S A. 1998;95(11):6151-6. Epub 1998/05/30.

214. Estivill-Torrus G, Llebrez-Zayas P, Matas-Rico E, Santin L, Pedraza C, De Diego I, et al. Absence of LPA1 signaling results in defective cortical development. Cereb Cortex. 2008;18(4):938-50. Epub 2007/07/28.

215. Harrison SM, Reavill C, Brown G, Brown JT, Cluderay JE, Crook B, et al. LPA1 receptor-deficient mice have phenotypic changes observed in psychiatric disease. Molecular and cellular neurosciences. 2003;24(4):1170-9. Epub 2003/12/31.

216. Campbell DS, Holt CE. Chemotropic responses of retinal growth cones mediated by rapid local protein synthesis and degradation. Neuron. 2001;32(6):1013-26. Epub 2002/01/05.

217. Fukushima N, Weiner JA, Chun J. Lysophosphatidic acid (LPA) is a novel extracellular regulator of cortical neuroblast morphology. Developmental biology. 2000;228(1):6-18. Epub 2000/11/23.

218. Fukushima N, Weiner JA, Kaushal D, Contos JJ, Rehen SK, Kingsbury MA, et al. Lysophosphatidic acid influences the morphology and motility of young, postmitotic cortical neurons. Molecular and cellular neurosciences. 2002;20(2):271-82. Epub 2002/07/03.

219. Weiner JA, Fukushima N, Contos JJ, Scherer SS, Chun J. Regulation of Schwann cell morphology and adhesion by receptor-mediated lysophosphatidic acid signaling. J Neurosci. 2001;21(18):7069-78. Epub 2001/09/11.

220. Inoue M, Rashid MH, Fujita R, Contos JJ, Chun J, Ueda H. Initiation of neuropathic pain requires lysophosphatidic acid receptor signaling. Nat Med. 2004;10(7):712-8. Epub 2004/06/15.

221. Svetlov SI, Ignatova TN, Wang KK, Hayes RL, English D, Kukekov VG. Lysophosphatidic acid induces clonal generation of mouse neurospheres via proliferation of Sca-1- and AC133-positive neural progenitors. Stem cells and development. 2004;13(6):685-93. Epub 2005/02/03.

222. Matas-Rico E, Garcia-Diaz B, Llebrez-Zayas P, Lopez-Barroso D, Santin L, Pedraza C, et al. Deletion of lysophosphatidic acid receptor LPA1 reduces neurogenesis in the mouse dentate gyrus. Molecular and cellular neurosciences. 2008;39(3):342-55. Epub 2008/08/19.

223. Zheng ZQ, Fang XJ, Qiao JT. Dual action of lysophosphatidic acid in cultured cortical neurons: survival and apoptogenic. Sheng li xue bao : [Acta physiologica Sinica]. 2004;56(2):163-71. Epub 2004/05/06.

224. Pilpel Y, Segal M. The role of LPA1 in formation of synapses among cultured hippocampal neurons. J Neurochem. 2006;97(5):1379-92. Epub 2006/04/28.

225. Spohr TC, Choi JW, Gardell SE, Herr DR, Rehen SK, Gomes FC, et al. Lysophosphatidic acid receptor-dependent secondary effects via astrocytes promote neuronal differentiation. J Biol Chem. 2008;283(12):7470-9. Epub 2008/01/17.

226. Shano S, Moriyama R, Chun J, Fukushima N. Lysophosphatidic acid stimulates astrocyte proliferation through LPA1. Neurochem Int. 2008;52(1-2):216-20. Epub 2007/08/19.

227. Manning TJ, Jr., Sontheimer H. Bovine serum albumin and lysophosphatidic acid stimulate calcium mobilization and reversal of cAMP-induced stellation in rat spinal cord astrocytes. Glia. 1997;20(2):163-72. Epub 1997/06/01.

228. Sorensen SD, Nicole O, Peavy RD, Montoya LM, Lee CJ, Murphy TJ, et al. Common signaling pathways link activation of murine PAR-1, LPA, and S1P receptors to proliferation of astrocytes. Molecular pharmacology. 2003;64(5):1199-209. Epub 2003/10/24.

229. Tham CS, Lin FF, Rao TS, Yu N, Webb M. Microglial activation state and lysophospholipid acid receptor expression. International journal of developmental neuroscience : the official journal of the International Society for Developmental Neuroscience. 2003;21(8):431-43. Epub 2003/12/09.

230. Bernhart E, Kollroser M, Rechberger G, Reicher H, Heinemann A, Schratl P, et al. Lysophosphatidic acid receptor activation affects the C13NJ microglia cell line proteome leading to alterations in glycolysis, motility, and cytoskeletal architecture. Proteomics. 2010;10(1):141-58. Epub 2009/11/10.

231. Fujita R, Ma Y, Ueda H. Lysophosphatidic acid-induced membrane ruffling and brain-derived neurotrophic factor gene expression are mediated by ATP release in primary microglia. J Neurochem. 2008;107(1):152-60. Epub 2008/08/06.

232. Schilling T, Stock C, Schwab A, Eder C. Functional importance of Ca2+-activated K+ channels for lysophosphatidic acid-induced microglial migration. The European journal of neuroscience. 2004;19(6):1469-74. Epub 2004/04/07.

233. Allard J, Barron S, Diaz J, Lubetzki C, Zalc B, Schwartz JC, et al. A rat G protein-coupled receptor selectively expressed in myelin-forming cells. The European journal of neuroscience. 1998;10(3):1045-53. Epub 1998/09/30.

234. Weiner JA, Hecht JH, Chun J. Lysophosphatidic acid receptor gene vzg-1/lpA1/edg-2 is expressed by mature oligodendrocytes during myelination in the postnatal murine brain. The Journal of comparative neurology. 1998;398(4):587-98. Epub 1998/08/26.

235. Yu N, Lariosa-Willingham KD, Lin FF, Webb M, Rao TS. Characterization of lysophosphatidic acid and sphingosine-1-phosphate-mediated signal transduction in rat cortical oligodendrocytes. Glia. 2004;45(1):17-27. Epub 2003/12/04.

236. Cervera P, Tirard M, Barron S, Allard J, Trottier S, Lacombe J, et al. Immunohistological localization of the myelinating cell-specific receptor LP(A1). Glia. 2002;38(2):126-36. Epub 2002/04/12.

237. Nogaroli L, Yuelling LM, Dennis J, Gorse K, Payne SG, Fuss B. Lysophosphatidic acid can support the formation of membranous structures and an increase in MBP mRNA levels in differentiating oligodendrocytes. Neurochemical research. 2009;34(1):182-93. Epub 2008/07/03.

238. Weiner JA, Chun J. Schwann cell survival mediated by the signaling phospholipid lysophosphatidic acid. Proc Natl Acad Sci U S A. 1999;96(9):5233-8. Epub 1999/04/29.

239. Li Y, Gonzalez MI, Meinkoth JL, Field J, Kazanietz MG, Tennekoon GI. Lysophosphatidic acid promotes survival and differentiation of rat Schwann cells. J Biol Chem. 2003;278(11):9585-91. Epub 2003/01/14.

240. Frohnert PW, Stonecypher MS, Carroll SL. Lysophosphatidic acid promotes the proliferation of adult Schwann cells isolated from axotomized sciatic nerve. Journal of neuropathology and experimental neurology. 2003;62(5):520-9. Epub 2003/05/29.

241. Goldshmit Y, Munro K, Leong SY, Pebay A, Turnley AM. LPA receptor expression in the central nervous system in health and following injury. Cell and tissue research. 2010;341(1):23-32. Epub 2010/05/25.

242. Savaskan NE, Rocha L, Kotter MR, Baer A, Lubec G, van Meeteren LA, et al. Autotaxin (NPP-2) in the brain: cell type-specific expression and regulation during development and after neurotrauma. Cell Mol Life Sci. 2007;64(2):230-43. Epub 2006/12/29.

243. Umemura K, Yamashita N, Yu X, Arima K, Asada T, Makifuchi T, et al. Autotaxin expression is enhanced in frontal cortex of Alzheimer-type dementia patients. Neuroscience letters. 2006;400(1-2):97-100. Epub 2006/03/15.

244. Shi J, Dong Y, Cui MZ, Xu X. Lysophosphatidic acid induces increased BACE1 expression and Abeta formation. Biochim Biophys Acta. 2013;1832(1):29-38. Epub 2012/10/06.

245. Sayas CL, Moreno-Flores MT, Avila J, Wandosell F. The neurite retraction induced by lysophosphatidic acid increases Alzheimer's disease-like Tau phosphorylation. J Biol Chem. 1999;274(52):37046-52. Epub 1999/12/22.

246. Hwang SH, Shin EJ, Shin TJ, Lee BH, Choi SH, Kang J, et al. Gintonin, a ginseng-derived lysophosphatidic acid receptor ligand, attenuates Alzheimer's disease-related neuropathies: involvement of non-amyloidogenic processing. Journal of Alzheimer's disease : JAD. 2012;31(1):207-23. Epub 2012/05/01.

247. Ueda H, Matsunaga H, Olaposi OI, Nagai J. Lysophosphatidic acid: chemical signature of neuropathic pain. Biochim Biophys Acta. 2013;1831(1):61-73. Epub 2012/09/11.

248. Tsujiuchi T, Araki M, Hirane M, Dong Y, Fukushima N. Lysophosphatidic acid receptors in cancer pathobiology. Histology and histopathology. 2014;29(3):313-21. Epub 2013/11/07.

249. Hoelzinger DB, Nakada M, Demuth T, Rosensteel T, Reavie LB, Berens ME. Autotaxin: a secreted autocrine/paracrine factor that promotes glioma invasion. J Neurooncol. 2008;86(3):297-309. Epub 2007/10/12.

250. Kishi Y, Okudaira S, Tanaka M, Hama K, Shida D, Kitayama J, et al. Autotaxin is overexpressed in glioblastoma multiforme and contributes to cell motility of glioblastoma by converting lysophosphatidylcholine to lysophosphatidic acid. J Biol Chem. 2006;281(25):17492-500. Epub 2006/04/22.

251. Khalil BD, El-Sibai M. Rho GTPases in primary brain tumor malignancy and invasion. J Neurooncol. 2012;108(3):333-9. Epub 2012/04/25.

252. Manning TJ, Jr., Parker JC, Sontheimer H. Role of lysophosphatidic acid and rho in glioma cell motility. Cell motility and the cytoskeleton. 2000;45(3):185-99. Epub 2000/03/08.

253. Annabi B, Lachambre MP, Plouffe K, Sartelet H, Beliveau R. Modulation of invasive properties of CD133+ glioblastoma stem cells: a role for MT1-MMP in bioactive lysophospholipid signaling. Molecular carcinogenesis. 2009;48(10):910-9. Epub 2009/03/28.

254. Salhia B, Rutten F, Nakada M, Beaudry C, Berens M, Kwan A, et al. Inhibition of Rho-kinase affects astrocytoma morphology, motility, and invasion through activation of Rac1. Cancer Res. 2005;65(19):8792-800. Epub 2005/10/06.

255. Corcoran A, O'Connor JJ. Hypoxia-inducible factor signalling mechanisms in the central nervous system. Acta Physiol (Oxf). 2013;208(4):298-310. Epub 2013/05/23.

256. Lee J, Park SY, Lee EK, Park CG, Chung HC, Rha SY, et al. Activation of hypoxia-inducible factor-1alpha is necessary for lysophosphatidic acid-induced vascular endothelial growth factor expression. Clinical cancer research : an official journal of the American Association for Cancer Research. 2006;12(21):6351-8. Epub 2006/11/07.

257. Lee SJ, No YR, Dang DT, Dang LH, Yang VW, Shim H, et al. Regulation of hypoxia-inducible factor 1alpha (HIF-1alpha) by lysophosphatidic acid is dependent on interplay between p53 and Kruppel-like factor 5. J Biol Chem. 2013;288(35):25244-53. Epub 2013/07/25.

258. Herr KJ, Herr DR, Lee CW, Noguchi K, Chun J. Stereotyped fetal brain disorganization is induced by hypoxia and requires lysophosphatidic acid receptor 1 (LPA1) signaling. Proc Natl Acad Sci U S A. 2011;108(37):15444-9. Epub 2011/09/01.

259. Savitz SI, Dhallu MS, Malhotra S, Mammis A, Ocava LC, Rosenbaum PS, et al. EDG receptors as a potential therapeutic target in retinal ischemia-reperfusion injury. Brain research. 2006;1118(1):168-75. Epub 2006/10/10.

260. Ploeger A, Raijmakers ME, van der Maas HL, Galis F. The association between autism and errors in early embryogenesis: what is the causal mechanism? Biological psychiatry. 2010;67(7):602-7. Epub 2009/11/26.

261. Castilla-Ortega E, Escuredo L, Bilbao A, Pedraza C, Orio L, Estivill-Torrus G, et al. 1-Oleoyl lysophosphatidic acid: a new mediator of emotional behavior in rats. PloS one. 2014;9(1):e85348. Epub 2014/01/11.

262. Moolenaar WH, van Meeteren LA, Giepmans BN. The ins and outs of lysophosphatidic acid signaling. Bioessays. 2004;26(8):870-81. Epub 2004/07/27.

263. Knowlden S, Georas SN. The autotaxin-LPA axis emerges as a novel regulator of lymphocyte homing and inflammation. J Immunol. 2014;192(3):851-7. Epub 2014/01/21.
264. Liu S, Murph M, Panupinthu N, Mills GB. ATX-LPA receptor axis in inflammation and cancer. Cell Cycle. 2009;8(22):3695-701. Epub 2009/10/27.
265. Sevastou I, Kaffe E, Mouratis MA, Aidinis V. Lysoglycerophospholipids in chronic inflammatory disorders: the PLA(2)/LPC and ATX/LPA axes. Biochim Biophys Acta. 2013;1831(1):42-60. Epub 2012/08/08.
266. Yin Z, Carbone LD, Gotoh M, Postlethwaite A, Bolen AL, Tigyi GJ, et al. Lysophosphatidic acid-activated Cl- current activity in human systemic sclerosis skin fibroblasts. Rheumatology (Oxford). 2010;49(12):2290-7. Epub 2010/09/09.
267. Park GY, Lee YG, Berdyshev E, Nyenhuis S, Du J, Fu P, et al. Autotaxin production of lysophosphatidic acid mediates allergic asthmatic inflammation. American journal of respiratory and critical care medicine. 2013;188(8):928-40. Epub 2013/09/21.
268. Zhao C, Fernandes MJ, Prestwich GD, Turgeon M, Di Battista J, Clair T, et al. Regulation of lysophosphatidic acid receptor expression and function in human synoviocytes: implications for rheumatoid arthritis? Mol Pharmacol. 2008;73(2):587-600. Epub 2007/11/17.
269. Miyabe Y, Miyabe C, Iwai Y, Takayasu A, Fukuda S, Yokoyama W, et al. Necessity of lysophosphatidic acid receptor 1 for development of arthritis. Arthritis and rheumatism. 2013;65(8):2037-47. Epub 2013/05/15.
270. Mototani H, Iida A, Nakajima M, Furuichi T, Miyamoto Y, Tsunoda T, et al. A functional SNP in EDG2 increases susceptibility to knee osteoarthritis in Japanese. Human molecular genetics. 2008;17(12):1790-7. Epub 2008/03/08.
271. Deierborg T. Preparation of primary microglia cultures from postnatal mouse and rat brains. Methods Mol Biol. 2013;1041:25-31. Epub 2013/07/03.
272. Kozian DH, Evers A, Florian P, Wonerow P, Joho S, Nazare M. Selective non-lipid modulator of LPA5 activity in human platelets. Bioorganic & medicinal chemistry letters. 2012;22(16):5239-43. Epub 2012/07/18.
273. Harikumar KB, Kunnumakkara AB, Ochi N, Tong Z, Deorukhkar A, Sung B, et al. A novel small-molecule inhibitor of protein kinase D blocks pancreatic cancer growth in vitro and in vivo. Molecular cancer therapeutics. 2010;9(5):1136-46. Epub 2010/05/06.
274. Waetzig V, Czeloth K, Hidding U, Mielke K, Kanzow M, Brecht S, et al. c-Jun N-terminal kinases (JNKs) mediate pro-inflammatory actions of microglia. Glia. 2005;50(3):235-46. Epub 2005/03/02.

275. Livak KJ, Schmittgen TD. Analysis of relative gene expression data using real-time quantitative PCR and the 2(-Delta Delta C(T)) Method. Methods. 2001;25(4):402-8. Epub 2002/02/16.

276. McCall MN, McMurray HR, Land H, Almudevar A. On non-detects in qPCR data. Bioinformatics. 2014;30(16):2310-6. Epub 2014/04/26.

277. Halliwell B, Whiteman M. Measuring reactive species and oxidative damage in vivo and in cell culture: how should you do it and what do the results mean? Br J Pharmacol. 2004;142(2):231-55. Epub 2004/05/25.

278. Walker FR, Beynon SB, Jones KA, Zhao Z, Kongsui R, Cairns M, et al. Dynamic structural remodelling of microglia in health and disease: a review of the models, the signals and the mechanisms. Brain, behavior, and immunity. 2014;37:1-14. Epub 2014/01/15.

279. Hickman SE, Kingery ND, Ohsumi TK, Borowsky ML, Wang LC, Means TK, et al. The microglial sensome revealed by direct RNA sequencing. Nat Neurosci. 2013;16(12):1896-905. Epub 2013/10/29.

280. Ridley AJ, Schwartz MA, Burridge K, Firtel RA, Ginsberg MH, Borisy G, et al. Cell migration: integrating signals from front to back. Science. 2003;302(5651):1704-9. Epub 2003/12/06.

281. Vicente-Manzanares M, Webb DJ, Horwitz AR. Cell migration at a glance. Journal of cell science. 2005;118(Pt 21):4917-9. Epub 2005/10/29.

282. Rozengurt E, Rey O, Waldron RT. Protein kinase D signaling. J Biol Chem. 2005;280(14):13205-8. Epub 2005/02/11.

283. Huang C, Jacobson K, Schaller MD. MAP kinases and cell migration. Journal of cell science. 2004;117(Pt 20):4619-28. Epub 2004/09/17.

284. Lauffenburger DA, Horwitz AF. Cell migration: a physically integrated molecular process. Cell. 1996;84(3):359-69. Epub 1996/02/09.

285. Rozengurt E. Protein kinase D signaling: multiple biological functions in health and disease. Physiology (Bethesda). 2011;26(1):23-33. Epub 2011/03/02.

286. McHugh D, Hu SS, Rimmerman N, Juknat A, Vogel Z, Walker JM, et al. N-arachidonoyl glycine, an abundant endogenous lipid, potently drives directed cellular migration through GPR18, the putative abnormal cannabidiol receptor. BMC neuroscience. 2010;11:44. Epub 2010/03/30.

287. Harry GJ, Kraft AD. Neuroinflammation and microglia: considerations and approaches for neurotoxicity assessment. Expert Opinion on Drug Metabolism & Toxicology. 2008;4(10):1265-77.

288. Chhor V, Le Charpentier T, Lebon S, Ore MV, Celador IL, Josserand J, et al. Characterization of phenotype markers and neuronotoxic potential of polarised primary microglia in vitro. Brain, behavior, and immunity. 2013;32:70-85. Epub 2013/03/05.

289. Medzhitov R, Horng T. Transcriptional control of the inflammatory response. Nature reviews Immunology. 2009;9(10):692-703.

290. Shih RH, Wang CY, Yang CM. NF-kappaB Signaling Pathways in Neurological Inflammation: A Mini Review. Frontiers in molecular neuroscience. 2015;8:77. Epub 2016/01/07.

291. Herdegen T, Waetzig V. AP-1 proteins in the adult brain: facts and fiction about effectors of neuroprotection and neurodegeneration. Oncogene. 2001;20(19):2424-37. Epub 2001/06/13.

292. Kaplan MH. STAT signaling in inflammation. Jak-Stat. 2013;2(1):e24198. Epub 2013/09/24.

293. Tigyi G, Hong L, Yakubu M, Parfenova H, Shibata M, Leffler CW. Lysophosphatidic acid alters cerebrovascular reactivity in piglets. The American journal of physiology. 1995;268(5 Pt 2):H2048-55. Epub 1995/05/01.

294. Santos-Nogueira E, Lopez-Serrano C, Hernandez J, Lago N, Astudillo AM, Balsinde J, et al. Activation of Lysophosphatidic Acid Receptor Type 1 Contributes to Pathophysiology of Spinal Cord Injury. J Neurosci. 2015;35(28):10224-35. Epub 2015/07/17.

295. Crack PJ, Zhang M, Morganti-Kossmann MC, Morris AJ, Wojciak JM, Fleming JK, et al. Anti-lysophosphatidic acid antibodies improve traumatic brain injury outcomes. Journal of neuroinflammation. 2014;11:37. Epub 2014/03/01.

296. Kishi Y, Okudaira S, Tanaka M, Hama K, Shida D, Kitayama J, et al. Autotaxin Is Overexpressed in Glioblastoma Multiforme and Contributes to Cell Motility of Glioblastoma by Converting Lysophosphatidylcholine TO Lysophosphatidic Acid. Journal of Biological Chemistry. 2006;281(25):17492-500.

297. Tabuchi S. The autotaxin-lysophosphatidic acid–lysophosphatidic acid receptor cascade: proposal of a novel potential therapeutic target for treating glioblastoma multiforme. Lipids in Health and Disease. 2015;14(1):56.

298. Mills GB, Moolenaar WH. The emerging role of lysophosphatidic acid in cancer. Nat Rev Cancer. 2003;3(8):582-91.

299. Xiang SY, Dusaban SS, Brown JH. Lysophospholipid receptor activation of RhoA and lipid signaling pathways. Biochim Biophys Acta. 2013;1831(1):213-22. Epub 2012/09/19.

300. Eyo UB, Dailey ME. Microglia: key elements in neural development, plasticity, and pathology. Journal of neuroimmune pharmacology : the official journal of the Society on NeuroImmune Pharmacology. 2013;8(3):494-509. Epub 2013/01/29.

301. Madore C, Joffre C, Delpech JC, De Smedt-Peyrusse V, Aubert A, Coste L, et al. Early morphofunctional plasticity of microglia in response to acute lipopolysaccharide. Brain, behavior, and immunity. 2013;34:151-8. Epub 2013/09/03.

302. Sunkaria A, Bhardwaj S, Halder A, Yadav A, Sandhir R. Migration and Phagocytic Ability of Activated Microglia During Post-natal Development is Mediated by Calcium-Dependent Purinergic Signalling. Mol Neurobiol. 2016;53(2):944-54. Epub 2015/01/13.

303. Kanazawa H, Ohsawa K, Sasaki Y, Kohsaka S, Imai Y. Macrophage/microglia-specific protein Iba1 enhances membrane ruffling and Rac activation via phospholipase C-gamma -dependent pathway. J Biol Chem. 2002;277(22):20026-32. Epub 2002/03/28.

304. Imai Y, Kohsaka S. Intracellular signaling in M-CSF-induced microglia activation: role of Iba1. Glia. 2002;40(2):164-74. Epub 2002/10/16.

305. Torres-Platas SG, Comeau S, Rachalski A, Bo GD, Cruceanu C, Turecki G, et al. Morphometric characterization of microglial phenotypes in human cerebral cortex. Journal of neuroinflammation. 2014;11:12. Epub 2014/01/23.

306. Wirjatijasa F, Dehghani F, Blaheta RA, Korf HW, Hailer NP. Interleukin-4, interleukin-10, and interleukin-1-receptor antagonist but not transforming growth factor-beta induce ramification and reduce adhesion molecule expression of rat microglial cells. Journal of neuroscience research. 2002;68(5):579-87. Epub 2002/07/12.

307. Jacob SW, Herschler R. Pharmacology of DMSO. Cryobiology. 1986;23(1):14-27.

308. Penazzi L, Lorengel J, Sundermann F, Golovyashkina N, Marre S, Mathis CM, et al. DMSO modulates CNS function in a preclinical Alzheimer's disease model. Neuropharmacology. 2017;113(Pt A):434-44. Epub 2016/10/25.

309. Blacher E, Ben Baruch B, Levy A, Geva N, Green KD, Garneau-Tsodikova S, et al. Inhibition of glioma progression by a newly discovered CD38 inhibitor. International journal of cancer. 2015;136(6):1422-33. Epub 2014/07/24.

310. Elisia I, Nakamura H, Lam V, Hofs E, Cederberg R, Cait J, et al. DMSO Represses Inflammatory Cytokine Production from Human Blood Cells and Reduces Autoimmune Arthritis. PloS one. 2016;11(3):e0152538. Epub 2016/04/01.

311. Doppler HR, Bastea LI, Lewis-Tuffin LJ, Anastasiadis PZ, Storz P. Protein kinase D1-mediated phosphorylations regulate vasodilator-stimulated phosphoprotein (VASP) localization and cell migration. J Biol Chem. 2013;288(34):24382-93. Epub 2013/07/13.

312. Rey O, Yuan J, Rozengurt E. Intracellular redistribution of protein kinase D2 in response to G-protein-coupled receptor agonists. Biochem Biophys Res Commun. 2003;302(4):817-24. Epub 2003/03/21.

313. Rey O, Sinnett-Smith J, Zhukova E, Rozengurt E. Regulated nucleocytoplasmic transport of protein kinase D in response to G protein-coupled receptor activation. J Biol Chem. 2001;276(52):49228-35. Epub 2001/10/20.

314. Wille C, Seufferlein T, Eiseler T. Protein Kinase D family kinases: roads start to segregate. Bioarchitecture. 2014;4(3):111-5. Epub 2014/05/23.

315. Zhang ER, Liu S, Wu LF, Altschuler SJ, Cobb MH. Chemoattractant concentration-dependent tuning of ERK signaling dynamics in migrating neutrophils. Science signaling. 2016;9(458):ra122. Epub 2016/12/15.

316. Wang Y, Waldron RT, Dhaka A, Patel A, Riley MM, Rozengurt E, et al. The RAS effector RIN1 directly competes with RAF and is regulated by 14-3-3 proteins. Molecular and cellular biology. 2002;22(3):916-26. Epub 2002/01/11.

317. Song J, Li J, Qiao J, Jain S, Mark Evers B, Chung DH. PKD prevents H2O2-induced apoptosis via NF-kappaB and p38 MAPK in RIE-1 cells. Biochemical and biophysical research communications. 2009;378(3):610-4. Epub 2008/12/09.

318. Bernhart E, Damm S, Heffeter P, Wintersperger A, Asslaber M, Frank S, et al. Silencing of protein kinase D2 induces glioma cell senescence via p53-dependent and -independent pathways. Neuro Oncol. 2014;16(7):933-45. Epub 2014/01/28.

319. Alcantara-Hernandez R, Hernandez-Mendez A, Campos-Martinez GA, Meizoso-Huesca A, Garcia-Sainz JA. Phosphorylation and Internalization of Lysophosphatidic Acid Receptors LPA1, LPA2, and LPA3. PLoS One. 2015;10(10):e0140583. Epub 2015/10/17.

320. Olayioye MA, Barisic S, Hausser A. Multi-level control of actin dynamics by protein kinase D. Cell Signal. 2013;25(9):1739-47. Epub 2013/05/22.

321. Eiseler T, Doppler H, Yan IK, Kitatani K, Mizuno K, Storz P. Protein kinase D1 regulates cofilin-mediated F-actin reorganization and cell motility through slingshot. Nat Cell Biol. 2009;11(5):545-56. Epub 2009/03/31.

322. Peterburs P, Heering J, Link G, Pfizenmaier K, Olayioye MA, Hausser A. Protein kinase D regulates cell migration by direct phosphorylation of the cofilin phosphatase slingshot 1 like. Cancer research. 2009;69(14):5634-8. Epub 2009/07/02.

323. Eiseler T, Hausser A, De Kimpe L, Van Lint J, Pfizenmaier K. Protein kinase D controls actin polymerization and cell motility through phosphorylation of cortactin. J Biol Chem. 2010;285(24):18672-83. Epub 2010/04/07.

324. Alpsoy A, Gunduz U. Protein kinase D2 silencing reduced motility of doxorubicin-resistant MCF7 cells. Tumour biology : the journal of the International Society for Oncodevelopmental Biology and Medicine. 2015;36(6):4417-26. Epub 2015/04/16.

325. Bernhart E, Damm S, Wintersperger A, DeVaney T, Zimmer A, Raynham T, et al. Protein kinase D2 regulates migration and invasion of U87MG glioblastoma cells in vitro. Exp Cell Res. 2013;319(13):2037-48.

326. Zou Z, Zeng F, Xu W, Wang C, Ke Z, Wang QJ, et al. PKD2 and PKD3 promote prostate cancer cell invasion by modulating NF-kappaB- and HDAC1-mediated expression and activation of uPA. Journal of cell science. 2012;125(Pt 20):4800-11. Epub 2012/07/17.

327. Hao Q, Wang L, Zhao ZJ, Tang H. Identification of protein kinase D2 as a pivotal regulator of endothelial cell proliferation, migration, and angiogenesis. J Biol Chem. 2009;284(2):799-806.

328. Doppler H, Bastea LI, Borges S, Spratley SJ, Pearce SE, Storz P. Protein kinase d isoforms differentially modulate cofilin-driven directed cell migration. PLoS One. 2014;9(5):e98090. Epub 2014/05/21.

329. Sinnett-Smith J, Ni Y, Wang J, Ming M, Young SH, Rozengurt E. Protein kinase D1 mediates class IIa histone deacetylase phosphorylation and nuclear extrusion in intestinal epithelial cells: role in mitogenic signaling. American journal of physiology Cell physiology. 2014;306(10):C961-71. Epub 2014/03/22.

330. Vicente-Manzanares M, Choi CK, Horwitz AR. Integrins in cell migration--the actin connection. Journal of cell science. 2009;122(Pt 2):199-206. Epub 2009/01/02.

331. Christoforides C, Rainero E, Brown KK, Norman JC, Toker A. PKD controls alphavbeta3 integrin recycling and tumor cell invasive migration through its substrate Rabaptin-5. Developmental cell. 2012;23(3):560-72. Epub 2012/09/15.

332. Milner R, Crocker SJ, Hung S, Wang X, Frausto RF, del Zoppo GJ. Fibronectin- and vitronectin-induced microglial activation and matrix metalloproteinase-9 expression is mediated by integrins alpha5beta1 and alphavbeta5. J Immunol. 2007;178(12):8158-67. Epub 2007/06/06.

333. Paolillo M, Serra M, Schinelli S. Integrins in glioblastoma: Still an attractive target? Pharmacological Research. 2016;113, Part A:55-61.

334. Ghazaleh T, Jorg-Christian T, Roger S, Michael W. The Role of Integrins in Glioma Biology and Anti-Glioma Therapies. Current Pharmaceutical Design. 2011;17(23):2402-10.

335. Seiki M. The cell surface: the stage for matrix metalloproteinase regulation of migration. Current opinion in cell biology. 2002;14(5):624-32. Epub 2002/09/17.

336. Eiseler T, Wille C, Koehler C, Illing A, Seufferlein T. Protein Kinase D2 Assembles a Multiprotein Complex at the Trans-Golgi Network to Regulate Matrix Metalloproteinase Secretion. J Biol Chem. 2016;291(1):462-77. Epub 2015/10/29.

337. VanMeter TE, Rooprai HK, Kibble MM, Fillmore HL, Broaddus WC, Pilkington GJ. The Role of Matrix Metalloproteinase Genes in Glioma Invasion: Co-dependent and Interactive Proteolysis. Journal of Neuro-Oncology. 2001;53(2):213-35.

338. Veeravalli KK, Rao JS. MMP-9 and uPAR regulated glioma cell migration. Cell Adhesion & Migration. 2012;6(6):509-12.

339. Hambardzumyan D, Gutmann DH, Kettenmann H. The role of microglia and macrophages in glioma maintenance and progression. Nat Neurosci. 2016;19(1):20-7. Epub 2015/12/30.

340. Konnecke H, Bechmann I. The role of microglia and matrix metalloproteinases involvement in neuroinflammation and gliomas. Clinical & developmental immunology. 2013;2013:914104. Epub 2013/09/12.

341. Azoitei N, Pusapati GV, Kleger A, Moller P, Kufer R, Genze F, et al. Protein kinase D2 is a crucial regulator of tumour cell-endothelial cell communication in gastrointestinal tumours. Gut. 2010;59(10):1316-30. Epub 2010/08/25.

342. Forstreuter F, Lucius R, Mentlein R. Vascular endothelial growth factor induces chemotaxis and proliferation of microglial cells. Journal of neuroimmunology. 2002;132(1–2):93-8.

343. Liu H, Wang J, Wang J, Wang P, Xue Y. Paeoniflorin attenuates Abeta1-42-induced inflammation and chemotaxis of microglia in vitro and inhibits NF-kappaB- and VEGF/Flt-1 signaling pathways. Brain Res. 2015;1618:149-58. Epub 2015/06/07.

344. Ryu JK, Cho T, Choi HB, Wang YT, McLarnon JG. Microglial VEGF receptor response is an integral chemotactic component in Alzheimer's disease pathology. J Neurosci. 2009;29(1):3-13. Epub 2009/01/09.

345. Lee S, Chung CY. Role of VASP phosphorylation for the regulation of microglia chemotaxis via the regulation of focal adhesion formation/maturation. Molecular and cellular neurosciences. 2009;42(4):382-90. Epub 2009/09/08.

346. Ma L, Uchida H, Nagai J, Inoue M, Chun J, Aoki J, et al. Lysophosphatidic acid-3 receptor-mediated feed-forward production of lysophosphatidic acid: an initiator of nerve injury-induced neuropathic pain. Molecular pain. 2009;5:64. Epub 2009/11/17.

347. Lin ME, Rivera RR, Chun J. Targeted deletion of LPA5 identifies novel roles for lysophosphatidic acid signaling in development of neuropathic pain. J Biol Chem. 2012;287(21):17608-17. Epub 2012/03/31.

348. Ma L, Nagai J, Ueda H. Microglial activation mediates de novo lysophosphatidic acid production in a model of neuropathic pain. Journal of neurochemistry. 2010;115(3):643-53. Epub 2010/08/21.

349. Aly H, Khashaba MT, El-Ayouty M, El-Sayed O, Hasanein BM. IL-1beta, IL-6 and TNF-alpha and outcomes of neonatal hypoxic ischemic encephalopathy. Brain & development. 2006;28(3):178-82. Epub 2005/09/27.

350. Gyoneva S, Ransohoff RM. Inflammatory reaction after traumatic brain injury: therapeutic potential of targeting cell-cell communication by chemokines. Trends Pharmacol Sci. 2015;36(7):471-80. Epub 2015/05/17.

351. Liu B, Gao HM, Wang JY, Jeohn GH, Cooper CL, Hong JS. Role of nitric oxide in inflammation-mediated neurodegeneration. Annals of the New York Academy of Sciences. 2002;962:318-31. Epub 2002/06/22.

352. Hsieh HL, Yang CM. Role of redox signaling in neuroinflammation and neurodegenerative diseases. BioMed research international. 2013;2013:484613. Epub 2014/01/24.

353. Saha RN, Pahan K. Regulation of inducible nitric oxide synthase gene in glial cells. Antioxid Redox Signal. 2006;8(5-6):929-47. Epub 2006/06/15.

354. Kumar A, Chen SH, Kadiiska MB, Hong JS, Zielonka J, Kalyanaraman B, et al. Inducible nitric oxide synthase is key to peroxynitrite-mediated, LPS-induced protein radical formation in murine microglial BV2 cells. Free Radic Biol Med. 2014;73:51-9. Epub 2014/04/22.

355. Tarpey MM, Wink DA, Grisham MB. Methods for detection of reactive metabolites of oxygen and nitrogen: in vitro and in vivo considerations. American journal of physiology Regulatory, integrative and comparative physiology. 2004;286(3):R431-44. Epub 2004/02/06.

356. Ebadi M, Sharma SK. Peroxynitrite and mitochondrial dysfunction in the pathogenesis of Parkinson's disease. Antioxidants & redox signaling. 2003;5(3):319-35. Epub 2003/07/26.

357. Baud O, Li J, Zhang Y, Neve RL, Volpe JJ, Rosenberg PA. Nitric oxide-induced cell death in developing oligodendrocytes is associated with mitochondrial dysfunction and apoptosis-inducing factor translocation. The European journal of neuroscience. 2004;20(7):1713-26. Epub 2004/09/24.

358. Ding R, Chen Y, Yang S, Deng X, Fu Z, Feng L, et al. Blood-brain barrier disruption induced by hemoglobin in vivo: Involvement of up-regulation of nitric oxide synthase and peroxynitrite formation. Brain Res. 2014;1571:25-38. Epub 2014/05/13.

359. Popa-Wagner A, Mitran S, Sivanesan S, Chang E, Buga AM. ROS and brain diseases: the good, the bad, and the ugly. Oxidative medicine and cellular longevity. 2013;2013:963520. Epub 2014/01/02.

360. Valko M, Leibfritz D, Moncol J, Cronin MT, Mazur M, Telser J. Free radicals and antioxidants in normal physiological functions and human disease. The international journal of biochemistry & cell biology. 2007;39(1):44-84. Epub 2006/09/19.

361. Awada R, Saulnier-Blache JS, Gres S, Bourdon E, Rondeau P, Parimisetty A, et al. Autotaxin downregulates LPS-induced microglia activation and pro-inflammatory cytokines production. J Cell Biochem. 2014;115(12):2123-32. Epub 2014/07/24.

362. Fan H, Zingarelli B, Harris V, Tempel GE, Halushka PV, Cook JA. Lysophosphatidic acid inhibits bacterial endotoxin-induced pro-inflammatory response: potential anti-inflammatory signaling pathways. Mol Med. 2008;14(7-8):422-8. Epub 2008/04/24.

363. Fu R, Shen Q, Xu P, Luo JJ, Tang Y. Phagocytosis of microglia in the central nervous system diseases. Molecular neurobiology. 2014;49(3):1422-34. Epub 2014/01/08.

364. Brown GC, Neher JJ. Microglial phagocytosis of live neurons. Nat Rev Neurosci. 2014;15(4):209-16. Epub 2014/03/22.

365. Sierra A, Abiega O, Shahraz A, Neumann H. Janus-faced microglia: beneficial and detrimental consequences of microglial phagocytosis. Frontiers in cellular neuroscience. 2013;7:6. Epub 2013/02/07.

366. Neher JJ, Neniskyte U, Zhao JW, Bal-Price A, Tolkovsky AM, Brown GC. Inhibition of microglial phagocytosis is sufficient to prevent inflammatory neuronal death. J Immunol. 2011;186(8):4973-83. Epub 2011/03/16.

367. Neher JJ, Emmrich JV, Fricker M, Mander PK, Thery C, Brown GC. Phagocytosis executes delayed neuronal death after focal brain ischemia. Proceedings of the National Academy of Sciences of the United States of America. 2013;110(43):E4098-107. Epub 2013/10/09.

368. Fricker M, Oliva-Martin MJ, Brown GC. Primary phagocytosis of viable neurons by microglia activated with LPS or Abeta is dependent on calreticulin/LRP phagocytic signalling. Journal of neuroinflammation. 2012;9:196. Epub 2012/08/15.

369. Yung YC, Stoddard NC, Chun J. LPA Receptor Signaling: Pharmacology, Physiology, and Pathophysiology. J Lipid Res. 2014. Epub 2014/03/20.

370. Kozian DH, von Haeften E, Joho S, Czechtizky W, Anumala UR, Roux P, et al. Modulation of Hexadecyl-LPA-Mediated Activation of Mast Cells and Microglia by a Chemical Probe for LPA5. Chembiochem : a European journal of chemical biology. 2016;17(9):861-5. Epub 2016/01/27.

371. Bennett BL, Sasaki DT, Murray BW, O'Leary EC, Sakata ST, Xu W, et al. SP600125, an anthrapyrazolone inhibitor of Jun N-terminal kinase. Proceedings of the National Academy of Sciences of the United States of America. 2001;98(24):13681-6. Epub 2001/11/22.

372. Rozengurt E. Protein Kinase D Signaling: Multiple Biological Functions in Health and Disease. Physiology. 2011;26(1):23-33.

373. Chiu TT, Leung WY, Moyer MP, Strieter RM, Rozengurt E. Protein kinase D2 mediates lysophosphatidic acid-induced interleukin 8 production in nontransformed human colonic epithelial cells through NF-kappaB. Am J Physiol Cell Physiol. 2007;292(2):C767-77. Epub 2006/08/25.

374. Storz P, Doppler H, Toker A. Activation loop phosphorylation controls protein kinase D-dependent activation of nuclear factor kappaB. Molecular pharmacology. 2004;66(4):870-9. Epub 2004/07/01.

375. Storz P, Doppler H, Toker A. Protein kinase Cdelta selectively regulates protein kinase D-dependent activation of NF-kappaB in oxidative stress signaling. Molecular and cellular biology. 2004;24(7):2614-26. Epub 2004/03/17.

376. Mihailovic T, Marx M, Auer A, Van Lint J, Schmid M, Weber C, et al. Protein kinase D2 mediates activation of nuclear factor kappaB by Bcr-Abl in Bcr-Abl+ human myeloid leukemia cells. Cancer Res. 2004;64(24):8939-44. Epub 2004/12/18.

377. Yoo J, Chung C, Slice L, Sinnett-Smith J, Rozengurt E. Protein kinase D mediates synergistic expression of COX-2 induced by TNF-{alpha} and bradykinin in human

colonic myofibroblasts. Am J Physiol Cell Physiol. 2009;297(6):C1576-87. Epub 2009/10/02.

378. Zhu H, Yang Y, Zhang H, Han Y, Li Y, Zhang Y, et al. Interaction between protein kinase D1 and transient receptor potential V1 in primary sensory neurons is involved in heat hypersensitivity. Pain. 2008;137(3):574-88. Epub 2007/12/08.

379. Kaminska B, Gozdz A, Zawadzka M, Ellert-Miklaszewska A, Lipko M. MAPK signal transduction underlying brain inflammation and gliosis as therapeutic target. Anat Rec (Hoboken). 2009;292(12):1902-13. Epub 2009/11/28.

380. Whitmarsh AJ. Regulation of gene transcription by mitogen-activated protein kinase signaling pathways. Biochimica et biophysica acta. 2007;1773(8):1285-98. Epub 2007/01/02.

381. Kim EK, Choi EJ. Pathological roles of MAPK signaling pathways in human diseases. Biochimica et biophysica acta. 2010;1802(4):396-405. Epub 2010/01/19.

382. Perez M, Moran MA, Ferrer I, Avila J, Gomez-Ramos P. Phosphorylated tau in neuritic plaques of APP(sw)/Tau (vlw) transgenic mice and Alzheimer disease. Acta neuropathologica. 2008;116(4):409-18. Epub 2008/08/06.

383. Puig B, Gomez-Isla T, Ribe E, Cuadrado M, Torrejon-Escribano B, Dalfo E, et al. Expression of stress-activated kinases c-Jun N-terminal kinase (SAPK/JNK-P) and p38 kinase (p38-P), and tau hyperphosphorylation in neurites surrounding betaA plaques in APP Tg2576 mice. Neuropathology and applied neurobiology. 2004;30(5):491-502. Epub 2004/10/19.

384. Marques CA, Keil U, Bonert A, Steiner B, Haass C, Muller WE, et al. Neurotoxic mechanisms caused by the Alzheimer's disease-linked Swedish amyloid precursor protein mutation: oxidative stress, caspases, and the JNK pathway. J Biol Chem. 2003;278(30):28294-302. Epub 2003/05/06.

385. Shen C, Chen Y, Liu H, Zhang K, Zhang T, Lin A, et al. Hydrogen peroxide promotes Abeta production through JNK-dependent activation of gamma-secretase. J Biol Chem. 2008;283(25):17721-30. Epub 2008/04/26.

386. Colombo A, Bastone A, Ploia C, Sclip A, Salmona M, Forloni G, et al. JNK regulates APP cleavage and degradation in a model of Alzheimer's disease. Neurobiology of disease. 2009;33(3):518-25. Epub 2009/01/27.

387. Muresan Z, Muresan V. The amyloid-beta precursor protein is phosphorylated via distinct pathways during differentiation, mitosis, stress, and degeneration. Molecular biology of the cell. 2007;18(10):3835-44. Epub 2007/07/20.

388. Klegeris A, Pelech S, Giasson BI, Maguire J, Zhang H, McGeer EG, et al. Alpha-synuclein activates stress signaling protein kinases in THP-1 cells and microglia. Neurobiology of aging. 2008;29(5):739-52. Epub 2006/12/15.

389. Rawal N, Parish C, Castelo-Branco G, Arenas E. Inhibition of JNK increases survival of transplanted dopamine neurons in Parkinsonian rats. Cell death and differentiation. 2007;14(2):381-3. Epub 2006/07/22.

390. Bendotti C, Bao Cutrona M, Cheroni C, Grignaschi G, Lo Coco D, Peviani M, et al. Inter- and intracellular signaling in amyotrophic lateral sclerosis: role of p38 mitogen-activated protein kinase. Neuro-degenerative diseases. 2005;2(3-4):128-34. Epub 2006/08/16.

391. Ackerley S, Grierson AJ, Banner S, Perkinton MS, Brownlees J, Byers HL, et al. p38alpha stress-activated protein kinase phosphorylates neurofilaments and is associated with neurofilament pathology in amyotrophic lateral sclerosis. Molecular and cellular neurosciences. 2004;26(2):354-64. Epub 2004/06/23.

392. Brownlees J, Yates A, Bajaj NP, Davis D, Anderton BH, Leigh PN, et al. Phosphorylation of neurofilament heavy chain side-arms by stress activated protein kinase-1b/Jun N-terminal kinase-3. Journal of cell science. 2000;113 (Pt 3):401-7. Epub 2000/01/20.

393. Weston CR, Davis RJ. The JNK signal transduction pathway. Current opinion in cell biology. 2007;19(2):142-9. Epub 2007/02/17.

394. Sabapathy K. Role of the JNK pathway in human diseases. Progress in molecular biology and translational science. 2012;106:145-69. Epub 2012/02/22.

395. Hunot S, Vila M, Teismann P, Davis RJ, Hirsch EC, Przedborski S, et al. JNK-mediated induction of cyclooxygenase 2 is required for neurodegeneration in a mouse model of Parkinson's disease. Proceedings of the National Academy of Sciences of the United States of America. 2004;101(2):665-70. Epub 2004/01/06.

396. Zhu X, Raina AK, Rottkamp CA, Aliev G, Perry G, Boux H, et al. Activation and redistribution of c-jun N-terminal kinase/stress activated protein kinase in degenerating neurons in Alzheimer's disease. Journal of neurochemistry. 2001;76(2):435-41. Epub 2001/02/24.

397. Mitsios N, Gaffney J, Krupinski J, Mathias R, Wang Q, Hayward S, et al. Expression of signaling molecules associated with apoptosis in human ischemic stroke tissue. Cell biochemistry and biophysics. 2007;47(1):73-86. Epub 2007/04/05.

398. Vukic V, Callaghan D, Walker D, Lue LF, Liu QY, Couraud PO, et al. Expression of inflammatory genes induced by beta-amyloid peptides in human brain endothelial cells and in Alzheimer's brain is mediated by the JNK-AP1 signaling pathway. Neurobiology of disease. 2009;34(1):95-106. Epub 2009/01/24.

399. Eynott PR, Xu L, Bennett BL, Noble A, Leung SY, Nath P, et al. Effect of an inhibitor of Jun N-terminal protein kinase, SP600125, in single allergen challenge in sensitized rats. Immunology. 2004;112(3):446-53. Epub 2004/06/16.

400. Zhuang ZY, Wen YR, Zhang DR, Borsello T, Bonny C, Strichartz GR, et al. A peptide c-Jun N-terminal kinase (JNK) inhibitor blocks mechanical allodynia after spinal nerve ligation: respective roles of JNK activation in primary sensory neurons and spinal astrocytes for neuropathic pain development and maintenance. The Journal of neuroscience : the official journal of the Society for Neuroscience. 2006;26(13):3551-60. Epub 2006/03/31.

401. Guan QH, Pei DS, Liu XM, Wang XT, Xu TL, Zhang GY. Neuroprotection against ischemic brain injury by SP600125 via suppressing the extrinsic and intrinsic pathways of apoptosis. Brain research. 2006;1092(1):36-46. Epub 2006/05/06.

402. Wang Y, Zhang Y, Wei Z, Li H, Zhou H, Zhang Z, et al. JNK inhibitor protects dopaminergic neurons by reducing COX-2 expression in the MPTP mouse model of subacute Parkinson's disease. Journal of the neurological sciences. 2009;285(1-2):172-7. Epub 2009/07/17.

403. Borsello T, Clarke PG, Hirt L, Vercelli A, Repici M, Schorderet DF, et al. A peptide inhibitor of c-Jun N-terminal kinase protects against excitotoxicity and cerebral ischemia. Nature medicine. 2003;9(9):1180-6. Epub 2003/08/26.

404. Bodles AM, Barger SW. Secreted β-amyloid precursor protein activates microglia via JNK and p38-MAPK. Neurobiology of aging. 2005;26(1):9-16.

405. Goldmann T, Wieghofer P, Muller PF, Wolf Y, Varol D, Yona S, et al. A new type of microglia gene targeting shows TAK1 to be pivotal in CNS autoimmune inflammation. Nature neuroscience. 2013;16(11):1618-26.

406. Yang L, Liu C-C, Zheng H, Kanekiyo T, Atagi Y, Jia L, et al. LRP1 modulates the microglial immune response via regulation of JNK and NF-κB signaling pathways. Journal of neuroinflammation. 2016;13(1):304.

407. Kacimi R, Giffard RG, Yenari MA. Endotoxin-activated microglia injure brain derived endothelial cells via NF- κ B, JAK-STAT and JNK stress kinase pathways. Journal of Inflammation. 2011;8(1):7.

408. Raivich G. c-Jun expression, activation and function in neural cell death, inflammation and repair. Journal of neurochemistry. 2008;107(4):898-906. Epub 2008/09/17.

409. Vallabhapurapu S, Karin M. Regulation and function of NF-kappaB transcription factors in the immune system. Annual review of immunology. 2009;27:693-733. Epub 2009/03/24.

410. Lawrence T. The nuclear factor NF-kappaB pathway in inflammation. Cold Spring Harbor perspectives in biology. 2009;1(6):a001651. Epub 2010/05/12.

411. Kaltschmidt B, Kaltschmidt C. NF-kappaB in the nervous system. Cold Spring Harbor perspectives in biology. 2009;1(3):a001271. Epub 2010/01/13.

412. Parisi C, Napoli G, Amadio S, Spalloni A, Apolloni S, Longone P, et al. MicroRNA-125b regulates microglia activation and motor neuron death in ALS. Cell death and differentiation. 2016;23(3):531-41.

413. Frakes Ashley E, Ferraiuolo L, Haidet-Phillips Amanda M, Schmelzer L, Braun L, Miranda Carlos J, et al. Microglia Induce Motor Neuron Death via the Classical NF-κB Pathway in Amyotrophic Lateral Sclerosis. Neuron.81(5):1009-23.

414. Khasnavis S, Jana A, Roy A, Mazumder M, Bhushan B, Wood T, et al. Suppression of Nuclear Factor- κ B Activation and Inflammation in Microglia by Physically Modified Saline. Journal of Biological Chemistry. 2012;287(35):29529-42.

415. Yao L, Kan EM, Kaur C, Dheen ST, Hao A, Lu J, et al. Notch-1 Signaling Regulates Microglia Activation via NF- κ B Pathway after Hypoxic Exposure In Vivo and In Vitro. PloS one. 2013;8(11):e78439.

416. Nicolas CS, Amici M, Bortolotto ZA, Doherty A, Csaba Z, Fafouri A, et al. The role of JAK-STAT signaling within the CNS. Jak-Stat. 2013;2(1):e22925. Epub 2013/09/24.

417. O'Shea JJ, Plenge R. JAK and STAT signaling molecules in immunoregulation and immune-mediated disease. Immunity. 2012;36(4):542-50. Epub 2012/04/24.

418. Gu J, Li G, Sun T, Su Y, Zhang X, Shen J, et al. Blockage of the STAT3 signaling pathway with a decoy oligonucleotide suppresses growth of human malignant glioma cells. J Neurooncol. 2008;89(1):9-17. Epub 2008/04/17.

419. Chen F, Xu Y, Luo Y, Zheng D, Song Y, Yu K, et al. Down-regulation of Stat3 decreases invasion activity and induces apoptosis of human glioma cells. Journal of molecular neuroscience : MN. 2010;40(3):353-9. Epub 2010/01/14.

420. Yang X, He G, Hao Y, Chen C, Li M, Wang Y, et al. The role of the JAK2-STAT3 pathway in pro-inflammatory responses of EMF-stimulated N9 microglial cells. Journal of neuroinflammation. 2010;7:54. Epub 2010/09/11.

421. Huang C, Ma R, Sun S, Wei G, Fang Y, Liu R, et al. JAK2-STAT3 signaling pathway mediates thrombin-induced proinflammatory actions of microglia in vitro. Journal of neuroimmunology. 2008;204(1-2):118-25. Epub 2008/08/20.

422. Rauch I, Muller M, Decker T. The regulation of inflammation by interferons and their STATs. Jak-Stat. 2013;2(1):e23820. Epub 2013/09/24.

423. Herrera-Molina R, Flores B, Orellana JA, von Bernhardi R. Modulation of interferon-γ-induced glial cell activation by transforming growth factor β1: A role for STAT1 and MAPK pathways. Journal of neurochemistry. 2012;123(1):113-23.

424. Delgado M. Inhibition of Interferon (IFN) γ-induced Jak-STAT1 Activation in Microglia by Vasoactive Intestinal Peptide: INHIBITORY EFFECT ON CD40, IFN-INDUCED PROTEIN-10, AND INDUCIBLE NITRIC-OXIDE SYNTHASE EXPRESSION. Journal of Biological Chemistry. 2003;278(30):27620-9.

425. Rezai-Zadeh K, Ehrhart J, Bai Y, Sanberg PR, Bickford P, Tan J, et al. Apigenin and luteolin modulate microglial activation via inhibition of STAT1-induced CD40 expression. Journal of neuroinflammation. 2008;5(1):41.

426. De-Fraja C, Conti L, Magrassi L, Govoni S, Cattaneo E. Members of the JAK/STAT proteins are expressed and regulated during development in the mammalian forebrain. Journal of neuroscience research. 1998;54(3):320-30. Epub 1998/11/18.

427. Hashioka S, Klegeris A, Schwab C, McGeer PL. Interferon-gamma-dependent cytotoxic activation of human astrocytes and astrocytoma cells. Neurobiology of aging. 2009;30(12):1924-35. Epub 2008/04/01.

428. Okada S, Nakamura M, Katoh H, Miyao T, Shimazaki T, Ishii K, et al. Conditional ablation of Stat3 or Socs3 discloses a dual role for reactive astrocytes after spinal cord injury. Nature medicine. 2006;12(7):829-34. Epub 2006/06/20.

429. Satriotomo I, Bowen KK, Vemuganti R. JAK2 and STAT3 activation contributes to neuronal damage following transient focal cerebral ischemia. Journal of neurochemistry. 2006;98(5):1353-68. Epub 2006/08/23.

430. Choi SH, Lee DY, Kim SU, Jin BK. Thrombin-induced oxidative stress contributes to the death of hippocampal neurons in vivo: role of microglial NADPH oxidase. The Journal of neuroscience : the official journal of the Society for Neuroscience. 2005;25(16):4082-90. Epub 2005/04/22.
431. Planas AM, Gorina R, Chamorro A. Signalling pathways mediating inflammatory responses in brain ischaemia. Biochemical Society transactions. 2006;34(Pt 6):1267-70. Epub 2006/11/01.

Appendix I

Reagents	Company
1-bromo-3(S)-hydroxy-4-(palmitoyloxy)butyl]phosphonate (BrP-LPA)	Echelon Biosciences, Salt Lake City, UT, USA
1-Oleoyl-2-hydroxy-sn-glycero-3-phosphate (LPA)	Sigma Aldrich, St. Louis, MO, USA
1,9-Pyrazoloanthrone (SP 600125)	Merck Millipore, Billerica, MA, USA
2-[4-[[(2R)-2-Aminobutyl] amino]-2-pyrimidinyl]-4-(1-methyl-1H-pyrazol-4-yl)-phenol hydrochloride (CRT 0066101)	Sigma Aldrich, St. Louis, MO, USA
5-(3-Chloro-4-cyclohexylphenyl)-1-(3-methoxyphenyl)-1H-pyrazole-3-carboxylic acid (TCLPA5)	Tocris Bioscience, Bristol, UK
Acrylamide	Thermo Fisher Scientific, Waltham, USA
Alexa Fluor® 488 Phalloidin	Invitrogen, Waltham, MA, USA
Ammoniumpersulfate (APS)	Sigma Aldrich, St. Louis, MO, USA
Aprotinin	Sigma Aldrich, St. Louis, MO, USA
BD Cell Fix (10x)	BD Biosciences, San Jose, CA, USA
Bis-Acrylamide	Sigma Aldrich, St. Louis, MO, USA
Dako Antibody Diluent with background reducing agents	Agilent Technologies, Santa Clara, CA, USA
Dako Fluorescence Mounting Medium	Agilent Technologies, Santa Clara, CA, USA
Dako Pen	Agilent Technologies, Santa Clara, CA, USA
Dimethyl sulfoxide (DMSO)	Sigma Aldrich, St. Louis, MO, USA
DMEM (Dulbecco's modified Eagle's medium) Cell Culture Medium	Invitrogen, Waltham, MA, USA
Ethylenediaminetetraacetic Acid (EDTA)	Sigma Aldrich, St. Louis, MO, USA
Fatty Acid Free Bovine Serum Albumin (BSA)	SERVA Electrophoresis GmbH, Heidelberg, Germany
Fetal Calf Serum (FCS)	Sigma Aldrich, St. Louis, MO, USA
FITC-tomato-lectin	Sigma Aldrich, St. Louis, MO, USA
Formaldehyde	Sigma Aldrich, St. Louis, MO, USA
Glutamine	Invitrogen, Waltham, MA, USA
Glycerol	Sigma Aldrich, St. Louis, MO, USA
Halt™ Phosphatase Inhibitor Cocktail	Thermo Fisher Scientific, Waltham, MA, USA

HEPES	Invitrogen, Waltham, MA, USA
Hoechst 33342	Thermo Fisher Scientific, Waltham, USA
KCl	Sigma Aldrich, St. Louis, MO, USA
KH_2PO_4	Sigma Aldrich, St. Louis, MO, USA
Leupeptin	Sigma Aldrich, St. Louis, MO, USA
LPS from E. coli (O111:B4)	Sigma Aldrich, St. Louis, MO, USA
Mercaptoethanol	Sigma Aldrich, St. Louis, MO, USA
Methanol	New England Biolabs, Ipswich, MA, USA
Na_2HPO_4	Sigma Aldrich, St. Louis, MO, USA
NP-40	Sigma Aldrich, St. Louis, MO, USA
Penicillin	Invitrogen, Waltham, MA, USA
Pepstatin	Sigma Aldrich, St. Louis, MO, USA
Phenylmethylsulfonylfluorid (PMSF)	Sigma Aldrich, St. Louis, MO, USA
Phosphate Buffered Saline (PBS)	Sigma Aldrich, St. Louis, MO, USA
Recombinant murine IL-4	Peprotech, Rocky Hill, NJ, USA
Recombinant murine IL-10	Peprotech, Rocky Hill, NJ, USA
RPMI 1640 Cell Culture Medium	Invitrogen, Waltham, MA, USA
Sodium Chloride (NaCl)	Sigma Aldrich, St. Louis, MO, USA
Sodium Dodecyl Sulfate (SDS)	Sigma Aldrich, St. Louis, MO, USA
Sodium Fluoride (NaF)	Sigma Aldrich, St. Louis, MO, USA
Sodium Orthovanadate (Na_3VO_4)	Sigma Aldrich, St. Louis, MO, USA
Streptomycin	Invitrogen, Waltham, MA, USA
Tetramethylethylenediamine (Temed)	New England Biolabs, Ipswich, MA, USA
Tris-HCl	Sigma Aldrich, St. Louis, MO, USA
TritonX	Sigma Aldrich, St. Louis, MO, USA
Trypsin	Invitrogen, Waltham, MA, USA
Tween 20	Sigma Aldrich, St. Louis, MO, USA
Ultra V Block	Thermo Fisher Scientific, Waltham, USA

Antibodies	Company
β-actin (mouse)	Sigma Aldrich, St. Louis, MO, USA
β-Tubulin (mouse)	Sigma Aldrich, St. Louis, MO, USA
Akt (rabbit)	Cell Signaling, Beverly, MA, USA
APC-CD86	e-Bioscience, San Diego, CA, USA
Arg-1 (rabbit)	Cell Signaling, Beverly, MA, USA
Arg-1 (rabbit)	Santa Cruz, Dallas, TX, USA
CD11b (rat)	Novus Biologicals, Littleton, CO, USA
c-Jun (H-79) (rabbit)	Cell Signaling, Beverly, MA, USA
COX-2 (rabbit)	Cell Signaling, Beverly, MA, USA
COX-2 (goat)	Santa Cruz, Dallas, TX, USA
Cyanine (Cy-2)-goat anti-rabbit	GE Healthcare, Vienna, Austria
Cyanine (Cy-3)-goat anti-mouse	GE Healthcare, Vienna, Austria
Cyanine (Cy-3)-goat anti-rabbit	GE Healthcare, Vienna, Austria
Cyanine (Cy-3)-rabbit anti-goat	GE Healthcare, Vienna, Austria
Horse Radish Peroxidase Conjugated Anti-goat (HRP anti-goat)	Santa Cruz, San Diego, CA, USA
Horse Radish Peroxidase Conjugated Anti-mouse (HRP anti-mouse)	Santa Cruz, San Diego, CA, USA
Horse Radish Peroxidase Conjugated Anti-rabbit (HRP anti-rabbit)	Thermo Fisher Scientific, Waltham, USA
Iba-1 (rabbit)	Wako Chemicals, Neuss, Germany
iNOS (mouse)	BD Biosciences, San Jose, CA, USA
iNOS (rabbit)	Abcam, Cambridge, UK
IκBα (rabbit)	Santa Cruz, Dallas, TX, USA
NF-kB p65 (rabbit)	Cell Signaling, Beverly, MA, USA
p38 MAPK (rabbit)	Cell Signaling, Beverly, MA, USA
p44/42 MAPK (Erk1/2) (137F5) (rabbit)	Cell Signaling, Beverly, MA, USA
phospho-Akt (Ser473) (rabbit)	Cell Signaling, Beverly, MA, USA
phospho-c-Jun (Ser63) II (rabbit)	Cell Signaling, Beverly, MA, USA
phospho-IκBα (Ser32)-R (rabbit)	Cell Signaling, Beverly, MA, USA
phospho-NF-kB p65 (Ser536) (93H1) (rabbit)	Cell Signaling, Beverly, MA, USA
phospho-IKK (rabbit)	Cell Signaling, Beverly, MA, USA
phospho-p38 MAPK (Thr180/Tyr182) (D3F9) XP (rabbit)	Cell Signaling, Beverly, MA, USA
phospho-p44/42 MAPK (Erk1/2) (Thr202/Tyr204) (rabbit)	Cell Signaling, Beverly, MA, USA
phospho-PKD/PKCμ (pPKD1, Ser744/748) (rabbit)	Cell Signaling, Beverly, MA, USA
phospho-PKD2 (Ser848) (rabbit)	Abcam, Cambridge, UK

phospho-SAPK/JNK (Thr183/Tyr185) (rabbit)	Cell Signaling, Beverly, MA, USA
phospho-STAT1 (Tyr701) (rabbit)	Cell Signaling, Beverly, MA, USA
phospho-STAT3 (Tyr705) (D3A7) XP (rabbit)	Cell Signaling, Beverly, MA, USA
PE-CD206	e-Bioscience, San Diego, CA, USA
PE-CD40	e-Bioscience, San Diego, CA, USA
PKD1 (rabbit)	Cell Signaling, Beverly, MA, USA
PKD2 (mouse)	Abcam, Cambridge, UK
PKD3/PKCν (D57E6) (rabbit)	Santa Cruz, San Diego, CA, USA
RELMα (FIZZ-1) (rabbit)	Novus Biologicals, Littleton, CO, USA
SAPK/JNK (rabbit)	Cell Signaling, Beverly, MA, USA
STAT1 (rabbit)	Cell Signaling, Beverly, MA, USA
STAT3 (Tyr705) (D3A7) XP (rabbit)	Cell Signaling, Beverly, MA, USA

Assay Kits	Company
DCFDA Cellular ROS Detection Kit	Abcam, Cambridge, UK
Elisa Development Kit ABTS Murine IL-1 beta	Peprotech, Rocky Hill, NJ, USA
Elisa Development Kit ABTS Murine IP-10 (CXCL10)	Peprotech, Rocky Hill, NJ, USA
Elisa Development Kit ABTS Murine MIP-2 (CXCL2)	Peprotech, Rocky Hill, NJ, USA
Elisa Development Kit Murine IL-6 (TMB EDK)	Peprotech, Rocky Hill, NJ, USA
Elisa Development Kit Murine Rantes (CCL5) (TMB EDK)	Peprotech, Rocky Hill, NJ, USA
Elisa Development Kit Murine TNF alpha (TMB EDK)	Peprotech, Rocky Hill, NJ, USA
LDH Cytotoxicity Assay Kit	Cayman Chemical, Ann Arbor, MI, USA
Nitric Oxide (Total) Detection Kit	Enzo Life Sciences (ELS) AG, Lausen, Switzerland
Phagocytosis Assay Kit (IgG PE)	Cayman Chemical, Ann Arbor, MI, USA
Pierce BCA Protein Assay Kit	Thermo Fisher Scientific, Waltham, USA
Pierce ECL Western Blotting Substrate	Thermo Fisher Scientific, Waltham, USA
Pierce ECL Plus Western Blotting Substrate	Thermo Fisher Scientific, Waltham, USA

Solutions-Buffers-WB Gels	
Acrylamide-Bis (100mL)	Acrylamide 30g, Bis-Acrylamide 0.8g
Blocking Solution	Low-fat Milk Powder 5g, Wash Buffer 100mL
Blotting Buffer (1L)	Tris 1.21g, Glycine 3.0g, Methanol 200mL
PAGE Running Gel (per Gel)	Acrylamide-Bis 2.9mL, 1.5M Tris Buffer pH 8.8 2.17mL, H_2O 3.53mL, SDS 10% 86µL, Temed 4.36µL, APS 10% 76 µL
PAGE Stacking Gel (per Gel)	Acrylamide-Bis 0.326mL, 0.5M Tris-Buffer pH 6.8 0.5mL, Glycerol 50% 1.65mL, SDS 10 % 21.5µL, Temed 1.25µL, APS10% 19µL
PBS Buffer (1L)	NaCl 8g, KCl 0.2g, Na_2HPO_4 2.2g, KH_2PO_4 0.2g
Ripa Buffer pH 7.4 (100mL)	Tris 605.7mg, NaCl 876.6mg, EDTA 37.22mg, NP-40 1% 1g, Na_3VO_4 [200mM] 500µL, NaF [200mM] 500µL
Sample Buffer pH 6.8	Glycerol 10mL, SDS 2.15g, Tris 0.76g, Mercaptoethanol 2.25mL, Bromphenol Blue
SDS-PAGE Running Buffer (1L)	Tris 3.03g, Glycine 15.01g, SDS 1g
Stripping Buffer pH 6.8 (0.5L)	Tris HCl 3.63g, SDS 10g, Mercaptoethanol 3.5mL
TBST Buffer pH 7.5 (1L)	Tris 3.03g, NaCl 8.77g, Tween 20 0.5g,
Wash Buffer pH 7.4 (1L)	Tween 20 0.5g, NaCl 9g, Tris 1.21g

Table 1. Primers (Qiagen) used for qPCR analyses

Gene	Detected transcripts	Amplicon Length
Lpar1	NM_010336 (3362 bp)	94
	NM_172989 (3451 bp)	
Lpar2	NM_020028 (5701 bp)	94
Lpar3	NM_022983 (2494 bp)	99
Lpar4	NM_175271 (4237 bp)	96
Lpar5	NM_001163268 (1458 bp)	100
	NM_001163269 (1393 bp)	
	XM_355812 (1458 bp)	
	XM_917685 (1458 bp)	
	XM_981874 (1387 bp)	
	XM_006506340 (2537 bp)	
Lpar6	NM_175116 (2468 bp)	118
Prkd1	NM_008858 (3778 bp)	149
	XM_006515586 (3805 bp)	
	XM_006515588 (4308 bp)	
	XM_006515589 (3220 bp)	
	XM_006515590 (3422 bp)	
	XM_006515591 (2593 bp)	
Prkd2	NM_001252458 (3340 bp)	116
	NM_178900 (3625 bp)	
	XM_006539444 (2087 bp)	
Prkd3	NM_001171004 (5887 bp)	100
	NM_001171005 (5083 bp)	
	NM_029239 (5884 bp)	
	XM_006525065 (5194 bp)	

Table 2. Gene primers utilized in qPCR arrays

Gene	Detected transcripts	Amplicon Size
Itga4	NM_010576.3	161
Itga5	NM_010577.3	131
Itgav	NM_008402.3	117
Itgb1	NM_010578.2	135
Itgb3	NM_016780.2	146
Itgb5	NM_010580.2	135
Mmp2	NM_008610.2	141
Mmp9	NM_013599.2	95
Mmp12	NM_008605.3	153
Mmp14	NM_008608.3	99
Myh9	NM_022410.3	114
Rac2	NM_009008.3	90
Tbcb	NM_025548.3	127
Vasp	NM_009499.3	102
Vim	NM_011701.4	134
Wasf2	NM_153423.6	121
Vegfa	NM_009505.4	141
B2m	NM_009735	112
Gusb	NM_010368.1	148
Hprt	NM_013556.2	152
Hsp90ab1	NM_008302.3	134

Table 3. Primers (Qiagen) used for qPCR analyses

Gene	Detected transcripts	Amplicon Length
Itga4	NM_010576 (9833 bp)	72
Itga5	NM_010577 (4397 bp)	136
Itgav	NM_008402 (7055 bp)	66
Mmp9	NM_013599 (3174 bp)	104
Mmp14	NM_008608 (2597 bp)	122
Vasp	NM_009499 (2267 bp)	88
Wasf2	NM_153423 (4088 bp)	129
Vegfa	NM_001025250 (3547 bp)	62

Table 4. Primers (Invitrogen) used for qPCR analyses

Gene	Forward primer (5'-3')	Reverse primer (5'-3')	Length (bp)
Ccl5	GCTGCTTTGCCTACCTCTCC	TCGAGTGACAAACACGACTGC	104
Cxcl10	AGTGCTGCCGTCATTTTCTG	ATTCTCACTGGCCCGTCAT	122
Cxcl2	AGTGAACTGCGCTGTCAATG	GCCCTTGAGAGTGGCTATGA	126
Il1β	TGTGAAATGCCACCTTTTGA	GGTCAAAGGTTTGGAAGCAG	94
Il6	TGATGCACTTGCAGAAAACA	ACCAGAGGAAATTTTCAATAGGC	109
Tnfα	CCACCACGCTCTTCTGTCTAC	AGGGTCTGGGCCATAGAACT	103

Appendix II

Table 1 Physiological roles for LPA signaling

	Phenotype	Established roles for LPA signaling
Nervous system	Growth/development	Proliferation and differentiation of neural progenitor cells (NPCs) Neurogenesis Ionic conductance changes Neuronal survival LPA production by neurons Astrocyte proliferation
	Morphology	Morphological changes in NPCs, neurons, and astrocytes Cortical actin assembly in *Xenopus* neurons Synapse formation
	Cellular interaction	Neuronal differentiation by astrocyte-derived soluble factors
	Myelination	Differentiation of oligodendrocytes Morphological changes in Schwann cells Proliferation and survival of Schwann cells Upregulation of myelin P0 protein
Vascular system	Vasculogenesis Angiogenesis	Frontal cephalic hemorrhages in *Lpar1*$^{-/-}$ and *Lpar1*$^{-/-}$/*Lpar2*$^{-/-}$ Severe vascular defects in ATX null Vasculature maintenance
	Vasoregulation	Hypertension or hypotension by LPA Endothelial cell death Loss of vascular integrity Increase in hydraulic permeability
Immune system	T cell functions	Chemotaxis Cytokine production Apoptosis Trafficking (regulation by ATX)
	Dendritic cell functions	Maturation Chemotaxis of immature dendritic cells
Reproductive system	Embryo implantation	Timing and spacing of implantation Regulation of prostaglandin pathways
	Spermatogenesis	Survival factor for germ cell Sperm motility
	Others	Possible role in male sexual function, ovarian functions, fertilization, decidualization, pregnancy maintenance, and parturition

Table 2 Pathophysiological roles for LPA signaling

Pathological conditions	Established roles for LPA signaling	
Neuro-inflammation	Astrogliosis by LPA injection LPA_3 upregulation in activated microglia	
Nerve injury	LPA_1 and LPA_2 upregulation after nerve transection Neuropathic pain by LPA injection Substance P release by LPA Resistance to partial sciatic nerve ligation–induced neuropathic pain in *Lpar1*$^{-/-}$ or ATX null	
Schizophrenia	Cranial dysmorphism in *Lpar1*$^{-/-}$ Defect in the prepulse inhibition in *Lpar1*$^{-/-}$ Alteration of 5-HT system in *Lpar1*$^{-/-}$ Reduction of Risperidone efficacy	
Atherosclerosis	LPA accumulation in atherosclerotic plaques Platelet activation De-differentiation of vascular smooth muscle cells (VSMCs) by LPA Defect in migration of SMCs from *Lpar1*$^{-/-}$/*Lpar2*$^{-/-}$ Reduction in neointimal lesions of carotid artery ligation in *Lpar1*$^{-/-}$/*Lpar2*$^{-/-}$	
Wound healing	Secretion of LPA from activated platelets Mitogenic/migratory effect on endothelial cells, SMCs, and fibroblasts Closure of wounded endothelial monolayers Promotion of repair processes in wounds	
Cancer	Ovarian	LPA as ovarian cancer activating factor Potent protumorigenic effect (by LPA_2; partially by LPA_1 or LPA_3) LPA_2 upregulation in some cancers Involvement in hypoxia-stimulated tumorigenic processes
	Gastrointestinal	Protumorigenic effect (by LPA_1 and LPA_2) LPA_2-mediated tumor formation Regulation of known signaling molecules
	Lung	Promotion of cancer aggressiveness
	ATX as a motility stimulating factor for cancer cells Stimulation of angiogenesis during tumor formation Possible involvement in breast cancer, prostate cancer, and glioma	
Airway disease	Increased LPA levels in asthma Possible role for LPA signaling as an anti-inflammatory factor	
Fibrosis	Pulmonary fibrosis (PF)	Increased LPA level in PF Reduced mortality in *Lpar1*$^{-/-}$
	Tubulo-interstitial fibrosis (TIF)	Reduced TIF by genetic and pharmacological inhibition of LPA_1 activity Enhanced LPA secretion and LPA_1 up-regulation in TIF
	Liver fibrosis	Enhanced LPA level and ATX activity in patients or animal models LPA-induced proliferation of stellate cells and hepatocytes
Obesity	ATX upregulation during adipocyte differentiation ATX upregulation in obese-diabetic mice or in glucose-intolerant obese women Anti-adipogenesis LPA or ATX secretion by adipocytes Stimulation of motility and proliferation in preadipocytes Higher adiposity in *Lpar1*$^{-/-}$ compared to wild type Regulation of blood glucose metabolism	